LEABHARLANN CHOLÁISTE NA TRÍONÓIDE, BAILE ÁTHA CLIATH | TRINITY COLLEGE LIBRARY DUBLIN
Ollscoil Átha Cliath | The University of Dublin

Terms and Conditions of Use of Digitised Theses from Trinity College Library Dublin

Copyright statement

All material supplied by Trinity College Library is protected by copyright (under the Copyright and Related Rights Act, 2000 as amended) and other relevant Intellectual Property Rights. By accessing and using a Digitised Thesis from Trinity College Library you acknowledge that all Intellectual Property Rights in any Works supplied are the sole and exclusive property of the copyright and/or other IPR holder. Specific copyright holders may not be explicitly identified. Use of materials from other sources within a thesis should not be construed as a claim over them.

A non-exclusive, non-transferable licence is hereby granted to those using or reproducing, in whole or in part, the material for valid purposes, providing the copyright owners are acknowledged using the normal conventions. Where specific permission to use material is required, this is identified and such permission must be sought from the copyright holder or agency cited.

Liability statement

By using a Digitised Thesis, I accept that Trinity College Dublin bears no legal responsibility for the accuracy, legality or comprehensiveness of materials contained within the thesis, and that Trinity College Dublin accepts no liability for indirect, consequential, or incidental, damages or losses arising from use of the thesis for whatever reason. Information located in a thesis may be subject to specific use constraints, details of which may not be explicitly described. It is the responsibility of potential and actual users to be aware of such constraints and to abide by them. By making use of material from a digitised thesis, you accept these copyright and disclaimer provisions. Where it is brought to the attention of Trinity College Library that there may be a breach of copyright or other restraint, it is the policy to withdraw or take down access to a thesis while the issue is being resolved.

Access Agreement

By using a Digitised Thesis from Trinity College Library you are bound by the following Terms & Conditions. Please read them carefully.

I have read and I understand the following statement: All material supplied via a Digitised Thesis from Trinity College Library is protected by copyright and other intellectual property rights, and duplication or sale of all or part of any of a thesis is not permitted, except that material may be duplicated by you for your research use or for educational purposes in electronic or print form providing the copyright owners are acknowledged using the normal conventions. You must obtain permission for any other use. Electronic or print copies may not be offered, whether for sale or otherwise to anyone. This copy has been supplied on the understanding that it is copyright material and that no quotation from the thesis may be published without proper acknowledgement.

The Spatial and Non-Spatial Properties of Single-Units in the Anterior Retrosplenial Cortex of the Freely-Moving Rat



A Thesis Submitted to the University of Dublin for the Degree of Doctor of Philosophy

By

Paul Wynne

September 2016

Under the Supervision of Prof. Shane O'Mara

School of Psychology, Institute of Neuroscience

Trinity College Dublin

Ireland

TRINITY COLLEGE DUBLIN
28 SEP 2016
ACADEMIC REGISTRY
PhD
PSYCHOLOGY

TRINITY LIBRARY
0 8 MAR 2017
DUBLIN
Thesis 11282

Declaration

I declare that this thesis has not been submitted as an exercise for a degree at this or any other university and it is entirely my own work.

I agree to deposit this thesis in the University's open access institutional repository or allow the library to do so on my behalf, subject to Irish Copyright Legislation and Trinity College Library conditions of use and acknowledgement.

Signed

Summary

Summary of methods

The purpose of this study was to describe the spatial and non-spatial properties of single-units in the anterior retrosplenial cortex (RSC) of the freely moving rat. A total of five male Lister Hooded rats were implanted with bundles of four or eight tetrodes aimed at the anterior RSC. Each tetrode was made of a bundle of four microwires which were mounted onto a small driveable microdrive. Rats were connected to the recording system which allowed for animal position tracking via two mounted infrared LEDs. Rats were then placed onto a raised circular platform, with 0.3cm high perimeter walls, screened for the presence of single-units while performing a pellet chasing task for 16 minutes. Units recorded were quickly analysed for any spatial or head direction firing preference as well as theta-modulation. Units which displayed either location or head direction dependent firing then underwent recording sessions where the environment was changed, see Table 1. Units which displayed no location or head direction dependent firing were not subject to these recording sessions. Units which were theta-modulated or theta-skipping were also not subject to the recordings sessions. However, the screening session for these units were saved for further analysis.

Table 1. Overview of recording sessions rats with units which displayed location or head direction dependent firing in this study underwent.

	Trials undertaken in each session		
	Trial 1	Trial 2	Trial 3
Session 1	Light 1	Dark	Light 2
Session 2	Circle 1	Circle w/walls	Circle 2
Session 3	Small circle 1	Large circle	Small circle 2
Session 4	Circle 1	Square	Circle 2

See chapter 3 methods section (3.2.1) for details of arena and recording duration.

The waveform and firing properties of all units recorded in this study were described. The strength of the correlation between the firing rates of all units in this study with running speed and angular head velocity was also assessed. Head direction units were described using conventional head direction analyses (see methods 3.2.2). The firing properties of all HD units (e.g. preferred firing direction) were statistically compared between each trial in a recording session (see results 3.5.1-3.54). Units which displayed similar location specific firing but no head directionality were grouped together based on visual inspection of their firing rate maps. Firing rate maps were inspected across recordings sessions (Table 1) to visually identify any change or disruption to firing patterns. Location specific firing units were formally tested by statistically comparing mean firing rates (Hz) between each trial for all recording sessions. The waveform and firing characteristics of all units

recorded in this study were described using Neurochat® analysis toolbox created in-house using Matlab®.

Summary of results

Approximately 71% of all units in this study displayed no location or head direction dependent firing. These units were classified based on waveform properties and firing characteristics (e.g. propensity to burst). The firing activity of most of these units were correlated with the running speed and/or angular head velocity. Theta-modulated and theta-skipping units were described in the anterior RSC and accounted for approximately 5% of all units recorded. The firing rates of these units were also found to be correlated with running speed and/or angular head velocity.

Head direction units accounted for approximately 15% of all units recorded in this study. The firing rates for the majority of these units were correlated with angular head velocity and/or running speed. Anterior RSC head direction unit's firing activity was not dependent on location and preferred direction was established upon entry to arena. Head direction units were also found to anticipate future heading direction by approximately 41 ms. Preferred firing direction for head direction units was maintained despite environmental changes, similar to head direction units described in other brain areas.

Approximately 11% of all units recorded in anterior RSC whose activity appeared dependent on the rat's location within the environment, or more specifically, its proximity to the perimeter of the arena. Units which displayed similar location specific firing were grouped together based on visual inspection of their firing rate maps. These groups were: Perimeter units (including partial perimeter units), corona units, gradient units and centre firing units (see section 4.3.1 for definitions). The firing rates of most of these units were found to be correlated with running speed and/or angular head velocity. Perimeter units were active only around the arena perimeter and their firing rates were not disrupted by environmental changes. However, partial perimeter units, became active around the entire arena perimeter when arena walls were present. Corona units, were active throughout the arena but had a higher firing frequency either before or at the arena perimeter. The firing activity of these units were only disrupted by the presence of arena walls. Gradient units were most active in the centre of the arena then their firing rates decreased until near zero at the arena perimeter. The firing pattern of these units were not disrupted by environmental changes. Centre firing units were active throughout the arena but were silent when the rodent stretched its head out over the arena perimeter. The firing activity of centre firing units were strongly correlated with running speed but not angular head velocity, this would explain their firing pattern when arena walls were not present.

Acknowledgements

I would like to thank, my supervisor, Prof. Shane O'Mara for giving me the opportunity to study and work towards a PhD in his lab. I would also like to thank him for his endless enthusiasm and constant encouragement throughout this project.

I am very grateful to past and present lab members of the O'Mara lab for their encouragement and humour throughout the PhD. I am especially grateful to Kim Ronnqvist, M.D. Nurul Islam and Maciej Jankowski for all their help and advice over the years.

I have been fortunate to be blessed with wonderful friends, both in Scotland and Ireland, who have stuck with me for the duration of this PhD. I am especially grateful to Denis Johnstone, Ryan O'Neill and Robbie Sage, for their never-ending encouragement and support.

Most of all, I want to thank my parents Anne Wynne and Joseph Wynne for all their love, support and advice throughout my life. Although you are not here to see this thesis completed, I have always kept your words of advice and encouragement close me, Dad.

Table of Contents

Contents

Table of Contents 1

1. General introduction 5

1.1 The cognitive map and navigation strategies 6

1.2 The neural substrates of the cognitive map and spatial navigation 7

1.2.1 Place cell properties – Basic firing properties 9

1.2.2 Factors which modulate place cell firing 10

1.2.3 Place cells and goal navigation 11

1.2.4 Place cells outside the hippocampus 11

1.2.5 Grid cells 11

1.2.6 Head direction cells 12

1.2.7 Boundary cells 13

1.2.8 The role of the theta rhythm in spatial cognition and memory 14

1.3 The retrosplenial cortex (RSC) 15

1.3.1 Location and Cytoarchitectonic organisation of RSC 17

1.3.2 Connections of the rodent RSC 17

1.3.3 Rostro-caudal connections vary along RSC axis 20

1.3.4 Rostro-caudal efferent connections vary along Rgb axis 20

1.3.5 Rostro-caudal afferent connections vary along Rgb axis 20

1.4 Rodent behaviour and lesion studies of the RSC 20

1.4.1 Summary of rodent behaviour and lesion studies of the RSC 25

1.5 Human neurophysiological studies 26

1.5.1 Summary of human neurophysiological studies 28

1.6 Local field potential (LFP) recordings in RSC 29

1.7 Importance of single-unit recordings 29

1.8 Single-unit recordings in RSC of the freely-moving rat 30

1.81 Summary of single-unit recordings in RSC of freely-moving rat 31

1.9 Aims of the thesis 32

2. Units with No Obvious Spatial Firing Properties and Theta-Modulated Units Recorded in the Anterior Retrosplenial Cortex of the Freely-Moving Rat 34

2.1 Introduction 35

2.2 Methods 37

2.2.1 Animals and surgical implantation of electrodes 37
2.2.2 Recording technique and recordings session 38
2.2.3 Firing analysis 39
2.2.4 Spatial analyses & head direction analyses 39
2.2.5 Interspike interval and bursting unit analysis 41
2.2.6 Unit Classification 41
2.2.7 Autocorrelation histograms: theta index and theta-skipping analyses 42
2.2.8 Running speed and, angular head velocity correlation with spike rate. 43
2.2.9 Statistical analysis 44
2.3 Histology 45
2.4 Results 46
2.4.1 Units which displayed no obvious spatial or theta-modulation 46
2.4.2 Formal statistical comparison between unit classes. 47
2.4.3 Non-spatially modulated and non-theta-modulated units whose firing rates where correlated with running speed. 52
2.4.4. The effects of angular head velocity on spike rate of non-spatially modulated and, non-theta-modulated units 53
2.4.5 Units whose firing rates were correlated with angular head velocity for either clockwise only or counter-clockwise only head turns 53
2.4.6 Units whose firing rates were correlated with angular head velocity for both clockwise and counter-clockwise head turns 54
2.5 Units which displayed no obvious spatial firing properties but demonstrated theta frequency modulation 56
Descriptive parameters shown are represented as mean ± standard error of the mean, units as indicated. 59
2.5.1 Formal statistical comparison between unit class and theta index report 59
2.5.2 Theta-modulated and theta-skipping units were positively or negatively correlated with running speed 59
2.5.3 Theta-modulated and theta-skipping units whose firing rates were positively or negatively correlated with angular head velocity for either clockwise only or, counter-clockwise only head turns 61
2.6 Discussion 64
3. Head Direction Units Recorded in the Anterior Retrosplenial Cortex of the Freely-Moving Rat 69
3.1 Introduction 70
3.2 Methods 74
3.2.1 Recording sessions 74

3.2.2 HD analysis 75
3.2.3 Calculation of the separation angle 75
3.2.4 Calculation of the anticipatory time interval 76
3.3 Results 78
3.3.1 Baseline properties of head direction units in the anterior RSC in the freely-moving rat..... 78
3.3.2 Separation angle (clockwise versus counter-clockwise head turns) is present. 83
3.3.3 Anticipatory properties of anterior RSC head direction units 84
3.4.1 RSC HD unit's firing rates were positively and negatively correlated with running speed 85
3.4.2 HD units whose firing rates were correlated with angular head velocity for clockwise only or counter-clockwise only head turns 88
3.4.3 HD Units whose firing rates were correlated with angular head velocity for both clockwise and counter-clockwise head turns. 89
3.5.1 Firing and directional properties of head direction units in anterior RSC in light and dark conditions. 90
3.5.2 Firing and directional properties of head direction units in anterior RSC in the open-field arena without perimeter walls and with perimeter walls. 92
3.5.3 Firing and directional properties of head direction units in anterior RSC in a varying size but same shape open-field arena. 93
3.5.4 Firing and directional properties of head direction units in anterior RSC in different shaped open-field arena. 94
3.6 Discussion 96
4. Perimeter, Corona, Centre-Firing and Gradient (Boundary sensitive) Units Recorded in the Anterior Retrosplenial Cortex of the Freely-Moving Rat 100
4.1 Introduction 101
4.2 Methods and statistics 104
4.3 Results 105
4.3.1 Definitions of Perimeter, Corona, gradient and centre-firing units. 105
4.3.2 Formal statistical comparison of firing properties between unit classes 105
4.3.3 Boundary sensitive units whose firing rates were correlated with running speed 112
4.3.4 Boundary sensitive units whose firing rates were correlated with angular head velocity for either clockwise only or counter-clockwise only head turns 113
4.3.4 Boundary sensitive units whose firing rates were correlated with angular head velocity for both clockwise and counter-clockwise head turns 114
4.4.1 Firing activity of perimeter units during environmental changes 115
4.4.2 Firing activity of gradient units during environmental changes 121
4.4.3 Firing activity of corona units during environmental changes 126

4.4.4 Firing activity of centre firing units during environmental changes 131
4.5 Discussion 136
5. General discussion 141
6. Conclusion 148
7. References 150
8. Appendix – Conformation of ethical approval for experimentation 167

1. General introduction

1.1 The cognitive map and navigation strategies

The theory that the environment, that one is located in, is represented in the brain was first introduced by Tolman (1948). Tolman placed rats in a cross shaped maze and allowed the rat to explore the entire maze. Once familiar with the maze, the rodent was placed into one arm of the maze and the arm to the immediate right was baited with a food reward. This exact procedure was repeated so the rat was conditioned to turn right to gain a food reward. However, when the rodent was placed into different arms of the maze but the food reward remained in the same location, the rat did not automatically turn right to look for the food reward but navigated to the correct arm where the reward was located. Tolman hypothesised that navigation is guided by internal cognitive maps, these maps flexibly represent the overall spatial relationships between landmarks and environment (i.e. allocentric navigation). In 1971, O'Keefe and Dostrovsky discovered neurons in the rat CA1 hippocampus which were only active when the rat was in a certain location (i.e. place field) and when the rat moved out of the cell's place field the cell became silent (see Figure 1A & B for examples of typical CA1 place cell firing activity). The place fields of many place cells are thought to map the entire environment so the rodent's position within the environment is always known (Muller, 1996; O'Keefe & Nadel, 1978). Place cells active in one environment were also found to be active in other environments but the location of firing fields differed between environments (Muller, 1987; Muller et al., 1991). This finding suggests that a unique cognitive map is generated for each environment. Therefore place cells were proposed to provide the rat with a dynamic, continuously updated allocentric representation of the rodent's own location within its environment.

A common behavioural paradigm used to assess spatial navigation and memory is the Morris water maze (MWM) (Morris, 1981). The MWM is a large circular pool with a platform which is hidden just below the surface of the water. The walls of the room where the MWM is located usually contain large pictures or cue cards. The task requires the rat to be placed into the MWM and the rat swims until it finds the platform then the trial ends. Upon re-entry to the MWM the time taken to find the platform is much shorter, this time decreases upon further re-entry until the rodent swims straight to the safety platform. A rodent familiar with the location of the platform will swim quickly to it because it has remembered the location of the platform in relation to external cues. Removal of the hippocampus from rodents (Morris *et al.*, 1982) severely impaired the rodent's ability to navigate to the hidden platform, even after many successive trials with the platform in the same location. These findings suggest the hippocampus is indeed the location of the cognitive map which is important for allocentric navigation as proposed by O'Keefe and Nadel (1978).

Mammals can also navigate in familiar environments using egocentric navigation. Here the rodent uses itself as its own point of reference so all external cue points are encoded and processed in relation to the rodent's own body axis. Egocentric navigation relies on self-generated movement cues such as the vestibular system for head orientation and the kinaesthetic systems (Burgess *et al.*, 2004; Moghaddam & Bures, 1996). In the absence of visual cues the rodent can learn the location of the platform for the MWM task, from a constant starting position, using self-generated motion cues. For example, the rat can learn that if it has its back to the wall then the platform is 60 degrees to the left and 80 cm distant (Moghaddam & Bures, 1996). Self-generated cues used for egocentric navigation are also used for a specific type of navigation in an unfamiliar environment with no cues present (e.g. in the dark) called path integration. Mittelstaedt & Mittelstaedt (1980) used the strong drive of the mother to retrieve a pup displaced from the nest to demonstrate rodents use path integration. During dark conditions, a pup was moved from the starting location (nest) to a location within the adjacent arena. The mother left the nest to find the pup, after some time searching, the mother found the pup. Despite a complex outgoing path, involving many turns, the mother with the pup returned directly to the nest. To test the importance of the vestibular system for this type of navigation the experiment was repeated and when the mother left the nest to retrieve the pup the arena was rotated slowly, to not activate the vestibular system. This resulted in a return trajectory error of the same magnitude of the arena rotation. On the outbound journey from the nest the speed, distance and head movements are thought to be used to generate and ongoing vector representation of the journey. The summing up of outbound vectors are thought to be used to calculate the direct homing vector back to the nest (Etienne *et al.*, 1998; McNaughton *et al.*, 2006; Mittelstaedt & Mittelstaedt, 1980).

1.2 The neural substrates of the cognitive map and spatial navigation

In order to survive and procreate mammals must leave their home location and seek food, water and a mate. To navigate between home and known location, e.g. a food source, the mammal must first have knowledge of where it is located within the environment, secondly it must also have a sense of heading direction. If one does not have a heading direction then the success rate of navigating from home to a food source is minimal. Place cells within the hippocampus are thought to form a cognitive map of the environment and provide the mammal with information as to where it is currently located in the environment (see Figure 1A & B for examples of typical place cell firing). However, place cells do not provide the mammal with a sense of heading direction which is crucial for route planning. In the postsubiculum of the rat neurons were discovered which were only active when the rodent faced in a certain direction (Ranck, 1984).

These neurons were called head direction cells, fired independently of the animal's location, but were active as long as the head was orientated in the preferred firing direction for that HD cell, usually over a 90 degree range (Taube, 1990 a; Taube, 1990 b), see Figure 1E & F for examples of typical head direction cell firing activity. A third type of spatially correlated neuron was discovered in the medial entorhinal cortex (mEC) of the rodent, called the grid cell (see Figure 1C & D for firing activity of two typical grid cells). Grid cells were observed to be active throughout the environment with a periodic triangular array firing pattern, like a grid, that covered the whole environment (Hafting *et al.*, 2005). The constant grid like firing pattern, lead researchers to suggest, grid cells may be part of a metric system for measuring distance and rodent's path over time (Hafting *et al.*, 2005; Jeffery & Burgess, 2006). The entorhinal cortex (EC) receives direct projections from the postsubiculum and the EC projects via the perforrant pathway to the hippocampus (Vago & Kesner, 2008). The EC receives feedback from the hippocampus via the subiculum (Taube, 2007). Therefore, due the anatomical connections to brain regions containing spatially correlated neurons, the EC is likely to participate in the process of integrating both direction and locational information.

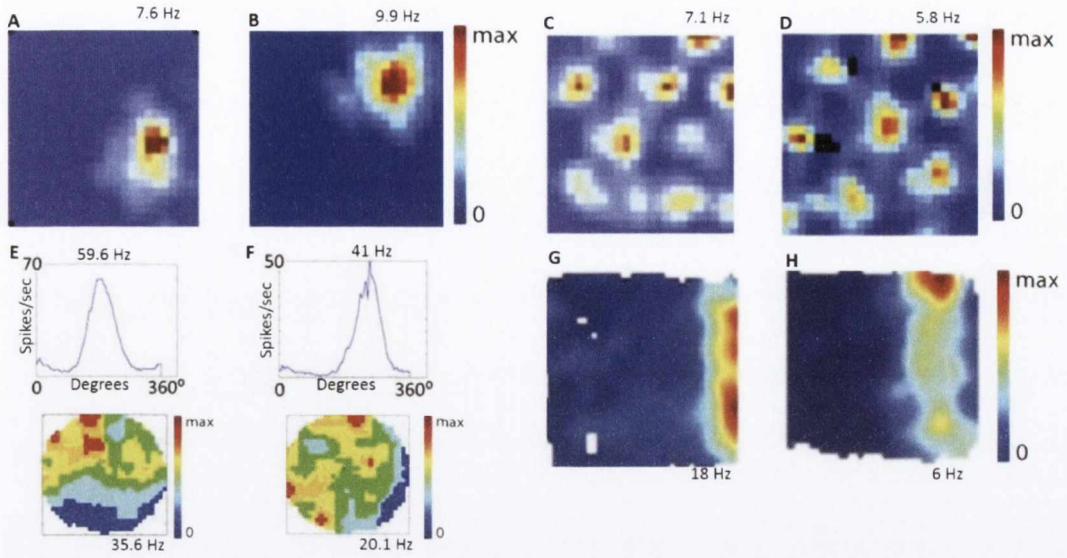


Figure 1. Examples of firing rates maps of spatially-tuned cells recorded in the rodent brain whilst the rat was foraging for food (A-H). The red areas on the map indicate the cells highest firing frequency whilst blue indicates no firing activity, maximum firing rate for each cell is indicated either above or below the firing rate map. A & B) firing rate maps of two place cells recorded in the CA1 of the rodent hippocampus (adapted from Koenig *et al.*, 2011). C & D) Two grid cells recorded in the mEC (adapted from Solstad *et al.*, 2008). E & F) top, tuning curve for two different head direction cells recorded in rostral thalamus, peak firing frequency for preferred direction top (adapted from Jankowski *et al.*, 2015). G and H) firing rate maps for two different border cells recorded in the mEC (adapted from Koenig *et al.*, 2011).

1.2.1 Place cell properties – Basic firing properties

O'Keefe and Dostrovsky (1971) discovered place cells in the rodent hippocampus and found the rodent's location rather than other variables such a running speed or direction was the determining factor for activity. The firing frequency of place cells is also found to be correlated with theta firing frequency (4-12 Hz) (Huxter *et al.*, 2003; O'Keefe & Recce, 1993). Subsequently the firing properties of place cells have been studied extensively, most commonly in the rodent but place cells have been found in the bat (Yartsev & Ulanovsky, 2013) primate (O'Mara, 1995) and human (Ekstrom *et al.*, 2003) hippocampus. In the rodent hippocampus place cells have been recorded in CA3 and CA1 (O'Keefe, 1979), granule cells with place like properties have also been found in the rodent dentate gyrus (Neunuebel & Knierim, 2012). Place fields created and established quickly upon entry into a novel environment (Frank et al., 2004; Hill, 1978). Firing location can be maintained for long periods of time, place cells were found to be stable for up to

153 days (Thompson & Best, 1990). In a small open-field arena place cells have one place field but in larger arena they can have two or more place fields (Fenton, 2008). Place field locations are not topographically arranged within the hippocampal pyramidal layer, therefore, two place fields of place cells recorded close together could have overlapping place fields or place fields far apart (Redish *et al.*, 2001). The location in an environment where a place cell is active may change if the environment is changed (e.g. recording in a circle arena then a square arena) (Muller *et al.*, 1991). A place cell can also be active in one arena and then be silent in another arena (Muller, 1987). The probability of a place cell being active in one arena (e.g. a circle) then being active in another arena (e.g. a square) is around 0.4 (Guzowski *et al.*, 1999; Muller *et al.*, 1987).

1.2.2 Factors which modulate place cell firing

The firing activity of place cells recorded in the open-field do not display any correlation with heading direction. However, if the place cell is recorded in a radial-arm maze, where directionality is enforced onto the navigating rodent, the firing activity of the cell will demonstrate direction dependence (Muller *et al.*, 1994). A place cell's firing field is orientated to distal visual cues (e.g. extra-maze cue card). If the extra-maze cue is rotated, when the rat is not present, then the place field of the place cell will also rotate from its original position by the same magnitude of the cue card (Muller *et al.*, 1987). If the distal cue card is rotated by a small degree (<45 degrees) when the rat is present, the place field will also rotate by the same magnitude. However, if there is a large rotation of the distal cue card (>180 degrees), in the presence of the rodent, the place field will not rotate (Rotenberg & Muller, 1997). Objects (e.g. bottles) placed at the arena perimeter can also serve as cues for place cells. When bottles at the arena perimeter were rotated place fields also rotate by the same magnitude of the rotation. When the bottles were moved to the centre of the arena and rotated they demonstrated a less modulatory effect on place fields (Cressant *et al.*, 1997). If extra-maze cue cards are removed from the arena then place field of that place cell remains, distinguishing their firing activity from visual system neurons (Muller et al., 1987; O'Keefe & Speakman, 1987). Place cells are present in the hippocampus of blind rats (Save *et al.*, 1998) and in normal rats, place fields persist in the dark (Save *et al.*, 2000). This information strongly suggests that self-generated movement cues contribute to generate and maintain place fields. However, if a place cell is recorded during light conditions then the arena is cleaned, thus removing odour cues (e.g. urine or dander), when re-recorded in light conditions some place fields were not stable (Save *et al.*, 2000). When the same experiment was repeated and the place cell was recorded after the arena was cleaned with no lights, half of place cells were not active (Save *et al.*, 2000). This study suggests that odour is an

important cue for place cell stability and may compensate for lack of visual cues. The firing properties of most place cells in the mouse CA1, performing a virtual reality task, were found to be modulated by both visual cues and self-generated movement cues (Chen *et al.*, 2013).

1.2.3 Place cells and goal navigation

An efficient navigational system must be able to represent a place of significance. O'Keefe and Nadel (1978) suggested in their model that place cells do not code for goals or hedonic aspects of spatial navigation. Later, it was demonstrated that goal location change did not alter the place fields of place cells in the hippocampus (Speakman and O'Keefe, 1990). Also, in support of this theory, place cell's firing field remain stable even when the rat chases food reward pellets in the open-field arena (Muller *et al.*, 1987). However, Hok *et al.* (2007) trained rats to wait in a discrete location within an arena (i.e. goal zone), if the rodent did this then a food reward pellet would be dropped into the arena. Hok *et al.* (2007) observed that although place fields were active in discrete locations, separate to the goal zone, when the rodent waited in the goal zone place cells also demonstrated some firing activity there. The authors propose that place cells not only provide a geometric representation of the current environment but also reflect that the rat is located correctly at the goal location or a place of significance. Hok *et al.* (2007) suggest that hippocampal place cells are part of a complex neural network, along with frontal areas which also contain goal related cells (Hok et al., 2005), which allows the rat to plan accurate trajectories in space.

1.2.4 Place cells outside the hippocampus

Place cells have been recorded throughout the hippocampus proper (Barnes *et al.*, 1990). Place cells have also been recorded in ventral portions of the mEC (Quirk *et al.*, 1992). Place fields of Place cells in ventral mEC had a smaller signal to noise ratio compared to CA1 place cells. Ventral mEC place cells firing activity were similar to those of CA1 place cells because their firing activity was due only to the location of the animal and not to variations of the rat's behaviour. Ventral mEC place cells firing location also rotated when a distal cue cards were rotated, like CA1 place cells. However, when the shape of the arena changed from circle to a square arena ventral mEC place cells did not remap, like CA1 place cells, but the place field appeared to stretch. Quirk *et al.* (1992) suggested that ventral mEC place cells were more dependent on sensory input than CA1 place cells, but mEC place cells were less sensitive to changes in the environment.

1.2.5 Grid cells

Anatomical studies demonstrated that the hippocampus receives a principle neocortical projection from the ventral mEC (Van Strien et al., 2009). Single-unit recordings in the ventral

mEC revealed the existence of cells whose firing activity was location specific, called grid cells (Hafting *et al.*, 2005; Jeffery & Burgess, 2006). Grid cells fired in multiple locations throughout the environment in a repeating regular lattice of equilateral triangles (Hafting *et al.*, 2005). Grid cell firing activity like a place cells was found to correlate with theta frequency (Koenig *et al.*, 2011). Grid cells firing activity was found not to depend on head direction but only location (Hafting *et al.*, 2005). Later, single-unit recordings in dorsal mEC revealed grid cells whose firing activity was modulated by the rat's head direction and running speed (Sargolini *et al.*, 2006). In familiar environments grid cell firing remains stable, that is the distance and angle between peak firing areas remain constant (Hafting *et al.*, 2005). Initial studies suggested that the activity of grid cells were independent of the environment and their firing activity was only dependent only self-generated movement cues such as vestibular and proprioceptive input (Etienne & Jeffery, 2004; Jeffery & Burgess, 2006; Jeffery, 2007). To support this theory the firing activity of grid cells also remains constant when the rodent navigates in dark conditions (Hafting *et al.*, 2005). The the grid like firing pattern of grid cells have been suggested to provide a metric for calculating distance travelled which is important for navigation, particularly path integration (Hafting *et al.*, 2005). Grid cell activity is considered by some to be crucial determinate for place cell firing location (Fuhs *et al.*, 2006; Solstad *et al.*, 2006) but other researchers suggest grid cells only contribute to place cell firing location only under certain circumstances (e.g. dark conditions) (Poucet *et al.*, 2014). Interestingly, grid cells have also been reported in the post and para subiculum (Boccara *et al.*, 2010).

1.2.6 Head direction cells

Head direction (HD) cells were first discovered in the rodent postsubiculum by Ranck (1984) but later their general firing properties were described in detail by Taube (1990 a,b). Taube (1990 a,b) found that HD cells fire only when the rat's head is orientated in specific direction, usually over a 90 degree range. HD cell firing activity was found to not depend on the location of the animal. HD cell firing activity was also correlated with speed of head movement, termed angular head velocity (Taube, 1995). The firing activity of some head direction cells were also found to correlate with the running speed the rodent (Taube, 1995). The preferred firing direction of a HD cell is controlled by different types of allothetic cues. Rotation of an extramaze cue card results in the preferred firing direction of the HD cell rotating by the same magnitude (Taube *et al.*, 1990b; Taube, 1995). Removal of an extramaze cue card does not abolish the HD cell's preferred firing direction. Furthermore, HD cell firing activity persists during recordings in dark conditions, but the preferred firing direction may drift over time (Goodridge *et al.*, 1998). However, 80 ms after switching lights on the HD cell automatically returns to its original preferred firing direction

(Zugaro *et al.*, 2003). This information suggests that idiothetic, self-generated motion cues are able to maintain HD cell firing properties in the absence of visual cues but visual cues are important for maintaining directional accuracy. Non-visual, landmark cues were also found to be capable of controlling a HD cell's preferred firing direction (Goodridge *et al.*, 1998). Goodridge et al. (1998) found that rotation of a scented cotton bud 90 degrees resulted in the HD cell preferred firing direction rotating by the same magnitude. When well-known visual cues are placed in conflict with idiothetic cues, the preferred firing direction of the HD cell was aligned approximately with the visual cue (Blair and Sharp, 1996; Zugaro *et al.*, 2000). However, it was also apparent that the HD cell's preferred firing direction was not as accurately aligned with the visual cue when idiothetic cues were not in conflict (Blair and Sharp, 1996; Zugaro *et al.*, 2000). This suggests that during light conditions idiothetic cues still exert some control over HD cell firing activity. HD cells have been found in many different structures throughout the rodent brain (see Taube, 2007 for list of brain regions with HD cells).

1.2.7 Boundary cells

Boundary cells are most active at arena boundaries, for instance, this could be at one wall of a square arena (Lever *et al.*, 2009; Solstad *et al.*, 2008), see Figure 1G & H for examples of border cells recorded in mEC. Some border cells can fire around the entire boundary of the arena (Jankowski *et al.*, 2015; Jankowski & O'Mara, 2015). Boundary cells which were active at one boundary (e.g. one side of a square arena) were described in the subiculum and the mEC (Lever *et al.*, 2009; Solstad *et al.*, 2008). The firing activity of boundary cells in the subiculum and mEC were dependent on the type of environmental boundary. Subiculum boundary cells were active along the boundary of one side of the arena when arena walls were present. When this cell was recorded on a raised platform, with no arena walls, the cell displayed no specific firing activity but instead fired throughout the arena (Lever *et al.*, 2009). In a similar experiment mEC boundary cells were active along the edge of a specific arena boundary when walls were present. When the same cell was recorded on a raised platform with no walls, the location where the cell was active changed. The unit would either be active at another boundary or fire throughout the arena, displaying no boundary selectivity (Solstad *et al.*, 2008). Boundary cells in both subiculum and mEC are considered by some researchers to be an important determinant of place cell firing location (Barry *et al.*, 2006; Bush *et al.*, 2014). This theory arose from experimental observations where place cell firing locations tend to maintain a fixed distance from one or more boundaries following changes to the geometry of a familiar environment (Barry et al., 2006; O'Keefe & Burgess, 1996). Boundary cells active around the entire arena perimeter have be recorded in the

rodent claustrum, nucleus reuniens and rostral thalamus (Jankowski *et al.*, 2015; Jankowski & O'Mara, 2015).

1.2.8 The role of the theta rhythm in spatial cognition and memory

The first invasive electrophysiological studies used large electrodes (200 - 400μm) to measure a local field potential (LFP), typically in the rat brain. A LFP reflects the activity of a large number of cells, likely including excitatory and inhibitory synaptic potentials; dendritic and glial slow potentials, as well as, action potentials in disparate cells types (Andersen *et al.*, 2006). LFP recordings in the rat hippocampus revealed a dominant frequency in the range of 6-12 Hz, termed theta (Vanderwolf, 1969; Whishaw & Vanderwolf, 1973). Vanderwolf (1969), found that the theta-wave increased in spectral power when the rodent voluntarily moved, this was referred to as movement theta (Kramis *et al.*, 1975). Another less well described theta has been reported, in the hippocampus termed attention theta; it is observed to increase in spectral power just before animal moves and is associated with attention (Kramis *et al.*, 1975). Although the precise function the theta-wave is unknown it has been proposed to act as a global synchronising mechanism (Bullock *et al.*, 1990; Mitchell and Ranck, 1980). This is important, as described in the previous sections, there are many different brain areas processing different aspects of spatial information and which must be conveyed to the spatial cognition and memory network. In order to navigate correctly, these brain areas must function in one global processing mode, it is thought the theta-wave facilitates this. In support of this theory, during navigation the theta-wave in other brain areas which contain spatially tuned cells becomes phase locked to the hippocampal theta-wave (Andersen *et al.*, 2006). Single-unit studies have also demonstrated the presence of theta-modulated units amongst place cells in the hippocampus. These unit fire in the theta frequency and often display the same firing correlates as the underlying theta-wave and are often fire in phase with it (Ranck, 1973). Therefore, brain areas which contain theta-modulated units are likely to be part of the spatial cognition and memory network.

Frontal theta or also known as delta frequency modulation has been described in the prefrontal cortex, here the wave oscillates at 4 Hz (Fujisawa and Buzaki, 2011). The prefrontal cortex, amongst other things, is associated with working memory, this is memory which is useful to solve a task during a trial but is not needed when the trial finishes (Fujisawa and Buzaki, 2011; Vann *et al.*, 2009). When a rodent uses working memory there is an increase in the power of the 4Hz signal in prefrontal cortex. For example, a study of working memory, using an alternating t-maze, trained rats to turn left or right upon presentation of a specific odour to receive a food reward. Before the trial started rats were prompted with the odour to turn either left or right, at this point there was an increase in the power of the 4 Hz firing frequency in prefrontal cortex. The

power of the 4 Hz firing frequency returned to baseline once the animal made the correct turn, this suggests that the presence of a 4 Hz firing frequency reflects the use of working memory (Fujisawa and Buzaki, 2011). Furthermore, it was demonstrated that the pre-frontal 4 Hz firing frequency was phase locked to the theta-wave present in the hippocampus. This suggests that both prefrontal and hippocampal areas function together in order to complete this spatial cognition test. Interestingly, there are single-units which fire at both the 4 Hz and 8 Hz firing frequency called theta-skipping cells. These units are present in the nucleus reuiniens (Jankowski *et al.*, 2014) and the medial entorhinal cortex (Brandon *et al.*, 2013) both these structures are reciprocally connected to frontal areas and hippocampal areas (Eleore *et al.*, 2011; Witter et al., 1989). The presence of these units in a brain area suggest that it is important for spatial cognition as it could facilitate the communication of working memory, in frontal areas, and spatial memory, in hippocampal areas, ensuring correct navigation.

1.3 The retrosplenial cortex (RSC)

There are many different brain areas involved in spatial navigation such as hippocampal formation, subicular areas, and cortical areas such as the RSC. The RSC is one of the largest brain structures of the rodent brain spanning, rostral to caudal, approximately 8.5mm. Rodents with RSC lesions demonstrate similar impairments to rodents with hippocampal lesions during spatial navigation tasks (Harker & Whishaw, 2004; St-Laurent *et al.*, 2009; Sutherland *et al.*, 1988; Vann & Aggleton, 2002; Whishaw et al., 2001). Furthermore, The RSC is reciprocally connected with brain structures essential for spatial navigation, such as CA1 hippocampus, EC, postsubiculum, Anterior thalamic nuclei (ATN), visual areas, motor areas, frontal areas (Sugar *et al.*, 2011; Van Groen & Wyss, 1990; Van Groen & Wyss, 1992; Van Groen & Wyss, 2003; Wyass & Van Groen, 1992). See Figure 2 for representation of the location of the RSC in the rat brain, as well as, other brain areas important for spatial cognition and memory.

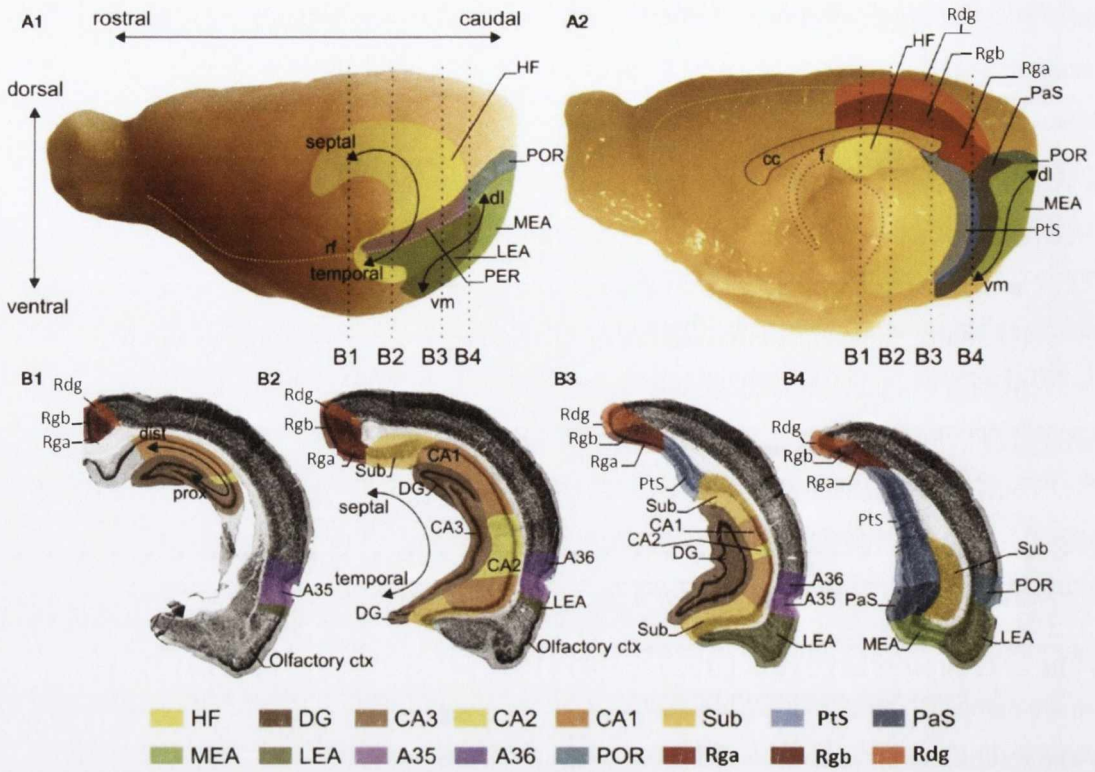


Figure 2. Representations of the retrosplenial cortex (RSC), hippocampal formation (HF) and parahippocampal formation (PHR) in the rat brain (Figure and text adapted from Sugar et al., 2011). Lateral (A1) and midsagittal (A2) views of the rat brain. The RSC is subdivided into Rdg, Rga, and Rgb. For orientation a rostrocaudal and dorsoventral axis is indicated (A1). The HF consists of the dentate gyrus (DG), CA3, CA2, CA1, and the subiculum (Sub). The PHR is subdivided into the postsubiculum (PtS), parasubiculum (PaS), the entorhinal cortex, which has a lateral (LEA) and a medial (MEA) subdivision, the perirhinal cortex (PER; consisting of Brodmann areas (A)35 and A36) and the postrhinal cortex (POR). For orientation in HF the long or septotemporal axis is used [also referred to as the dorsoventral axis; (A1,B2)]. Another commonly used axis is referred to as the proximodistal axis which indicates a position closer to DG or closer to PHR, respectively (B1). The main axis applied in case of PtS and PaS is also the septotemporal axis, in PER and POR a rostrocaudal axis and in the entorhinal cortex is a dorsolateral-to-ventromedial axis [dl and vm; (A1,A2)]. The dashed vertical lines in panels (A1,A2) indicate the levels of four coronal sections (B1–B4), which are shown in (B). The gray stippled line in (A1) represents the position of the rhinal fissure (rf) and in (A2) they represent the global delineation from the dorsal surface of the brain with the midsagittal and occipital surfaces. (B) Four coronal sections of the rat brain; the levels of these sections are indicated in (A). The subfields of the HF, PHR and RSC are color-coded, see colour panel above (B).

1.3.1 Location and Cytoarchitectonic organisation of RSC

In the rodent the RSC is the most caudal subdivision of the cingulate cortex. The rat RSC is sub divided into two distinct regions granular (29) and dysgranular (30) and the granular portion can be further divided into two (Van Groen & Wyss, 1990) or three (Vogt & Peters, 1981) portions depending on the authority. In this thesis I will refer to RSC regions using the same nomenclature as described by Van Groen and Wyss (1990), therefore, dysgranular (Rdg), granular a (Rga) and granular b (Rgb) are the defined regions of the RSC. This is the most appropriate description of this area as the majority of connectivity studies and all studies of selectively lesions in the RSC have used this nomenclature (Vann *et al.*, 2009).

The Rga is the most ventral RSC area and is the thinnest, smallest and least differentiated (Vogt & Peters, 1981). The Rgb region is the larger of the two granular regions and sits superior to the Rga but inferior to the Rdg. The RSC granular portions have 6 distinct layers: I, outer plexiform; II-III, a cell dense region of large stellate and vertical fusiform cells; IV, inner plexiform; V, medium and large pyramidal cells; VI, polymorph (Vogt & Peters, 1981). As described by Vogt and Peter's (1981) The Rdg region when compared with the granular portions have two distinct differences: Firstly, layers II and III which significantly expand in width and have a reduction in cell packing density. Secondly, layer IV has slightly larger and less densely packed neurons.

The RSC is present in both human and the primate and located with brain areas 23 and 31, together forming the posterior cingulate cortex (Kobayashi & Amaral, 2000; Kobayashi & Amaral, 2003). However, in the rat brain areas 23 and 31 have not been described. Despite lacking areas 23 and 31 the rodent RSC has a similar cytoarchitecture and connections to other brain areas as the primate RSC. The human and the primate RSC, like the rat, are is divided into dysgranular (area 30) and granular (29).

1.3.2 Connections of the rodent RSC

An overview of projections to and from RSC areas Rga (Figure 3), Rgb (Figure 4) and Rdg (Figure 5) as well as intrinsic projections within RSC will be presented here. See Sugar *et al.* (2011) interactive connectome for more details of ipsilateral connections between the RSC and the hippocampal formation, parahippocampal formation and, intrinsic RSC connections. For details of ipsilateral and contralateral connections between RSC and sub/cortical brain areas see Van Groen & Wyss, 1990, 1992, 2003 and Wyass & Van Groen, 1992.

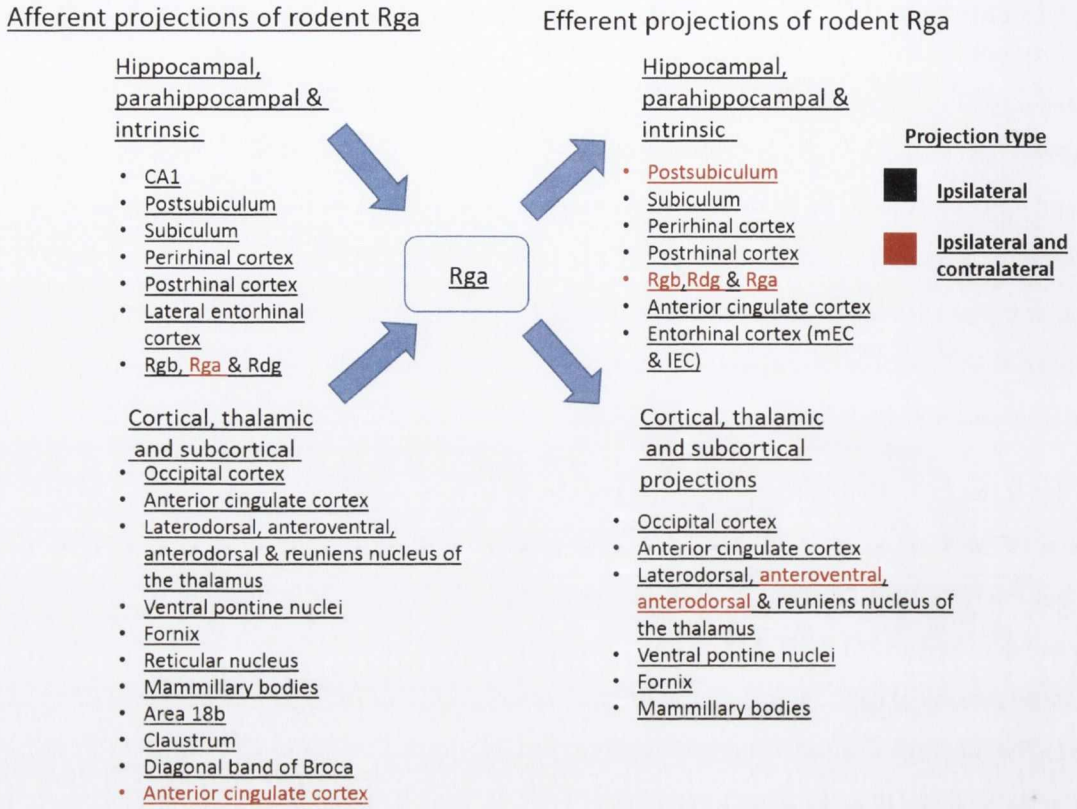


Figure 3. Afferent and efferent connections of the rodent retrosplenial granular a cortex (Rga). Retrosplenial granular b cortex (Rgb) and retrosplenial dysgranular cortex (Rdg). Medial entorhinal cortex (mEC) and lateral entorhinal cortex (lEC).

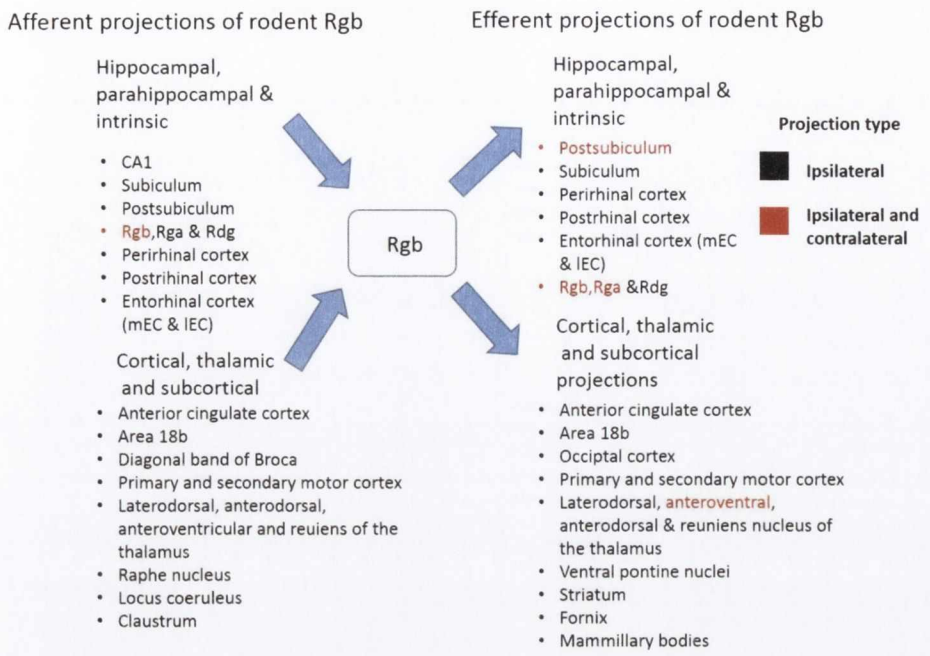


Figure 4. Afferent and efferent connections of the rodent retrosplenial granular b cortex (Rgb). Retrosplenial granular a cortex (Rga) and retrosplenial dysgranular cortex (Rdg). Medial entorhinal cortex (mEC) and lateral entorhinal cortex (lEC).

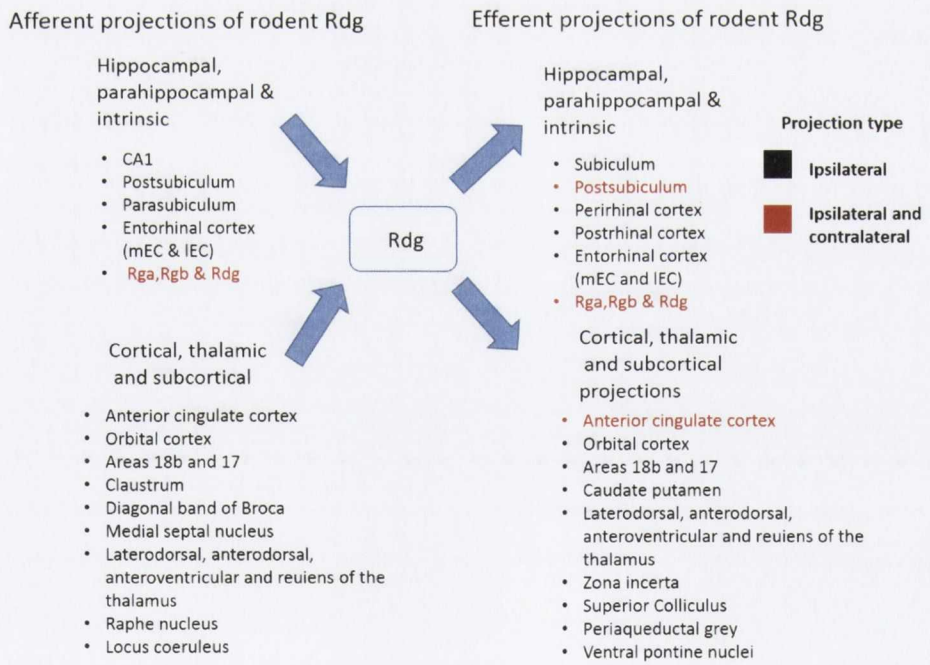


Figure 5. Afferent and efferent connections of the rodent retrosplenial dysgranular cortex (Rgb). Retrosplenial granular a cortex (Rga) and retrosplenial granular b cortex (Rgb). Medial entorhinal cortex (mEC) and lateral entorhinal cortex (lEC).

1.3.3 Rostro-caudal connections vary along RSC axis

The varying density of projections along the rostro-caudal axis from Rga and Rdg to other brain areas will not be described here. For detailed information on the varying afferent and efferent connections along the rostro-caudal axis of Rga and Rdg see Sugar *et al.*, 2011; Van Groen & Wyss, 1990, 1992, 2003 and Wyass & Van Groen, 1992.

1.3.4 Rostro-caudal efferent connections vary along Rgb axis

Anterior Rgb projects to posterior anterior cingulate cortex, whereas posterior Rgb projects to rostral anterior cingulate cortex (Van Groen & Wyss, 2003). Projections from Rgb to postsubiculum are topographically organised along the rostro-caudal axis. Anterior Rgb projects to septal and intermediate postsubiculum, intermediate Rgb projects to intermediate postsubiculum and posterior Rgb projects to the entire septo-temporal extent (Gonzalo-Ruiz & Bayona, 2001; Meibach and Siegel, 1977; Sugar *et al.*, 2011). Projections to mEC and lEC arise only in caudal Rgb (Jones & Witter, 2007; Shibata, 1994). Anterior Rgb projects to rostral postsubiculum and posterior Rgb projects to posterior postsubiculum. Anterior RSC projects predominantly to posterior portions of anteroventral and medial portions of laterodorsal nucleus of the thalamus compared to posterior Rgb (Van Groen & Wyss, 2003).

1.3.5 Rostro-caudal afferent connections vary along Rgb axis

Proximal septal subiculum projects to anterior Rgb whereas intermediate septotemporal and distal subiculum project to posterior Rgb (Miyashita & Rockland, 2007; Vogt & Miller, 1983). Distal area of CA1 projects to anterior Rgb (Van Groen & Wyss, 2003). Anterior Rgb receives more projections from anterior cingulate cortex compared to caudal Rgb (Van Groen & Wyss, 2003). Anterior Rgb receives projections from caudal anterodorsal, ventral portion of anteroventral and medial laterodorsal thalamic nuclei (Van Groen & Wyss, 2003). Posterior Rgb receives projections from rostral anterodorsal, rostral and dorsal anteroventricular and medial laterodorsal thalamic nuclei (Van Groen & Wyss, 2003).

1.4 Rodent behaviour and lesion studies of the RSC

In the advent of discovery of place cells in the hippocampus, it was hypothesised that this brain structure contains a cognitive map of the environment (O'Keefe & Nadel, 1978). The hippocampus receives no direct projections from any sensory areas (e.g. the visual cortex), therefore, other brain regions which receive sensory information, like the RSC, could be involved in processing spatial information and convey this to the hippocampus. Early gene-imaging studies indicated that the entire rostro-caudal axis RSC was active while the rat performed the eight-arm radial maze (see below for more information on this task) as well as the hippocampus (Vann *et al.*, 2000). However, this does not indicate if the RSC is passively relaying sensory information to the HF or if it is has a

specific function. As a result of this finding, further studies were conducted where rodents with RSC lesions were tested in a variety of behavioural tasks to attempt to understand its role in spatial cognition and memory.

It is worthy to note, in early RSC behaviour and lesion studies there was controversy in the literature regarding the lesion extent used to identify the function of the RSC (for details see Vann *et al.*, 2009). Previous RSC studies lesioned anterior portions but inadvertently spared posterior portions of RSC, as a result, there were very little behavioural deficits described during tasks designed to test spatial cognition and memory (e.g water maze and 8-arm radial maze) (Harker & Wishaw, 2004; Vann and Aggleton, 2004). Rats with lesions of the entire rostro-caudal extent of RSC did indeed demonstrate impairment during spatial cognition and spatial memory tasks. Lesion deficits will be described and discussed below for each behavioural task, the inconsistent lesion extent provides insight into the possible differences in anterior and posterior RSC function.

Rats with RSC lesions performance was tested during the Morris water maze (MWM), see section 1.1 for more information on this task; briefly, the rodent swims to a safety platform, hidden under the surface of the water, the rodent has to learn and remember where the hidden safety platform is in relation to extra-maze cues. Spatial memory is tested when the rat is put into the MWM for either the same starting location or different starting locations over a period of a few days or, the position of the platform changes daily and the same procedure is repeated. Rodents with hippocampal lesions are severely impaired in this task as they cannot remember where the platform is in relation to extra-maze cues (Morris *et al.*, 1982). It was hypothesised that because the RSC receives projections from visual areas and projects to the HF it could be important for providing visual information to the HF to solve this task correctly. Rats with RSC lesions of entire RSC were found to be mildly impaired on the fixed and daily changing versions of the MWM, suggesting that the ATN, and other brain areas within the HF could have adapted to compensate for the loss of RSC function (Harker and Wishaw, 2004; Whishaw et al., 2001; Sutherland et al., 2002; Vann and Aggleton, 2002; Vann et al., 2003). No deficit was found in similar experiments where posterior RSC was spared (Vann and Aggleton, 2004), perhaps it is also the case that the remaining RSC adapted to compensate for the loss of the anterior portion's function. It was apparent that further lesion and behaviour work must be undertaken to gain more insight into what role RSC plays within the spatial cognition and memory network.

The MWM is a very specific behavioural test which specifically tests allocentric navigation and hippocampal dependent spatial memory. In the absence of visual cues animals, such as rats, can accurately navigate using other strategies such a path integration, this is the use of self-

generated (idiothetic) movement information to keep track of its position in space and memory of the route taken. As a result, rats have demonstrated the ability to take a direct route back where they started navigating from (i.e. a nest) despite taking a complex outgoing route (e.g. locating a hidden food reward (Cooper *et al.*, 2001) The RSC was hypothesised to be important for this type of navigation as it receives self-generated movement information in the form of motor-efference copy from the motor cortices (Van Groen & Wyss, 1990, 1992, 2003 and Wyass & Van Groen, 1992) and vestibular information, relayed via its projections with the ATN (Dillingham *et al.*, 2015). In order to test this hypothesis Elduayen and Save (2014) assessed the ability of rats to forage for a hidden food reward on a circular platform, with no visual, auditory or olfactory cues and then to return to the starting location. Rats with RSC lesions, once the food reward was found, did not return to the starting location; rats without RSC lesions could find the food reward and return home accurately. This suggests that RSC is important for processing self-generated movement cues to enable accurate path integration.

The importance of RSC for path integration was expanded further by Cooper *et al.* (2001). Here, rats were trained in the open field arena, in a room with many visual cues, to retrieve a food reward always placed in the same location then return to the starting location. The experiment was then repeated in dark conditions with the rat placed into the arena from different starting locations. The rodent retrieved the food reward but returned to the learned starting location (learned during light trials) and not the novel location of entry for the dark trial. If the rat was simply relying on a path integration strategy then it would have returned to the novel starting location and not the learned location. This suggests that the rats utilised mnemonic representation of the familiar arena to return to the learned starting location. Rats with RSC lesions could perform this task in light but in darkness, once the pellet was located, did not return to the learned or the novel location. This suggests that rats with RSC lesions could not path integrate correctly and could not utilise the mnemonic representation of the environment to return to the starting location. The findings of this study suggest that RSC is important for correct path integration and also for providing a mnemonic representation of the environment to increase navigational accuracy, in the absence of visual cues, in a familiar environment.

The radial eight-arm maze is behavioural test which requires rats to use both working memory (i.e. remember which arms the rat has visited) associated with frontal brain areas and spatial memory (i.e. use extra-maze cues to locate and orientate itself in maze) associated with the HF. The maze has a central area which has eight doors, which are all open and the rat picks one to move through to receive a food reward, the rat then returns to the central area and all doors are closed. After a

short delay, all doors are open the rat must visit another arm, which it has not previously visited to collect a food reward; this process is repeated until all arms have been visited. Damage to both frontal areas (Yoon *et al.*, 2008) and hippocampal areas (Wincour, 1982) dramatically increase the incorrect choices made by the rat. Anatomically, the RSC is reciprocally connected with both frontal brain areas and structures within the HF (Van Groen & Wyss, 1990, 1992, 2003 and Wyass & Van Groen, 1992), this prompted researchers to test if rats with RSC lesions were impaired during this task; results would suggest what RSC role was within the spatial cognition and memory network. Rats with lesions of only anterior portions of RSC were not impaired, whereas rats with entire RSC lesions were mildly impaired (Vann and Aggleton 2004). The results of this study suggest that RSC is important for integrating prefrontal working memory and HF spatial memory. The mild deficit observed suggests that other brain areas could compensate for the loss of RSC function. For instance, the nucleus reuniens of the thalamus (Eleore *et al.*, 2011) and the claustrum (Atlan *et al*, 2016) are both reciprocally connected with prefrontal areas and the HF, when RSC is damaged these brain areas could compensate for its loss of function.

The role of the RSC for solving the 8-arm radial maze was further explored when the rat made four correct choices and returned to the central choice area, the maze was rotated 45 degrees and the trial continued. By rotating the maze 45 degrees extra-maze cues e.g. cue cards were now placed in conflict with intra-maze cues (e.g. urine or dander). In these trials the rats with RSC lesions were severely impaired and incorrectly re-visited several arms but non-lesioned rats were not impaired (Vann *et al.*, 2003). In order to solve the 8-arm radial maze task the rat can use an allocentric spatial strategy (e.g. use extra-maze cues) or it can use egocentric strategies (e.g. use urine, dander and self-motion cues). It appears that non-lesioned rats were able to integrate both strategies and when cues were placed in conflict the rat could was able to pick the most reliable strategy to correctly solve the task. Whereas, RSC lesioned rats were not be able to integrate both navigational strategies and when they were placed in conflict the rat was unable to resolve the conflict. Similarly, deficits have also been described when the rat performs the first four choices in light conditions then lights are turned off for the last four choices, an increased incorrect arm choices is found (Cooper and Mizumori, 1999). Anatomically, the RSC receives projections from visual areas and areas which project self-generated, idiothetic information (e.g. vestibular and motor-efference). These findings suggest a function of the RSC is to integrate external sensory information with internally generated sensory information to ensure correct navigation is maintained in the absence of one (e.g. maintain correct navigation when move from light to dark conditions).

Furthermore, rats with RSC lesions were tested in the alternating t-maze experiment. This experiment, like the radial arm maze, tests both working memory and spatial memory. Rats are placed in maze shaped like a T, they start off in the stem of the maze and are given a forced choice to turn either left or right, at the top of the stem, to receive a food reward. The rat is then placed in the start position again and has to remember to turn in the opposite direction at the choice area to receive a food reward. The delay between choices can be altered to examine working memory, intra-maze cues and extra-maze cues can be altered to test navigational strategies. Rats with the entire RSC lesions were mildly impaired while performing the alternating t-maze task in standard conditions (Nelson *et al.*, 2015). However, significant impairment was observed when, after making the first choice, the maze was rotated 90 degrees (similarly procedure for 8-arm radial maze described previously) so that intra-maze cues were in conflict with extra-maze cues. Impairment was also demonstrated when the rat performed the forced choice in the dark in one maze and placed, in the dark, to make the choice decision in an adjacent t-maze (Nelson *et al.*, 2015). During this trial the rat could not depend on intra-maze cues to solve the task, but instead only rely on a path integration strategy. Rats with RSC lesions were also impaired when they were forced to use only an extramaze visual cue as a point of reference to provide to alternate around (Nelson *et al.*, 2015; Pothuizen et al., 2008). Here the rat, in light conditions, performed the first part of the task (i.e. the forced choice) then it was transferred to an adjacent t-maze, which was rotated 90 degrees to make the choice. The rat couldn't rely on idiothetic cues but only on a distal visual cue to derive a heading direction to alternate. Finally, the biggest deficit occurred when the RSC was temporarily lesioned, in this case severe impairments were observed when the rat performed the task in the light with access to intra and extra-maze cues (Nelson *et al.*, 2015). These findings, with the 8-arm radial maze studies, suggest that the RSC functions to integrate different spatial navigational strategies (i.e. allocentric and egocentric). The severe impairment observed during temporal RSC lesions suggest that other structures (e.g. ATN or brain areas within the HF compensate for RSC, this would explain the mild effects observed with chronic RSC lesions on standard spatial cognition tasks.

Novel object recognition is a highly validated test for recognition memory, the animal is exposed to two objects and allowed to explore for a set time. If one object is replaced with a novel object then the animal will spend much more time investigating the novel object compared to the old object. Rats with a RSC lesions demonstrate no deficit in this task compared to control animals (Vann & Aggleton, 2002). However, rats with the RSC lesions demonstrate impairment when performing the object-in-place task (Vann & Aggleton, 2002). In the open-field the rat is allowed to explore four unique objects located in the corner of a square arena. After a short break, the rat

is reintroduced but two objects on one side have changed location. The RSC lesion rats spent significantly less time exploring the novel arrangement than control rats. Object-in-place task tests not if the object is novel but tests the context of its position is novel or familiar within the environment. This study suggests that the RSC could work in concert with other brain regions involved with novel object recognition to determine if the environment is familiar or novel. This would presumably be important for determining if a new cognitive map has to be created or an old one retrieved from memory, or if the retrieved map has to be updated to reflect some environmental change.

Indeed, the RSC is not only important for spatial memory but also contextual fear conditioning (Keen and Bucci, 2008). In rodent studies of contextual memory a context is usually defined as the chambers in which conditioning occurs and are composed of various visual, tactile, and olfactory cues (Todd and Bucci, 2015). For instance, rats will display a freezing behaviour when they are returned to a specific context (e.g. white box) where they had previously received a foot shock (Bouton, 2002 & 2004), therefore, contexts can directly elicit conditioned fear responses. Experimental studies have demonstrated that the RSC is particularly important for post-encoding, which includes consolidation, storage and retrieval of previously formed associations between stimuli in the environment (Todd and Bucci, 2015). This has been shown experimentally when rats were trained to associate placement in a training box with a shock, upon re-entry to the training box, rats would immediately freeze. However, rats which received RSC lesions before re-entry to the training box demonstrated a significant lack of freezing response (Keene and Bucci, 2008). Furthermore, RSC is important in the inhibitory avoidance task where the rat has to learn and recall that an aversive stimuli is paired to a specific environment (Bouton and Todd, 2014). In this task, the rat is placed in box with two compartments: one with bright light shone on it and the other dimly lit. Rats tend to move towards the dimly lit section to avoid the bright light, but in this experiment, the rat is foot-shocked upon entry to the dimly lit section. Healthy rats, once having experienced the foot shock in the dimly lit section, upon return to the two compartment box do not return to the dimly lit section for several minutes or not at all (Todd and Bucci, 2015). This suggests that these rats have a memory of receiving a shock in the darkened area. However, RSC lesion rats return to the dark section in a significantly shortened time period, suggesting that these rats cannot recall memory of the foot shock (Shettleworth, 2010). As a result of these studies, it appears that RSC is important for recalling memories for contexts.

1.4.1 Summary of rodent behaviour and lesion studies of the RSC

Rodent behaviour and lesion studies indicate that the RSC is important for correct spatial cognition and memory. The findings of the rodent behaviour and lesion studies indicate that a role of the

RSC is to integrate self-generated motion information with extra-sensory information (e.g. visual information) to ensure accurate navigation if navigational strategies change (i.e. from light to dark). RSC also appears to be important for providing mnemonic representation of a familiar environment to increase accuracy of navigation in dark conditions. The RSC is also important for contextual memory, the ability to recognise familiar environments is important for accurate navigation and future route planning. It is also evident from the severity of spatial deficits observed during temporal lesions of rodent RSC that the ATN and HF and other brain areas may adapt to compensate over time for its loss during spatial cognition tests. The prior controversy in the RSC lesion literature, where lesions of RSC accidently spared the posterior portions, demonstrated that rodents with posterior portions of RSC intact were not impaired during spatial cognition tests. It is most likely that the role of anterior RSC in spatial cognition and behaviour is masked by the adaption and compensation of posterior RSC. Therefore, it would be incorrect to assume that because no deficit was observed during behavioural tasks designed to test spatial cognition and memory that anterior RSC has no function or the same function as posterior RSC. This is further evidenced by the synaptic weight of projections from brain structures important for spatial navigation varying along the anterior-posterior axis of the RSC; furthermore, the anterior RSC receives direct projections from the CA1 of the hippocampus but posterior RSC does not. Due to these anatomical differences it is likely anterior RSC could have a different role in spatial navigation and memory which, due to compensation of spared portions of RSC and other brain areas, has been masked in these studies.

1.5 Human neurophysiological studies

In humans, damage to the RSC is likely to occur following cerebral haemorrhages or tumours of the splenium of the corpus callosum (Maguire, 2001). Like rodents, humans with damaged RSC consistently present with deficits in spatial cognition and memory. Humans with RSC damage, in a familiar environment, can recognise landmarks but cannot derive a directional heading (Ino et al., 2007). This is similar to rodent studies where rats could not use familiar landmarks to provide a sense of direction during the spatial alternation test (Pothuizen *et al.*, 2008). Humans with hippocampal lesions are also unable to navigate around familiar environments, unlike patients with RSC lesions, they still have a sense of direction (Maguire, 2001). Humans with RSC lesions are also impaired in utilising allocentric navigational strategies as subjects cannot place landmarks on a familiar map (i.e. landmarks on familiar route taken by the subject every day to work) (Takahashi et al., 1997) or locate oneself on a map of a familiar environment (Katayama et al., 1999).

However, egocentric representation of space is not impaired with RSC damage, so that the patient can point to objects in a testing room from memory or recall the positions of landmarks which can

be seen from their current position (Miller et al., 2014). For example, a patient with RSC lesions, when presented with map of a familiar city which contained only streets and rail roads the patient could not recall the position of a principle building (i.e. the town hall). However, when the examiner indicated a position on the map and told the patient its name, the subject was able to recall the name and locations of those buildings within sight of the indicated location (Miller et al., 2001; Takahashi et al., 1997, patient 2). This is similar to reports in the rodent RSC lesion literature where rats cannot alternate spatial navigational strategies e.g. when allocentric cues are placed in conflict with intra-maze (egocentric) cues (Vann *et al.*, 2003). Also in concordance with animal RSC lesion data humans with only partial lesions of RSC, where one hemisphere is damaged, are spatially impaired for a short period (approximately 8 weeks). In this period, the healthy portion of RSC increases in and size and is thought to compensate for the functional loss of the damaged portion of RSC (Maguire. 2001).

Spatial memory deficits are not the only cognitive impairment reported after RSC damage, ability to acquire new information verbally or visually and, recent but not remote autobiographical memory recall have all been reported as impaired (Bottini et al., 1990; Maguire, 2001; McDonald et al., 2001). These reports are also similar to those found in rodent RSC lesion studies, where rats were unable to remember that a certain context was associated with a shock (Keene and Bucci, 2008). Also, studies in humans have Highlighted the significance of projections from the ATN and HF, if either of these brain areas are damaged, then atrophy is experienced in RSC (Albasser et al., 2007; Garden et al., 2009; Jenkins et al., 2004). This is demonstrated in Alzheimer's disease, here the hippocampus undergoes severe atrophy leading to deafferentation of projections to RSC resulting in severe RSC atrophy. The resulting atrophy of the hippocampus, RSC and other brain areas are likely to exacerbate the spatial and cognitive decline of these patients (Minoshima et al., 1997).

Functional MRI (fMRI) is a non-invasive method for measuring brain activity in humans (Logothetis, 2008). Neurons in the brain receive oxygen bound to haemoglobin and glucose from arterioles which are essential for neuronal function as the cell cannot make these itself. The magnetic properties of haemoglobin are altered when oxygen is taken up by the neuron, so haemoglobin bound to oxygen has a different magnetic property to that of haemoglobin not bound to oxygen. Areas of the brain which increase in activity during a certain task (e.g. hippocampus during a spatial cognition test) will require more oxygen; such areas, therefore, will have a higher proportion of haemoglobin not bound to oxygen. Using statistical analyses images of the brain are produced providing a map of areas with high and low activity.

fMRI recordings can be undertaken whilst the human performs specific tasks using virtual reality or during sensory stimulation. Studies have demonstrated that RSC increases in activity when subjects were presented with an image of a familiar location and asked to mentally navigate from it to another location compared to passively looking at the image (Morgan *et al.*, 2011). Also, RSC activity increased when subjects were shown the mirror reversal of a familiar picture of some objects compared to when the normal image was shown (Dilks *et al.*, 2011). This finding is similar to the rodent literature where rats with RSC lesions were impaired in the ability to determine if the familiar layout of objects was altered or not (Vann & Aggleton, 2002). fMRI studies have also demonstrated that RSC is involved in determining the permanence of landmarks, this is important to build a long-term spatial representation of an environment (Miller *et al.*, 2014). This was demonstrated when subjects were shown several landmark cues of varying permanency (e.g. passing car or fire hydrant) (Auger et al., 2012; Auger and Maguire, 2013). RSC was found to be most active when viewing landmark cues of high permanency (i.e. fire hydrant). Also, subjects whose RSC was most active when shown cues of high permanency were also found to be the best navigators. RSC fMRI studies have also demonstrated that the RSC is important for development of memory representations (Wolbers and Buchel, 2005). Here, subjects were repeatedly shown first-person point of view snapshots of a virtual maze which contained prominent visual landmarks. Overtime, subjects when shown one cue, could instruct the examiner where another cue was located in relation to it in the maze. Throughout this task, the subjects' accuracy increased at instructing the examiner where one cue was related to another in the maze. Moreover, RSC demonstrated increased activity throughout these trials and activity increased further when subjects indicated where one cue was located with respect to another cue. This suggests that the RSC is important for transforming spatial reference frames (i.e. egocentric to allocentric). This finding is similar to rats with RSC lesions which cannot pick the most reliable navigational cue when egocentric and allocentric cues are in conflict (Vann *et al.*, 2003). It is likely that one of the roles of RSC is to translate egocentric information, received via projections from visual areas, to an allocentric representation which could then be utilised by the hippocampus.

1.5.1 Summary of human neurophysiological studies

Studies of humans with RSC lesions bear a striking resemblance to the spatial cognition and memory deficits observed in rodents with similar lesions. The inability of humans with RSC lesions to derive directional information from familiar cues has also been described in rodent studies. fMRI studies of humans also demonstrate that the RSC is important for recognising the familiarity of the orientation of cues, this is also in concordance with the rodent RSC lesion literature. Human RSC also appears to be important for providing information of the permanence

of spatial cues, this has not been described before in rodent studies. After partial RSC lesion, remaining healthy RSC tissue increases in size over a period of around 8 weeks, and at this point spatial cognition and memory deficits subside. Therefore, it is likely that the remaining healthy RSC tissue adapts to compensate for the loss of the damaged RSC. This is a similar finding to that reported in rodent RSC literature where partial RSC lesions did not affect spatial cognition and memory but complete lesions did. Despite the obvious importance of the RSC for spatial cognition and memory and clear difference of projections from important brain regions along its anterior-posterior axis, to date, there are no human studies which have examined the functional differences of anterior and posterior RSC.

1.6 Local field potential (LFP) recordings in RSC

Like the hippocampus, RSC also shows a clear theta-wave oscillation during LFP recordings (Borst *et al.*, 1987; Talk *et al.*, 2004). The underlying theta-wave in hippocampus is thought to play a critical role organizing the spike timing of many neurons to enable neural plasticity (Brandon *et al.*, 2013; Skaggs et al., 1996); it is also thought to be important for providing a mechanism for coordinating the spiking activity of neurons in hippocampus with neurons on other brain areas (Jones and Wilson, 2005; Sirota *et al.*, 2008). The theta-wave in RSC, like the hippocampal theta-wave, increases in spectral power during locomotion. Also, during locomotion hippocampal and RSC theta-waves are phased locked (Leung and Borst, 1987; Young and McNaughton 2009). RSC and hippocampal theta both decrease in spectral power simultaneously as the rat enters a new environment (Young and McNaughton 2009), this suggests that RSC supports the hippocampal areas with forming spatial representations.

1.7 Importance of single-unit recordings

fMRI is an important non-invasive tool to examine brain activity. However, one caveat of human fMRI studies is imaging resolution: the typical resolution of any given brain area, called a voxel, is approximately 55 mm^3 (55 µl) (Logothetis, 2008). Within this voxel there are approximately 5.5 million neurons, this resolution enables the experimenter to appreciate that a specific brain area is involved in a spatial task (Logothetis, 2008). Similarly, LFP recordings in small rodents sample the membrane activity of many neurons within a local area and therefore provide an overall view of a brain areas activity. In order to gain a fuller understanding of a brain areas function, one must measure the activity of single neurons in response to a stimuli. For example, in the CA1 of the hippocampus, neighbouring pyramidal cells share the property of representing place in the environment. However, different cells become active in different parts of the environment, this property is not revealed in current fMRI studies or LFP recordings. However, implantation of fine recordings electrodes (~ 25 µm diameter, LFP electrodes ~ 200 µm diameter) into a specific brain

region provide the resolution to examine the response of a single neuron to stimuli, thus providing a very detailed picture of that brain regions function. Due to the invasive surgical implant of electrodes required to record single neurons the majority of experiments are conducted in small mammals.

1.8 Single-unit recordings in RSC of the freely-moving rat

Chen *et al.* (1994a) published the first single-unit study in the freely-moving rodent while the rat performed the 8-arm radial maze. The authors reported that, for both Rdg and Rgb layers, 8.5% of all of units recorded were HD units. HD units in Rdg and Rgb maintained preferred firing direction in the dark (i.e. absence of visual cues). Chen et al (1994a) also reported that HD units firing activity was not only correlated with the direction the rodent faced but also with running speed and angular head velocity (i.e. speed of head movement for clockwise or counter-clockwise head turns. The preferred firing direction for some RSC HD units was dependent on extra-maze visual cues as rotation of the visual cue resulted in rotation of the preferred firing direction of the HD cell. However, the majority of HD cell's preferred firing direction were not altered as a result of rotation of extra-maze visual cues (Chen *et al.*, 1994a, Chen *et al.*, 1994b).

Cho and Sharp (2001) recorded single-units from the mid-caudal portion rodent RSC in a large circular arena while the rodent chased small food pellets. Cho and Sharp (2001) found that approximately 10 % of all units recorded in RSC were HD units. They also found that these units anticipated future heading direction by around 25ms. Cho and Sharp (2001), like Chen *et al.* (1994a,b) found that HD units firing activity were also correlated with running speed and, angular head velocity. Furthermore, in this study, units whose firing activity were strongly correlated with place, head direction and movement were described, called direction-dependent place cells. Cho and Sharp (2001) also described units whose firing activities were not correlated with head direction or place but only correlated with rodent's running speed and/or head direction. Lesion of the rodent anterior RSC, where posterior portions were inadvertently left intact, did not impair HD cell firing activity in the anteriordorsal thalamus (ADN) (unpublished observations in Taube, 2007). However, lesions of the entire RSC resulted in a decrease in firing stability for the preferred firing direction of the HD cells in ADN, even in the presence of visual cues (Clark *et al.*, 2010). Temporary inactivation of the rodent RSC results in disruption of location specific place cell firing in the hippocampus (Cooper & Mizumori, 2001).

Cho and Sharp (2001) also reported a population of 30 to 50 % of theta-modulated units in mid-caudal RSC. Theta-modulated unit fire rhythmically in an 8Hz frequency, are often phase-locked to the underling theta-wave (Ranck, 1973) and often display the same firing correlates (e.g.

increased firing rate during locomotion). These findings suggest that the RSC is part of the hippocampal dependent spatial cognition and memory network. Interestingly, despite RSC connectivity with frontal areas, theta-skipping units were not described in mid-caudal RSC. These units exhibit a complex firing frequency which includes both the 8 Hz and 4 Hz firing frequency. The 4Hz firing frequency, termed frontal theta, is present during working memory tasks in frontal areas and is phase locked to hippocampal theta during spatial cognition tasks (Fujisawa and Buzaki, 2011).

Alexander and Nitz (2015) recorded the firing activity of RSC units while the rodent traversed a simple "W" shaped maze. RSC units were observed to be active when the rodent had to make a right turn and other units were only active when the rodent had to make a left turn. Alexander and Nitz (2015) suggested that the presence of these units in RSC which demonstrated turn specific firing are indicative of an egocentric navigational strategy. Other units were reported to fire in a complex, but reliable manner, as the rat traversed maze route. For example, these units demonstrated higher firing activity prior to turns on the "W" maze or higher firing rate when the rat traversed specific sections of the "W" maze (Alexander and Nitz, 2015). Alexander and Nitz (2015) also found that RSC units firing activity also influenced by allocentric cues as the firing activity for RSC units differed depending on the location of the maze. For instance, a unit which was active for left turns, then allocentric cues are altered, would then either be silent or be active for only one of the two left turns on the "W" maze.

1.81 Summary of single-unit recordings in RSC of freely-moving rat

The presence of spatially-tuned units in RSC provide evidence, along with lesion studies in rodents and fMRI studies in humans, that it is an important component of the spatial cognition and memory system. Rodent and human lesion studies indicate that the RSC is important for providing a sense of direction, the presence of HD units in RSC supports this theory. The presence of units whose firing rates are correlated with running speed, angular head velocity, as well as, head direction, are of theoretical importance for path integration (e.g. navigating in the dark). For example, in order to maintain a sense of direction in the dark one would have to know in which direction one's heard was orientated and after a movement which direction it is now orientated in; HD cells whose firing rates are also correlated with angular head velocity would provide this information. Also, the combined activity of units whose firing rates are correlated with running speed and angular head velocity could provide an ongoing vector representation of the rodent's movements. This would enable the rat to sum up a complex outgoing journey (i.e. a series of vectors) and calculate a direct return route back to the starting point (McNaughton *et*

al., 2006). This finding complements rodent RSC lesion studies where the rat could not accurately return to a starting point in the dark.

In order to navigate effectively, self-generated movement information has to be integrated with extra-sensory information (e.g. visual cues). The RSC is the likely location where this function takes place as it receives visual information from areas 17 and 18b, as well as, motor efference copy from the motor cortices and, vestibular information via the ATN. HD units in RSC, whose firing activity is correlated with running speed or angular head velocity also appear to be sensitive to rotation of external cues, that is, if a salient cue is rotated then the preferred firing direction will also rotate by the same magnitude. The importance of RSC for integrating self-generated and extra-sensory signals is highlighted when RSC lesions result in ADN HD units preferred firing direction shifts every few minutes despite visual access to salient visual cues. This lends support to the finding that rats with RSC lesions cannot integrate visual cues and self-motion cues to solve the 8-arm radial maze when conditions change from light to dark.

The presence of theta-modulated units RSC provide further support that this brain area is part of the spatial cognition and memory network. The presence of single-units in RSC which encode left and right turns through a route (i.e. egocentric navigation) whose firing is altered by extra-maze cues (i.e. allocentric navigation) provides further evidence that this brain area is important for switching between different spatial reference frames essential for accurate navigation. This is in concordance with human fMRI studies which demonstrate that RSC is active when egocentric spatial representations (i.e. first person view) are translated into allocentric representations (i.e. map like view).

1.9 Aims of the thesis

Single-unit recordings provide a detailed and precise measurement of an individual neuron's activity in response to stimuli, thus giving great insight into its function and the possible function of that brain area. Importantly, electrodes can be implanted into discrete portions of a brain structures with minimal disturbance of surrounding brain tissue. This permits the study of individual neurons with their surrounding efferent and afferent connections intact. RSC single-unit recordings, thus far, have demonstrated that RSC contains spatially-tuned cells, in concordance with the animal and human behavioural studies. However, these studies have been conducted in the same mid-caudal portion (Alexander and Nitz, 2015; Cho and Sharp, 2001) or, in the case of Chen et al., (1994a and b) did not compare units recorded in anterior and posterior areas, but chose to group them as one sample; possibly due a low sample size. Despite the importance of the RSC for spatial cognition and memory and, obvious anatomical differences of

anterior and posterior regions no single-unit study, thus far, has sought to systematically record single-units in the anterior portion of the RSC. Therefore, a detailed systematic study of the spatial firing properties of single-units in anterior RSC is warranted as it would further our understanding of this structures role in spatial cognition and memory.

Therefore, the purpose of this study is to describe the spatial and non-spatial properties of single-units in the anterior RSC of the freely-moving rat. This study will be undertaken as follows: Chapter two will contain a description of units whose firing rates which are correlated with angular head velocity and, running speed. Units with these firing properties would indicate that anterior RSC functions to facilitate navigation based on self-generated cues (i.e. path integration). The second part of this chapter will describe any theta-modulated or theta-skipping cells in anterior RSC. The presence of these units provides further evidence that it is involved in the spatial cognition and working memory network. The purpose of the third chapter is to firstly report the population of HD units present, their waveform and firing characteristics, as well as, their firing rate correlations with running speed and angular head velocity. The second part of this chapter will include a description of the firing properties of HD units in response to environmental manipulations. Manipulations include arena size, shape, boundary type and dark conditions. The response of HD units to these environmental manipulations will give further insight into their function and allow for comparisons with HD units recorded in posterior RSC and other brain regions. Anterior RSC receives direct projections from CA1 of the hippocampus which contains place cells, as well as, the subiculum which contains border cells. The presence of cells with place like firing properties or border firing activity would strongly indicate that the anterior RSC has a different role within the spatial cognition and memory network than posterior portions; any unit which demonstrates place or border like firing will undergo recordings during the same environmental manipulations as HD units. Overall, the findings of this study will provide, for the first time, a detailed description of the spatial and non-spatial properties of single-units in anterior RSC which will contribute and expand our understanding of RSC role in spatial cognition and memory.

2. Units with No Obvious Spatial Firing Properties and Theta-Modulated Units Recorded in the Anterior Retrosplenial Cortex of the Freely-Moving Rat

2.1 Introduction

The RSC is thought to be important for spatial navigation because rodent behavioural studies have demonstrated that a damaged RSC due to lesions cause impairment in spatial navigation tasks (Cooper & Mizumori, 1999; Cooper *et al.*, 2001; Harker & Wishaw, 2004; Vann & Aggleton, 2002; Vann *et al.*, 2003). Anatomical connection studies of the RSC also implicate it as important for spatial navigation and memory, it has many reciprocal connections (strong and weak) with the hippocampal formation, ATN and other cortical areas (Van Groen & Wyss, 1990; Van Groen & Wyss, 1992; Van Groen & Wyss, 2003; Wyass & Van Groen, 1992). Electrophysiological studies have demonstrated the RSC contains single-units whose firing activity are dependent on heading direction, and place (Alexander & Nitz, 2015; Chen *et al.*, 1994a; Chen *et al.*, 1994b Cho & Sharp, 2001). Single-units which demonstrate spatial firing properties are likely to be large pyramidal neurons (O'Keefe & Dostrovsky, 1971; O'Keefe, 1976)

RSC, like other cortical brain areas, contains not only pyramidal cells but other neuronal subtypes such as stellate and fusiform cells (Vogt & Peters, 1981). While previous single-unit studies have described firing and waveform properties of large pyramidal cells (i.e. cells which are spatially-tuned) in rodent RSC they have not reported the firing and waveform properties of other neuronal subtypes present (e.g. stellate and fusiform cells). However, the waveform and firing properties of these neuronal subtypes have been described, using single-unit recordings in the freely-moving rat, in nearby mPFC (Baeg *et al.*, 2001; Jung *et al.*, 1998). Therefore, cells recorded in anterior RSC, which are not spatially-tuned (e.g. place cells or HD cells), should be classified based on the same firing and waveform parameters used to describe non-pyramidal cells in nearby, mPFC (see methods section 2.2.6 for definitions). The parameters used to describe non-pyramidal cells in mPFC are suitable to use in this study, like RSC, mPFC is a 6-layered cortical structure. Also, the recording site in mPFC was 0.2mm anterior to the most rostral portion of the RSC where recordings in this study were done. It is likely that in previous single-unit studies in RSC that non-pyramidal cells have been ignored because they may demonstrate no obvious spatial firing properties. However, these units' firing rates may convey running speed and angular head velocity which have important theoretical implications for navigation. Therefore, the correlation of these cells' firing rates with angular head velocity and running speed will be examined in this study.

In the absence of visual cues animals successfully navigate using self-motion cues (e.g. vestibular and motor efference copy), called egocentric navigation (Rancz *et al.*, 2015; Shinder & Taube, 2010). Path integration is a specific form of egocentric navigation, the animal sums up the vectors of distance and direction travelled from an outgoing journey and uses this information to

plot a direct return trajectory home (Etienne *et al.*, 1998; Etienne & Jeffery; 2004; McNaughton *et al.*, 2006; Mittelstaedt & Mittlestaedt, 1980). This type of navigation is particularly important in the absence of visual cues e.g. dark or in an unfamiliar environment with few visual cues. Path integration was demonstrated in the rodent using the strong will of a mother to retrieve a pup displaced from the nest to a location within an adjacent arena during dark conditions (Mittelstaedt & Mittlestaedt, 1980). The mother left the nest and despite searching throughout the arena for some time, it located the pup and returned to the nest in a direct trajectory. In order to test the importance of the vestibular system for this type of navigation, when the mother left to find the pup the arena was rotated below vestibular activation. This resulted in the mother not returning to the nest but to a position which was equal to the rotation of the arena relative to the nest (Mittelstaedt & Mittlestaedt, 1980). A brain area which contains units whose firing activities are correlated with running speed and angular head velocity, likely providing an ongoing vector representation of an outgoing journey, suggest it is important for path integration (Etienne *et al.*, 1998)

In order for animals to successfully navigate through an environment many different brain regions are required to work together in synchrony. The mechanism which coordinates this synchrony is likely to be the underlying theta frequency (4-10Hz) oscillations observed during freely-moving rodent electroencephalogram (EEG) recordings (Hasselmo, 2005). Single-unit recordings in the hippocampus found individual cells whose firing activity demonstrated strong phase correlation to the underlying EEG theta wave, they were termed theta-modulated units (O'Keefe & Dostrovsky, 1971; Ranck, 1973). Theta-modulated units recorded in the hippocampus, have demonstrated some of the same behavioural correlates of the underlying EEG theta wave (Colom & Bland, 1987). Single-unit recordings also revealed another type of theta cell, in the entorhinal cortex (Brandon *et al.*, 2011; Brandon *et al.*, 2013) and nucleus reunions of the thalamus (Jankowski *et al.*, 2014), named the theta-skipping unit. The underlying mechanism driving these cells to skip is not fully understood or what their function could be. Some researchers have hypothesised it may provide a pace-maker like function for synchronising some early components of the head direction system (Jankowski *et al.*, 2014).

Despite being one of the largest brain structures in the rodent brain and lesion studies implicating it in spatial memory and navigation. There have been remarkably few single-unit studies in the RSC of the freely moving rat. Furthermore, studies have consistently aimed their recording tetrodes at the same mid-caudal area of RSC (Alexander & Nitz, 2015; Cho and Sharp, 2001) or recorded in behavioural apparatus which imposes head direction and restricts

movement (Chen *et al.*, 1994a; Chen *et al.*, 1994b). The synaptic weighting of connections along the anterior-posterior gradient of the RSC to and from other brain areas also important for spatial navigation varies (Van Groen & Wyss, 1990; Van Groen & Wyss, 1992; Van Groen & Wyss, 2003; Wyass & Van Groen, 1992). Furthermore, the anterior RSC is the only part of the RSC which receives a projection from CA1 (Van Groen & Wyss, 1992; Wyass & Van Groen, 1992) and has reciprocal projections with the primary motor, M1 and M2 cortices (Vogt & Miller, 1983).

The aims of this chapter are to first, report the firing and waveform properties of non-spatially and non-theta-modulated units in the anterior RSC. This description will complement existing cytoarchitectonic studies, and allow comparison between these units with similar units in nearby structures, this may help to elucidate the function of the anterior RSC. The firing activity of these units will also be correlated with running speed and angular head velocity to observe if there is a relationship. The presence of units whose firing activity is correlated with running speed and angular head velocity in anterior RSC suggests it is important for navigation, especially path integration. The second part of this chapter will describe the firing and waveform properties of theta-modulated and theta-skipping units. The firing rates of these units will also be correlated with running speed and angular head velocity as this may provide information to their function in anterior RSC. All experiments will be conducted in the open-field arena so no directionality or movement restrictions are imposed on the animal which could confound results.

2.2 Methods

2.2.1 Animals and surgical implantation of electrodes

In this study, a total of five male Lister Hooded (Harlan, UK) were used for anterior RSC recording trials (250-300g, age 3-5 months at time of implant). Rats were housed individually, in a temperature (20 -24 °C) controlled laminar airflow unit (Scanbur Technology) and maintained on a 12 hour light and 12 hour dark cycle (0800 – 2000hrs). All recording sessions were carried out between the hours of 0930 and 1730. Rats received 15g of food as standard each day, water *ad libitum* and, 20mg of food pellets (TestDiet, Formula 5TUL, USA) during each trial. Animals were habituated to the housing conditions for two weeks before any procedure or protocol was undertaken. Prior to testing, animals were handled for approximately three to four days to become accustomed to the experimenter. Experiments were carried out in strict accordance with the European Union derivatives on animal experimentation (86/609/EEC), and Cruelty to Animals Act, 1876, and followed Bioresources Ethics Committee, Trinity College Dublin, Ireland, and international guidelines of good practice (see appendix for copy of Animal Research Ethics Committee (AREC) approval)

The recording electrodes consisted of bundles of four (16 channel microdrives) or eight bundles (32 channel microdrives) of four/eight platinum-iridium wires (90% platinum, 10% iridium; Heavy Polymide Enamel (HML)insulated, 25µm bare wire diameter, California Fine Wire LTD., USA) twisted together. The bundles were cut at a small angle of approximately 10° so the tips were separated by a small distance. Tetrodes were threaded through a guide cannula, 25 gauge, and protected by a 21 gauge cover. Tetrodes were then mounted in a small driveable microdrive (Axona Ltd.,UK) and implanted in the anterior RSC (-2.76 mm anterior posterior, ±0.6 mm mediolateral and 1mm dorso-ventral to dura layer of the rodent brain (Paxino & Watson, 2005). Rats were anaesthetised with isoflurane (Abbott Laboratories, UK) via a gas anaesthesia system (Medical Supply Services, UK) and maintained under anaesthesia (average flow rate of 1.0±0.2 litres per minute) during the whole procedure. Rats were placed into a stereotaxic apparatus (Kopf Instruments, USA), the skull was exposed, and a small hole was drilled over the respective electrode implantation site. Six bone screws (one of which served as the ground) were inserted into the exposed skull to anchor the microdrive. The microdrives were placed on the respective implantation hole and the electrodes were lowered to the required depth. The exposed area between the cannula and the surrounding skull was packed with sterile gel (Granugel, Convatec, IRL), and the entire apparatus was cemented to the skull with dental acrylic (Associated Dental, UK). After surgery, the wound area was dusted with antibiotic powder (Cicatrin, Wellcome, IRL), and the rats were kept under observation for several hours. To ensure a full recovery, rats were administered an antibiotic (Baytril, Bayer Healthcare, Germany) and the analgesic (Rimidyl, Pfizer, UK). Electrodes were implanted in the right hemisphere.

2.2.2 Recording technique and recordings session

Once rats had recovered from surgery and could explore the arena sufficiently, subjects were connected, via 16 or 32 channel headstage (Axona Ltd., UK), to a recording system which also allowed for animal position tracking via two mounted infrared LEDs (Axona Ltd., UK). Signals were amplified between 1000 to 3000 times and bandpass-filtered between 380 Hz and 6 kHz for single-unit detection. Spikes were recorded whenever the signal exceeded a predefined user set threshold based on the signal to noise ratio present on the oscilloscope. To minimise noise electrodes were referenced to other channels from other tetrodes of similar background noise with no cell activity. Candidate waveforms were then discriminated off-line using graphical cluster-cutting software Tint® (Axona Ltd., UK), which allows waveform separation based on multiple features. Such features include spike amplitude, spike duration, maximum and minimum voltage and the time of occurrence of maximum and minimum voltages. It was also possible to discriminate waveforms further according to the voltage at a specified time.

Rats were connected to the recording equipment and screened for the presence of single-units. Screening session were conducted in a circle (diameter 77cm, perimeter wall height 0.3cm) raised 32cm from the ground on a stable platform for 16 minutes. Three quarters of the recording arena were surrounded by thick black curtains with a cue card placed on one curtain. The section of the test area where the curtain was not present allowed the experimenter to throw 25mg sucrose pellets (TestDiet, Formula 5TUL, USA) into the arena for the rodent to chase during the recording session. The purpose of this was to encourage the rat to be in constant locomotion and to visit all parts of the arena as equal as possible. If there were no units present then the microdrive was advanced 25 μm, no more than twice per day; with at least a 3 hour interval between advancements. After the screening session rats were transferred back to their home cage. The arena was then cleaned with a 70% alcohol solution.

Units recorded in the screening session were quickly analysed using Tint® to check for any spatial and HD properties as well as any theta-modulation. Firing rate maps, HD polar plots and -1000ms and +1000ms autocorrelation histograms were carefully compared between previous screening sessions to ensure that no units were recorded twice enabling an accurate population description in this study. In this chapter only units which displayed no obvious spatial or HD properties are described, units which are presented in this chapter are described only using data from the 16 minute screening session.

2.2.3 Firing analysis

It should be noted that all analysis of firing characteristics were done with Neurochat® analysis toolbox, created in-house using Matlab® (The MathWorks, Inc, USA). Analysis methods which were used from peer-reviewed publications will be cited where applicable or else novel methods which were developed in-house which were employed will be described.

2.2.4 Spatial analyses & head direction analyses

Spatial analyses methodologies which were used in this study are described in details elsewhere (see Jankowski *et al.*, 2014; Tsanov *et al.*, 2011; Tsanov *et al.*, 2014). Briefly, creating firing rate maps allowed for visual inspection of units preferred areas of firing (i.e. place fields). They were constructed by normalising the number of spikes which occurred in specific pixel coordinates by the total trial time the animal spent in that coordinate (Cacucci *et al.*, 2004). This produced maps depicting the spatial firing activity of the unit in Hertz (Hz). The firing map reflected the frequency of firing calculated from the top firing bins down to the lowest firing bins, this was done by scaling in decreasing intervals of 20% of peak firing. Average frequency was calculated for each unit as the total number of spikes divided by the total recording time and is expressed in

Hz. The spatial information content (Skaggs) was calculated for selected units and is displayed as bits per spike, for details of the Skaggs calculation see Skaggs *et al.*, 1996.

Details of the directional analyses that were undertaken in this study are also reported elsewhere (see, Jankowski *et al.*, 2014; Tsanov *et al.*, 2011 Tsanov *et al.*, 2014). Briefly, the rat's head direction was calculated for each time the camera sampled the orientation of the relative position of the two LEDs (present on the recording cable above the rats head) onto the horizontal plane. The directional tuning function for each cell was calculated by plotting the firing rate as a function of the rat's directional heading, divided into bins of 6°. The firing rate was computed based on the total time in that bin (Taube *et al.*, 1990a). Data was only accepted if all directional bins were used by the rat this was to restrict the influence of inhomogeneous sampling.

To overcome the problems of sampling bias, we also used the "distributive hypothesis" method (Muller et al., 1994; Cacucci et al., 2004) exactly as described in Tsanov *et al.*, (2011). The distributive hypothesis procedure was applied to quantify the influence of head direction on the spatial firing. The calculation of locational distributive ratio is based on the estimation of directional firing that one would predict under the null hypothesis that the firing of a cell is only modulated by location and that the only influence of head direction arises from the sampling bias discussed above. The predicted rate as a function of direction is as follows:

$$R_{pred}(\theta) = \frac{\sum (R_p T_p(\theta))}{\sum T_p(\theta)}$$

where Rp is the firing rate in one pixel and Tp(θ) is the time spent facing head direction θ in that pixel. Then we tested whether the observed directional tuning for the cell, $R_{obs}(\theta)$, differs from the one calculated under the assumption that the effect of direction is purely artifactual, $R_{pred}(\theta)$. We achieved this by computing a "distributive ratio" (DR) as follows:

$$DR = \frac{\sum \left| \frac{\ln((1+R_{Obs}))}{((1+R_{\mathrm{Pred}}(\theta)} \right|}{N}$$

where N is the number of directional bins considered. For a perfect prediction, DR is zero. A perfect prediction indicates that the null hypothesis is true, namely, place cell firing is only modulated by location and the directional influence on place cell firing is only attributable to the

inhomogeneity of sampling referred to above, whereas high values of this ratio would indicate a poor prediction (indicating that head direction accounts for some of the variability in the firing rate of the cell). This value is then represented on each head direction cell's polar plot as the green line, this represents the distribution of time heading in different directions across all time bins of the trial, whereas the black line represents the distribution of head directions for time bins when a spike was recorded from the cell.

2.2.5 Interspike interval and bursting unit analysis

Interspike interval histograms (ISIHs) show the temporal relationship between spikes fired by the same unit. The x-axis shows the range of different times between each spike of that unit. The y-axis shows the number of times the time difference between each spike occurred.

A burst was defined as a series of spikes in which each inter-spike interval (ISI) was <5 ms. Bursts, therefore consisted of a minimum of two spikes. A propensity to burst index was calculated (Anderson & O'Mara, 2003) to calculate the likelihood of a unit to fire in bursting mode, with the 0 value indicating the cell never bursts and 1 indicating the unit fires constantly in bursting mode.

2.2.6 Unit Classification

The mPFC firing and waveform classifications were chosen to describe non-pyramidal cells because mPFC and RSC are both structures in the cortex, and the recording location was nearby (0.2 mm anterior) to where tetrodes were aimed to target anterior RSC (Baeg *et al.*, 2001; Jung *et al.*, 1998). Therefore, the following working definitions for each unit class are as follows:

Regular spiking units were defined as units where mean firing frequency were greater than 2Hz but less than 12Hz, usually a large spread on the ISIHs with no clearly marked peaks and, no apparent theta-modulation on its ±1000ms autocorrelation, see Figure 9 for an example

Fast spiking units – low propensity to burst units were defined as units which had an average firing frequency greater than 12Hz, propensity to burst less than 0.1 and no apparent theta-modulation on visible upon inspection of its ±1000ms autocorrelation.

Fast spiking units – High propensity to burst units were defined as units which had a 12Hz or greater average firing rate, propensity to burst of 0.1 or greater and no theta-modulation upon inspection of its ±1000ms autocorrelation, see Figure 8 for example.

Unspecified low firing units were defined as units which had an average firing frequency of less than 2Hz which had no apparent spatial or theta-modulation.

2.2.7 Autocorrelation histograms: theta index and theta-skipping analyses

Autocorrelation histograms of the ISI distribution were first calculated for ISI lags of -10 ms and +10 ms between spikes with 1 ms width bins to make sure each unit had a clear refractory period (no count before 2ms). This is indicative of good unit isolation, any unit with activity within the first 2ms period was discarded. Autocorrelation histograms were also calculated for an ISI lag of -1000ms and +1000ms with 1ms wide bins. These histograms are useful to identify any rhythmic properties the unit may have, of particular interest is activity in the theta range (4-12Hz). A sine wave of decaying amplitude was then fitted to the +/- 1000 ms autocorrelation histograms of theta-modulated units to calculate the theta index, see equation below:

$$\left[a\left(\sin\left(\frac{\pi}{2}-\omega t\right)\right)+b\right].e^{\frac{-|t|}{\tau_1}}+ce^{\frac{-t^2}{\tau_2}}$$

t refers to time and *a,b,c*, τ1,τ2 and ω are fit parameters. The fit parameters are estimated using the least squares fitting method. The theta index is defined as the ratio of the fitted parameters *a/b*, where *a* is amplitude of the oscillation and *b* is the offset of the oscillation (Royer et al., 2010; Tsanov et al., 2011). Theta index value can be thought of as a measurement of how reliably the cell fires within the theta frequency band, a 0 measurement indicates that the cell does not fire in the theta frequency, whereas an index measurement of 1 indicates that the cell fires consistently and only in the theta frequency band.

The autocorrelation histogram for some theta-modulated units appeared to have alternating cycles of large peaks and small peaks, termed theta-skipping cells. A non-normalised autocorrelation signal was fitted to the equation below, this is an extended form of the equation used by Brandon *et al.*, 2013), developed by Jankowski *et al.*, 2014 and used here, from this equation the theta-skipping index (equation 4, Brandon et al., 2013) was calculated.

$$y(x)=[a_1\cos(\omega_1 x)+a_2\cos(\omega_2 x)]\times\exp\left(-\frac{|x|}{\tau_1}\right)+b+c_1\exp\left(-\frac{|x|}{\tau_2}\right)-c_2\exp\left(-\frac{|x|}{\tau_3}\right)$$

Here, *y* is the autocorrelation signal, *x* is the lag, a1 and a2 are the amplitude of the oscillating terms with frequency ω1 and ω2 modulated by exponential with decay constant τ1.The terms τ2 and τ3 are the decay constants for the exponentials with amplitude *c*1 and *c*2. The parameters *a*1, *a*2, *b*, *c*1 and *c*2 were allowed to vary in the range [0, N], where N is the peak of the autocorrelation signal. The range of decay constants are, τ1 = [0, 5000], τ2 = [0, 100], τ3 = [0, 10] in milisecond unit. ω1 and ω2 were varied in the range [12π, 24π] and [6π, 12π], respectively.

Assuming spikes were generated following a Poisson process, the ISI was considered to follow an exponential distribution, which also gives an exponential distribution in its autocorrelation, represented in the above equation by the positive exponential component comprised of ($c1$, $\tau2$). The initial dip in the autocorrelation for the refractory period in the ISI was given by the fast-decaying negative exponential ($c2$, $\tau3$). The alternating low and high peaks are modelled as the superposition of two oscillations, given by two slow decaying cosine functions, as if the high peaks are generated when the oscillations are in the same-phase and the low peaks are generated when they are in anti-phase. The baseline shifts for the cosine terms and all the constant errors are interpreted in constant b. The above equation does not hold the prior assumption that one of the periodic functions oscillates exactly at half-frequency of the other, as others have assumed (*Brandon et al., 2013*). The curve fitting followed the measurement of 'jump factor', defined as the relative contribution of the low frequency components in the higher peaks given by $a2/(a1 + a2)$. Frequency ratios of the cosine functions were also measured to verify the superposition model of the above equation, theta cycle skipping index, TS was measured by Equation 4; *Brandon et al., 2013*.

As described (*Brandon et al., 2013*), TS range should be [−1 to +1]. A positive TS is present if the second peak after the centre peak is larger than the first one; a negative TS is not expected according to the model in the above equation if it is fitted for the theta-skipping cycle cell with an alternative low and high peaks and low peaks appearing first after the centre peak. The greater the TS, the greater the larger peak is jumped from the theta-modulated signal, caused by the interference of the second oscillation. We measured this effect with an alternative index 'jump factor' defined as $a2/(a1+ a2)$, which provides a direct measurement of the relative contribution of the two oscillations. A jump factor >0.5 means the contribution of the slow varying interfering oscillation in the jump is greater than the theta-range oscillation. If the frequency ratio follows a 2:1 ratio (or closer), then the mathematical basis of using two cosine functions of different frequency ranges to obtain consecutive in-phase or anti-phase superposition to yield lower and higher peaks respectively, is verified.

2.2.8 Running speed and, angular head velocity correlation with spike rate.

Raw speed data was smoothed using a moving average filter with rectangular window of duration 100ms (five samples). The histogram count of the speeds generated from the recording session, and hence the number of times the rat moved with certain speed, were measured using 1ms bins up to 40ms/sec (max speed analysed). For each position data sample, number of spikes corresponding to the speed at that time were counted. The spike rate was finally calculated by

dividing the total number of spikes belonging to each running speed bin by total time the rat maintained that speed. Speed bins at which rats did not travel for at least 1sec were then excluded. The remaining raw data were fitted to a linear regression equation. The quality of the linear fit were assessed using the Pearson's correlation coefficient between the raw spike rate vs fitted rate.

To calculate the angular head velocity, head direction was first smoothed using a moving circular mean filter over 100ms rectangular window. The angular velocity at time t(i) was then calculated as the slope of the linear regression line passing through head direction at t(i-2) to t(i+2) time samples after adjustment of circular zero-crossing (Bassett & Taube, 2001). The negative and positive angular head velocities were taken as the clockwise (CW) and counter-clockwise (CCW) angular velocities respectively. For each of these groups, the spike rate was calculated using the similar approach as that used for running speed. The bin size and the maximum angular velocity were set as 10 deg/sec and 500 deg/sec respectively. Bins with trailing zeros at higher angular velocities and those not visited for at least one second were removed. Both the CW and CCW spike rates were separately fitted to a linear equation, and the quality of the fit were assessed using the Pearson's correlation coefficient between the fitted spike rate and the raw rate.

The value at which significance was detected for the Pearson's test ($p<0.01$) was chosen to reduce the chance of a type I statistical error. From inspection of the Pearson's correlation results, in this study, for angular head velocity and running speed it was found that significance was not detected for a correlation value (r) below 0.4. Units whose firing rates demonstrated a significant correlation with angular head velocity and running speed were divided into arbitrary groups based on their Pearson's r value; these groups were 0.4 to 0.6, 0.61 to 0.8 and 0.81 to 1.

2.2.9 Statistical analysis

All data were first tested for normality using the D'Agostino and Pearson omnibus normality test (GraphPad Prism®, USA). As a results it was found that the majority of the data in this study were not normally distributed. An un-paired non-parametric test was used to compare waveform or firing characteristics between unit classes. Specific tests used will be noted in results as appropriate, GraphPad Prism®, USA was used to make all statistical comparisons. Comparison was considered significantly different if $p<0.01$. The correct descriptive statistics for non-parametric data is median and inter-quartile range but for the sake of simplicity and comparison with other studies mean and standard error of the mean will be used in this chapter of results.

2.3 Histology

Recording sessions ended when the depth of 2.4mm was reached by the tetrodes, or the rat lost the headstage due to infection or age, or the ground wire was irreparably damaged. The brains of the rats which were sacrificed were collected for electrode position verification. Brains were stored in a 4% PFA solution (Sigma, UK) until they were shipped to the Histology & Microscopy, Institute of Medical Sciences, University of Aberdeen. In short, brains were embedded in paraffin, and the target region was microtome sliced into 20 µm sections. Thereafter, brain sections were stained with a standard haematoxylin and eosin staining protocol to allow cellular differentiation. Blue haematoxylin stains the cell nucleus whereas the eosinophilic counter-stain labels the cytoplasm in a pinkish colour. Tetrode tracks were verified by visual inspection of the experimenter under a standard microscope (Leica, GER) fitted with a 5x and a 20x lens (Leica, GER). Figure 6 is an example of a coronal brain slice (2.8 mm posterior to Bregma) from a rat in this study (right), the arrow with the dashed line represents the path of the electrodes. The accompanying schematic Figure (left) is the representative coronal section from Paxinos and Watson (2005).

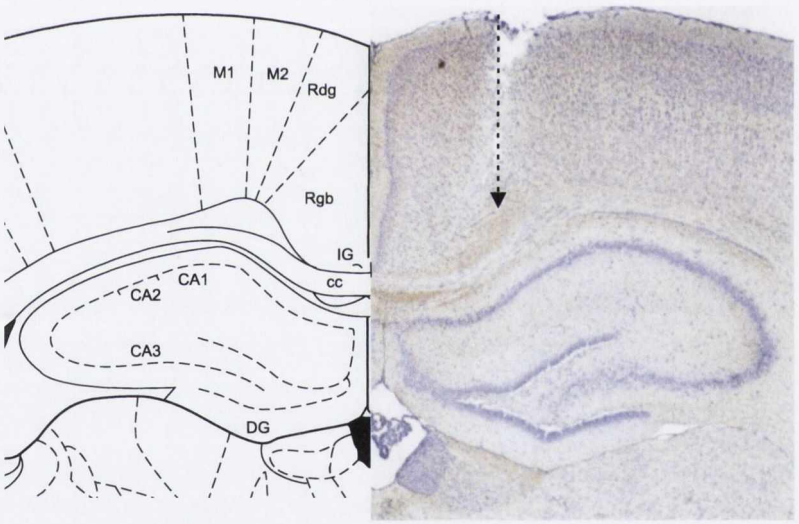


Figure 6. Schematic diagram of electrode implant site (left), adapted from Paxinos and Watson (2005). Representative histological specimen showing electrode track which is highlighted by dashed line. Tetrodes were implanted 2.8 mm to Bregman, 0.6 mm lateral to the midline; approximately 1 mm ventral to the surface of the brain. M1 Primary motor cortex; M2 Secondary motor cortex; Rdg Retrosplenial cortex dysgranular; Rgb Retrosplenial granular b area, Indusium griseum; cc Corpus callosum; CA1 field CA1 of hippocampus; CA2 field CA2 of hippocampus; field CA3 of hippocampus and DG Dentate gyrus.

2.4 Results

2.4.1 Units which displayed no obvious spatial or theta-modulation

There were 812 cells recorded from the anterior RSC from five different rats in this study. Of that, a total 584 cells had no spatial firing properties or were theta-modulated. Due to time limitations and a large data set, a sample population of 241 cells, from two rats, out of 584 cells were analysed for descriptive purposes. Based on their electrophysiological and firing characteristics, four broad categories of cells were defined: unspecified low firing units, regular spiking units, fast spiking units with low propensity to burst, fast spiking units with a high propensity to burst (table 2a and b). Cell classes from each one of these groups were further described based on how their spike rate correlated with running speed and/or angular head velocity. There were no discrete bursting unit class in this study, with a bursting cell usually defined as having a clear peak before 5ms on its ISIH. Most fast spiking cells which appeared with counts before 5ms also had many counts after 5ms this resulted in an ISIH plot with a broad peak outside of 5ms, therefore it is likely that these cells could switch from bursting mode to fast firing (Figure 7). Burst propensity was therefore used as an index to measure the proportion of spikes for each unit which fell within the bursting definition of ISI less than 5ms, a burst propensity greater than 0.1 was used as a threshold to indicate a high likelihood of bursting for fast spiking units.

Table 2a. Waveform and firing properties of units with no obvious spatial or frequency modulation

	Number of units in sample and (%)	Mean spike amplitude (μv)	Mean spike width (μs)
Regular spiking units	86 (36%)	122.5±4.00	132.3± 1.56
Fast spiking units, low propensity to burst	25(10%)	181.2±22.64	128.90±3.70
Fast spiking units, high propensity to burst	11 (5%)	170.4±23.04	122.2±3.0
Unspecified low firing units	119 (49%)	124.1±3.2	137.5±1.56

Values for each descriptive parameter represented using mean ± standard error of the mean.

Table 2b. Waveform and firing properties of units with no obvious spatial or frequency modulation continued

	Mean firing (Hz)	Propensity to burst (%)	Spatial information content, Skaggs (bits per spike)
Regular spiking units	4.60±0.25	0.03±0.002	0.58±0.21
Fast spiking units, low propensity to burst	22.94±2.32	0.05±0.001	0.21±0.03
Fast spiking units, high propensity to burst	34.04±4.4	0.11±0.001	0.12±0.03
Unspecified low firing units	1.01±0.05	0.01±0.002	NA*

Values for each descriptive parameter represented using mean ± standard error of the mean.

*Skaggs value for unspecified low firing units is omitted due to low spike rate confounding the result of the Skaggs calculation.

2.4.2 Formal statistical comparison between unit classes.

Kruskal-Wallis test with Dunn's multiple comparison were conducted to test for any significant differences in waveform or firing characteristics between unit classes.

The amplitude of all unit classes were compared and statistical significant differences were present ($x^2(3)=22.31, p<0.01$). Dunn's post hoc test revealed significant differences between regular spiking units and fast spiking, low propensity to burst as well as fast spiking high propensity to burst. Statistical significance was also detected between unspecified low firing units and fast spiking, low propensity to burst as well as fast spiking, high propensity to burst. No significant difference was detected between unspecified low firing units and regular spiking units and, fast spiking low propensity to burst when compared to fast spiking high propensity to burst. Comparison between the spike width of each unit class also revealed significant difference existed ($x^2(3)=23.19, p<0.01$). Dunn's post hoc test revealed that a significant difference was detected between unspecified low firing and fast spiking low propensity to burst units as well as unspecified low firing units and fast spiking high propensity to burst, no other statistical significant differences were detected.

The mean firing rate from all unit classes were also compared and significance was detected ($x^2(3)=198.2, p<0.01$). Dunn's post-hoc test revealed that mean firing rate was significantly to each group when compared except between fast spiking low propensity to burst and fast spiking high propensity to burst. Burst propensity was found to be significantly different between all unit

classes ($x^2(3)=93.38, p<0.01$) except between regular spiking and fast spiking, low propensity to burst as well as between fast spiking, low propensity to burst and fast spiking, high propensity to burst. Spatial information content (Skaggs) was compared between each unit class, except low firing unspecified units due to Skaggs calculation requiring an adequate sample size of spikes, and significant difference were detected ($x^2(3)=63.45, p<0.01$). Dunn's post hoc revealed regular spiking units were significantly different to both fast spiking and, low propensity to burst. However, no significant difference was detected between fast spiking, low propensity to burst and fast spiking, high propensity to burst.

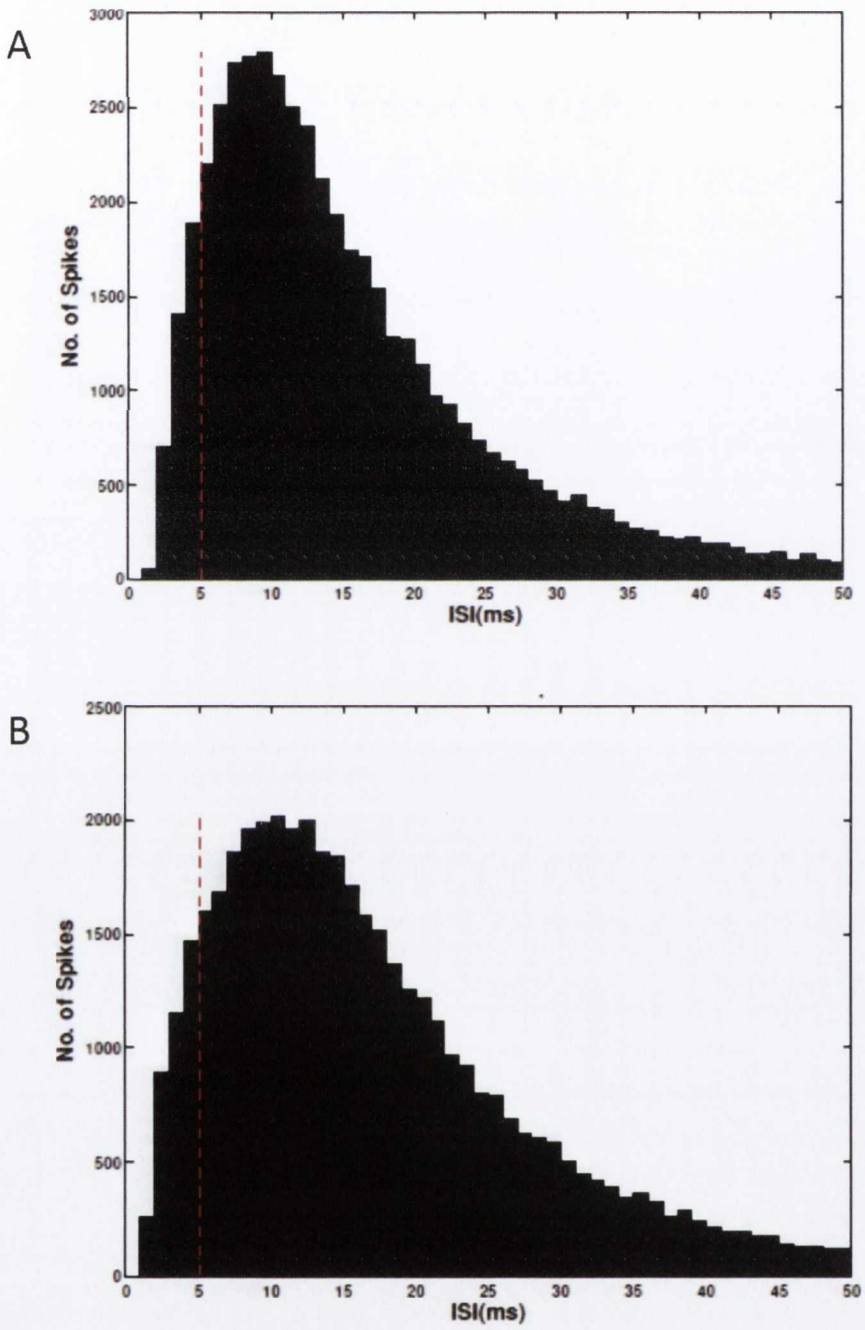


Figure 7. 50ms ISIH examples of two typical (A & B) of fast spiking, high propensity to burst neurons recorded in the anterior RSC. A) Mean firing rate was 55Hz and propensity to burst was 0.1, B) Mean firing frequency 51Hz and burst propensity 0.11. Note that counts before red dashed line are classified as bursts. This indicates that these fast spiking high propensity to burst neurons are not solely bursting units but likely switch between fast spiking and bursting modes.

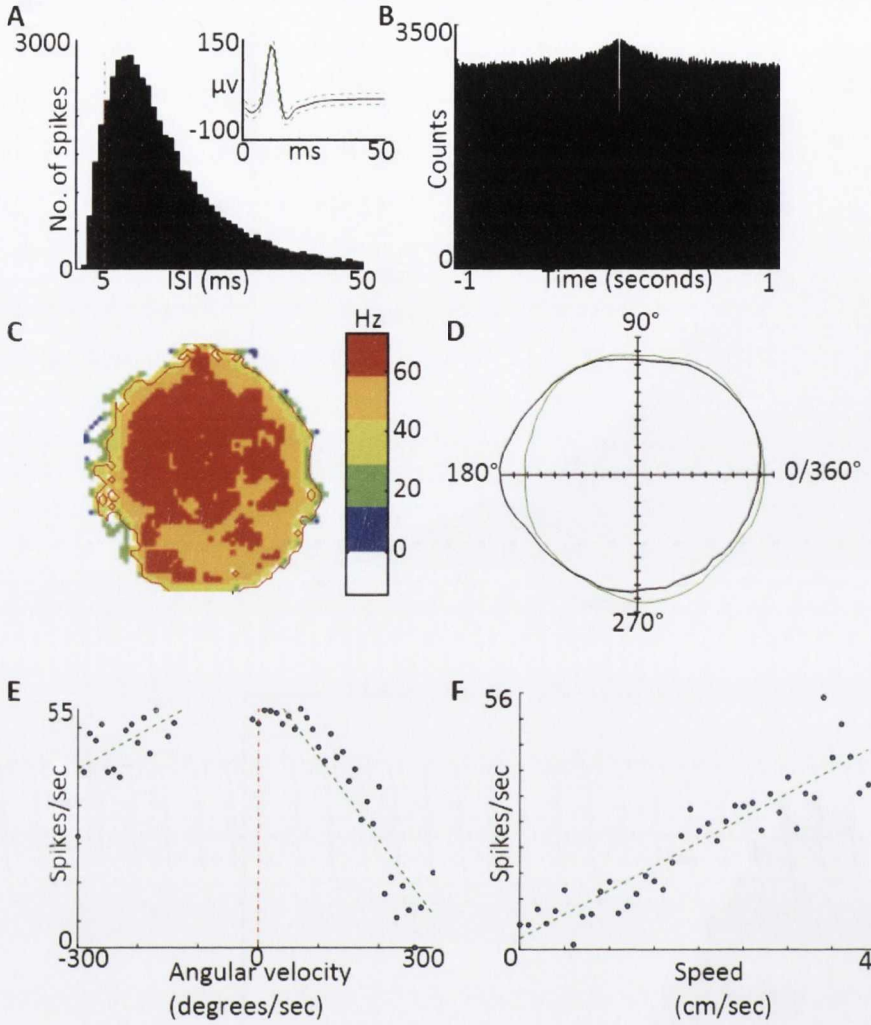


Figure 8. Example of a fast spiking high propensity to burst unit in the anterior RSC. Average firing frequency 55.71 Hz. A) 50 ms ISI, all counts before 5 ms (red dashed line) are considered bursting and spike waveform top right. B) ±1 second ACH showing no theta-modulation, Spike rate map (Hz) for cell during pellet chasing task showing no place specific firing (C). D) Head direction polar plot which shows the cell has no preferred head direction. E) The spike rate of this unit was negatively correlated with angular head velocity for both counter-clockwise head turns (r_{Pearse}=0.76; p_{Pearse}=7.25e^{-7}, p<0.01) and also for clockwise head turns (r_{Pearse}=0.91; p_{Pearse}=2.1e^{-12}, p<0.01). F) The firing rate of this units was positively correlated with running speed (r_{Pearse}=0.86; p_{Pearse}=2.5e^{-12}, p<0.01).

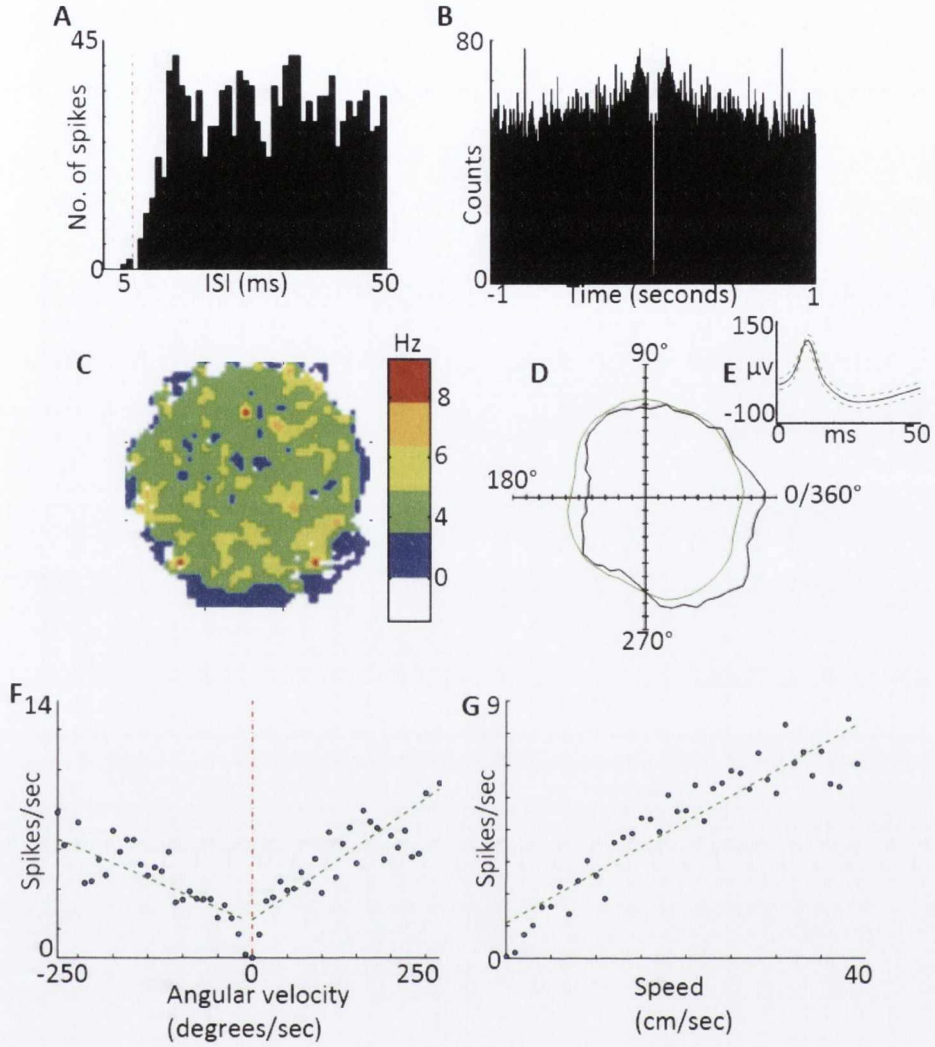


Figure 9. Example of a regular spiking unit in the anterior RSC. Average firing frequency 5 Hz. A) 50 ms ISI, all counts before 5 ms (red dashed line) are considered bursting. B) ±1 second ACH showing no theta-modulation, Spike rate map (Hz) for cell during pellet chasing task showing no place specific firing. D) Head direction polar plot which shows the cell has no preferred head direction. E) Spike waveform. F) The firing rate of this unit was positively correlated with angular head velocity for both counter-clockwise head turns ($r_{Pearson}$= 0.7; $p_{Pearson}$ =3.6e^{-5}, p<0.01) and clockwise head turns ($r_{Pearson}$= 0.8; $p_{Pearson}$ =2.2e^{-6}, p<0.01). G) The firing rate of this unit was positively correlated with running speed ($r_{Pearson}$= 0.92; $p_{Pearson}$ =5.3e^{-8}, p<0.01).

2.4.3 Non-spatially modulated and non-theta-modulated units whose firing rates where correlated with running speed.

See table 3a and b for full proportion and description of units whose firing rates were both positively and negatively correlated with running speed. Fast spiking (low propensity to burst) units had the biggest proportion of units whose firing rates were correlated with running speed. The firing rates of fast spiking (high propensity to burst) units which were correlated with running speed, demonstrated a preference to increase firing rate as the animal's running speed increased. Regular spiking units group had the smallest proportion of units whose firing rates were significantly correlated with running speed.

Table 3a. Non-spatially modulated and non-theta-modulated units whose firing rates which were positively correlated with running speed

Unit classification, n, (percentage)*	Running speed positive correlation (number of units, % proportion)+		
	r = 0.81 to 1	r = 0.61 to 0.8	r = 0.4 to 0.6
Fast spiking (low propensity) (*n*=9, 36%)	2 (8 %)	4 (16 %)	3 (12 %)
Fast spiking (high propensity) (*n*= 5, 45%)	2 (18 %)	2 (18%)	1 (9 %)
Regular spiking cells (*n*=24, 28%)	6 (7%)	12 (14%)	6 (7%)

* Percentage proportion of unit class who's firing rates demonstrated correlation with running speed. + Percentage proportion within each class of unit.

Table 3b. Non-spatially modulated and non-theta-modulated units whose firing rates which were negatively correlated with running speed

Unit classification, n, (percentage)*	Running speed negative correlation (number of units, % proportion)+		
	r = 0.81 to 1	r = 0.61 to 8	r = 0.4 to 0.6
Fast spiking (low propensity) (*n*=7, 28%)	7 (28%)		
Fast spiking (high propensity) (*n*= 1, 9%)			1(9 %)
Regular spiking cells (*n*=5, 6%)	2 (2%)	2 (2%)	1 (1%)

*Percentage proportion of unit class who's firing rates demonstrated correlation with running speed. + Percentage proportion within each class of unit.

2.4.4. The effects of angular head velocity on spike rate of non-spatially modulated and, non-theta-modulated units

The firing activity of non-spatially and non-theta-modulated units in anterior RSC were also found to be correlated with angular head velocity. Angular head velocity was measured for both clockwise and counter-clockwise head turns. These units were classified into two groups: units whose firing activity were only correlated with either velocity of head turns for clockwise only or counter-clockwise only head turns (table 4a and b) and units whose firing activity were correlated with the velocity of head turns in both clockwise and counter-clockwise directions. (table 5a and b).

2.4.5 Units whose firing rates were correlated with angular head velocity for either clockwise only or counter-clockwise only head turns

There appears to be an even spread between unit classes whose firing rates demonstrate a positive or a negative correlation with angular head velocity (table 4a and b). It is also apparent that there are no positive correlations with spike rate and angular head velocity for either clockwise or, counter-clockwise only head turns for any unit class within the r = 0.81 to 1 group. There are no units whose spike rate correlation demonstrates a negative correlation for any unit class within the 0.4 to 0.6 group.. Fast spiking (high propensity to burst) units had the highest proportion of units whose firing rates were correlated with angular head velocity (45%). The firing rates of two units from the fast spiking (high propensity to burst) class were negatively correlated with angular head velocity. There were eight units (32%) of fast spiking (low

propensity to burst) units whose firing rates were correlated with angular head velocity. The firing rates of only 14% of regular spiking units were correlated with angular head velocity.

Table 4a. Non-spatially modulated and non-theta-modulated units whose firing rates were positively correlated with angular head velocity for either clockwise only or counter-clockwise only head turns

Unit classification, n, (percentage)*	positive correlation (number of units, % proportion)+		
	r = 0.81 to 1	r = 0.61 to 0.8	r= 0.4 to 0.60
Fast spiking (low propensity) (*n*=3, 12%)			3 (12%)
Fast spiking (high propensity) (*n*=3, 27%)		2(18%)	1(9%)
Regular spiking (*n*=5, 6%)		4 (5%)	1(1%)

* Percentage proportion of unit class who's firing rates demonstrated correlation with angular head velocity. + Percentage proportion within each class of unit.

Table 4b. Non-spatially modulated and non-theta-modulated units whose firing rates were negatively correlated with angular head velocity for either clockwise only or counter-clockwise only head turns

Unit classification, n, (percentage)*	negative correlation (number of units, % proportion)+		
	r = 0.81 to 1	r = 0.61 to 0.8	r = 0.4 to 0.6
Fast spiking (low propensity) (*n*=5, 20%)		5(20%)	
Fast spiking (high propensity) (*n*=2, 18%)	2(18%)		
Regular spiking (*n*=6, 7%)	1(1%)	5 (6%)	

* Percentage proportion of unit class who's firing rates demonstrated correlation with angular head velocity. + Percentage proportion within each class of unit.

2.4.6 Units whose firing rates were correlated with angular head velocity for both clockwise and counter-clockwise head turns

All unit classes contained units whose spike rates were negatively correlated with angular head velocity for both clockwise and counter clockwise head turns (see table 5a and b). Units whose firing rates were negatively correlated for clockwise head turns were also negatively correlated with angular head velocity during counter-clockwise head turns. Proportionally, there were fewer units, across all unit classes, whose firing rates were correlated with angular head velocity for both clockwise and counter-clockwise head turns than clockwise only or counter-clockwise head

turns only (table 4a and b). Fast spiking (low and high propensity to burst) units whose spiking rates were correlated with angular head velocity for both clockwise and counter-clockwise head turns demonstrate only a negative correlation. The firing activity of only three regular spiking units were found to be correlated with angular head velocity for both clockwise and counter-clockwise head turns.

Table 5a. Non-spatially modulated and, non-theta-modulated units whose firing rates were positively correlated with angular head velocity for both clockwise and counter-clockwise head turns

Unit classification, n, (percentage)*	positive correlation (number of units, % proportion)+		
	r = 0.81 to 1	r = 0.61 to 0.8	r = 0.81 to 1
Fast spiking (low propensity) (*n*=0, na%)			
Fast spiking (high propensity) (*n*=0, na%)			
Regular spiking cells (*n*=1, 1%)		1(1%)	

* Percentage proportion of unit class who's firing rates demonstrated correlation with angular head velocity. + Percentage proportion within each class of unit.

Table 5b. Non-spatially modulated and, non-theta-modulated units whose firing rates were negatively correlated with angular head velocity for both clockwise and counter-clockwise head turns

Unit classification, n, (percentage)*	negative correlation (number of units, % proportion)+		
	r = 0.81 to 1	r = 0.61 to 0.8	r = 0.4 to 0.6
Fast spiking (low propensity) (*n*=6, 24%)	4(16%)	2(8%)	
Fast spiking (high propensity) (*n*=3, 27%)	1(9%)	2 (18%)	
Regular spiking cells (*n*=3, 3.5%)	1(1%)	1(1%)	

* Percentage proportion of unit class who's firing rates demonstrated correlation with angular head velocity. + Percentage proportion within each class of unit.

2.5 Units which displayed no obvious spatial firing properties but demonstrated theta frequency modulation

There were 34 theta-modulated and 6 theta-skipping units were recorded in the anterior RSC from 5 different animals. These units were classified based on the following criteria:

Theta-modulated units were defined as units which displayed peaks in the ±1000ms ACH which correspond to the theta frequency between 4-12Hz.

Theta-skipping units were defined as units which showed alternating large and small peaks on their ±1000ms ACH, these peaks corresponded to the theta frequency of 4-12Hz.

Waveform, firing properties, spatial information content, theta index of theta-modulated and theta-skipping units can be found on table 6a and b. Examples of theta-modulated units recorded in anterior RSC see Figure 10, for examples of theta-skipping units see Figure 11.

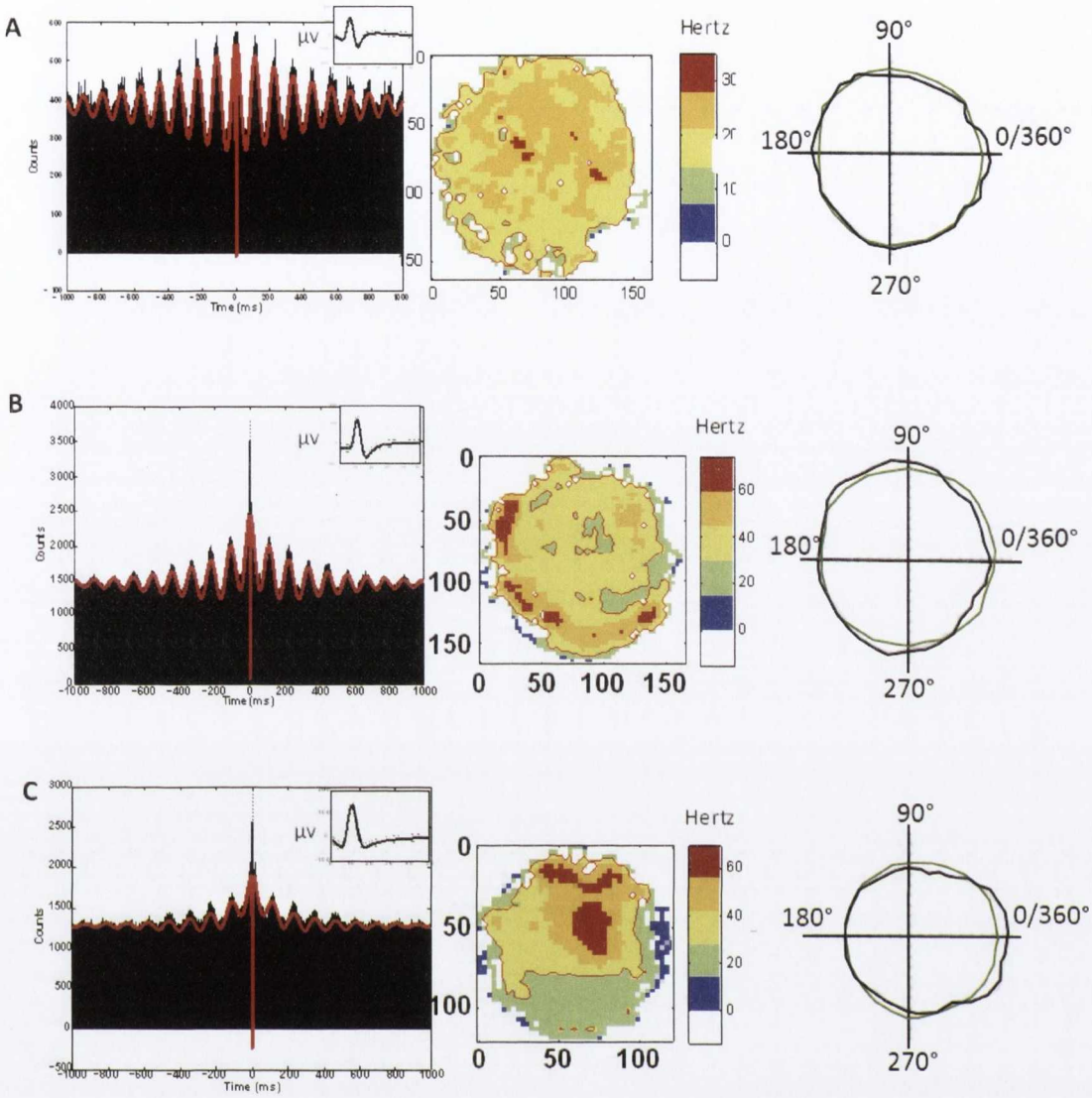


Figure 10. Examples of three different theta modulated units (A, B and C) recorded in anterior RSC. From left to right, ±1000ms ACH fitted with exponentially decaying sinusoids for calculation of theta index (top: 0.49; middle: 0.22; bottom: 0.16) with waveform top right. Top and middle firing rate maps (A and B) show no spatial preference whereas bottom (C) shows a slight preference for the top half of the arena. Head direction polar plots far right (A, B and C) show units display no direction dependent firing.

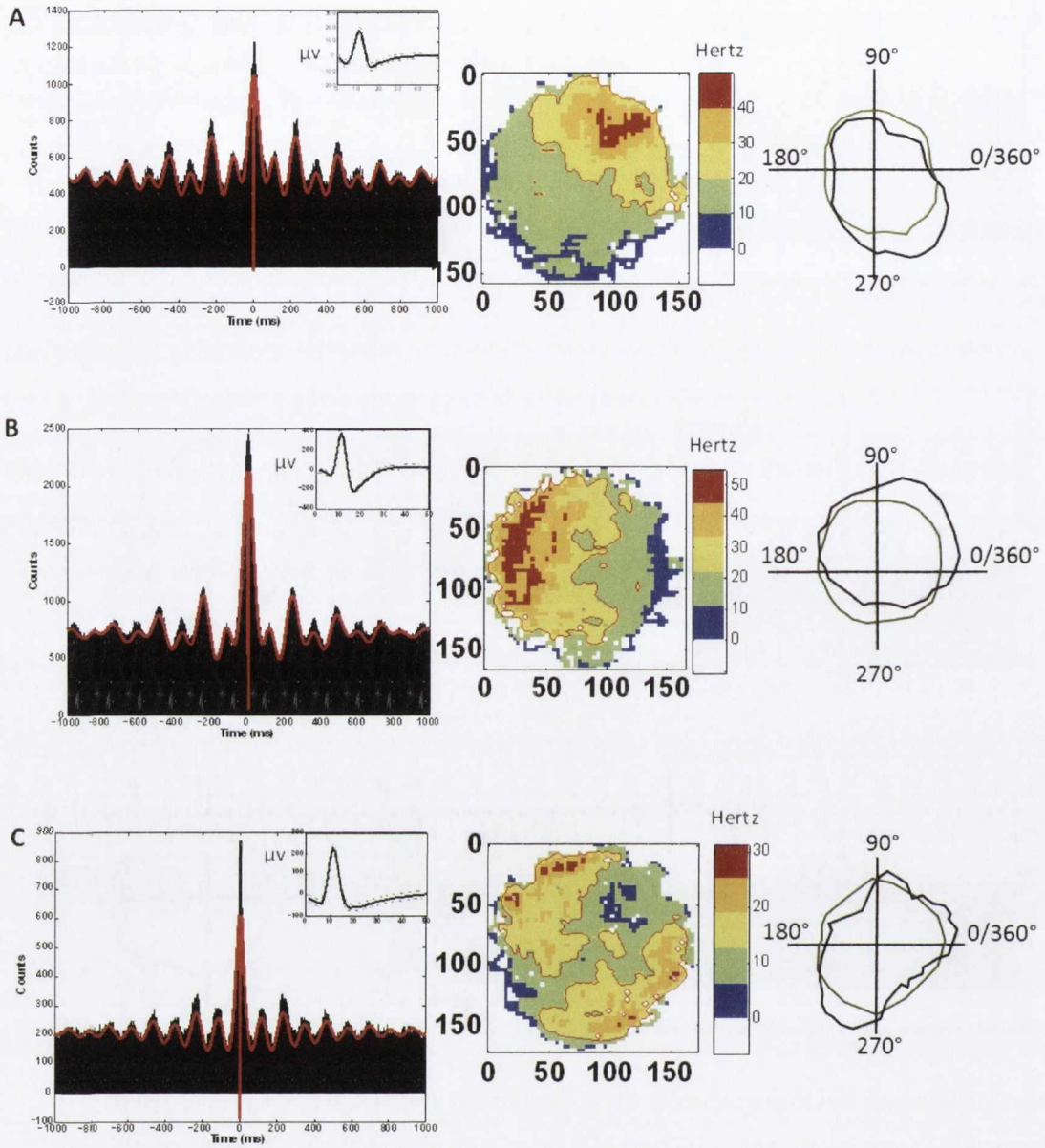


Figure 11. Examples of three different theta skipping units (A, B and C) recorded in anterior RSC. From right to left, ±1000ms ACH fitted with two exponentially decaying sinusoid where the frequency of one sinusoid lies in the theta range and other is half of that. Theta-skipping index top: 0.35; middle: 0.16; bottom: 0.11, with waveform top right. Firing rate map for unit A has a preference to fire in the top right corner, unit B prefers the left half of the arena and unit C appears to fire more frequently in the top left and bottom right. Head direction polar plots for each unit (far right) show the unit firing activity is not dependent on head direction.

Table 6a. Waveform and firing properties of theta-modulated and theta-skipping units

	Mean spike amplitude (μv)	Mean spike width (μs)	Mean firing (Hz)
Theta modulated units n=34	180.5±9.9	135±3.6	21.02±2.5
Theta modulated skipping units N=6	224.9±15.59	130±4.9	15.82±2.33

Descriptive parameters shown are represented as mean ± standard error of the mean, units as indicated.

Table 6b. Waveform and firing properties of theta-modulated and theta-skipping units continued

	Propensity to burst (%)	Spatial information content (Skaggs)	Theta Index
Theta modulated units n=34	0.13±0.01	0.31±0.05	0.37±0.05
Theta modulated skipping units N=6	0.21±0.03	0.38±0.03	0.21±0.06

Descriptive parameters shown are represented as mean ± standard error of the mean, units as indicated.

2.5.1 Formal statistical comparison between unit class and theta index report

Descriptive parameters for waveform and firing properties (table 6a and b) from theta-modulated and theta-skipping cells were found to be not normally distributed. An unpaired Mann-Whitney test were conducted to test for any significant differences between unit class's descriptive parameters. The only significant difference was observed between theta-modulated unit's propensity to burst (0.31±0.05) and theta-skipping unit's propensity to burst (0.21±0.01), $p<0.01$. There were no more statistically significant differences observed between these unit's parameters. Theta-modulated units' theta index was always positive, mean 0.37±0.05. The theta-skipping units skipping index is always positive, mean 0.21±0.06; jump factor 0.45±0.04, frequency ratio of 2.04±0.02 Hz. Frequency of the higher oscillation and lower oscillations were 8.58±0.01 Hz and 4.20±0.05 Hz respectively.

2.5.2 Theta-modulated and theta-skipping units were positively or negatively correlated with running speed

The firing rates of all but one theta-modulated unit were found to be correlated with running speed, in a positive direction (see table 7a and b). The firing rate of only one theta-modulated unit demonstrated a negative correlation with running speed within the r = 0.4 to 0.6 group, see Figure 12 for examples of theta-modulated units who firing activity is positively and negatively

correlated with running speed. The firing rate of only one theta-skipping unit was negatively correlated with running speed.

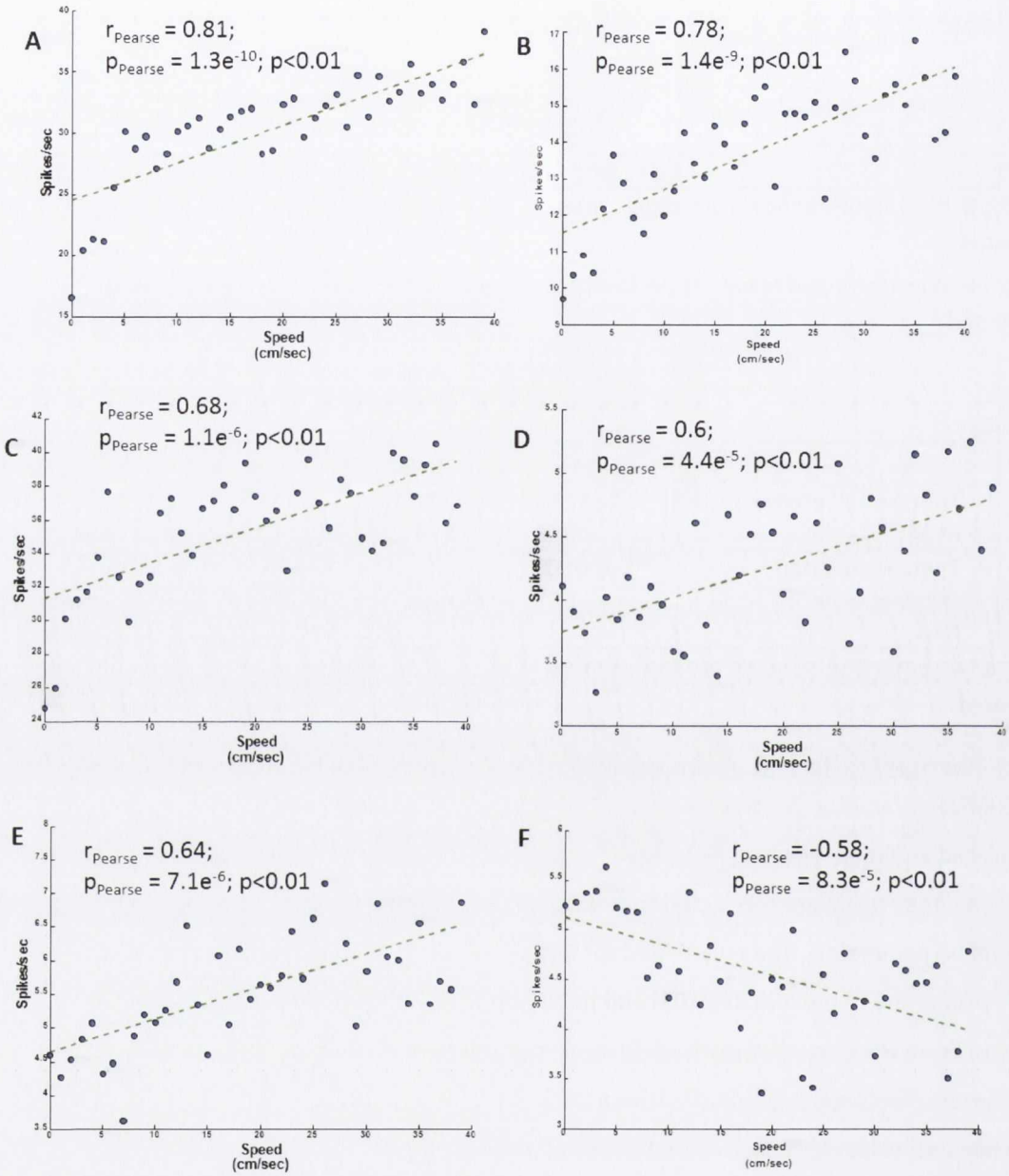


Figure 12. Examples of 6 different theta-modulated units whose spike rate is significantly correlated with running speed. A) A– E) 5 theta-modulated units whose firing rates were postively correlated with running speed F) An example of a theta-modulated unit whose firing rate was negatively correlated with running speed.

Table 7a. Theta-modulated and theta-skipping units whose firing rates which were positively correlated with running speed

Unit classification, n, (percentage)*	Running speed positive correlation (number of units, % proportion)+		
	r = 0.81 to 1	r = 0.61 to 0.8	r = 0.4 to 0.6
Theta-modulated (*n*=14, 44%)	2(6%)	11(32%)	1(3%)
Theta-skipping (n=1, 17%)			1 (17%)

* Percentage proportion of unit class who's firing rates demonstrated correlation with running speed. + Percentage proportion within each class of unit.

Table 7b. Theta-modulated and theta-skipping units whose firing rates which were negatively correlated with running speed

Unit classification, n, (percentage)*	Running speed negative correlation (number of units, % proportion)+		
	r = 0.81 to 1	r = 0.61 to 0.8	r = 0.4 to 0.6
Theta-modulated (*n*=1, 3%)			1(3%)
Theta-skipping (n=0, na%)			

* Percentage proportion of unit class who's firing rates demonstrated correlation with running speed. + Percentage proportion within each class of unit.

2.5.3 Theta-modulated and theta-skipping units whose firing rates were positively or negatively correlated with angular head velocity for either clockwise only or, counter-clockwise only head turns

Angular head velocity was found to be correlated with the spiking rates of five (15%) theta-modulated units, the majority demonstrated a negative correlation (table 8a and b). Only one theta-modulated unit's firing rate was positively correlated with angular head velocity. The firing rate of only one theta-skipping unit was negatively correlated with angular head velocity. The firing rates of only two theta-modulated units were significantly correlated with angular head velocity for both clockwise and counter-clockwise head turns. One of these units demonstrated a positive correlation while the other demonstrated a negative correlation. See Figure 13 for examples of theta-modulated units whose spike rates were positively and negatively correlated with angular head velocity.

Table 8a. Theta-modulated and theta-skipping units whose firing rates were positively correlated with angular head velocity for both clockwise only or counter-clockwise head turns only

Unit classification, n, (percentage)	Positive correlation (number of units, % proportion)		
	r = 0.81 to 1	r = 0.61 to 0.8	r = 0.4 to 0.6
Theta modulated (*n*=1, 3%)			1(3%)
Theta modulated skipping (n=0,na%)			

* Percentage proportion of unit class who's firing rates demonstrated correlation with angular head velocity. + Percentage proportion within each class of unit.

Table 8b. Theta-modulated and theta-skipping units whose firing rates were negatively correlated with angular head velocity for both clockwise only or counter-clockwise head turns only

Unit classification, n, (percentage)	Negative correlation (number of units, % proportion)		
	r = 0.81 to 1	r = 0.61 to 0.8	r = 0.4 to 0.6
Theta modulated (*n*=4, 12%)	1(3%)	2(6%)	1(3%)
Theta modulated skipping (n=1,17%)	1(17%)		

* Percentage proportion of unit class who's firing rates demonstrated correlation with angular head velocity. + Percentage proportion within each class of unit.

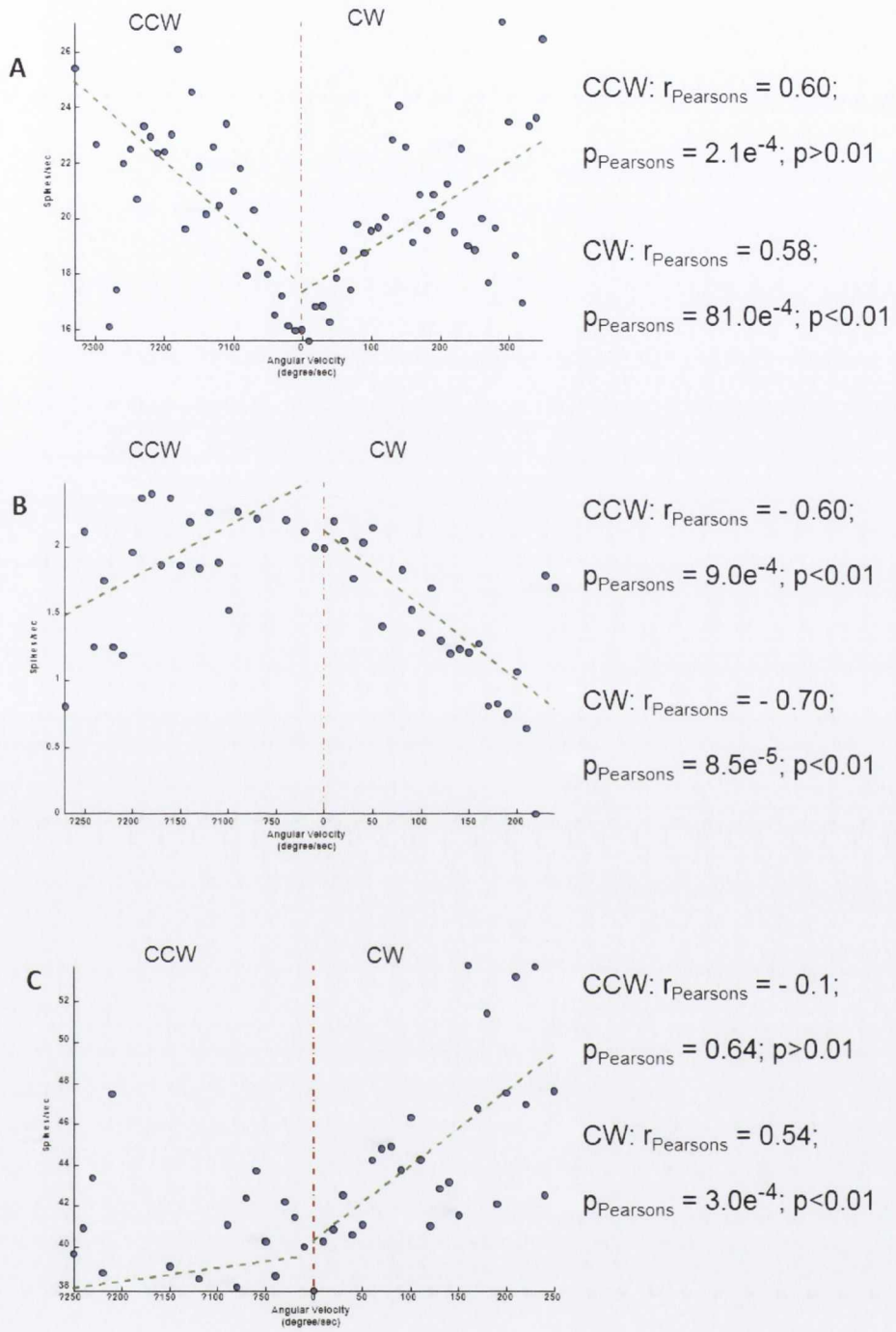


Figure 13. Three different examples of theta-modulated units whose firing rates were positively or negatively correlated with angular head velocity. A) The firing rate of this theta-modulated unit is positively correlated with angular head velocity for both CW and CCW head turns. B) The spike rate of this theta-modulated unit is negatively correlated with angular head velocity for both CW and CCW head turns. C) The firing rate of this theta-modulated unit is positively correlated with angular head velocity for CW head turns only.

2.6 Discussion

There have been few studies attempting classify RSC cells based on their waveform and firing characteristics in the freely-moving rat. Previous single-unit studies in rodent RSC reported only units which demonstrated location or head direction dependent firing, and, as such, may have been biased towards recording pyramidal cells (Alexander & Nitz, 2015; Chen *et al.*, 1994a; Chen *et al.*, 1994b; Cho & Sharp, 2001). Therefore, the purpose of this chapter was, firstly, to describe the waveform and firing properties of units which demonstrated no spatial firing properties or theta-modulation. The second aim was to observe if the firing rates of these units were correlated with angular head velocity or running speed. The third aim was to report the proportion and index of theta-modulated and theta-skipping cells in anterior RSC, describe their firing characteristics and waveform properties. The final aim was to observe if theta-modulated or theta-skipping units firing activity are correlated with running speed or angular head velocity.

Units whose firing activity demonstrated no obvious spatial properties or theta-modulation were separated into four distinct classes: regular spiking, fast spiking (low propensity to burst, fast spiking (high propensity to burst) and unspecified low firing units. This is the first time unit classification has been attempted for these cell types in RSC using only waveform and firing characteristics. Therefore, definitions for classification were adapted from those used to describe similar units in the medial prefrontal cortex (mPFC) (Baeg et al., 2001; Jung et al., 1998). The mPFC was chosen as it is cortical tissue and its proximity to anterior RSC. It is likely, in this study, that regular spiking cells are projecting neurons and fast spiking cells are likely inhibitory inter-neurons, similar to mPFC (Baeg et al., 2001; Jung et al., 1998). In support of this theory, fast spiking cells were also found to burst more frequently than regular spiking cells. Also in support of this classification we found anterior RSC units to have a similar spatial information content (Skaggs) as those similarly classified in the mPFC (Baeg et al., 2001; Jung et al., 1998). Late-spiking pyramidal neurons, described in-vitro, in the granular layer of the RSC (Kurotani *et al.*, 2013) could be unspecified low firing units due their low firing rate.

Upon inspection of the firing rate map after a recording session, the contribution of cells with no obvious location specific firing, for spatial navigation can easily be overlooked. Cho and Sharp (2001) performed a multiple regression analysis for the firing activity of each cell they recorded in RSC with head direction, place, running speed and angular head velocity. They found that the firing rates of almost all unit recorded were correlated with running speed and angular head velocity. A limitation of this analysis is that it gave no indication of the relationship of the correlation (e.g. positive or negative) between spike rate of the unit recorded and running speed or, angular head velocity. They also did not report the proportion of cells where angular head

velocity was correlated with spike rate in a clockwise only, counter-clockwise only direction or if they were correlated with both directional head turns.

Anterior RSC fast spiking, low and high propensity to burst cell classes all contain cells whose firing rate is significantly correlated with running speed. However, there are some discrepancies between cell classes as fast spiking low and high propensity to burst have approximately the same proportion of cells whose firing rate is correlated with running speed but regular spiking cells have less. Also, fast spiking high propensity to burst and regular spiking cells proportionally are more likely to have firing rate positively correlated with running speed whereas a more even spread of positive and negative correlations are observed in fast spiking low propensity to burst cells. The anterior RSC is reciprocally connected to the M1, M2 and primary motor cortices, it is likely that information received via these connections is integrated by the anterior RSC. This would account for anterior RSC units firing rates correlating with running speed. The posterior RSC is connected to the mEC, where cells with similar running speed correlates were found (Kropff *et al.*, 2015). The running speed signal could be projected from anterior RSC to posterior RSC via the RSC dense intrinsic connections (Sugar *et al.*, 2011). However, only units whose firing rates demonstrated a negative relationship with running speed were described in mEC. It is possible, that the posterior RSC projects units whose firing activity is negatively or positively correlated with running speed to different locations within the mEC.

A proportion of fast spiking (low and high propensity to burst) and regular spiking cells were also found to be correlated with angular head velocity in this study. Fast spiking low and high propensity to burst cells had approximately the same proportion of cells within class whose firing rate were correlated with angular head velocity for either CW or CCW directions only. Regular spiking cells, proportionally, had much fewer of these cells. However, the proportion of cells where firing rate is either negatively or positively correlated with spike rate is similar across all classes. Across all classes there were fewer cells whose spike rate correlated with both CW and CCW head turns; especially within the regular spiking group. It is also notable that both classes of fast spiking cells only displayed positive correlations whilst the only negative correlation was observed in regular spiking cell group. The role of the anterior RSC could be to integrate the vestibular signal then project this information to other brain areas within the spatial navigation network (e.g. mEC). This would account for the firing rates of cells, in anterior RSC, correlating with angular head velocity. The vestibular signal, originating in the vestibular nuclei is likely to reach the anterior RSC as follows: vestibular neuclei projects to nucleus prepositus, dorsal tegmental neucleus, lateral mammillary neucleus, anterior thalamus then to RSC (Dillingham et

al., 2014; Taube, 2007). Lesion to any one of these structures should eliminate the correlation of firing rate with angular head velocity in anterior RSC.

Rodents have demonstrated the ability to path integrate (Etienne *et al.*, 1998; Mittelstaedt & Mittelstaedt, 1980), that is the ability to sum up the vectors of distance and direction travelled from a starting point to estimate current position and a direct route home. Disruption of the RSC prevents rodents from successfully performing path integration (Cooper et al., 2001; Elduayen & Save, 2014). Rodents with EC lesions are similarly impaired when the ability to path integrate is examined (Van Cauter *et al.*, 2013). It is likely that the RSC continuously integrates running speed and angular head velocity, thus providing an ongoing vector representation of current route. This information is likely projected to the EC which contains grid cells. Grid cell's unique firing pattern provides a metric to measure distance travelled and could be integrated with the vector created in RSC. The RSC and EC are likely to work in collaboration to provide an ongoing vector representation of the rat's journey.

Theta-modulated units accounted for 4 % of all cells recorded in the anterior RSC. Approximately, half of all theta-modulated units firing activity were correlated with running speed. During the recording session the rat was in almost constant locomotion, therefore, it is likely that these theta cells are entrained to a type I theta wave oscillation (Vanderwolf, 1969). The other theta cells which were not significantly correlated to running speed could be entrained by a type II theta wave oscillation (Sainsbury *et al.*, 1987). However, this is a tentative conclusion as the underlying the EEG wave would have to be analysed, as well as measuring putative type II theta cells during immobility. Regardless, the fact that theta-modulated cells are present in the anterior RSC supports the theory that it is part of the network of brain regions involved in spatial navigation and memory (O'Keefe & Nadel, 1978). Theta-modulated cells whose firing rate were correlated with angular head velocity, could act as a method of integration of this signal from other brain areas. It is also important to note that Cho and Sharp (2001) found, in mid-caudal RSC, 20% of cell which were not spatially or temporally correlated were found to be theta-modulated. Perhaps, the projection from dorsal CA1 unique to anterior RSC could account for fewer theta-modulated cells in anterior RSC.

Theta-skipping cells were described for the first time in the RSC in this study. These cells appear on the 1000ms autocorrelation with the first side peak smaller than the second side peak, indicating that spikes are occurring on alternating theta cycles (Brandon *et al.*, 2011; Brandon *et al.*2013). Theta-skipping units were also reported in the nucleus reuniens (Jankowski *et al.*, 2014) and mEC (Brandon *et al.*, 2011; Brandon *et al.* 2013). The skipping behaviour could be due to

lower frequencies of intrinsic oscillations of cells in anterior RSC or lower frequency input from the prefrontal cortex (Fujisawa & Buzaki, 2011; Gevin *et al.*, 1997; Giocomo et al., 2007). Brandon *et al.* (2011, 2013) demonstrated that theta-skipping cells in the mEC also contain a head direction component, medial septum (MS) lesion abolished theta-skipping oscillation but preserved the head direction component (Brandon *et al.*, 2011). The origins of the theta-skipping signal are not clear but the MS is a possible candidate structure. The MS projects to RSC, the RSC is reciprocally connected to the neucleus reuniens and mEC. It is possible the head direction signal is received by RSC from the ADN and the theta-skipping is received in RSC from neucleus reuniens or MS. This signal is then integrated within the RSC and projected to the mEC, where theta-skipping units with head direction are observed (Brandon *et al.*, 2013). The head direction component is preserved but theta-skipping is abolished in mEC when medial septum is lesioned. In order to better understand the role of the theta-skipping signal in anterior RSC it would be of interest to lesion RSC and observe if theta-skipping head direction units are still present in mEC.

Theta-skipping units appear to have preferred location of firing in anterior RSC. It also appears that the larger the theta-skipping index the more clearly defined the place preference of firing is. This hypothesis would be demonstrated by a simple correlation of the spatial information content of these cells with theta-skipping index. The apparent place preference for these units is likely to arise from the CA1 projection to anterior RSC. However, the RSC also receives projections from brain areas containing visual, motor, vestibular and somatosensory information (Burcham *et al.*, 1997; Reep *et al.*, 1994; Van Groen & Wyss, 1990; Van Groen & Wyss, 1992; Van Groen & Wyss, 2003; Vogt & Peters, 1983; Wyass & Van Groen, 1992). It could be the case that the place preference observed for theta-skipping units is a result of the integration of these signals. The apparent place preference for theta-skipping units requires further investigation. It would be interesting to lesion the projection from CA1 to RSC to observe the effects of place preference for these units.

The firing and waveform properties for non-spatial and non-theta-modulated units of the anterior RSC were described for the first time. The properties of these cells were found to be similar to those found in the nearby mPFC. Furthermore, firing activity of these cells were also correlated with running speed and angular head velocity, similar to the mid-caudal RSC (Chen et al., 1994a; Chen et al., 1994b; Cho and Sharp, 2001). The presence of these units, along with lesion and behaviour studies strongly implicate the RSC is important for navigation, particularly path integration. Theta-modulated cells were also present in the anterior RSC, the population was found to be smaller than those measured mid-caudal RSC (Cho and Sharp, 2001). This may

indicate that there is a graded population of theta-modulated cells along the anterior-posterior axis of the RSC. This could be due to the different weighting of connections, along the anterior-posterior axis of the RSC, from other brain areas containing theta-modulated units. A small population of theta-skipping cells were described for the first time in the anterior RSC. While the exact function of these cells is not clear, their firing activity appears to demonstrate place preference, this has not been previously reported for this cell type.

3. Head Direction Units Recorded in the Anterior Retrosplenial Cortex of the Freely-Moving Rat

3.1 Introduction

Successful navigation for any mammal, in any environment, requires not only knowledge of where they are located but also which way they are heading, i.e. head direction (HD). HD cells were first discovered in the rodent postsubiculum (Ranck, 1984). HD cells were found to be only active when the animal's head was orientated in certain direction, usually over a 90 degree range (Taube, 2007). When the rat's head moved out of this preferred firing range the cell stopped firing (Taube *et al.*, 1990a). The firing activity of HD cells were also found not to be place dependent (Taube *et al.*, 1990a) as they fire at any location within the environment, as long as the head is orientated in the preferred firing direction for that cell. HD cells are thought to provide an ongoing representation of the animal's heading direction essential for navigation.

In some brain areas HD cell's activity is not only correlated with direction but also with the animal's running speed and/or angular head velocity (Bassett and Taube., 2001; Blair & Sharp, 1995; Blair *et al.*, 1998; Chen *et al.*, 1994a; Cho & Sharp, 2001; Taube & Bassett, 2003). HD cells with angular head velocity correlates, firing rates increase or decrease as the speed of the rat's head movement increases through the preferred firing direction. However, these cells remain silent regardless of the speed of movement when the head is not orientated in the preferred firing direction. If the HD cell is recorded in the same environment over many days, the firing properties of the cell remain unchanged (Jankowski *et al.*, 2014; Taube., 1995).

The direction dependent firing of HD cells relies on distal environmental (allothetic) cues (Taube *et al.,* 1990 a; Taube *et al.,* 1990b). Allothetic cues are those present in the environment which are interpreted by one's senses and used to navigate. For instance, visual landmarks can be used to navigate but also olfactory or auditory cues can be used too. The influence of visual landmarks on the direction specific firing activity of HD cells is most frequently studied. Taube (1990 b) found that rotation of visual cue, attached to one side of the arena wall, resulted in an equal rotation that HD cells preferred firing direction. Goodridge *et al.*, (1998) observed that, in a circular arena, rotation of an odour cue by 90° also resulted in HD preferred direction shift. However, rotation of an auditory tone did not alter the preferred firing direction of the HD cell (Goodridge *et al.*, 1998).

Taube *et al.,*(1990 a,b) found that HD cell's preferred firing direction was maintained when recorded in the dark and, when visual cues were removed from the arena while the rat was present. This would imply that the preferred firing direction of HD cells is not simply the result of visual information but preferred direction can be maintained by idiothetic cues. Idiothetic cues are self-generated information about the body's location in space. This information arises from

proprioceptors, vestibular system and motor efference copy. This information can facilitate spatial navigation in the absence of allothetic cues (Etienne, 1992; Etienne & Jeffery, 2004; Mittelstaed M. & Mittelstaed H., 1980; Whishaw & Brooks, 1999; Whishaw *et al.,* 2001). Some idiopathic information is crucial for generation of the HD signal as disruption of the vestibular system disrupts the HD signal even when visual cues are present (Stackman & Taube, 1997). Lesion and recording studies in rodents provide evidence that it is idiothetic information that generates the HD signal and allocentric information which is important for establishing and maintaining directionality. This is demonstrated, with vestibular apparatus intact, rotation of visual cues produce the same proportion of shift in preferred firing direction (Taube, 1990b; Taube, 2007). This is further demonstrated when the rodent navigates for prolonged periods in darkness, the preferred firing direction of the HD cell can drift. The preferred direction is then returned within 80ms of turning on the lights to allow visual identification of the cue (Zugaro *et al.*, 2003).

HD cells are not only present in the postsubiculum (Ranck, 1984) they were also described in other areas within the classical Papez circuit. These areas include the anterior dorsal thalamic nuclei (ADN) (Taube, 1995), nucleus reunions of the thalamus (Jankowski et al, 2014), lateral mammillary nuclei (LMN) (Stackman & Taube, 1998), retrosplenial cortex (RSC) (Cho & Sharp, 2001; Chen *et al.*, 1994 a), and EC (Sargolini *et al.*, 2006). HD cells have also been observed in large numbers in other brain areas out with this Papez circuit. Lateral dorsal thalamus (Mizumori & Williams, 1993), dorsal straitum (Mizumori *et al.*, 2000; Wiener 1993). Small populations of HD cells have also been described in the medial prestriate cortex (Chen *et al.*, 1994a), CA1 hippocampus (Leutgeb *et al.*, 2000), and dorsal tegmental nucleus (Sharp *et al.*, 2001). HD cells have been found in many different structures throughout the rodent brain. The reason as to why these cells are observed in so many different brain regions is not known.

Taube (2007) hypothesised a primary pathway for the head direction signal from generation to the hippocampal formation based on lesion and recording experiments. The HD signal is believed originate in the dorsal tegmental nucleus (DTN) and project to the lateral mammillary nucleus (LMN). The LMN then projects to the ADN, the ADN then projects to the postsubiculum. The HD signal then projects to the EC, hereby entering the hippocampal formation. Lesion to the LMN was found to abolish the HD signal in the ADN and the postsubiculum (Bassett *et al.*, 2007; Blair *et al.*, 1998; Sharp & Koester, 2006). Lesion to ADN disrupted the HD signal in the postsubiculum but not in the LMN and lesion to postsubiculum did not disrupt the HD signal in the ADN (Goodridge & Taube, 1997). The dual lesion and recording work provide evidence to support

Taube's (2007) hypothesis that this is the primary pathway for the HD signal to reach the hippocampal formation.

Lesion or temporary inactivation studies of the rodent RSC have demonstrated its importance for spatial navigation tasks (Cooper & Mizumori, 1999; Cooper & Mizumori, 2001; Meunier *et al.*, 1991; Nelson *et al.*, 2015; Sutherland *et al.*, 1988; Vann & Aggelton, 2002; Vann *et al.*, 2003; Vann & Aggelton, 2005). The RSC is one of the largest structures in the rodent brain, it also receives projections and projects to structures located within the HD primary pathway. These structures include the ADN, postsubiculum, and EC (Sugar *et al.*, 2011; Van Groen & Wyss, 1990; Van Groen & Wyss, 1992; Van Groen & Wyss, 2003; Wyass & Van Groen, 1992). Therefore, it was not surprising that Chen *et al.* (1994) recorded single-units from 2 to 6mm (posterior to bregma) in the rat and found a population of HD in RSC, which accounted for approximately 10% of all units recorded there. However, from this research it is not apparent how many HD cells were recorded from anterior or posterior RSC or if any differences were observed in HD firing properties along the RSC anterior-posterior axis. Chen *et al.* (1994a) recorded RSC HD units while the rat performed a behavioural task on the 8-arm radial arm maze. The rat could only move in one of eight directions, therefore it imposed directionality on the rat which may confound interpretation of the natural directionality of these cells. Also, the maze arms would impede the rats head movements, this also confounds any findings on the influence of angular head velocity on RSC HD activity. Therefore, in order to accurately describe the firing properties of HD cells in the RSC, recordings would have to be repeated in the open-field arena.

The findings of Chen *et al.* (1994a, b) were extended by Cho & Sharp (2001) as they recorded HD cells in RSC while the rodent navigated an open-field arena. Unlike the previous study, Cho & Sharp (2001) recorded only from mid-caudal RSC where it directly surrounds a large portion of the postsubiculum, known to contain HD cells (Ranck, 1984). They found that approximately 10% of all cells recorded were HD cells. They also found HD cells whose firing rates were correlated with running speed and angular head velocity. This information gives insight into the possible role of the RSC during spatial navigation. However, very little is known about the spatial properties of cells in the anterior of the structure. Furthermore, there appears to be a varying density of projections, from many brain regions important for spatial navigation, along the anterior – posterior axis of the RSC. These areas include the anterodorsal, medial and ventral thalamic nuclei, subiculum, postsubliculum and CA1 hippocampus (Sugar *et al.*, 2011; Van Groen & Wyss, 1990; Van Groen & Wyss, 1992; Van Groen & Wyss, 2003; Wyass & Van Groen, 1992). Therefore, anatomical connectivity studies suggests that HD cells found in the anterior portion of

RSC could have different firing properties to those recorded in mid-caudal RSC. Therefore, a full description and characterisation of HD cells in anterior RSC is needed. It will also be important to assess if the firing rates of any HD cells are correlated with angular head velocity and running speed. HD units with these firing correlates are of theoretical importance for navigation, in particular path integration. Finally, comparison of firing properties of anterior RSC HD cells during environmental changes will provide more information for the possible function these cells. The information from this study will provide more insight for this structures role in spatial navigation.

3.2 Methods

Animals used in this chapter are the same animals as those used in chapter 2. The surgical techniques, recording techniques and firing analyses are also the same as those used in chapter 2. Any, additional recordings sessions and analysis methods used uniquely in this chapter are described below.

3.2.1 Recording sessions

Upon lowering the microdrive, animals were connected to the recordings apparatus and pellet chased around the raised, circular platform with a small wall around the perimeter (height 0.3cm) for 16 minutes. At the end of the 16 minutes, the spatial properties of the cell were quickly analysed. If a HD cell or cells were observed, which had not been recorded before, then a recording session would begin. There were 4 sessions in total, each session was carried out in the same recording room as the screening session with the same open curtain set-up as described in chapter 2 methods section. An overview of the 4 sessions are shown on table 9 but not necessarily undertaken in the order displayed. Each session consisted of 3 trials each lasting 16 minutes. The headstage cables were never detached from the animal, at any point, for the duration of the three trials. After each trial, rats were placed in a holding tray beside the arena to check that the unit of interest was still present (5 minute duration). During this 5 minutes the arena was always cleaned with a 70% ethanol solution. All arena contained a small wall (0.3cm height) around the perimeter. All trails were conducted with the arena 32cm raised from the ground and all arena were painted matt black. The arena used for the initial 16 minute trial is the same as that used for all trials in *italics* shown in table 9. Therefore, If a new HD cell was discovered during the 16 minute screen, then this recording could be used as trial 1. To achieve darkness (dark trial, Session 1) all lights were turned off including the computer monitor and the curtains were closed as much possible to ensure darkness. However, the curtain remained partially open which permitted pellets to be manually thrown into the arena. The circle with walls arena (trial: circle w/walls, Session 2) is the same circular arena used during the initial 16 minute screen, but with black opaque walls present (height 48cm) around the entire perimeter. The small circle used (Session 3) was 51cm in diameter and the square used in session 4 had length of one side 81cm.

Table 9. Overview of recording session rats with HD units undertook.

	Trials undertaken in each session		
	Trial 1	Trial 2	Trial 3
Session 1	*Circle*	Square	*Circle*
Session 2	Small circle	*circle*	Small circle
Session 3	*Light*	*Dark*	*Light*
Session 4	*Circle*	*Circle w/walls*	*Circle*

See text for detailed description of each trial type and arena parameters.

3.2.2 HD analysis

How HD units were recorded is described in methods section of chapter 2 (section 2.2.4), only further analyses of HD firing properties specific to this chapter will be described here. The maximal firing intensity (Hz) for each HD unit was measured and called "peak HD rate". The corresponding angle at which peak HD rate occurred was taken as peak HD (degrees). The half peak width of each HD cell was measured as follows, the peak HD rate for that unit was found from that HD cell's tuning curve; this number was divided by 2. The width of the tuning curve at the calculated firing rate was measured, giving half width in degrees. All of the HD polar plots from each of the sessions were decomposed into discreet time events, from the start of the trial to end. The firing rate map at the end of each session, for each HD cell, were also decomposed into the cardinal orientations (0 to 360°, in 45° bins) to examine any place specific firing properties of these HD units.

3.2.3 Calculation of the separation angle

Calculation of separation angle and anticipatory time interval were based upon the methodology of Blair & Sharp (1995); Blair *et al.* (1998); Cho & Sharp (2001). A brief description of how separation angle and anticipatory time interval were calculated will be given below, any adjustments or additional analysis will also be described.

Tuning curves were created for clockwise (CW; angular velocity >120°/s) and counter-clockwise (CCW; angular velocity < -120°/s) head turns for each HD cell. It was apparent that there was a gap between the peaks of the CW and CCW tuning curves for most HD cells (fig 11A), this is defined as the separation angle. The separation angle is calculated as follows, the peak HD for CW head turns (degrees) is subtracted from the peak HD (degrees) of CCW turns. One way to interpret this separation angle, If positive (CW [peak HD]<CCW [peak HD]), where the CW peak HD is to the left of the CCW peak HD, is that the unit might anticipate, by a small temporal interval, the arrival at the immediately next directional heading. Conversely, a negative separation angle (CW>CCW) indicates that the CW peak occurs to the right of CCW peak HD. This could be interpreted as the unit encodes the past head direction, by some temporal interval.

3.2.4 Calculation of the anticipatory time interval

To calculate the anticipatory time interval each HD cell's firing rate was plotted as a function of the rodent's past and future heading direction. This resulted in a series of time shifted tuning curves that showed the cell's directional tuning for past and future head directions (fig 14B). Time shifts were performed in increments of 20 ms, due to sampling rate (50Hz). The separation angle for each for each time displacement (-150 ms, +150ms) was plotted together and a line was fitted to connect each data point. This allowed for accurate measurement of the time displacement when the separation angle reached zero. When the fitted line crossed zero (the separation angle = 0), the time displacement that this corresponded to was termed the anticipatory time interval if positive. If this number was negative then it was interpreted as the time by which the HD cell represented past HD.

This line was also subject to a Pearson's test, where significance was set $p<0.01$. This was felt necessary because some HD had a low firing rate which led to inconsistent calculation of the separation angle. This in-turn led to inconsistent data points when the separation angle was plotted against time displacement. The resulting time displacement when the separation angle equalled zero for these cells was uninterpretable. In this study peak HD was used instead of mean HD for CW and CCW, to calculate peak HD for the separation angle. This method was chosen as some HD cells had other, small peaks, on the tuning curve. If the mean HD were used in this situation large separation angles would occur, this could possibly confound the results

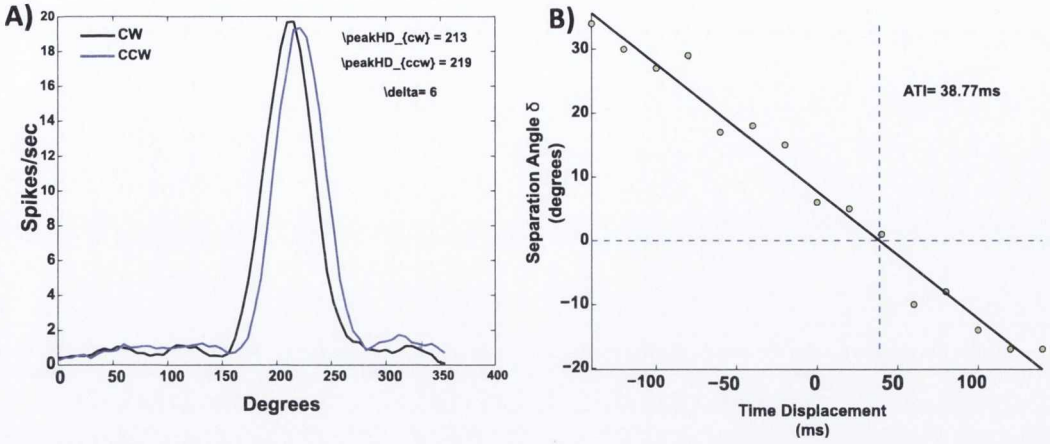


Figure 14 (A & B). Clockwise and counter-clockwise directional tuning functions for a HD cell recorded in anterior RSC (A) and calculation of anticipatory time interval (B). Firing rate is shown as a function of head direction (degrees). The difference in peak HD for CW and CCW tuning curves yielded a separation angle (A). To calculate the amount of time these cells anticipated future heading direction, the separation angle for each for each time displacement (-150 ms to +150ms) were plotted together with fitted line to connect each data point. The time displacement observed when the separation angle equalled zero was taken as the anticipatory time interval (B).

3.3 Results

3.3.1 Baseline properties of head direction units in the anterior RSC in the freely-moving rat.

Out of 812 cells recorded in this study, there were 119 different HD cells. The population of HD cells in the rodent anterior RSC is approximately 15%, see Figure 15 for examples. All units were likely from the RSG portion of the anterior RSC due to starting depth of tetrodes. Table 10 shows the baseline properties (mean and SEM) calculated from all head direction units recorded in this study. The half-peak tuning width of all head direction units recorded ranged from 36° to 108°. Peak rate for each head direction unit recorded ranged from 2Hz to 102Hz. There appears to be an even spread of possible directions the rat can face but there is an obvious peak (14 occurrences) at around 60°, and the lowest observation (1 occurrence) was observed around 300° (see Figure 16). The peak preferred direction, of all HD units, is observed from first exposure to the arena (0-1 minutes) and is maintained throughout the trial (16 minutes), Figure 17. No HD unit recorded in anterior RSC demonstrated any firing which was dependent on the animal's location in the environment (Figure 18).

Table 10. Mean basic directional properties of head direction units recorded in anterior RSC.

Spike Width (μs)	Spike Amplitude (μv)	Half-peak tuning width (degrees)	Peak rate (Hz)
132.1±1.7	154.5±7.5	63.7±1.1	32.3±2.3

Data displayed as mean ± SEM from all 119 HD found in this study.

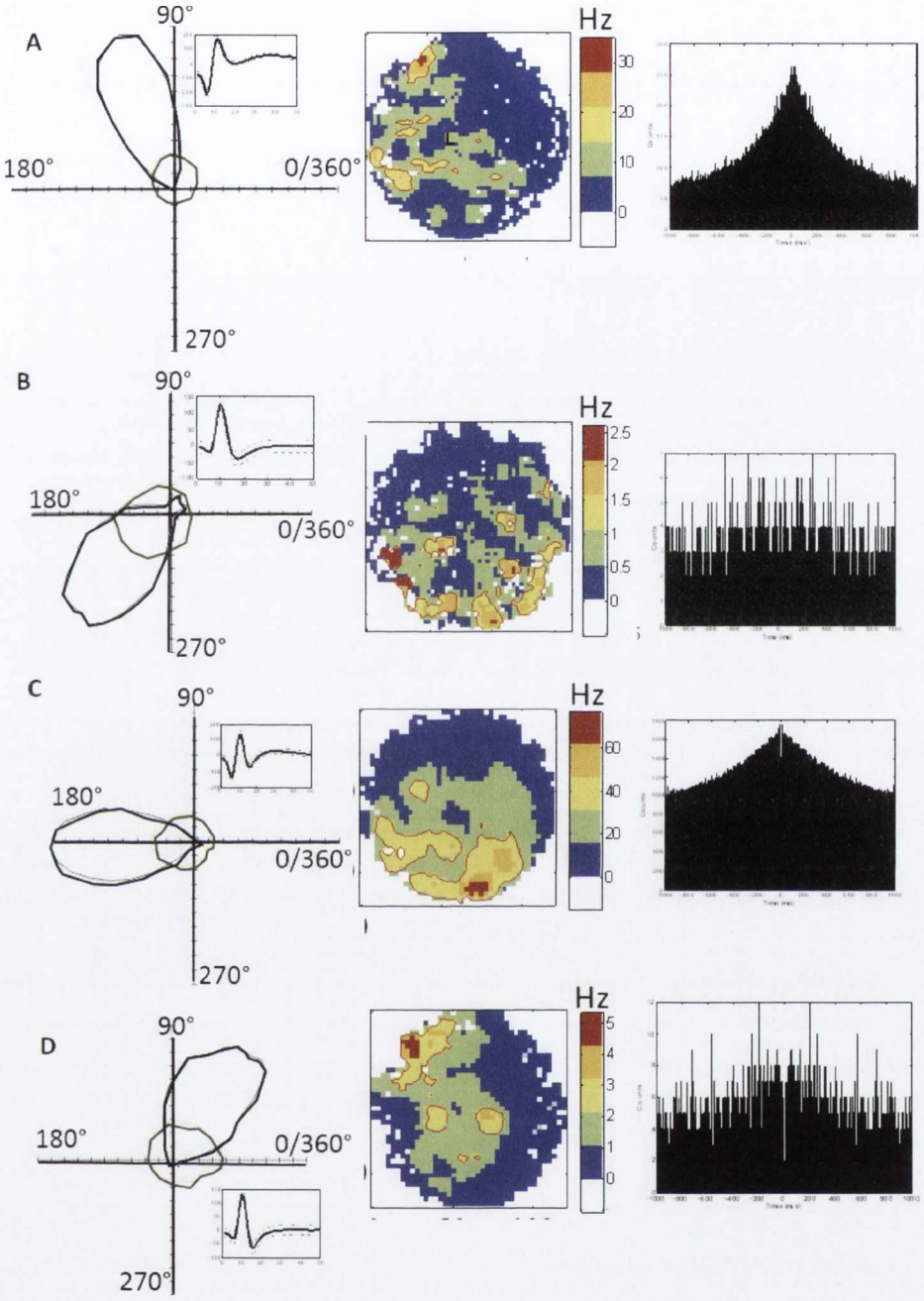


Figure 15. Four typical HD units recorded in anterior RSC of the freely-moving rat (A, B, C & D). From left to right, HD polar plot indicating preferred firing direction for unit, unit waveform, firing rate map and ±1000ms ACH indicating no obvious frequency modulation.

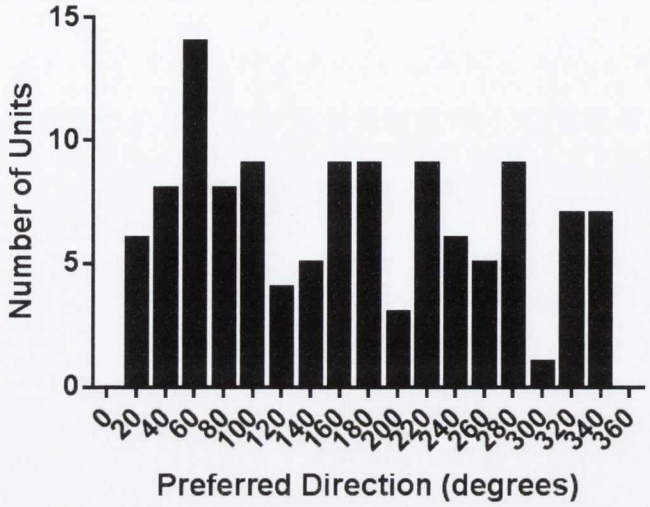


Figure 16. Frequency distribution of peak head direction for all 119 head direction units recorded in the anterior RSC of the freely moving rat. There appears to be an even spread across the peak firing rate for all possible directions the rat can face but there is an obvious peak (14 occurrences) at around 60° and the lowest observation (1 occurrence) was observed at 300°.

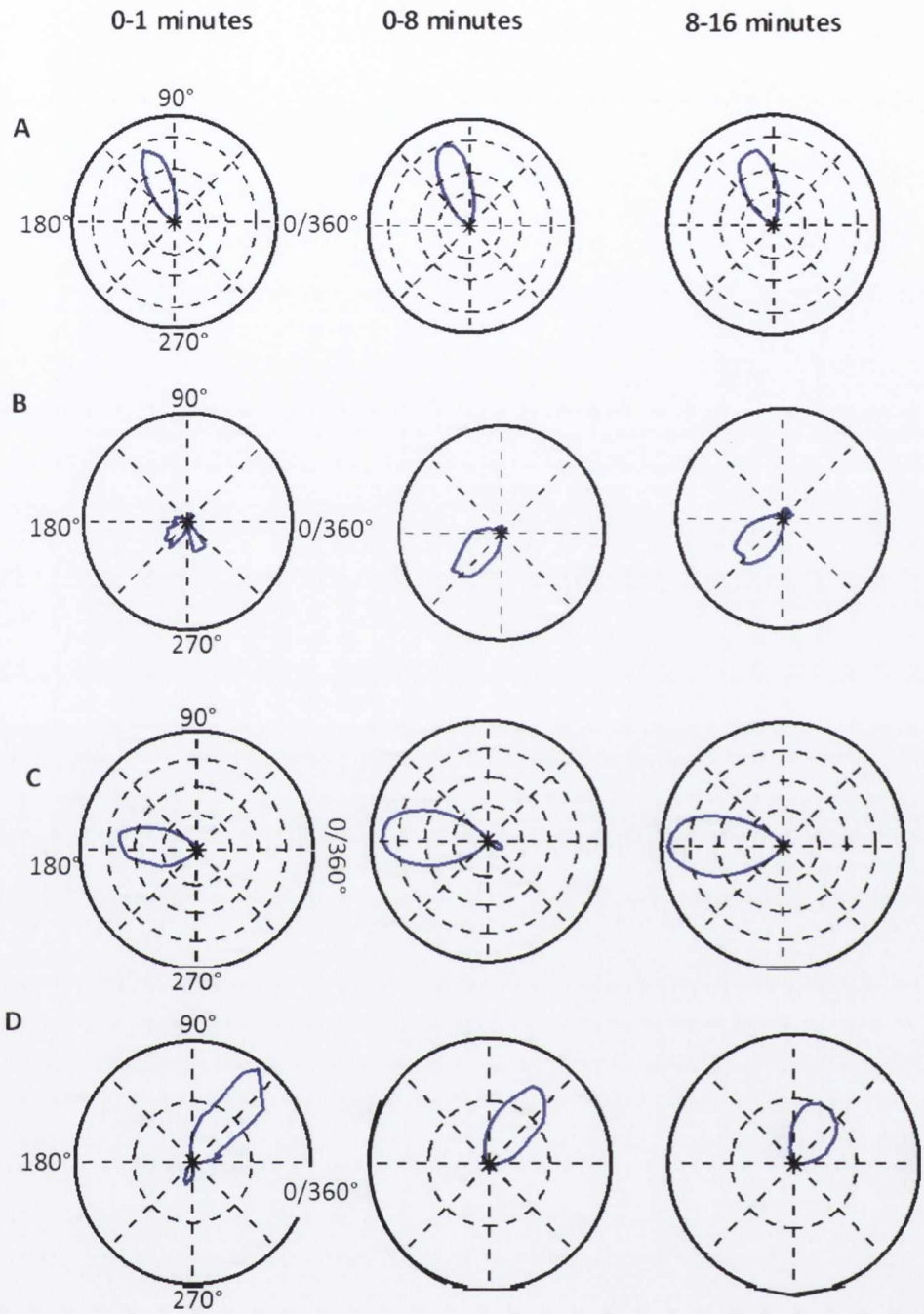


Figure 17. Temporal evolution of the 4 HD units represented in Figure 13 (A, B,C & D). Preferred firing direction is established upon first entry to the arena and remains constant throughout 16 minute trial.

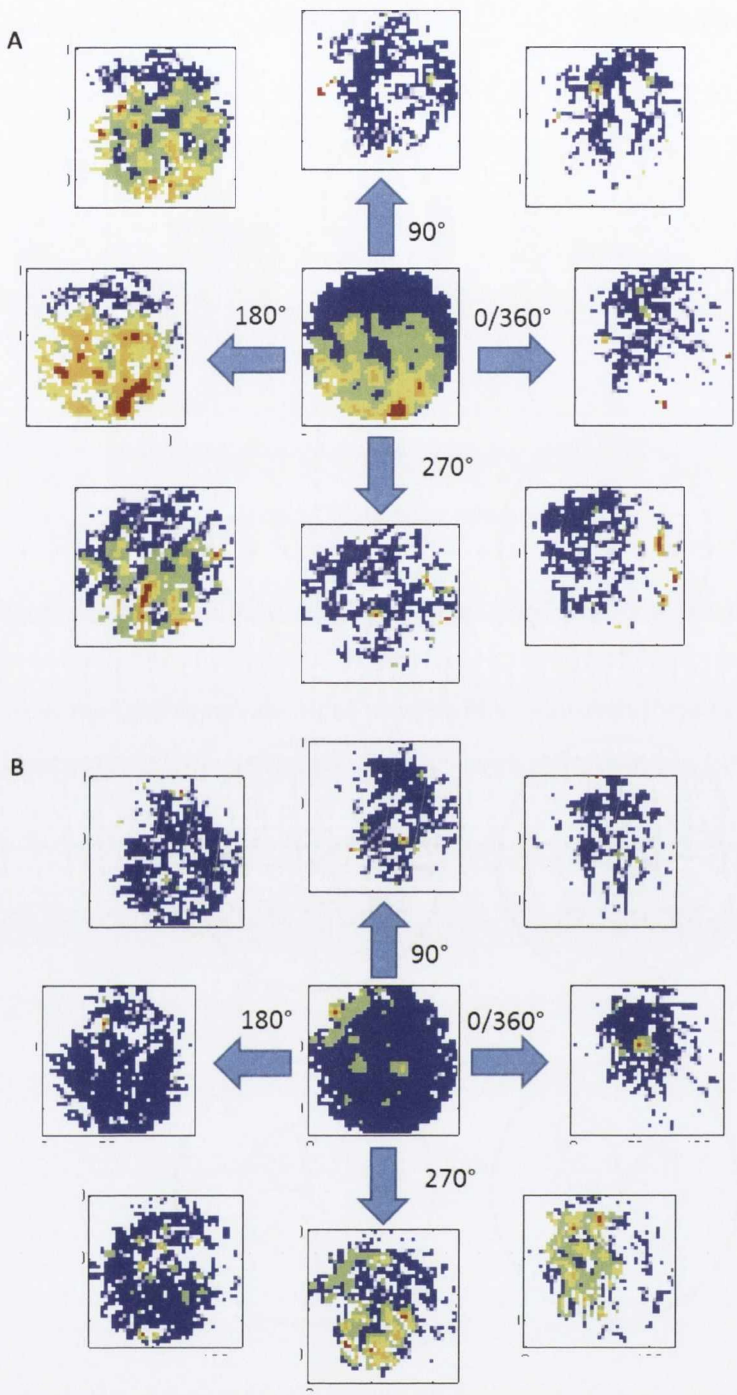


Figure 18. Spatial firing map at cardinal head orientations (0 to 360°, in 45° bins) for two HD units in the anterior RSC. A) Corresponds to HD unit C in Figure 13. B) Corresponds to HD unit D in Figure 13. It is apparent that there is no effect of spatial position on unit activity.

3.3.2 Separation angle (clockwise versus counter-clockwise head turns) is present.

For each HD unit recorded in anterior RSC two separate tuning curves were created with clockwise (CW) head turns only and counter-clockwise (CCW) head turns only (see fig 14A for an example). The difference (CW peak head direction subtracted from CCW peak head direction) between the two peaks can be calculated and is called the separation angle or delta. The separation angle for 93 out of the 119 HD units recorded in the anterior RSC was found. This was due to low firing rate and poor peak head directional identification, see chapter methods for details (section 3.2.4). Of the 93 head direction units analysed 82 units the CW peak were to the left of the CCW peak (CW<CCW), fig 19. The difference between CW peak firing and CCW peak firing were significantly different to 0 (1 sample Wilcoxon signed-ranks test; $p = 0.0001$, $p<0.01$). 9 units CW was to the right of CCW (CW>CCW) the separation angle was also found to be significantly different from 0 (1 sample Wilcoxon signed-ranks test; $p = 0.004$, $p<0.01$), fig 19. For only 2 units there was no difference ($p = 0.8$; $p>0.01$) between the peak head direction of the CW and CCW tuning curves (CW=CCW), see Figure 19. The frequency distribution of all separation angles from all anterior RSC head direction units can be observed in Figure 20.

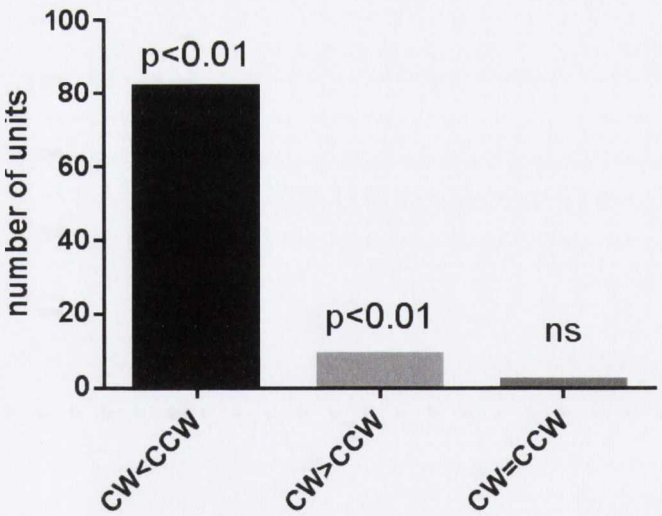


Figure 19. Bar graph showing the number of cells in anterior RSC that had significant difference between their clockwise peak firing direction and their counter-clockwise peak firing direction. The graph shows that there are 82 units where CW<CCW, 9 units where CW>CCW and 2 units where CW=CCW. Only 2 were observed where CW and CCW peak HD were not significantly different to one another.

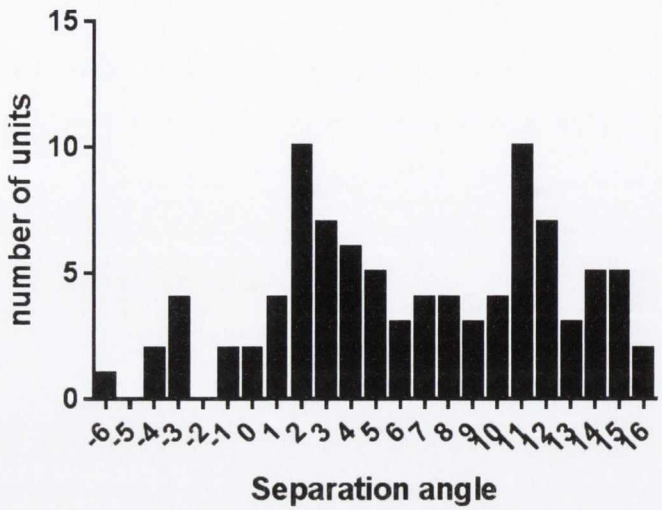


Figure 20. The frequency distribution of all 92 head direction units where a separation angle (CCW-CW) could be calculated. Negative separation angle when peak HD CW>CCW and positive separation angle when peak HD CW<CCW. Separation angle for anterior RSC HD cells ranged from -6° to 16° and is plotted on abscissa with number of units with this separation angle is plotted on the ordinate. There appears to be two peaks, one at 2° and the other at 11°.

3.3.3 Anticipatory properties of anterior RSC head direction units

The ATI could be calculated for 65 HD units out of 82, the other HD units the regression line did not cross zero or did not meet the statistical requirements. The mean ATI for these units was 40.9 ± 2.6 (SEM) ms. The mean temporal interval could be calculated for 4 out of the 9 HD units where (CW>CCW) was -16.4 ± 7.9 (SEM) ms. The negative value indicates that temporal interval is not strictly an ATI but is the time interval by which the unit encodes past head direction. Figure 21 shows the frequency distribution of all ATIs (positive numbers) and all HD units which were found to encode past head direction (negative ATI).

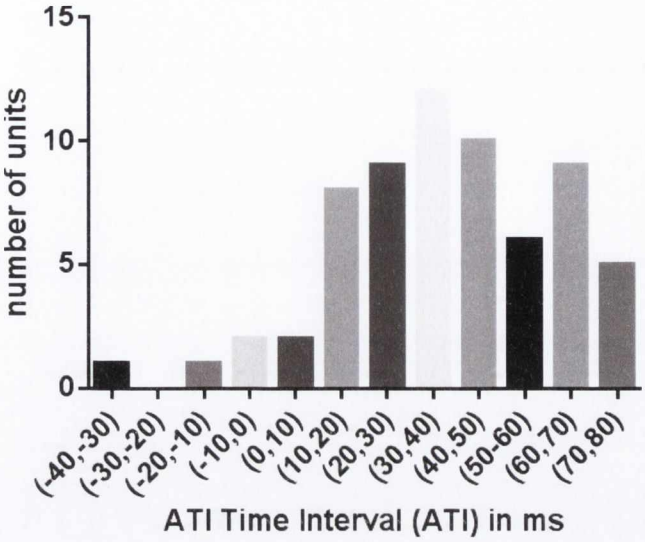


Figure 21. Grouped frequency distribution of ATI value (ms) for all 65 HD units in anterior RSC. ATI is grouped into 10ms bins on abscissa, and number of units falling into each 10ms bins is plotted on ordinate.

3.4.1 RSC HD unit's firing rates were positively and negatively correlated with running speed

The firing rates of only 35 out of 119 HD units recorded in the rodent anterior RSC were either positively or negatively correlated with running speed. Within this proportion there were 19 HD units demonstrated a positive correlation and 16 HD units which demonstrated a negative correlation with running speed. Table 11a and b provide a breakdown HD units whose firing rates were either positively or negatively correlated with running speed. See Figure 21 for examples.

Table 11a. Head direction units whose firing rates demonstrated a positive correlation with running speed

Unit classification, n, (percentage)*	Running speed, positive correlation number of units (% proportion)+		
	r = 0.4 to 0.6	r = 0.61 to 0.8	r = 0.81 to 1
Total units HD units (n=19,16%)	3(3%)	8(7%)	8(7%)

* Percentage proportion of unit class who's firing rates demonstrated correlation with running speed. + Percentage proportion.

Table 11b. Head direction units whose firing rates demonstrated a negative correlation with running speed

Unit classification, n, (percentage)*	Running speed, negative correlation number of units (% proportion)+		
	r = 0.4 to 0.6	r = 0.61 to 0.8	r=0.81 to 1
Total units HD units (n=16, 13%)	2(2%)	13(11%)	1(1%)

* Percentage proportion of unit class who's firing rates demonstrated correlation with running speed. + Percentage proportion.

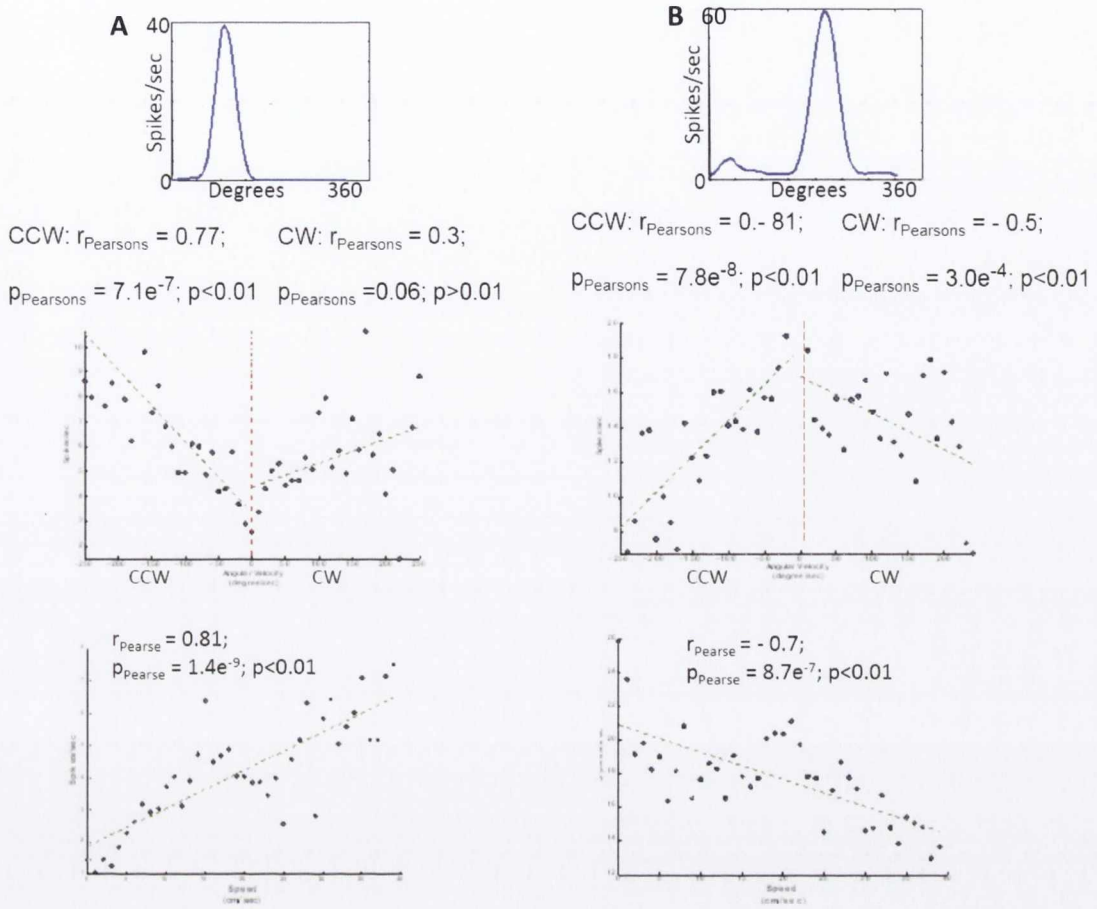


Figure 21 A and B. Example of 2 HD units, recorded in anterior RSC, spike rates correlated with angular head velocity (top) and running speed (bottom), - sign in front of r value denotes a negative correlation, no sign demonstrates a positive correlation. Pearson's r and p value are denoted above each Figure.

3.4.2 HD units whose firing rates were correlated with angular head velocity for clockwise only or counter-clockwise only head turns

The firing rates of 43 units out of 120 HD units were correlated with angular head velocity for either clockwise only or counter-clockwise only head turns (table 12a and b). There is an almost equal spread of HD units whose firing rates demonstrated positive or negative relationship with angular head velocity. See Figure 21A for an example of this type of unit.

Table 12a. HD units whose firing rates were positively correlated with angular head velocity for either clockwise only or counter clockwise only head turns

Unit classification, n, (percentage)*	Positive correlation (Number of units)+		
	r = 0.81 to 1	r = 0.61 to 0.8	r = 0.4 to 0.60
Proportion of HD units n=18, 15%)	3(3%)	15(13%)	

* Percentage proportion of unit class who's firing rates demonstrated correlation with angular head velocity. + Percentage proportion.

Table 12b. HD units whose firing rates were negatively correlated with angular head velocity for either clockwise only or counter clockwise only head turns

Unit classification, n, (percentage)*	Positive correlation (Number of units/% proportion)+		
	r = 0.81 to 1	r = 0.61 to 0.8	r = 0.4 to 0.6
Proportion of HD units n=16, (13%)	3(3%)	13(11%)	

* Percentage proportion of unit class who's firing rates demonstrated correlation with angular head velocity. + Percentage proportion.

3.4.3 HD Units whose firing rates were correlated with angular head velocity for both clockwise and counter-clockwise head turns.

There were also 33 HD units out of 119 recorded in anterior RSC whose spike rates were positively or negatively correlated with angular head velocity for both clockwise and counter-clockwise head turns (table 13a and b). The proportion of HD units whose spike rate demonstrated a positive or negative correlation with angular head velocity for both clockwise and counter-clockwise is equal. See Figure 21B for an example of this type of unit.

Table 13a. HD units whose firing activity was positively correlated with angular head velocity for both clockwise and counter-clockwise head turns.

Unit classification, n, (percentage)*	Negative correlation (Number of units)+		
	r= 0.81 to 1	r = 0.61 to 0.8	r = 0.4 to 0.6
Proportion of HD units (n=25, 21%)		19 (16%)	6(5%)

* Percentage proportion of unit class who's firing rates demonstrated correlation with angular head velocity. + Percentage proportion.

Table 13b. HD units whose firing activity was negatively correlated with angular head velocity for both clockwise and counter-clockwise head turns.

Unit classification, n, (percentage)*	Negative correlation (Number of units)+		
	r = 0.81 to 1	0.61 to 0.8	0.4 to 0.6
Proportion of HD units (n=17,14%)	4(3%)	13 (11%)	

* Percentage proportion of unit class who's firing rates demonstrated correlation with angular head velocity. + Percentage proportion.

3.5.1 Firing and directional properties of head direction units in anterior RSC in light and dark conditions.

The firing properties of 106 head direction units in anterior RSC were tested in the same open field arena in normal light conditions (light), dark conditions (dark) and then again in light conditions (light). Friedman's test revealed no statistical significant change ($x^2(2)=12.7$; $p = 0.017$, $p>0.01$) peak HD when measured in light 1 (Mdn 156; IQR 72 to 152) dark(Mdn 156; IQR 76 to 248) and light 2(Mdn 159; IQR 72 to 248) conditions (Figure 20). However, a Friedman's test revealed a significant change in peak HD firing rate ($x^2(2)=11.83$, $p = 0.002$, $p<0.01$), Figure 22. Dunn's post-hoc multiple comparison test revealed the only significant difference ($p=0.008$, $p<0.01$) was between light 1 (Mdn 49; IQR 14 to 50) and dark 2 conditions (Mdn 27; IQR 11, 47), there was no significance between light1 and light 2 (Mdn 29; IQR 10 to 47; $p = >0.99$) or between dark and light 2 ($p = 0.07$). Freidman's test also revealed no significant change occurred

to half-peak width of the HD tuning plot ($x^2(2)=1.048$; p = 0.59, p>0.01) during light 1 (Mdn 62;IQR 56 to 70), dark (Mdn 62; IQR 56,72) and light 2 (Mdn 62; IQR 56 to 72)conditions (Figure 22)

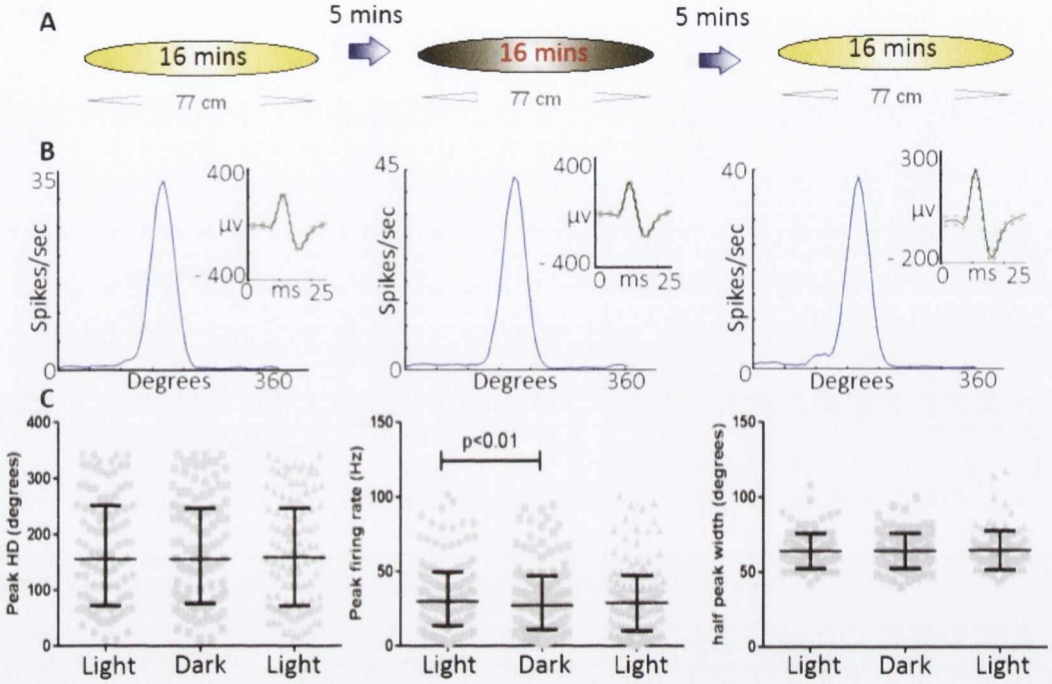


Fig 22. Head direction cells firing properties compared during different lighting conditions (n = 106). A) HD cells were first recorded in circular arena, lights on (left), circular arena, lights off (middle) and again in circle, lights on (right) each trial lasted 16 minutes with a 5 minute break between trials. B) An example of the same HD cell recorded during each trial, HD cell's tuning curve (left) and waveform (right) correspond to the above trial. C) Scatter plots (middle horizontal bar represents median and interquartile range is represented by the outer two horizontal bars) of peak HD, left; peak firing rate (Hz), middle and half peak width (degrees), right. See section 3.5.1 for median and interquartile ranges for each parameter during different lighting conditions and statistical comparisons.

3.5.2 Firing and directional properties of head direction units in anterior RSC in the open-field arena without perimeter walls and with perimeter walls.

There were 101 HD units recorded in the anterior RSC of the freely-moving rat whose directional and firing properties were observed firstly in the circle without perimeter walls (Circle 1), circle with perimeter walls present (Circle w/walls) and re-tested in the circle without perimeter walls present (Circle 2). No statistically significant change (Friedman's test (($x^2(2)=0.056$; $p = 0.97$, $p>0.01$) was observed in peak HD when HD units were recorded in Circle 1(Mdn 168;IQR 75 to 275), Circle w/walls (Mdn 150;IQR 78 to 249) and Circle 2 (Mdn 168;IQR 78 to 270), see Figure 23. Friedman's test also revealed there was no significant change to peak HD firing rate ($x^2(2)=6.02$; $p = 0.049$, $p>0.01$) when comparison was made between unit recording in Circle 1(Mdn 35;IQR 12 to 53), Circle w/walls (Mdn 29.66; IQR 12 to 51) and Circle 2(Mdn 32; IQR 14 to 55), see Figure 23. However, the Friedman's test revealed that half peak width of the HD tuning plot was significantly different ($x^2(2)=11.96$; $p = 0.003$, $p<0.01$) when comparisons were made between circle (Mdn 62; IQR 54 to 70), Circle w/walls (Mdn 62; IQR 56 to 74) and circle (Mdn 62; IQR 54 to 72). Dunn's post hoc multiple comparisons test revealed that the only significant difference in half peak tuning width was observed between Circle w/walls and the second recording session in circle ($p = 0.0056$; $p<0.01$), see Figure 23.

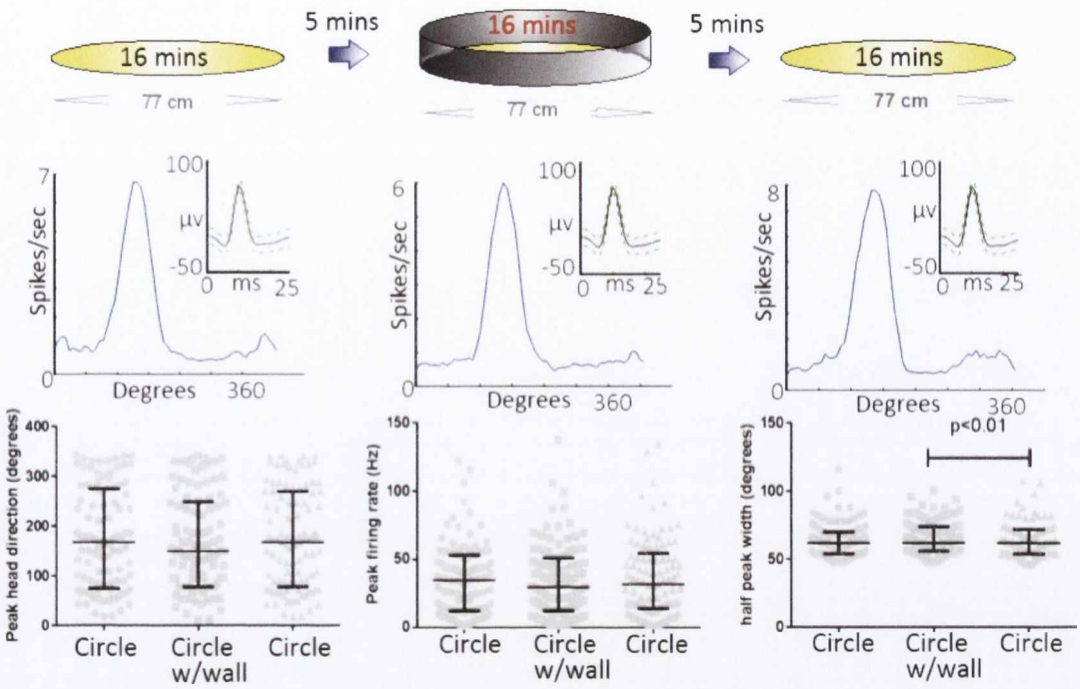


Fig 23. Head direction cells firing properties compared in the open arena without and with perimeter walls present (n = 101). A)) HD cells were first recorded in circular arena (left), no walls, circular arena with walls (middle) and again in circular arena, no walls (right) each trial lasted 16 minutes with a 5 minute break between trials. B) An example of the same HD cell recorded during each trial, HD cell's tuning curve (left) and waveform (right) correspond to the above trial.) recording session. C) Scatter plots (middle horizontal bar represents median and interquartile range is represented by the outer two horizontal bars) of peak HD, left; peak firing rate (Hz), middle and half peak width (degrees), right. See section 3.5.2 for median and interquartile ranges for each parameter during different lighting conditions and statistical comparisons.

3.5.3 Firing and directional properties of head direction units in anterior RSC in a varying size but same shape open-field arena.

The directional and firing properties of 94 HD units recorded in anterior RSC of the freely moving rat were compared in a small circular arena (small circle), large circular arena (circle), finally re-tested in the small circular arena (small circle). Friedman's test revealed no statistically significant change ($x^2(2)=1.88$; $p = 0.38$, $p>0.01$) in peak head direction when HD units were recorded in small circle (Mdn 177; IQR 78 to 287), circle (Mdn 174;IQR 73 to 281) and again in small circle (Mdn 180; IQR 77 to 287), Figure 24. Friedman's test also revealed no significant difference ($x^2(2)=4.23$; $p = 0.12$;$p>0.01$) was observed in peak rate when the first recording trial in small circle (Mdn 33; IQR 11 to 51), circle (Mdn 31; IQR 11 to 47) and the second recording trial in

small circle (Mdn 32; IQR 11 to 53) were compared, Figure 24. No statistical significant change ($x^2(2)=0.94$; $p = 0.62$, $p>0.01$) in half-peak tuning width for HD units was observed when first trial in small circle (Mdn 60; IQR 56 to 70), circle(Mdn 62; IQR 56 to 70) and second trial in small circle (Mdn 62; IQR 56 to 70) were compared, Figure 24.

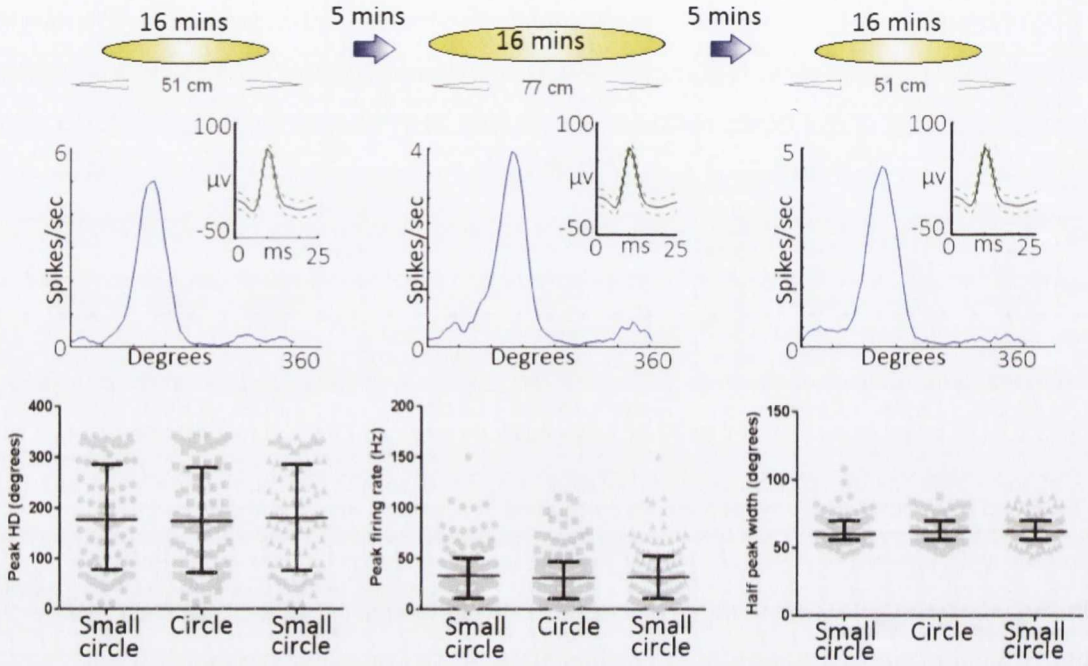


Fig 24. Head direction cells firing properties compared in the open arena without and with perimeter walls present (n = 94). A) HD cells were first recorded in small circular arena (left), large circular arena (middle) and again in small circle (right) each trial lasted 16 minutes with a 5 minute break between trials. B) An example of the same HD cell recorded during each trial, HD cell's tuning curve (left) and waveform (right) correspond to the above trial. C) Scatter plots (middle horizontal bar represents median and interquartile range is represented by the outer two horizontal bars) of peak HD, left; peak firing rate (Hz), middle and half peak width (degrees), right. See section 3.5.3 for median and interquartile ranges for each parameter when recorded in different sized arena and statistical comparisons.

3.5.4 Firing and directional properties of head direction units in anterior RSC in different shaped open-field arena.

86 HD units recorded in anterior RSC of the freely-moving rat were initially recorded in a circular arena (circle) then a square arena (square) and finally, again in the circular arena (circle) to assess any change in directional or firing properties as a result of arena shape. There was no significant effect of arena shape change on peak HD when circle 1 (Mdn 168; IQR 90 to 240),

square (Mdn 168; IQR 90 to 246) and circle 2 (Mdn 168; IQR 84 to 248) were compared using the Friedman test ($x^2(2)=4.45$; p = 0.11, p>0.01); Figure 29. Friedman's test revealed there was a significant change to peak HD rate as a result of arena shape change ($x^2(2)=13.6$; p = 0.002,p<0.01) when circle (Mdn 30; IQR 12 to 56), square (Mdn 26; IQR 12 to 49) and the second recording trial in circle (Mdn 27; IQR 12 to 50) were compared. Dunn's post-hoc multiple test comparison revealed the significant difference was observed between the recording trial in the first circle and square (p = 0.002, p<0.01); Figure 25. There was no significant effect of shape of arena on the half peak width of HD direction units recorded in anterior RSC, Friedman's test, $x^2(2)=4.24$; p = 0.12, p>0.01) when first trial in circle (Mdn 60; IQR 55 to 71), square (Mdn 60; IQR 52 to 72) and second trial in circle (Mdn 62; IQR 55 to 72) were compared (Figure 25).

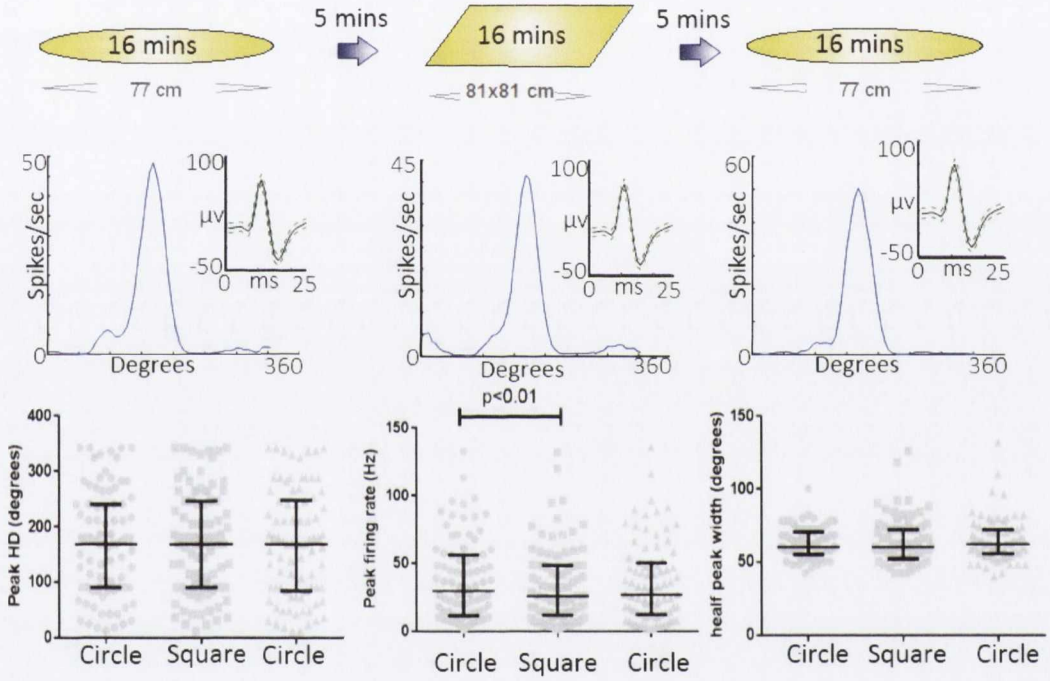


Fig 25. Head direction cells firing properties compared in the open arena without and with perimeter walls present (n = 86). A) HD cells were first recorded in circular arena (left), square arena (middle) and again in circular arena (right) each trial lasted 16 minutes with a 5 minute break between trials. B) An example of the same HD cell recorded during each trial, HD cell's tuning curve (left) and waveform (right) correspond to the above trial. C) Scatter plots (middle horizontal bar represents median and interquartile range is represented by the outer two horizontal bars) of peak HD, left; peak firing rate (Hz), middle and half peak width (degrees), right. See section 3.5.4 for median and interquartile ranges for each parameter when recorded in different shaped arena and statistical comparisons.

3.6 Discussion

The purpose of this chapter was to, first, describe the firing characteristics and waveform properties of any HD cells found in the anterior RSC and report their population. The second aim was to examine the effects of running speed and angular head velocity on HD cell firing activity. The third aim was to examine the effects of simple environmental changes on HD cells firing properties. In this study 15% of all cells recorded in the anterior RSC were HD cells. The population of HD cells in mid-caudal RSC was previously reported to be approximately 10% (Chen *et al.*, 1994 a; Chen *et al.*, 1994 b; Cho & Sharp, 2001). Anterior RSC HD cell activity did not depend on the location of the rat, firing activity was dependent on the rat orientating its head into the preferred firing direction for that HD cell. Anterior RSC HD cells were active in their preferred direction from first exposure into the arena and directionality was maintained throughout each trial. Peak firing rate for cells recorded in this study were almost identical to those found in mid-caudal RSC (Cho & Sharp, 2001). The tuning width of HD cells in this study were found to be more similar to those recorded in the postsubiculum and ADN than mid-caudal RSC (Blair & Sharp, 1995; Blair *et* al., 1997). The differences observed between anterior and mid-caudal RSC HD firing characteristics could be a result of varying density of projections, along its anterior-posterior axis, from other brain regions, which also contain HD cells (Van Groen & Wyss, 1990; Van Groen & Wyss, 1992; Van Groen & Wyss, 2003; Wyass & Van Groen, 1992).

Head direction units in anterior RSC like mid-caudal RSC (Chen *et al.*, 1994a; Chen *et al.*, 1994b; Cho and Sharp, 2001) firing activity were also correlated with running speed and angular head velocity. The source of the angular head velocity signal is likely to be the ADN which would relay projections from the vestibular neuclei (Fuchs & Kimm, 1975 and Keller & Kamath, 1975). The RSC is also connected with the primary, M1 and M2 cortices, it is likely that the RSC receives motor efference copy from either of these structures (Vogt & Miller, 1983). This may explain HD units whose firing rates were correlated with running speed. The function of the RSC is likely to be to integrate vestibular, head direction and running speed information (i.e. motor efference copy) received and project this information to the hippocampus via EC or subiculum. The ability to integrate these signals is likely to produce an ongoing vector representation of the rodent's trajectory this theoretically vital for the ability to be able to navigate in the dark and for path integration (Etienne *et al.*, 1998; McNaughton *et al.*, 2006; Mittelstaed M. & Mittelstaed H., 1980; Whishaw & Brooks, 1999). This would explain why lesion to the RSC impairs rodent's ability to navigate in the dark and to path integrate (Cooper et al., 2001; Elduayan & Save 2014).

In this study, HD cells in the anterior RSC were recorded during environmental changes, which included: shape of the arena; presence and absence of perimeter walls; light or dark conditions

and; size of the arena. Preferred head directionality was maintained throughout all sessions in this study, with only some changes to peak firing rate observed. Change to firing rate whilst directionality is maintained has been observed before when rodents have gone from light to dark conditions (Mizumori *et al.*, 2000). During darkness HD cells preferred direction was maintained, most likely, by idiothetic information (e.g. vestibular or motor efference copy). Peak firing rate was significantly different when comparisons were made between recordings in circle and square arena. For each trial the rat would have had access to the same visual cues so visual information could not explain this. One reason for this change could be that the rats' path or route around the square arena could be different to that of the circle. The activity of HD cells in anterior RSC were correlated with running speed and angular head velocity. The difference observed in firing rate here is likely due to a series of different body movements or running speeds which the rat employed in the square arena but not the circular arena.

A significant difference in half peak width of HD cells in anterior RSC was observed when the animal navigated the arena with opaque walls, compared to no arena walls. The rodent was present when walls placed on the arena, the removal of visual cues when the rat is present has been demonstrated to not alter the preferred directional firing of the HD cell (Goodridge *et al.*, 1998 and Taube *et al.*, 1990b). Also, there was a light on the ceiling which was on in every trial, perhaps serving as a visual landmark. However, when walls were present the rodent did not have access to other visual extramaze cues e.g. cue card on wall or recording room through the open part of the curtain. Perhaps the absence of these visual cues altered the range at which anterior RSC HD were active over. The mechanism or function whereby the direction that the HD cells are active over decrease when walls are present is not readily interpretable from these experiments. One might hypothesise that the directional specificity would decrease with opaque walls around the arena blocking visual landmarks. However, other studies have shown that RSC HD cells vary in their response to cue card rotation (Chen *et al.*, 1994 b). It could be the case that some HD cells in the anterior RSC depend more on visual cues than others. Another explanation is that when arena walls were present the rodent was able to touch them, through body contact or whiskers. This somatosensory information is likely to be projected to RSC via the parietal cortex (Burcham *et al.*, 1997; Reep *et al.*, 1994), could account for the difference in half-peak width observed here.

The changes in half peak width like firing rate during environmental manipulations, although statistically significant, were small. It should also be noted that the preferred firing directions of anterior RSC HD cells were not statistically different when compared during changes to the

environment. The environmental changes that anterior RSC HD cells were subject to were part of a wider experiment to examine the spatial properties of all cells in anterior RSC. Therefore, in order to understand the importance of visual or idiothetic information for anterior RSC HD cells more specific tests would have to be undertaken than those used in this study. More specific experiments may include recording anterior RSC HD cells during classic cue card rotations within a closed curtain environment and during behavioural navigation tasks designed to test the specific contributions of visual and idiothetic information specific for these cells activity.

The findings of this study question the origin of the HD signal. The HD signal is thought to originate in the DTN and LMN, project to ADN then enter the hippocampal formation via the postubiculum (Taube, 2007). The DTN contains several cell types whose activity are strongly correlated with only angular head velocity (Basset & Taube, 2001 and Sharp *et al.*, 2001). In addition the LMN also contains these cell types, as well as HD cells correlated with angular head velocity (Stackman & Taube, 1998). The presence of these cell types are thought to be crucial for the generation of the HD signal (Taube, 2007; Skaggs *et al.*, 1995). In support of this theory, lesion to the LMN disrupts the HD signal in the ADN (Bassett *et al.*, 2007 and Blair *et al.*, 1998) and postsubiculum (Sharp & Koeste, 2006) whereas lesion to the ADN only disrupts the HD signal in postsubiculum (Goodridge & Taube, 1997). Further support for this HD pathway was found when LMN cells were found to anticipate future head direction by approximately 40 ms (Blair & Sharp, 1998), ADN HD cells was found to anticipate by approximately 23ms (Blair & Sharp, 1995) whereas HD cells in the postsubiculum were found not to anticipate future head direction (Blair & Sharp, 1995). However, Cho & Sharp (2001) found that mid-caudal RSC HD cells anticipated future HD by approximately the same amount of time as ADN HD cells. Cho & Sharp (2001) also found cells who were correlated with angular head velocity and/or HD. This led Cho & Sharp (2001) to hypothesise that the HD signal is not just passively transferred to the cortex, but could contribute to its generation and transmission.

Like mid-caudal RSC anterior RSC contains cells whose activity is correlated with angular head velocity and HD cells whose activity is correlated with angular head velocity. However, to complicate the function of RSC HD cells further, anterior RSC HD cells were found to be more anticipatory than HD cells in the mid-caudal RSC. They were found to anticipate future HD by a similar time to the LMN. Mid-caudal RSC HD cells anticipate future head direction by a similar amount of time as the ADN. According to Cho and Sharp (2001) this could indicate that the RSC works in conjunction with LMN and DTN to generate the HD signal, for structures like the ADN. This theory, was tested as Taube lesioned the anterior portion of the RSC but left the posterior

portion intact. HD cells in the ADN were unaffected by this lesion (Reported in Taube, 2007 as unpublished observations). However, when the whole RSC was lesioned then ADN HD cells preferred firing direction would alter every few minutes (Clark *et al.*, 2010). However, due to the large size of the RSC and intrinsic as well as bilateral connections it is difficult to selectively lesion the RSC, the method is also important (Aggleton & Vann, 2004). One way to interpret these findings is that the anterior RSC receives projections from other brain areas which contain HD units, for example, the nucleus reuniens. It would be of interest to lesion anterior RSC and record HD units in other brain areas which contain HD cells which are connected to anterior RSC. Nonetheless, the findings of Clark *et al.*, (2010) give insight into the function of the RSC. The role of the RSC could be to integrate visual and idiothetic information with the HD signal received and project this to the postsubiculum or mEC. This would explain why RSC lesioned rodents demonstrate impairment during navigational tasks in light conditions; especially when the task taxes the head direction system (Pothuizen et al., 2008).

Anterior RSC HD cells are also not just simply cells which are driven by visual cues as their directionality is maintained in the dark. This is probably due to HD cell's activity also being driven by idiothetic inputs from the vestibular system and motor efference copy. HD units with angular head velocity correlates and running speed correlates, found in the anterior RSC, provide the neural basis of vector creation which is of theoretical importance for path integration. Angular head velocity units and HD units with angular head velocity correlates are hypothesised to be important for generation of the HD signal. Similar units are found in the LMB and DTN, thought to be the origin of the HD signal. Anterior RSC cortex HD cells were found to anticipate future head direction by the same amount of time as the LMN. Lesion of the whole RSC, but not anterior RSC impairs HD units in the ADN. The role of the anterior RSC during light conditions could be to integrate visual cues, via projections area 17 and 18b, with the HD signal projected to it from brain structures which contain HD units (e.g. nucleus reuniens). During dark conditions, the function of the anterior RSC is likely to be to integrate HD information from structures which project HD information to it, with motor efference copy and angular head velocity. It is more likely that the anterior RSC, during light conditions, integrates visual and idiothetic information at the same time. This would explain why lesion of the RSC disrupts navigation during light conditions and dark conditions. Further experiments are required to delineate what is the function of the anterior RSC and what contribution it makes to the head direction system.

4. Perimeter, Corona, Centre-Firing and Gradient (Boundary sensitive) Units Recorded in the Anterior Retrosplenial Cortex of the Freely-Moving Rat

4.1 Introduction

Place cells are pyramidal cells found in the CA1 and CA3 of the hippocampus, and are most commonly studied in the rat. Each place cell is active within a discrete area of the environment (ie. place field). Different place cells are active at different locations within an environment; the combination of activity of many place cells creates an internal neural map of the environment (O'Keefe, 1971; O'Keefe & Nadel, 1978). Approximately 90% of pyramidal cells in the CA1 and CA3 are place cells and approximately 15 to 50% of this population are active in any one environment (Gothard *et al.*, 1996; Thompson & Best, 1989; Wilson & McNaughton, 1993). Grid cells were discovered in both superficial and deeper layers of medial entorhinal cortex (mEC). Unlike place cells, which have a discrete firing location, grid cells fire in multiple locations within the environment that together form nodes of an extended hexagonal grid (Hafting *et al.*, 2005). Grid cell activity has been proposed by some researchers to be crucial for place cell activity and maintenance of place field location within an environment (de Almeida *et al.*, 2009; Hasselmo, 2009; Hayman & Jeffery, 2008; Lyttle *et al.*, 2013; Monaco & Abbott, 2011; O'Keefe & Burgess, 2005; Rolls *et al.*, 2006; Savelli & Knierim, 2010).

In support of this theory the mEC is the principal excitatory cortical input to the hippocampus (Van Strien *et al.*, 2009), and place cells in CA1 which receive the densest projections from mEC demonstrate the most spatial specificity (Henriksen *et* al., 2010). Place cells in ventral hippocampus have larger place fields than place cells recorded in dorsal hippocampus (Jung *et al.*, 1994; Kjelstrup *et al.*, 2008; Poucet *et al.*, 1994). Grid cells in mEC demonstrate a similar topography as ventral mEC grid cells have a larger grid scale than grid cells in the dorsal mEC (Barry *et al.*, 2007; Stensola *et al.*, 2012). Projections from mEC grid cells to hippocampal place cells are also topographic, ventral mEC grid cells project to ventral hippocampal place cells and dorsal mEC grid cells project to dorsal hippocampal place cells (Lyttle *et al.,* 2013; Solstad *et al.*, 2006).

In further support of grid cells importance, place cells, which were active at a specific phase of theta, were temporally silenced then reactivated, these cells were active at the same theta phase as before inactivation (Zugaro *et al.*, 2005). Grid cells from the mEC which project to the CA1 also display theta phase specific firing and could account for correct theta phase firing when place cells were reactivated (Hafting *et al.*, 2008). To test the theory that grid cells and not an intra-hippocampal circuit established and maintained place cell activity, rodent CA3 was lesioned but place cell activity in CA1 was not abolished (Brun *et al.*, 2002; Nakashiba *et al.*, 2008). Subsequently, based on these empirical findings, many theoretical models were created which

provided evidence that hippocampal place fields could be generated by combining grid cell firing patterns with different spatial scales (de Almeida *et al.*, 2009; Hasselmo, 2009; Hayman & Jeffery, 2008; Lyttle *et al.*, 2013; Monaco & Abbott, 2011; O'Keefe & Burgess, 2005; Rolls *et al.*, 2006; Savelli & Knierim, 2010). However, recent experimental findings and theoretical models have cast doubt on the importance of grid cells for place cell activity (Barry *et al.*, 2006; Bush *et al.*, 2014; Lever *et al.* 2009; Poucet *et al.*, 2014)

Single-unit recordings in pre-weanling rats leaving the nest for the first time revealed that grid cells with stable firing patterns did not appear for a few days. However, stable place cells were formed immediately after the rodent left the nest (Langston *et al.*, 2010; Wills *et al.*, 2010). Recordings of adult rodent place cells, with established firing fields in a known environment when recorded in a novel environment the preferred location of firing, i.e. the place field, is rapidly established (Frank *et al.*, 2004; Hill, 1978; Wilson & McNaughton, 1993). A temporary increase in the size of the place field is observed during initial navigation of the novel environment, but the size of the place field in the novel environment quickly returns to a similar size observed in the familiar environment (Barry *et al.*, 2012). However, during exposure to novel environments the grid scale of grid cells greatly increases in size (Barry *et al.*, 2012). Unlike place fields, grid cell firing properties do not return to baseline quickly and the enlarged firing properties persist for many hours in the novel environment (Barry *et al.*, 2012). Furthermore, complete bilateral lesion of the mEC did not completely abolish the activity of CA1 hippocampal place cells but did decrease the overall proportion of these cells (Hales *et al.*, 2014). Therefore, if place cells are still present in CA1 despite lesion to the mEC, then grid cells cannot solely account for establishment and maintenance of place cell firing fields.

Experimental data demonstrates that location of place fields in a novel environment can be predicted by its position relative to previous environmental boundaries (Hartley *et al.*, 2000; Lever *et al.*, 2002; O'Keefe & Burgess, 1996). Additional place fields often develop in the same relative position to addition of a boundary placed in a familiar environment (Bush *et al.*, 2014; Hartley *et al.*, 2000; O'Keefe & Burgess, 1996). Theoretical models hypothesised the existence of "boundary vector cells" within the hippocampal formation (Barry *et al.*, 2006) to explain this observation. These cells were predicted to encode the distance and direction of the rat relative to the environmental boundaries. This information is conveyed to hippocampal place cells via boundary vector cells, thus creating and maintaining stable firing fields. Cells which were active at the arena boundary, and demonstrated similar firing characteristics of those predicted in the boundary vector cell model were found in the rodent subiculum (Lever *et al.* 2009). Cells which

demonstrated similar firing properties were also described in the rodent mEC (Solstad *et al.*, 2008) and, post and para subiculum (Boccara *et al.*, 2010). Units which were active around the entire arena boundary, rather than just one section, were described in claustrum (Jankowski & O'Mara, 2015), nucleus reuniens and rosteral thalamus (Jankowski *et al.*, 2015). The reason why so many structures contain cells which encode environmental boundaries is not known. It is also not known if there is a hierarchy of importance between these structures, as the mEC is the primary input to the hippocampus it could provide the principal boundary input. To attempt to better understand boundary units, it would be of interest to delineate what inputs, from which structures, could drive boundary cell formation.

Interestingly, the rodent RSC receives projections and projects to brain areas which contain populations of boundary cells (Van Groen & Wyss, 1990; Van Groen & Wyss, 1992; Van Groen & Wyss, 2003; Wyass & Van Groen, 1992). Also, anatomical projections to and from these brain structures, as well as, other important brain areas associated with spatial navigation vary in density along the anterior-posterior axis of the RSC (Van Groen & Wyss, 1990; Van Groen & Wyss, 1992; Van Groen & Wyss, 2003; Wyass & Van Groen, 1992). The RSC receives projections from visual areas 18b and 17 and somatosenory information (e.g. vibrissae) from parietal cortex (Burcham *et al.*, 1997; Reep *et al.*, 1994; Van Groen & Wyss, 1990; Van Groen & Wyss, 1992; Van Groen & Wyss, 2003; Wyass & Van Groen, 1992) Lesions to RSC impairs the rodents ability to perform spatial navigation tasks and disrupts place cell firing fields (Cooper & Mizumori, 1999; Nelson *et al.*, 2015; Cooper & Mizumori, 2001; Meunier *et al.*, 1991; Sutherland *et al.*, 1988; Vann & Aggelton, 2002; Vann *et al.*, 2003; Vann & Aggelton, 2005).

Given the theoretical importance of environmental boundaries for spatial navigation, it is necessary to examine the RSC for the presence of cells which are active at or near the boundary of the arena. The presence of these cell types might explain the impaired performance of the rodent during spatial navigation tasks and CA1 place field disruption observed due to temporal lesioning of the RSC. It is also important to examine the firing properties of any boundary firing units during environmental manipulations. Comparison of firing properties in response to environmental change of boundary units in anterior RSC to those found elsewhere is important, as similar responses may give further insight into the connectivity of anterior RSC and its role in spatial navigation. The presence of boundary units in the anterior RSC would elude to the theory that anterior RSC could integrate the diverse sensory input probably needed to create boundary information and project this onto other brain regions which contain boundary cells.

4.2 Methods and statistics

The animals used in this chapter were the same animals used in chapters 2 and 3 (see chapter 2.2.1 methods section for implant coordinates). Recording sessions undertaken in this chapter were carried out in the same room as those for chapter 2 and chapter 3 methods section. The recording sessions and protocol in this chapter were identical to those described in chapter 3 (see section 3.2.1). But, see table 14, for each details of each recording session. The firing properties of single-units present in this chapter were subject to the same analysis as those described in methods chapter 2.

Table 14. Overview of recording session of rats in this chapter underwent.

	Trials undertaken in each session		
	Trial 1	Trial 2	Trial 3
Session 1	Light	Dark	Light
Session 2	Circle	Circle w/walls	Circle
Session 3	Small circle	circle	Small circle
Session 4	Circle	Square	Circle

See chapter 3 methods section (3.2.1) for details of arena and recording duration.

The frequency distribution of mean firing rates for each unit type for each trial, when plotted did not appear to be normally distributed. The distribution was formally tested for normality using the D'Agostino-Pearson omnibus test which also revealed the data were not normally distributed ($p>0.01$). Therefore, the Friedman's test with Dunn's post-hoc multiple comparison test, significance detected if $p<0.01$, was used to formally compare mean firing rates of all units within a unit class (e.g. perimeter units) between each trial in a recording session (e.g. light 1 vs dark vs light 2). The correct way to represent non-parametric data is to use median and interquartile range and this will be used throughout this chapter.

4.3 Results

4.3.1 Definitions of Perimeter, Corona, gradient and centre-firing units.

91 units of 812 recorded in anterior RSC whose activity appeared dependent on the rat's location within the environment, or more specifically, its proximity to the perimeter of the arena. No head direction dependent firing or theta-modulation was observed for any of these units. The terms used to describe these units and a working definitions are given below. Proportions, waveform properties and firing characteristics are presented in table 15.

Perimeter units: These units were only active around the arena perimeter (n=21) or, only one side or a discrete portion of the arena perimeter (n=15). Both of these types of perimeter units were combined into one group for analysis. See Figure 26 and 27 for example units.

Corona units: Corona units are active throughout the whole arena but have a higher firing frequency around the perimeter of the arena (n=12) or just before the perimeter of the arena (n=17). These groups were combined because it was not possible to exactly classify each cell into two groups only based on visual inspection of firing rate maps. See Figure 28 for an example units.

Centre firing units: These units were active throughout arena but when the rat moved its head over the arena perimeter firing activity decreased to below 20% of peak firing rate. See Figure 29 for an example unit.

Gradient units: The maximal firing rate was observed usually in the centre of the arena and decreased in a stepwise manner to less than 20% of peak firing rate around the perimeter of the arena. See Figure 30 for an example.

4.3.2 Formal statistical comparison of firing properties between unit classes

Kruskal-Wallace test with Dunn's multiple comparison were conducted to test for any significant differences in waveform or firing characteristics between unit classes.

The mean firing rates of all unit classes were compared and statistically significant differences were detected ($x^2(3) = 56.80$, $p<0.01$ (approximate p value = <0.0001). Dunn's post-hoc test revealed significant differences between mean firing rates of Perimeter units and Corona units (approximate pvalue = <0.0001), Gradient units (approximate pvalue = <0.0001) and, Centre firing units ($p = 0.0005$). The mean firing rates of no other unit classes, when compared, were statistically different.

Spike width of all unit classes were compared and statistically significant differences were detected ($x^2(3) = 29.63$, $p<0.01$ (approximate p value = <0.0001). Dunn's post-hoc test revealed significant differences between spike width of perimeter units and Corona units ($p<0.01$ approximate pvalue <0.0001) and, Gradient units ($p<0.01$, $p = 0.0021$). Spike width of Centre firing units was significantly different to Corona units ($p<0.01$, $p = 0.0037$). Spike width of no other unit classes, when compared, were statistically different. Spike amplitude of all unit classes were compared and no statistically significant differences were detected ($x^2(3) = 2.062$, $p>0.01$ ($p = 0.56$). Also, there was no statistically significant differences of propensity to burst when unit classes were compared (($x^2(3) = 8.95$, $p>0.01$ ($p = 0.029$).

Table 15. Proportion and basic firing properties of perimeter, corona, gradient and centre firing units recorded in the anterior RSC.

	Perimeter	Corona	Centre firing	Gradient
Number of units and proportion of total anterior RSC population (%).	36 (5%)	29 (4%)	6 (1%)	20(3%)
Mean firing rate (Hz)	1.52 ± 0.19	7.7 ± 1.2	2.8 ± 0.9	12.9 ± 1.9
Spike width (μS)	205.8 ± 6.7	152.7 ± 7.9	214.8 ± 21.4	160.9 ± 7.8
Spike amplitude (μV)	135 ± 7.3	150 ± 12.1	132.5 ± 7.3	155.7 ± 11.8
Propensity to burst	0.06 ± 0.02	0.02 ± 0.003	0.06 ± 0.2	0.06 ± 0.01

All unit data were recorded on the raised platform circle with no perimeter walls present (see methods 3.2.1 for recording session details). A total of 812 units were recorded, percentage proportion was calculated and rounded up to nearest whole number for each unit class. Descriptive parameters are shown as mean ± SEM.

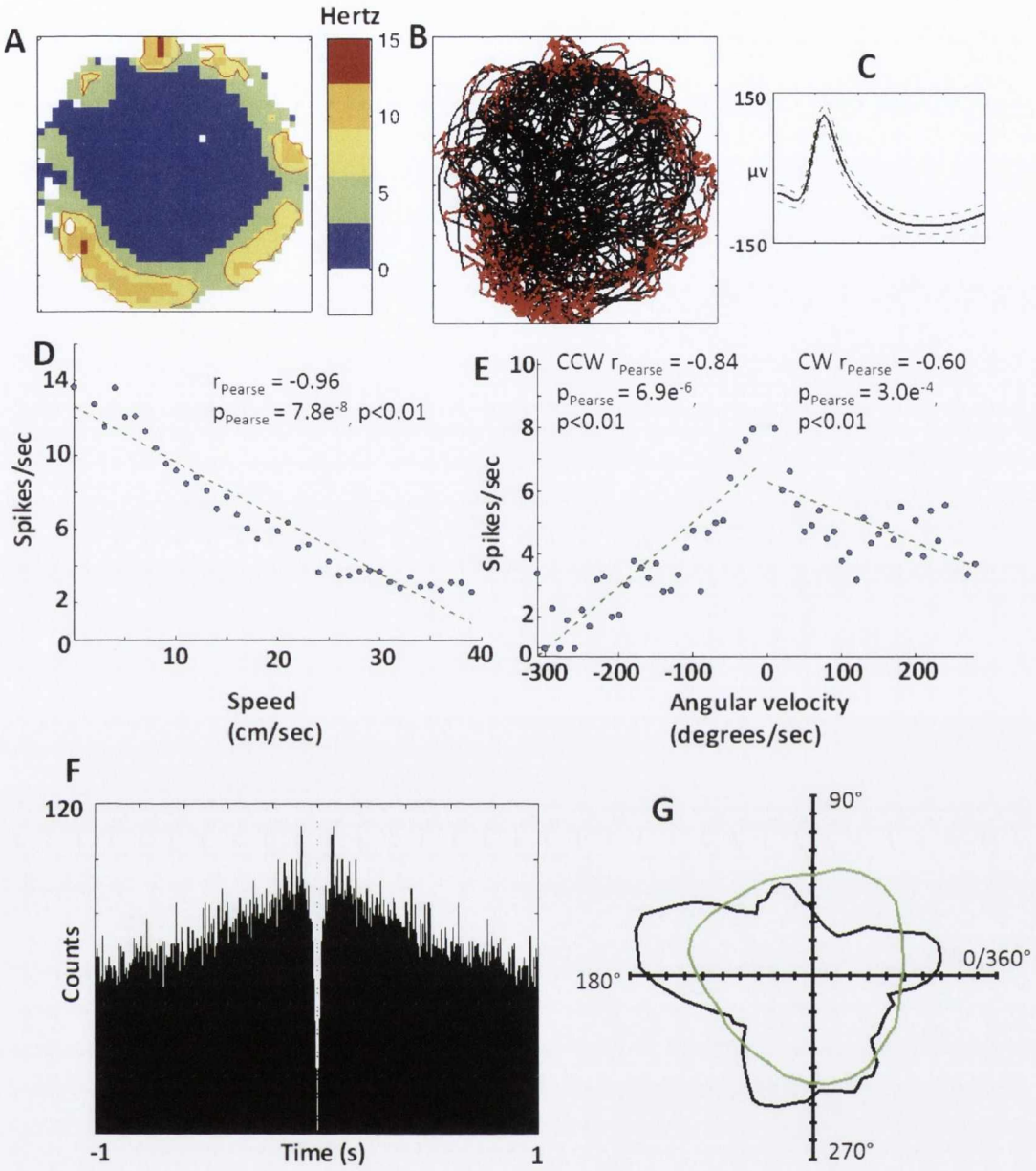


Figure 26. Spatial and temporal properties of a full perimeter unit in anterior RSC. A) Firing rate map: peak firing rate is red, blue is 20% of peak firing rate. B) Rats complete path through arena, red dots overlaid represent unit activity. C) Waveform of full perimeter unit. D) Spiking activity of this unit was negatively correlated with running speed. E) Spiking activity of this unit was negatively correlated with angular head velocity for both CCW and CW head turns. F) ±1000ms autocorrelation histogram demonstrating no theta frequency modulation. G) The firing activity of this unit was not dependent on head direction.

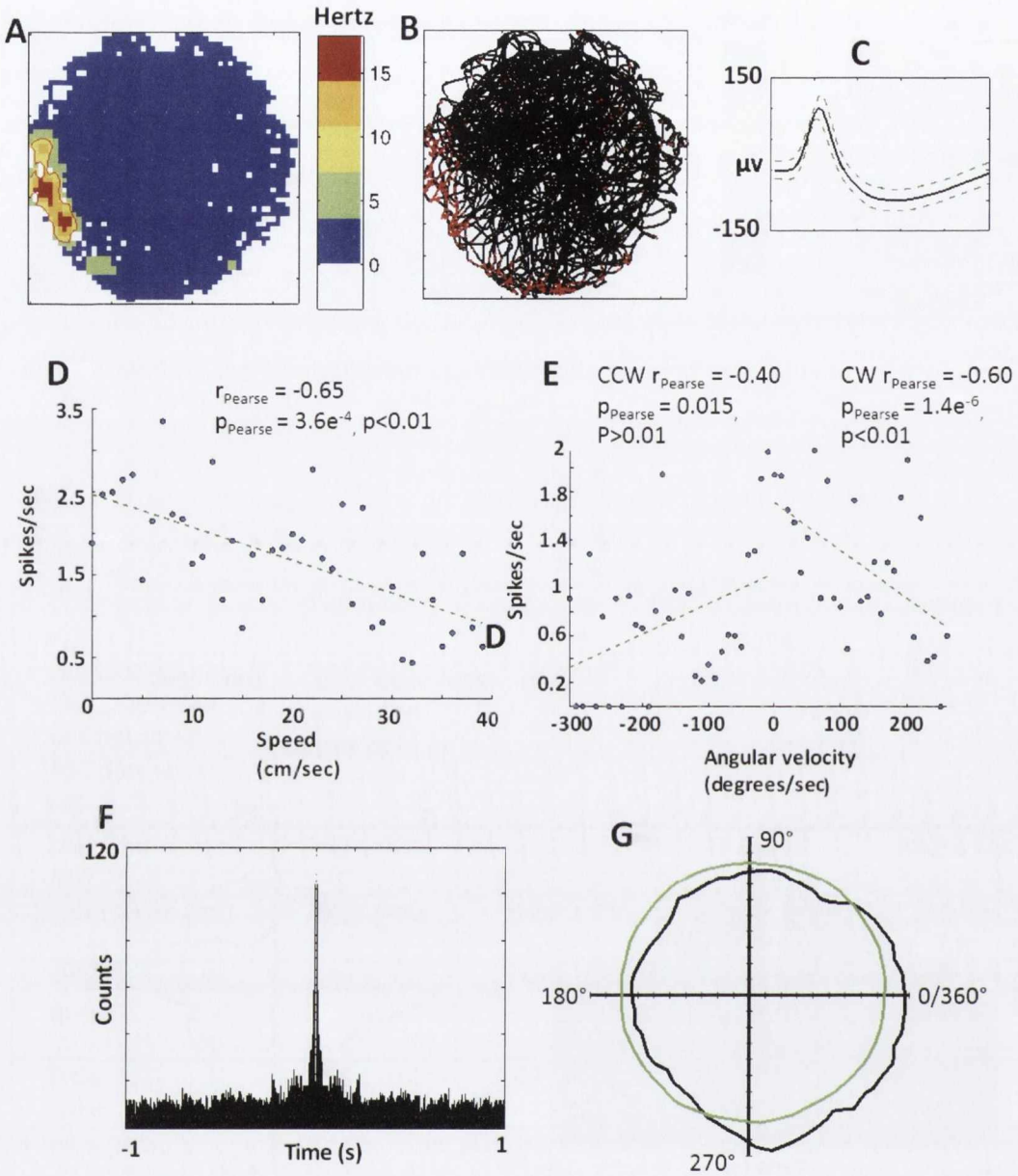


Figure 27. Spatial and temporal properties of a partial perimeter unit in anterior RSC. A) Firing rate map: peak firing rate is red, blue is 20% of peak firing rate. B) Rat's complete path through arena, red dots overlaid represent unit activity. C) Waveform of partial perimeter unit. D) Spiking activity of this unit was negatively correlated with running speed. E) Spiking activity of this unit was negatively correlated with angular head velocity for CCW direction but not CW head turns. F) ±1000ms autocorrelation histogram demonstrating no obvious theta frequency modulation. G) The firing activity of this unit was not dependent on head direction.

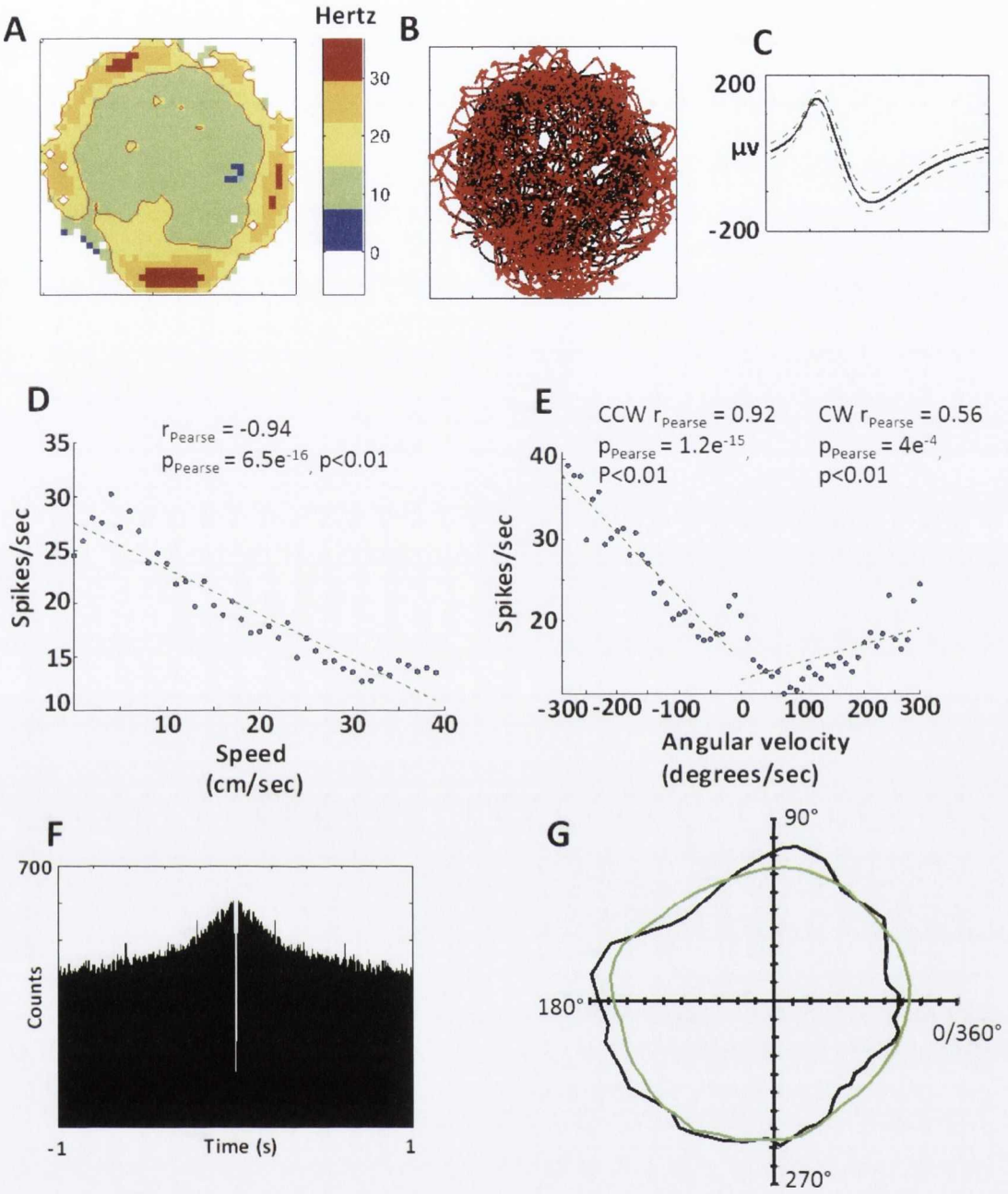


Figure 28. Spatial and temporal properties of a corona unit in anterior RSC. A) Firing rate map, firing rate map: peak firing rate is red, blue is 20% of peak firing rate. B) Rat's complete path through arena, red dots overlaid represent unit activity. C) Waveform of corona unit. D) Spiking activity of this unit was negatively correlated with running speed. E) Spiking activity of this unit was positively correlated with angular head velocity for both CCW and CW head turns. F) ±1000ms autocorrelation histogram demonstrating no obvious theta frequency modulation. G) The firing activity of this unit was not dependent on head direction.

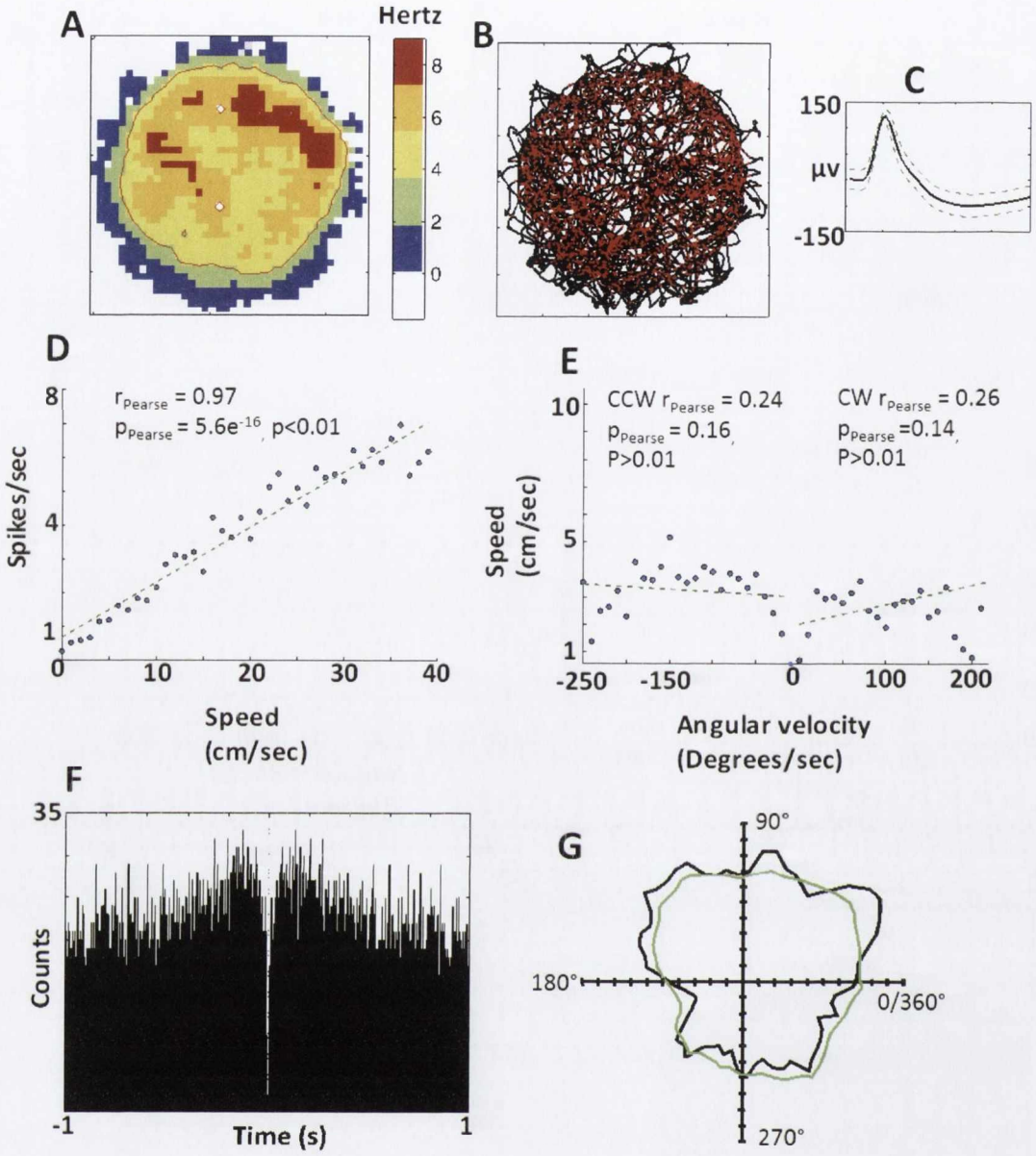


Figure 29. Spatial and temporal properties of a centre firing unit in anterior RSC. A) Firing rate map, firing rate map: peak firing rate is red, blue is 20% of peak firing rate. B) Rat's complete path through arena, red dots overlaid represent unit activity. C) Waveform of centre firing unit. D) Spiking activity of this unit was positively correlated with running speed. E) Spiking activity of this unit was not correlated with angular head velocity for either CCW or CW head turns. F) ±1000ms autocorrelation histogram demonstrating no obvious theta frequency modulation for this unit. G) The firing activity of this unit was not dependent on head direction.

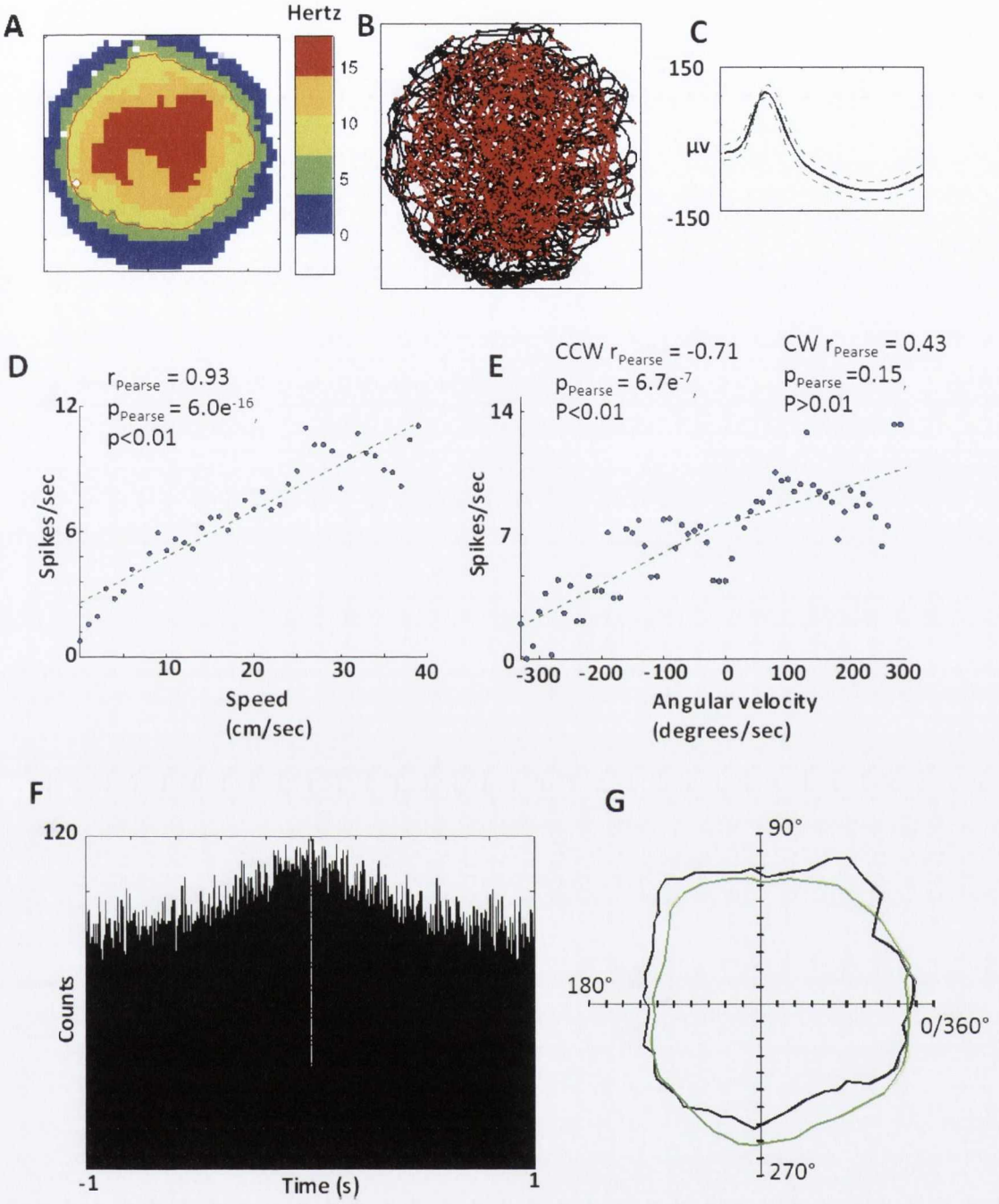


Figure 30. Spatial and temporal properties of a gradient unit in anterior RSC. A) Firing rate map: peak firing rate is red, blue is 20% of peak firing rate. B) Rat's complete path through arena, red dots overlaid represent unit activity. C) Waveform of gradient unit. D) Spiking activity of this unit was positively correlated with running speed. E) Spiking activity of this unit was negatively correlated with angular head velocity for only CCW head turns. F) ±1000ms autocorrelation histogram demonstrating no obvious theta frequency modulation for this unit. G) The firing activity of this unit was not dependent on head direction.

4.3.3 Boundary sensitive units whose firing rates were correlated with running speed

The firing activity of 23 perimeter units of 36 were either positively or negatively correlated with running speed. The firing activity of the majority of these units were negatively correlated with running speed. The firing activity of 23 corona units out of 29 were either positively or negatively correlated with running speed. The proportion of units whose firing rates were negatively correlated and positively correlated with running speed were equal. The firing rates of 5 out of 6 centre firing units were positively correlated with running speed. The firing rates of no centre firing units demonstrated a negative correlation with running speed. See table 16a and b for break of boundary sensitive units whose firing rates were either positively or negatively correlated with running speed.

Table 16a. Boundary sensitive units whose firing rates were positively correlated with running speed

Unit classification, n, (percentage)*	Running speed positive correlation (number of units, % proportion)+		
	r = 0.81 to 1	r = 0.61 to 0.8	r = 0.4 to 0.6
Perimeter (n=5,14%)		4(11%)	1(3%)
Corona (n=12, 41%)	6(21%)	5(17%)	1(3%)
Centre firing (n=5, 84%)	4 (67%)	1(17%)	
Gradient (n=15,75%)	10 (50%)	4 (20%)	1(5%)

* Percentage proportion of unit class who's firing rates demonstrated correlation with running speed. + Percentage proportion within each class of unit.

Table 16b. Boundary sensitive units whose firing rates were negatively correlated with running speed

Unit classification, n, (percentage)*	Running speed negative correlation (number of units, % proportion)+		
	r = 0.81 to 1	r = 0.61 to 0.8	r = 0.4 to 0.6
Perimeter (n=18, 50%)	9 (25%)	7(20%)	2(6%)
Corona (n=11, 38%)	5 (17%)	2 (7%)	4 (14%)
Centre firing (n=0, na%)			
Gradient (n=0,na%)			

* Percentage proportion of unit class who's firing rates demonstrated correlation with running speed. + Percentage proportion within each class of unit.

4.3.4 Boundary sensitive units whose firing rates were correlated with angular head velocity for either clockwise only or counter-clockwise only head turns

The firing rates of 13 perimeter units out of 36 were either positively or negatively correlated with angular head velocity for either clockwise or counter-clockwise only head turns (see table 17a and b). The firing rates for the majority of these units demonstrated a negative correlation with angular head velocity. The firing rates of 7 corona units out of 29 were either positively or negatively correlated with angular head velocity for either clockwise or counter-clockwise only head turns. The firing rates for the majority of these units demonstrated a negative correlation with angular head velocity. No centre firing units firing activity were found to be positively or negatively correlated with angular head velocity in this study. 6 of 20 gradient units firing activity were found to be either positively or negatively correlated with angular head velocity for clockwise head turns or counter-clockwise head turns only. The majority of these gradient units firing activity demonstrated a negative correlation with angular head velocity. See table 17a and b for details of the correlation between the firing rates of each unit class and angular head velocity for clockwise only or counter-clockwise only head turns.

Table 17a. Boundary sensitive units whose firing rates were positively correlated with angular head velocity for either clockwise only or counter-clockwise only head turns

Unit classification, n, (percentage)*	positive correlation (number of units, % proportion)+		
	r = 0.81 to 1	r = 0.61 to 0.8	r = 0.4 to 0.6
Perimeter (n=4,11%)		2(6%)	2(6%)
Corona (n=1,3%)			1(3%)
Centre firing (n=0,na%)			
Gradient (n=2,10%)			2(10%)

* Percentage proportion of unit class who's firing rates demonstrated correlation with angular head velocity. + Percentage proportion within each class of unit

Table 17b. Boundary sensitive units whose firing rates were negatively correlated with angular head velocity for either clockwise only or counter-clockwise only head turns

Unit classification, n, (percentage)*	negative correlation (number of units, % proportion)+		
	r = 0.81 to 1	r = 0.61 to 0.8	r = 0.4 to 0.6
Perimeter (n=9,25%)		9(25%)	
Corona (n=6,20%)		3(10%)	3(10%)
Centre firing (n=0,na%)			
Gradient (n=4,20%)		4(20%)	

* Percentage proportion of unit class who's firing rates demonstrated correlation with angular head velocity. + Percentage proportion within each class of unit

4.3.4 Boundary sensitive units whose firing rates were correlated with angular head velocity for both clockwise and counter-clockwise head turns

The firing rates of 6 perimeter units out of 36 were either positively or negatively correlated with angular head velocity for both clockwise and counter-clockwise head turns (see table 18a and b). The majority of these units firing rates demonstrated a negative correlation with angular head velocity. The firing rates of 5 corona units out of 29 demonstrated a negative correlation with angular head velocity for both clockwise and counter-clockwise head turns. There were no corona units whose firing rates were positively correlated with angular head velocity for both

clockwise and counter-clockwise head turns. There was one gradient unit whose firing activity was negatively correlated and one whose firing activity was positively correlated with angular head velocity for both clockwise and counter-clockwise head turns.

Table 18a. Boundary sensitive units whose firing rates were positively correlated with angular head velocity for both clockwise or counter-clockwise head turns

Unit classification, n, (percentage)*	positive correlation (number of units, % proportion)+		
	r= 0.81 to 1	0.61 to 0.8	0.4 to 0.6
Perimeter (n=1,3%)		1(3%)	
Corona (n=0,na%)			
Centre firing (n=0,na%)			
Gradient (n=1,5%)		1(5%)	

* Percentage proportion of unit class who's firing rates demonstrated correlation with angular head velocity. + Percentage proportion within each class of unit.

Table 18b. Boundary sensitive units whose firing rates were negatively correlated with angular head velocity for both clockwise or counter-clockwise head turns

Unit classification, n, (percentage)*	Negative correlation (number of units, % proportion)+		
	r= 0.81 to 1	r = 0.61 to 0.8	r = 0.4 to 0.6
Perimeter (n=5,14%)	2(5%)	3(8%)	
Corona (n=5,17%)	4(14%)	1(3%)	
Centre firing (n=0,na%)			
Gradient (n=1,5%)		1(5%)	

* Percentage proportion of unit class who's firing rates demonstrated correlation with angular head velocity. + Percentage proportion within each class of unit

4.4.1 Firing activity of perimeter units during environmental changes

Perimeter units, both those which were active around the full perimeter of the arena (Figure 31, cell #1) and those which were only active at discrete portions of the perimeter (Figure 31 cell #2)

maintain their place specific firing regardless of the shape of the arena. Friedman's test revealed no significant difference ($x^2(2)=4.5$; $p = 0.13$, $p>0.01$, $n=4$) in mean firing rate (Hz) when first trial in circle (Mdn 1.69 Hz; IQR 1.4 to 31), square (Mdn 1.2 Hz; IQR 0.9 to 33) and second trial in circle (Mdn 0.93 Hz; IQR 0.6 to 30) were compared.

Perimeter units, both those which were active throughout the whole perimeter of the arena (Figure 32, cell #3) and those which were only active at discrete portions of the perimeter (Figure 32, cell #4) maintain place specific firing in dark conditions. Friedman's test revealed no significant difference ($x^2(2)=1.75$; $p = 0.53$, $p>0.01$, $n=8$) in mean firing rate (Hz) of perimeter units when first light trial (Mdn 1.6 Hz; IQR 0.75Hz to 2.9), dark (Mdn 1.2 Hz; IQR 0.9 to 2.3) and second light trial (Mdn 1.2 Hz; IQR 0.9 to 2.4) were compared.

Visual inspection of the firing rate maps for perimeter cell #5 (Figure 33) reveals that, although this unit tends to fire more in the centre of the arena when walls were present, higher firing frequency was observed around the arena perimeter. There were four units in total like cell #6, in Figure 33, which were only active at discrete portions of the arena perimeter which were recorded in arena without walls and walls present. All four of these units, with arena walls present become active around the whole of the perimeter of the arena, Figure 33, cell #6. When perimeter walls were removed, all of these perimeter units returned to be active at the same discrete portion of the arena where it was previously active. Despite obvious visual changes to firing rate maps for these cells, Friedman's test revealed no statistical difference ($x^2(2)=3.0$; $p = 0.25$, $p>0.01$, $n=6$) in mean firing rate (Hz) when first circle trial (Mdn 2.7 Hz; IQR 0.7 to 3.8), circle with walls trial (Mdn 2.1 Hz; IQR 1.2 to 3.8) and second circle trial (Mdn 3.3 Hz; IQR 0.7 to 5.9) were compared.

Friedman's test revealed there was no significant difference ($x^2(2)=1.0$; $p = 0.74$, $p>0.01$, $n=6$) in mean firing rate (Hz) of perimeter units when first small circle trial (Mdn 1.9 Hz; IQR 1.1 to 2.8), circle trial (Mdn 2.9 Hz; IQR 1.3 to 4.1) and second small circle trial (Mdn 2.1 Hz; IQR 1.3 to 3.2) were compared. Visual inspection of the firing rate maps of perimeter units for small and large arena reveal no obvious changes to location of firing (Figure 34, cells #7 and #8).

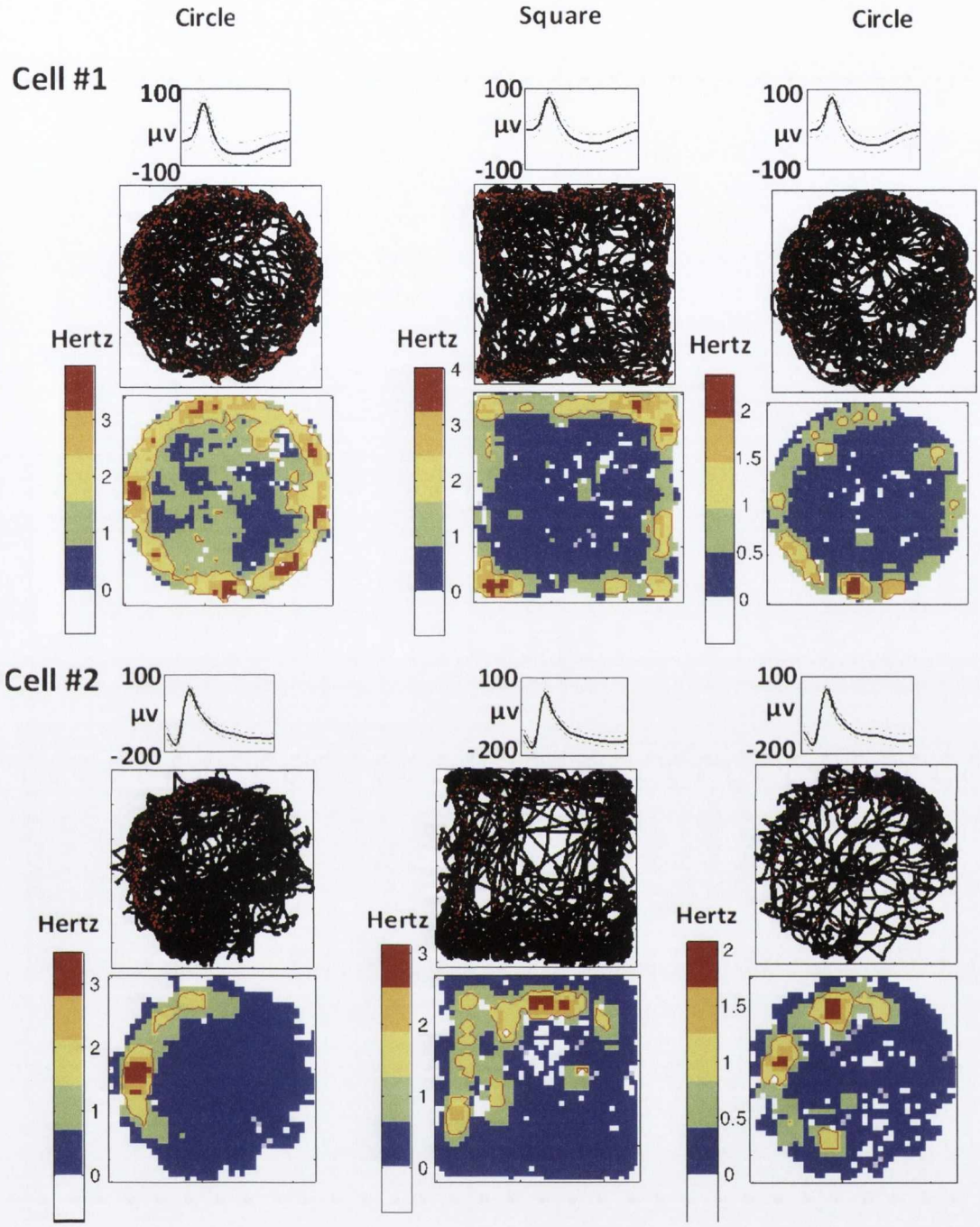


Figure 31. Waveform of and firing properties of perimeter units (cell #1 and #2) during circle, square then circle sessions. Firing rate map: peak firing rate is red, blue is 20% of peak firing rate. Cell #1 was active around the whole arena perimeter, cell #2 was active at only a discrete perimeter location.

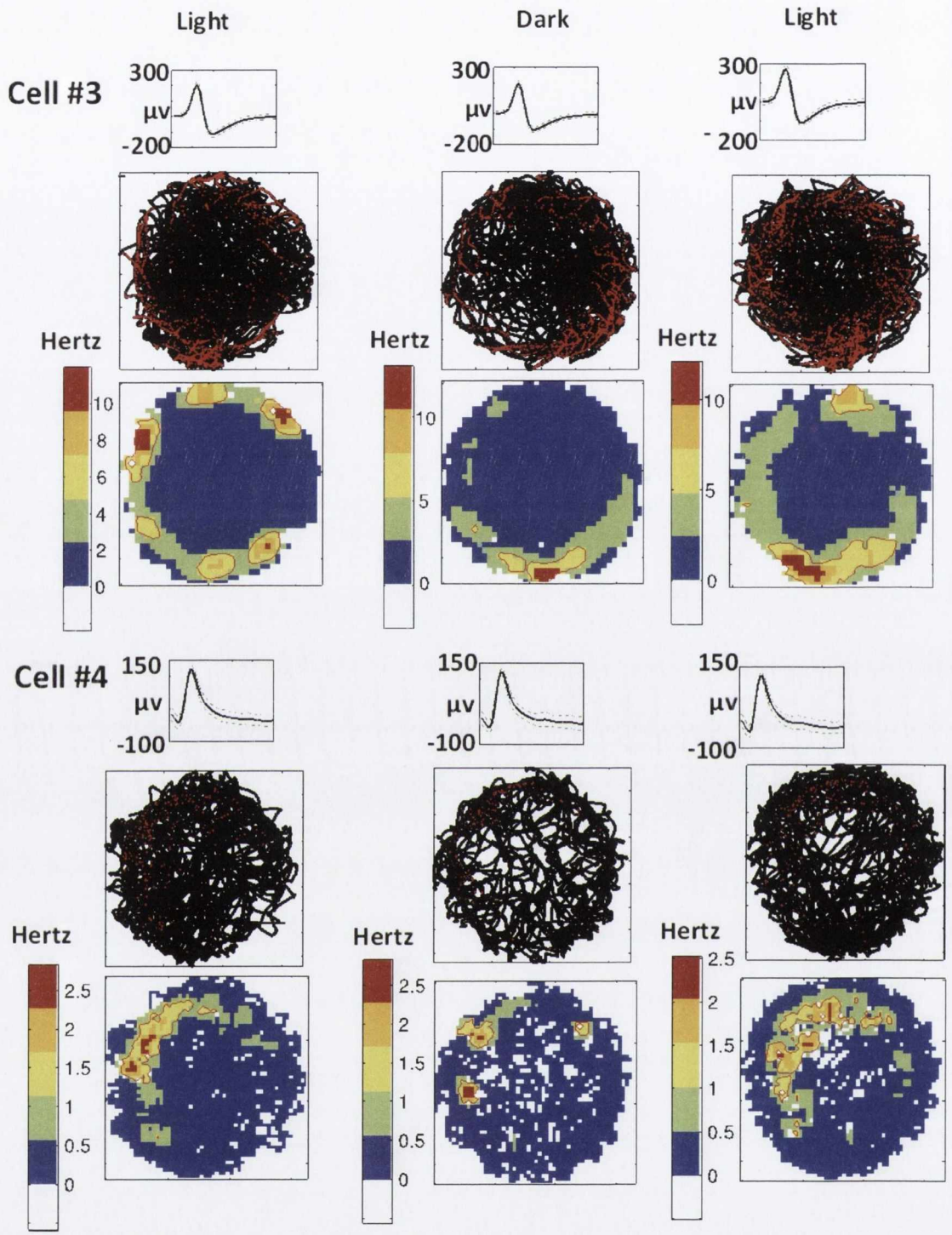


Figure 32. Waveform of and firing properties of perimeter units (cell #3 and #4) during light, dark then light sessions. Firing rate map: peak firing rate is red, blue is 20% of peak firing rate. Cell #3 was active around the whole arena perimeter, cell #4 was active at only a discrete perimeter location.

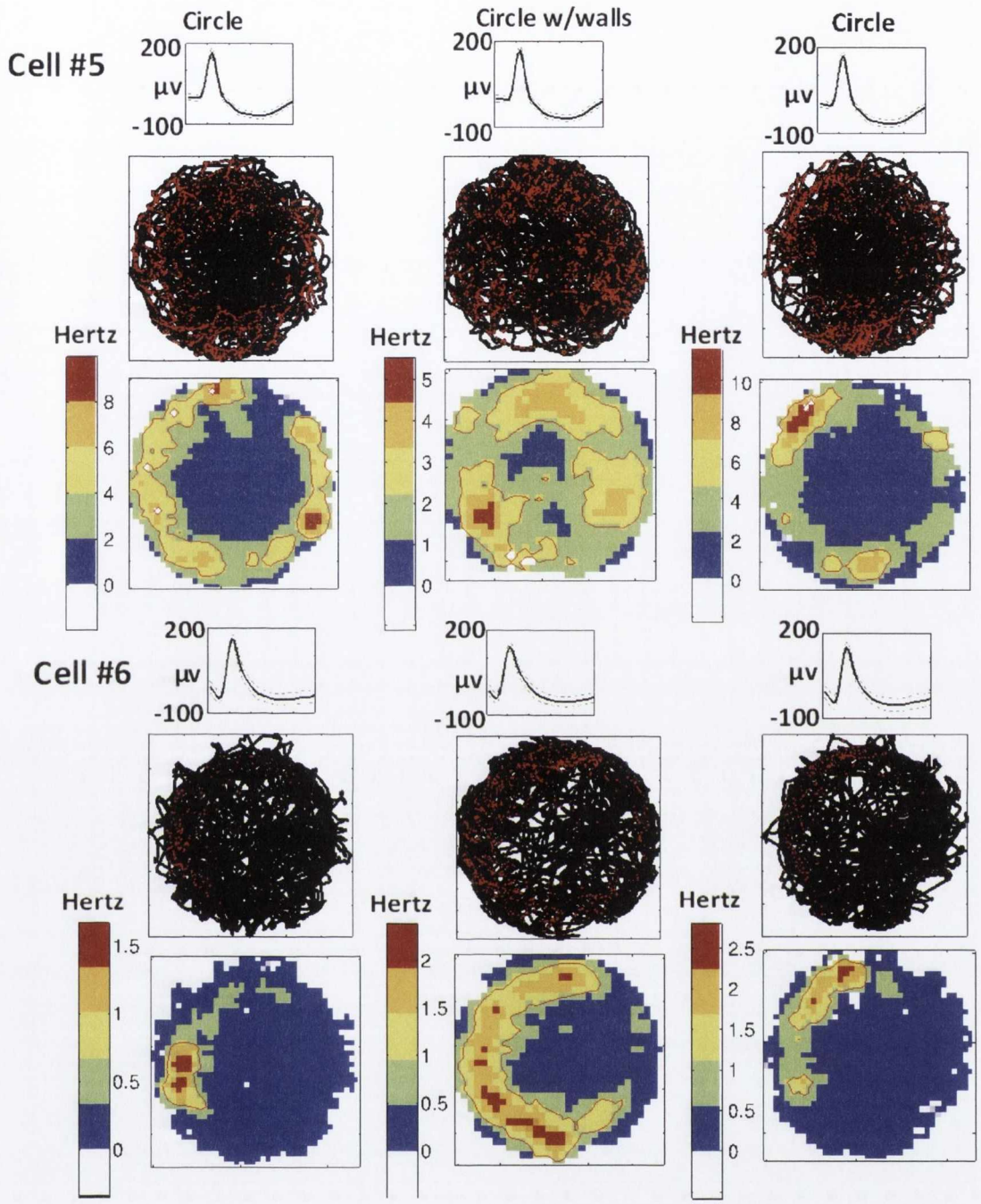


Figure 33. Waveform of and firing properties of perimeter units (cell #5 and #6) during circle, circle with walls then circle sessions. Firing rate map: peak firing rate is red, blue is 20% of peak firing rate. Cell #3 was active around the whole arena perimeter, cell #4 was active at only a discrete perimeter location but re-mapped to fire around the whole arena when walls were present.

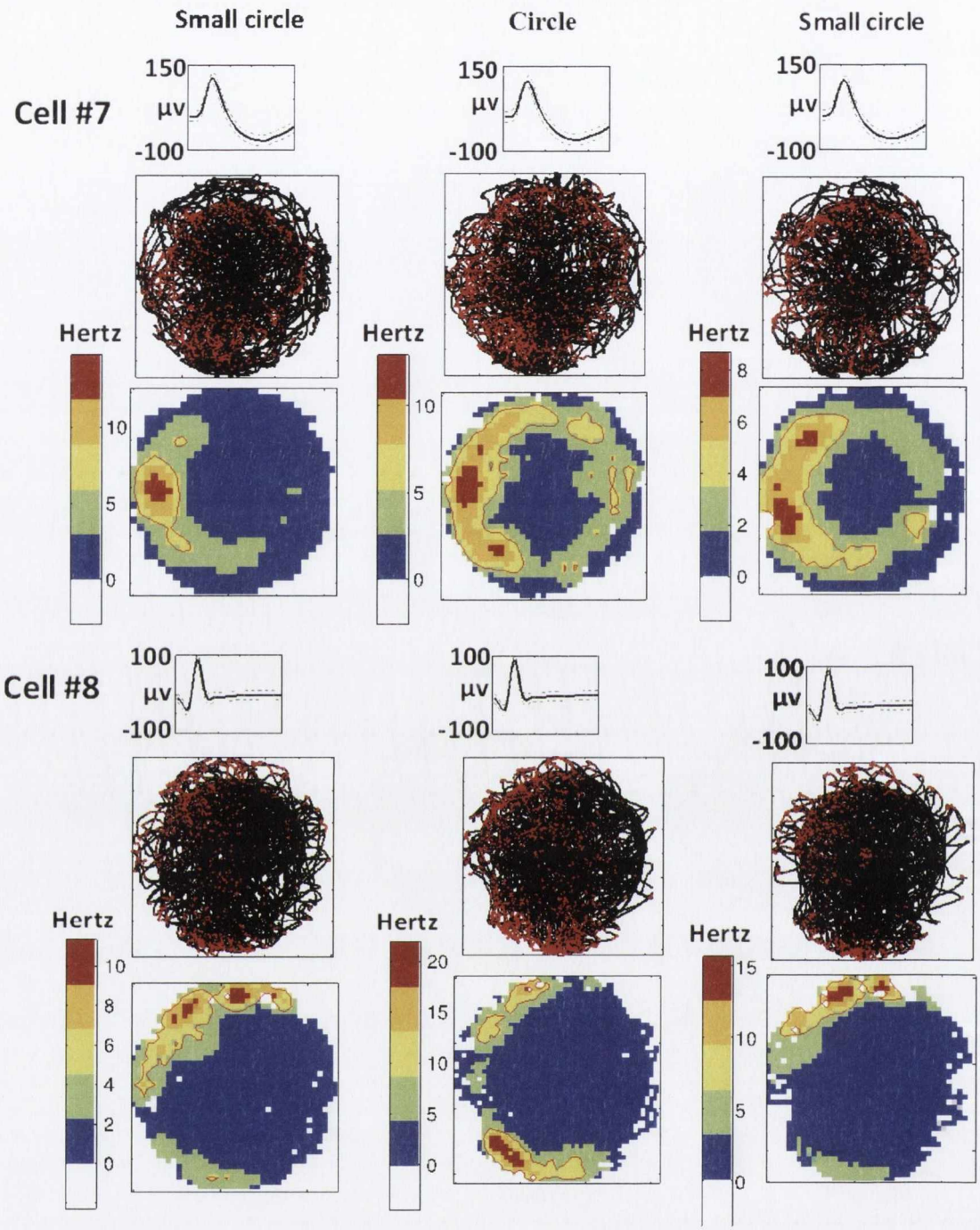


Figure 34. Waveform of and firing properties of perimeter units (cell #7 and #8) during small circle, circle then small circle sessions. Firing rate map: peak firing rate is red, blue is 20% of peak firing rate. Cells #7 and #8 remain active in the same location arena regardless change in size.

4.4.2 Firing activity of gradient units during environmental changes

Gradient units have a peak rate of activity at the centre of the arena, the activity of the cell decreases in stepwise manner, in all directions, to lowest firing rate at arena perimeter. Visual inspection of the firing rate maps for gradient cells in small and large arena (Figure 35, cells #9 and #10) demonstrate that the gradient of high activity in the centre of the arena to lowest activity at the perimeter was present in both arena sizes. Friedman's test revealed no significant difference ($x^2(2)=3.8$; $p = 0.82, p>0.01$, $n=21$) in mean firing rate (Hz) of gradient cells when comparisons were made between first small circle trial (Mdn 17.5 Hz; IQR 5.9 to 29), circle trial (Mdn 17.9 Hz; IQR 7.6 to 26) and second small circle trial (Mdn 15.6 Hz; IQR 6.8 to 26.6).

The presence of perimeter walls does not disrupt gradient like firing pattern for 8 out of 11 units recorded in this session (Figure 36, #11) but it does disrupt the gradient like firing pattern for 3 out of 11 units (Figure 36, #12). Friedman's test revealed no significant difference ($x^2(2)=3.45$; $p = 0.21, p>0.01$, $n=11$) in mean firing rate (Hz) when comparisons were made between first circle trial (Mdn 15.7 Hz; IQR 7.7 to 20.1), circle with walls trial (Mdn 15.3 Hz; IQR 10.4 to 19.9) and second circle trial (Mdn 11.5 Hz; IQR 7.7 to 18.5).

Gradient units maintain their gradient firing pattern of highest firing rate in the centre of the arena, decreasing to lowest firing rate at the perimeter of the arena in both the circular and square arena (Figure 37, cells #13 and 14). Interestingly the shape of firing activity, on the firing rate maps, for these cells appears to reflect the shape of the arena. Friedman's test revealed no significant difference ($x^2(2)=6.0$; $p = 0.81$, $p>0.01$, $n=4$) in mean firing rate (Hz) when comparisons were made between first circle trial (Mdn 14.3 Hz; IQR 7.6 to 28.4), square trial (Mdn 11.8 Hz; IQR 6.7 to 25.9) and second circle trial (Mdn 13.2 Hz; IQR 5.3 to 26.5).

The firing pattern of gradient units was maintained in dark conditions (Figure 38 cells #15 and 16). There was no significant difference ($x^2(2)=3.7$; $p = 0.19$, $p>0.01$, $n=7$) in mean firing rate (Hz) when comparisons were made between first light trial (Mdn 13.6 Hz; IQR 9.2 to 23), dark trial (16.3 Hz; IQR 7.3 to 21) and second light trial (Mdn 15.7 Hz; IQR 9.7 to 24.8) conditions.

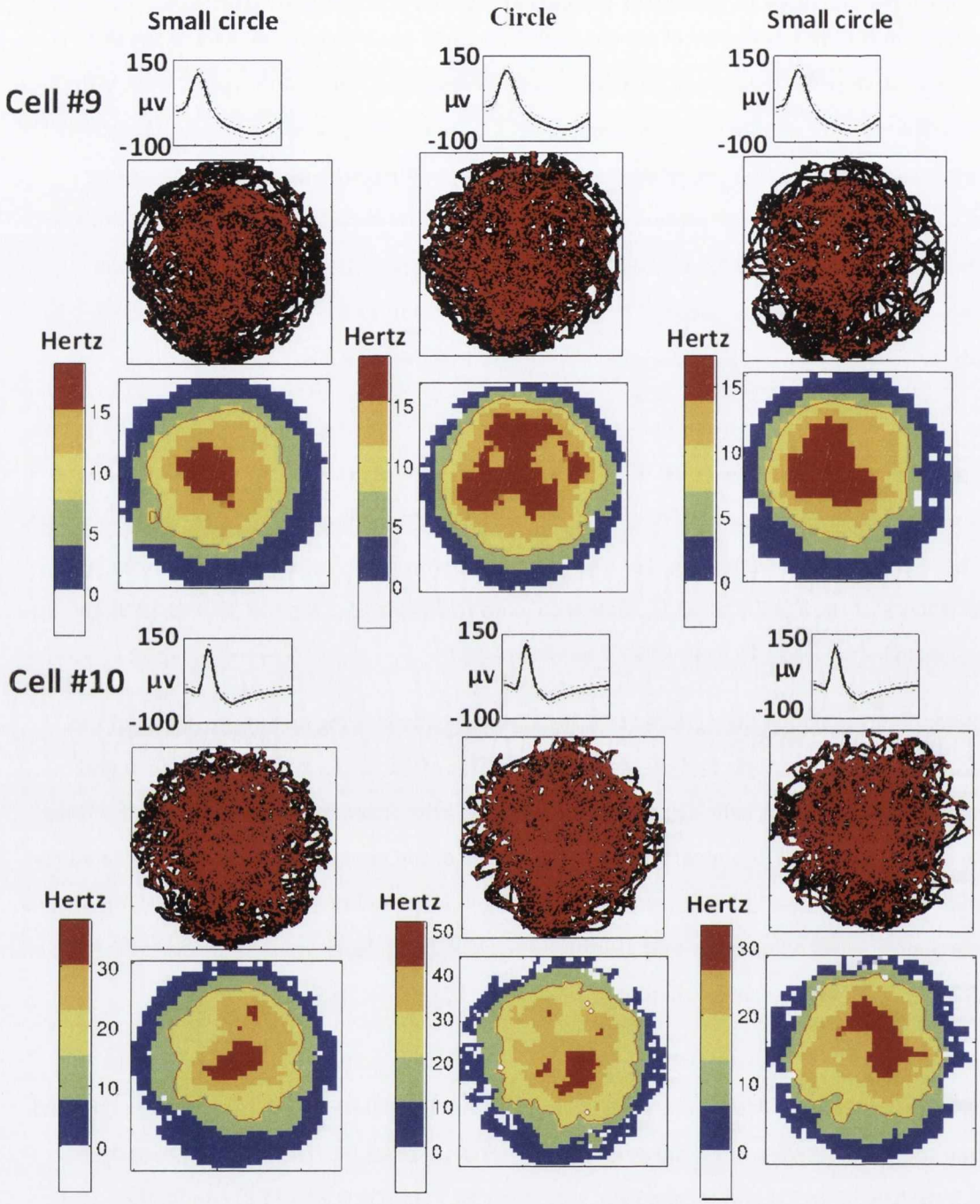


Figure 35. Waveform of and firing properties of gradient units (cell #9 and #10) during small circle, circle then small circle sessions. Firing rate map: peak firing rate is red, blue is 20% of peak firing rate. Firing activity re-scales to arena size so that the entire arena is mapped

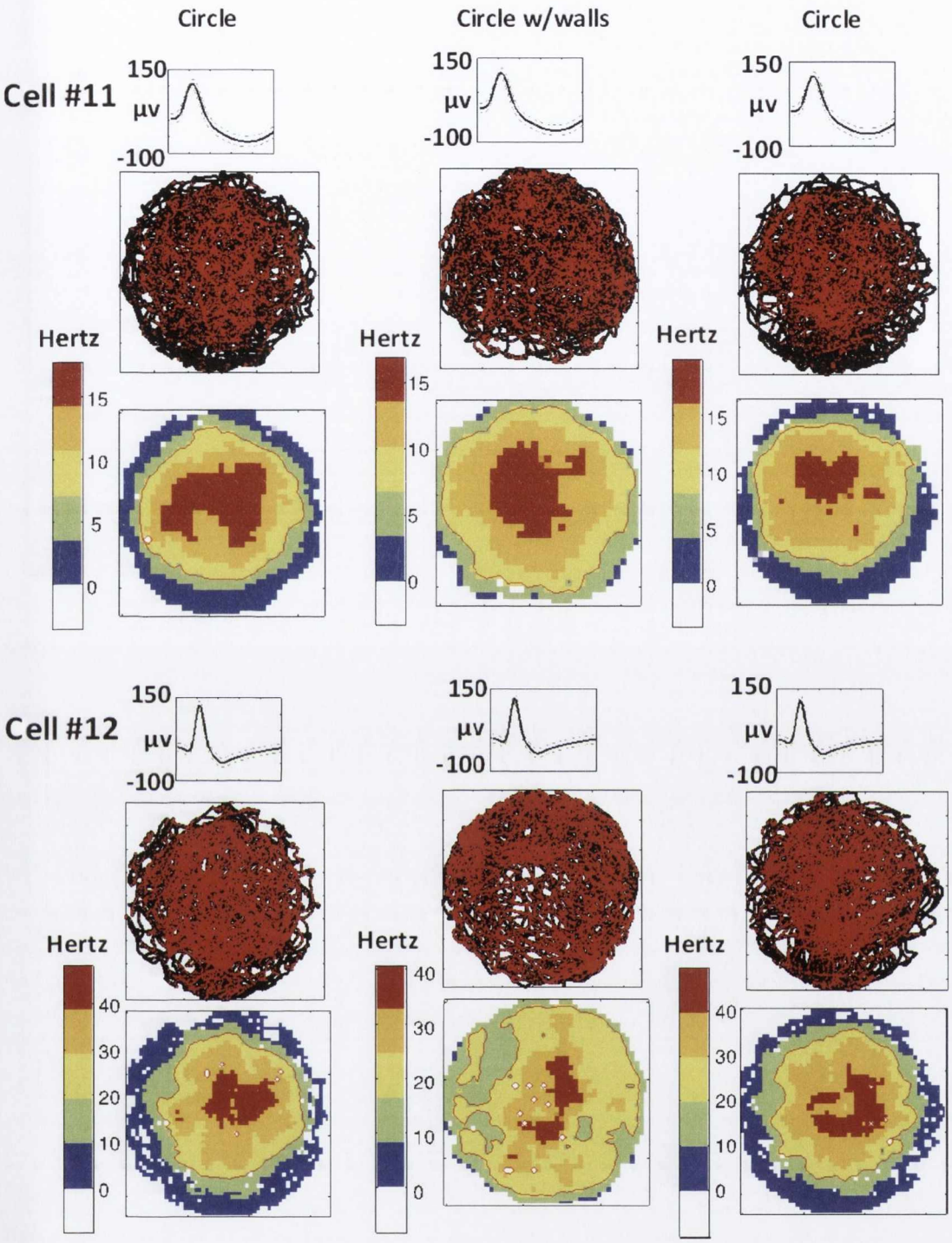


Figure 36. Waveform of and firing properties of gradient units (cell #11 and #12) during circle, circle with walls then circle sessions. Firing rate map: peak firing rate is red, blue is 20% of peak firing rate. Gradient activity is abolished for cell #12 but not cell #11 when arena walls were present.

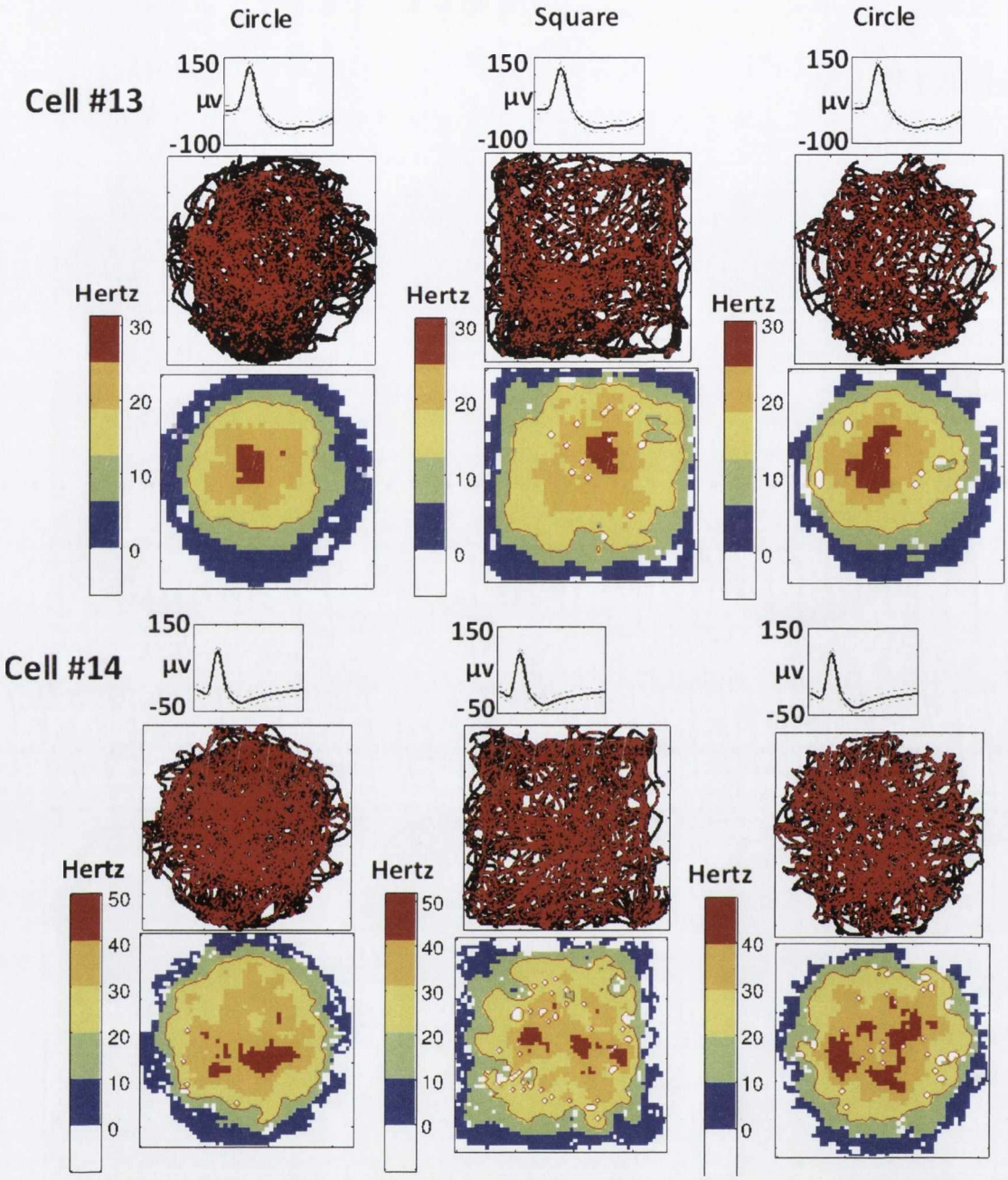


Figure 37. Waveform of and firing properties of gradient units (cell #13 and #14) during circle, square then circle sessions. Firing rate map: peak firing rate is red, blue is 20% of peak firing rate. Gradient firing activity was present square arena for both cells. The gradients of firing activity also reflected the shape of the recording arena.

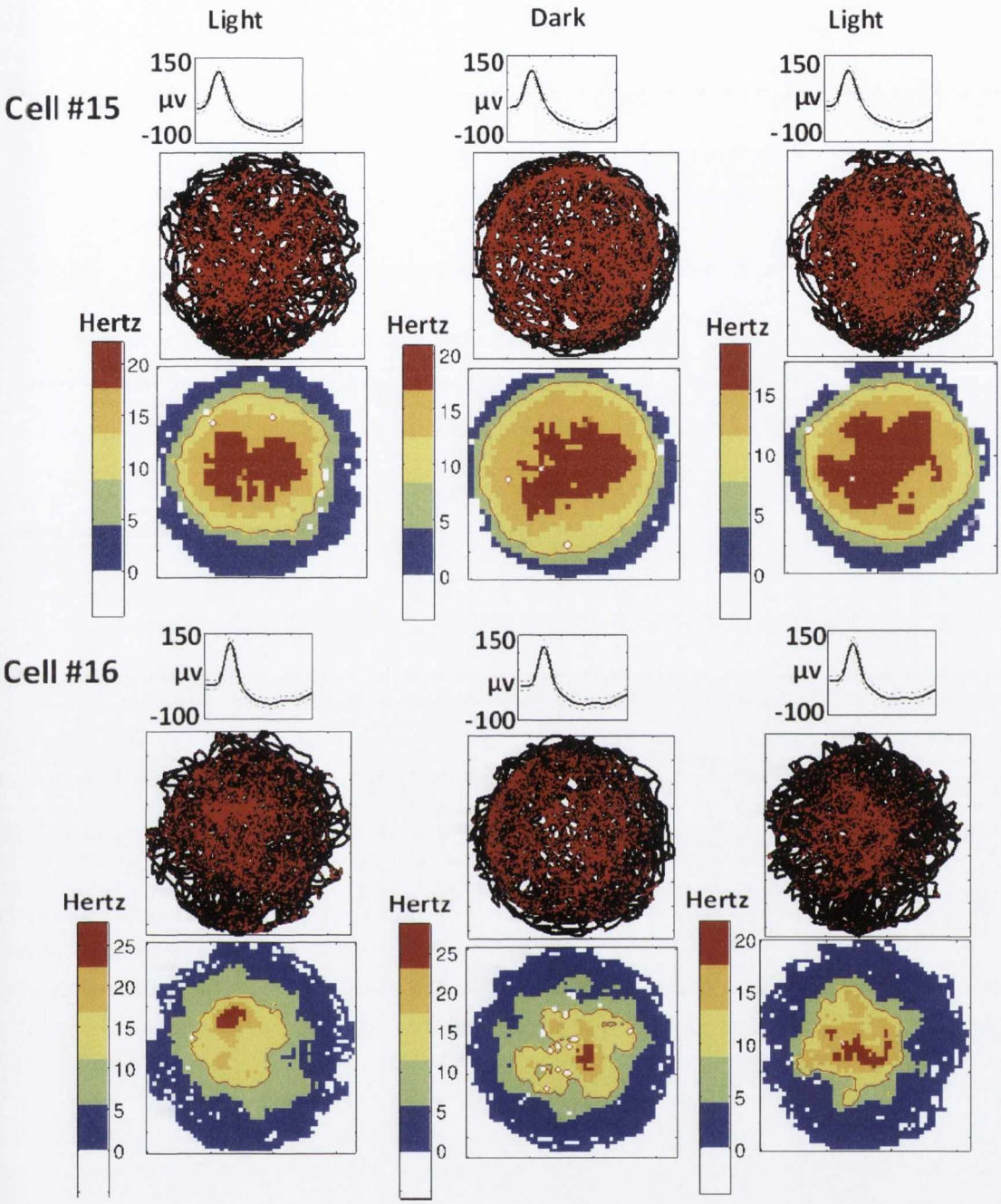


Figure 38. Waveform of and firing properties of gradient units (cell #15 and #16) during light, dark then light sessions. Firing rate map: peak firing rate is red, blue is 20% of peak firing rate. Gradient firing activity was maintained in dark recording conditions for both cells.

4.4.3 Firing activity of corona units during environmental changes

Corona units are active throughout the whole arena but have a higher firing frequency around the perimeter of the arena or just before the perimeter of the arena. The area of higher firing frequency for corona units, which occurred around the perimeter of the arena (Figure 39, cell #17) was present in both small and large arena. The area of higher firing frequency for those corona units whose area of higher activity occurred just before the perimeter of the arena was present in both small and large arena. Friedman's test revealed there was no significant difference ($x^2(2)=0.6;p = 0.83,p>0.01$, n=10) in mean firing rate (Hz) for corona units when first small circle trial (Mdn 17.5 Hz; IQR 5.9 to 28.8), circle trial (Mdn 17.9 Hz; IQR 7.6 to 25.8) and second small circle trial (Mdn 15.6 Hz; IQR 6.8 to 26.6) were compared.

The area of higher firing frequency for corona units which occurred before the arena perimeter (Figure 40, cell #19) and for other corona units whose area of higher firing frequency occurred around the perimeter of the arena (Figure 40, #20) were present when the arena shape changes from circle to square. The shape of the area of higher frequency activity around the perimeter for both these units reflects the shape of the arena. There was no significant difference (Friedman's test: $x^2(2)=2.0;p=0.39,p>0.01$, n=9) in mean firing frequency (Hz) when corona units when first circle trial (Mdn 7.5 Hz; IQR 2.8 to 22.7), square trial (Mdn 6.7 Hz; IQR 2.2 to 19.6) and second circle trial (Mdn 6.5 Hz; IQR 2.1 to 19.2) were compared.

The distinctive firing pattern of corona units (Figure 41, cells #21 and 22) was present in dark conditions. There was no significant difference (Friedman's test: $x^2(2)=1.56;p=0.57,p>0.01$, n=9) in mean firing rate (Hz) for corona units when first light trial (Mdn 11.2 Hz; IQR 8.8 to 22.4), dark trial (Mdn 10.7 Hz; IQR 7.2 to 21.8) and second light trial (Mdn 14.3 Hz; IQR 8.5 to 23.9) were compared.

The presence of arena walls did not disrupt the area of high activity around the perimeter for only 1 of 12 corona cells recorded in this session (Figure 42, cell #23). However, the distinctive area of high activity around the perimeter for 11 out of 12 corona cells was disrupted (Figure 42, cell #24). When walls were removed then the area of higher firing frequency around the perimeter of the arena returned (Figure 42, cell #24). The mean firing frequency (Hz) of corona units was not statistically significantly different (Friedman's test: $x^2(2)=5.3;p=0.07,p>0.01$, n=12) when first circle trial (Mdn 8.5 Hz; IQR 6.3 to 13.6), circle with walls trial (Mdn 6.3 Hz; IQR 4.5 to 13.5) and second circle trial (Mdn 7.6 Hz; IQR (4.8 to 13.4) were compared.

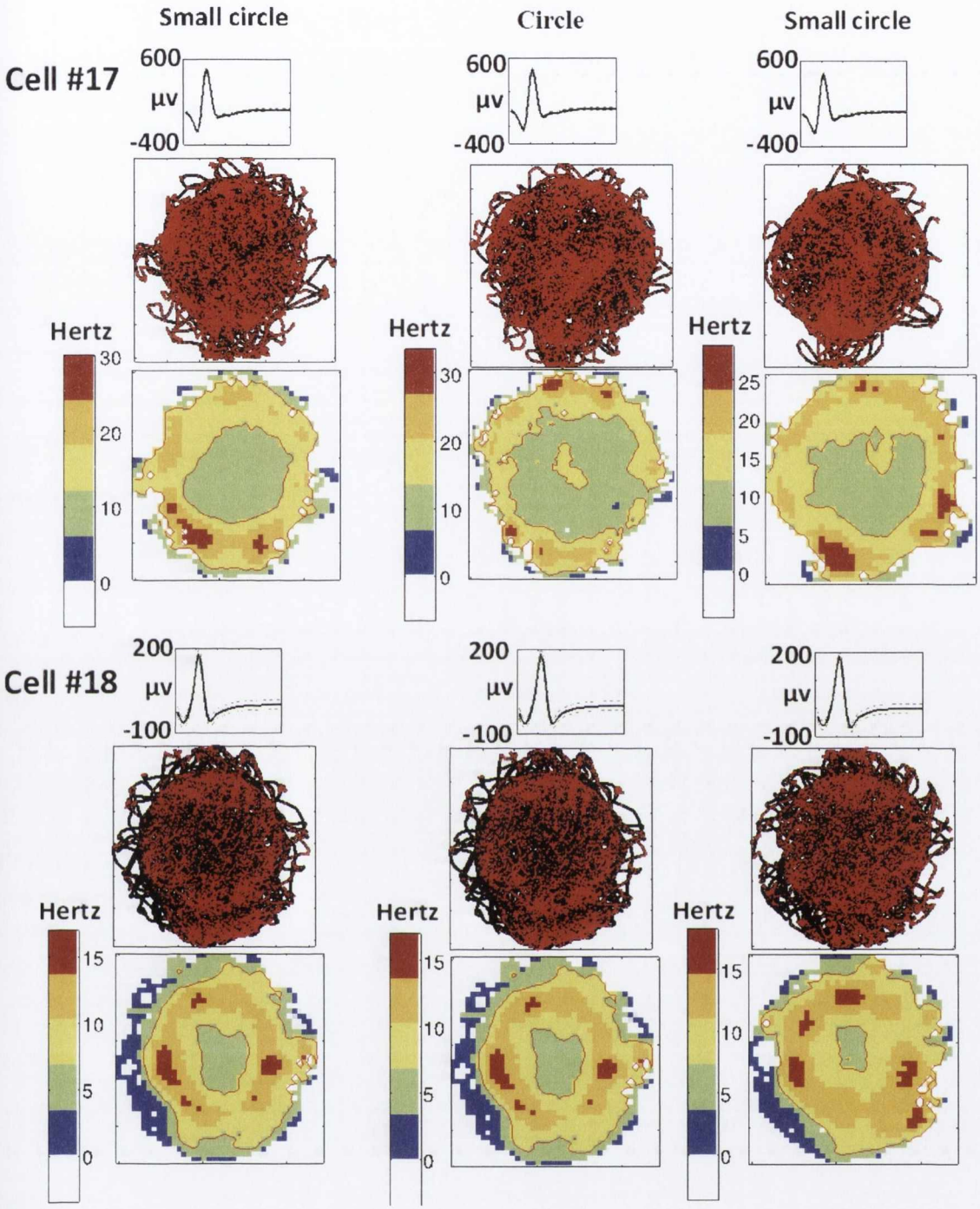


Figure 39. Waveform of and firing properties of corona units (cell #17 and #18) during small circle, circle then small circle sessions. Firing rate map: peak firing rate is red, blue is 20% of peak firing rate. Firing activity of corona units re-scales to appear similar in small and large arena.

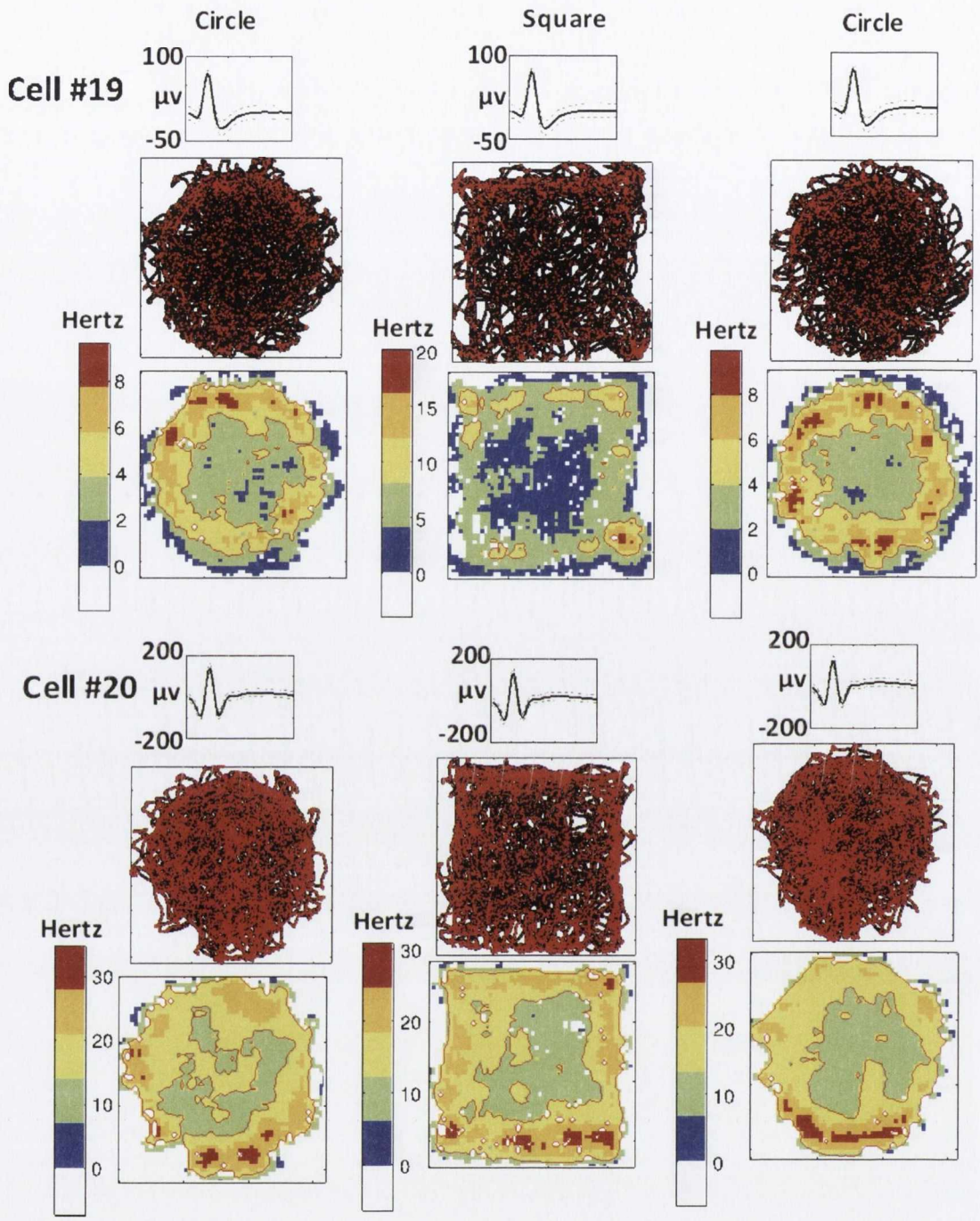


Figure 40. Waveform of and firing properties of corona units (cell #19 and #20) during circle, square then circle session. Firing rate map: peak firing rate is red, blue is 20% of peak firing rate. The Firing activity of corona units were maintained in the square arena.

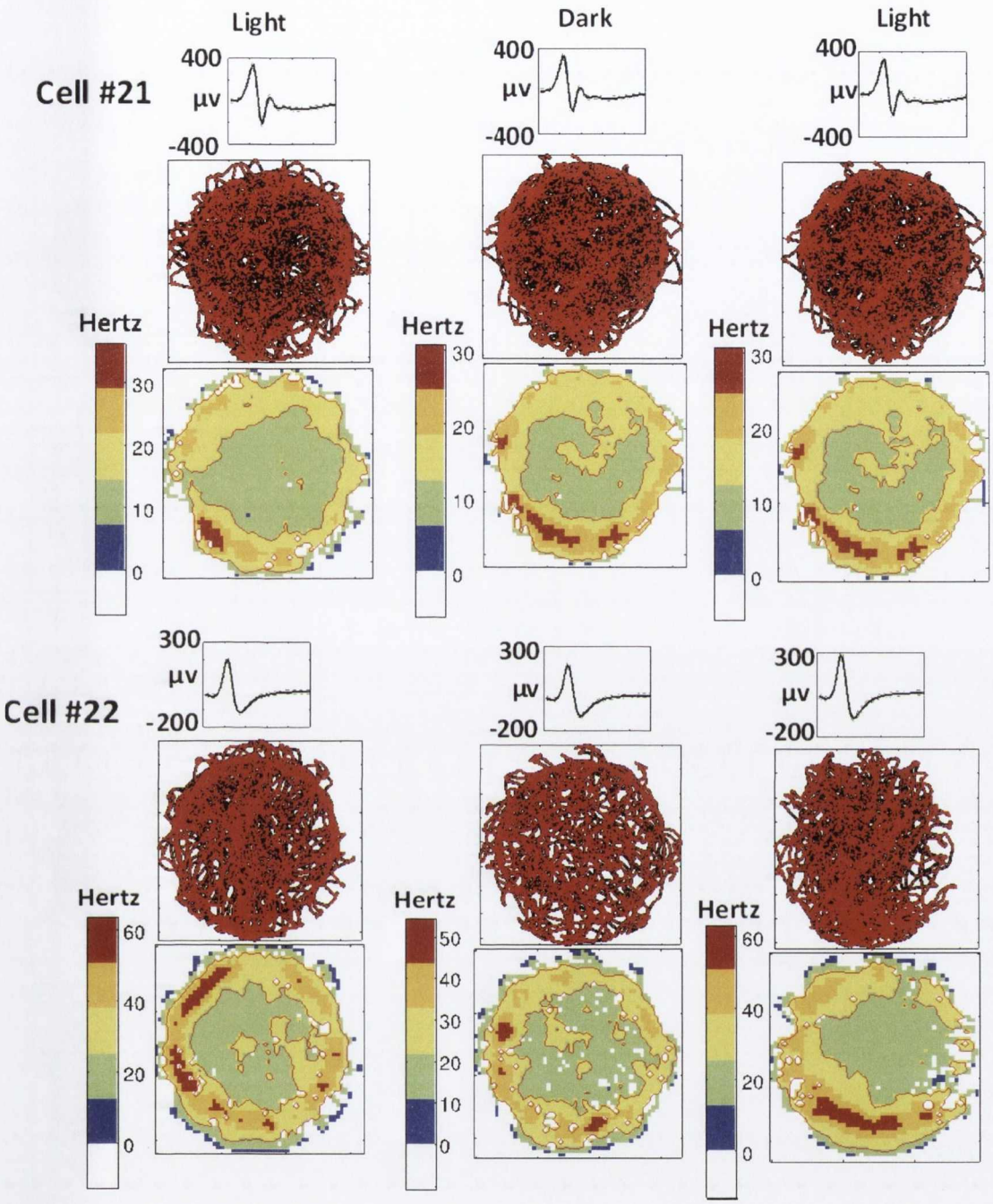


Figure 41. Waveform of and firing properties of corona units (cell #21 and #22) during light, dark then light session. Firing rate map: peak firing rate is red, blue is 20% of peak firing rate. The Firing activity of corona units were maintained in dark conditions.

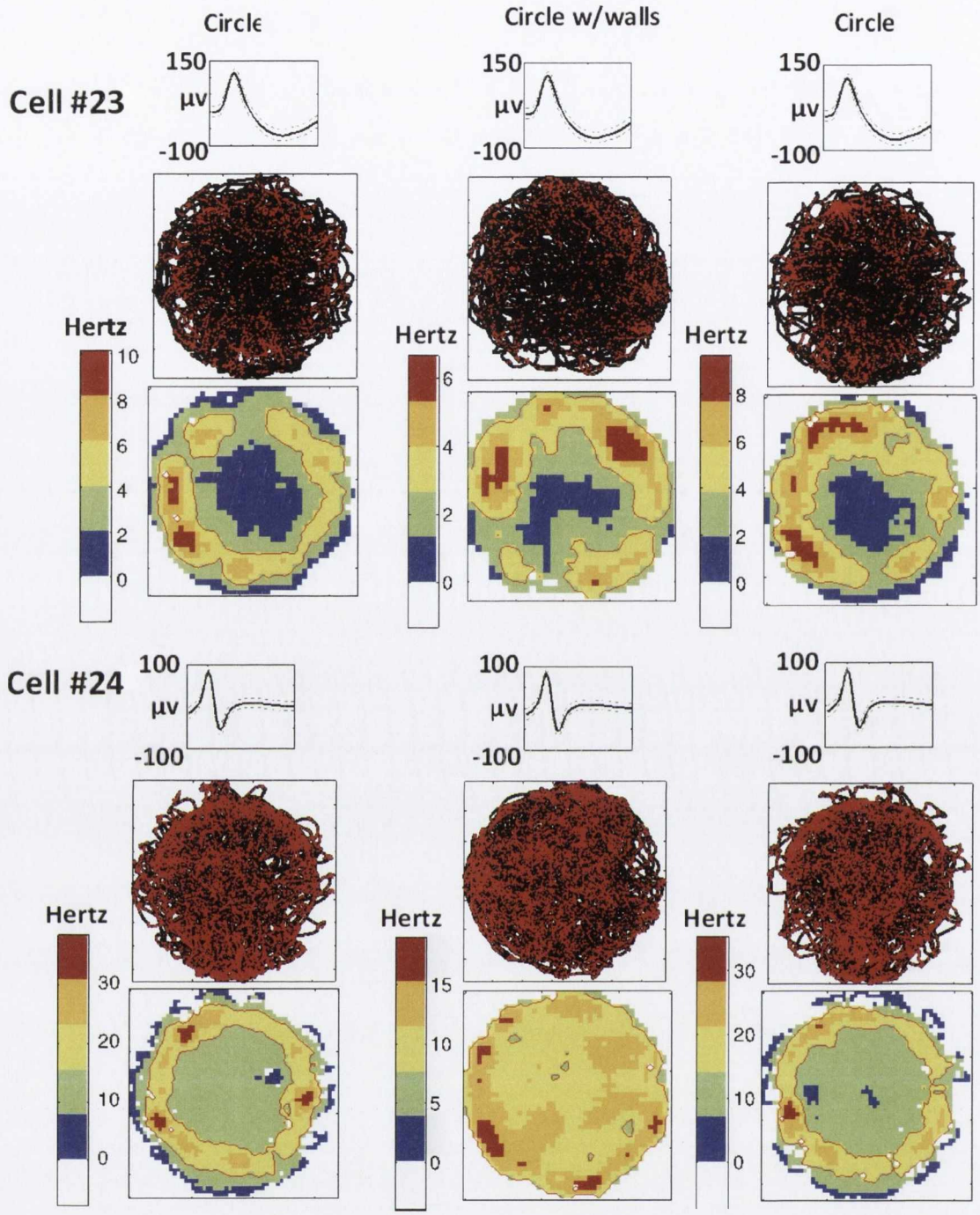


Figure 42. Waveform of and firing properties of corona units (cell #23 and #24) during circle, circle with walls then circle session. Firing rate map: peak firing rate is red, blue is 20% of peak firing rate. The Firing activity of corona unit #23 was maintained with arena walls present but abolished perimeter firing preference for cell #24.

4.4.4 Firing activity of centre firing units during environmental changes

Centre firing units were active throughout the arena but when the rat moved its head over the perimeter of the arena the firing rate of the unit decreased to below 20% of peak firing rate for that unit. No statistical analyses could be undertaken due to too few unit numbers in each recording session, but a description of firing rate maps during different environmental manipulations will be given below.

Firing rate maps for circle and square arena demonstrate (Figure 43, cells #25 and 26) that despite the shape of the arena, the unit's activity decreased to below 20% of peak firing rate when the rat's head moved off the perimeter of the arena. Firing activity of centre firing units was maintained in dark conditions as visual inspection of firing rate maps for units in dark conditions look the same as those recorded in light conditions (Figure 44, cells #27 and 28). Walls around the perimeter of the arena prevent the rat from moving its head over the arena perimeter, interestingly the lowest firing rate for these cells during walled arena recordings were around the arena perimeter (Figure 45, cells #29 and 30). The firing pattern of centre firing cells returns, lowest firing activity when the rat moves its head over the arena perimeter, when walls were removed. The firing activity of centre firing cells were similar to firing rate maps for both first small circle trial and second small circle trial, and for the circle when visually inspected (Figure 46, cells #31 and 32).

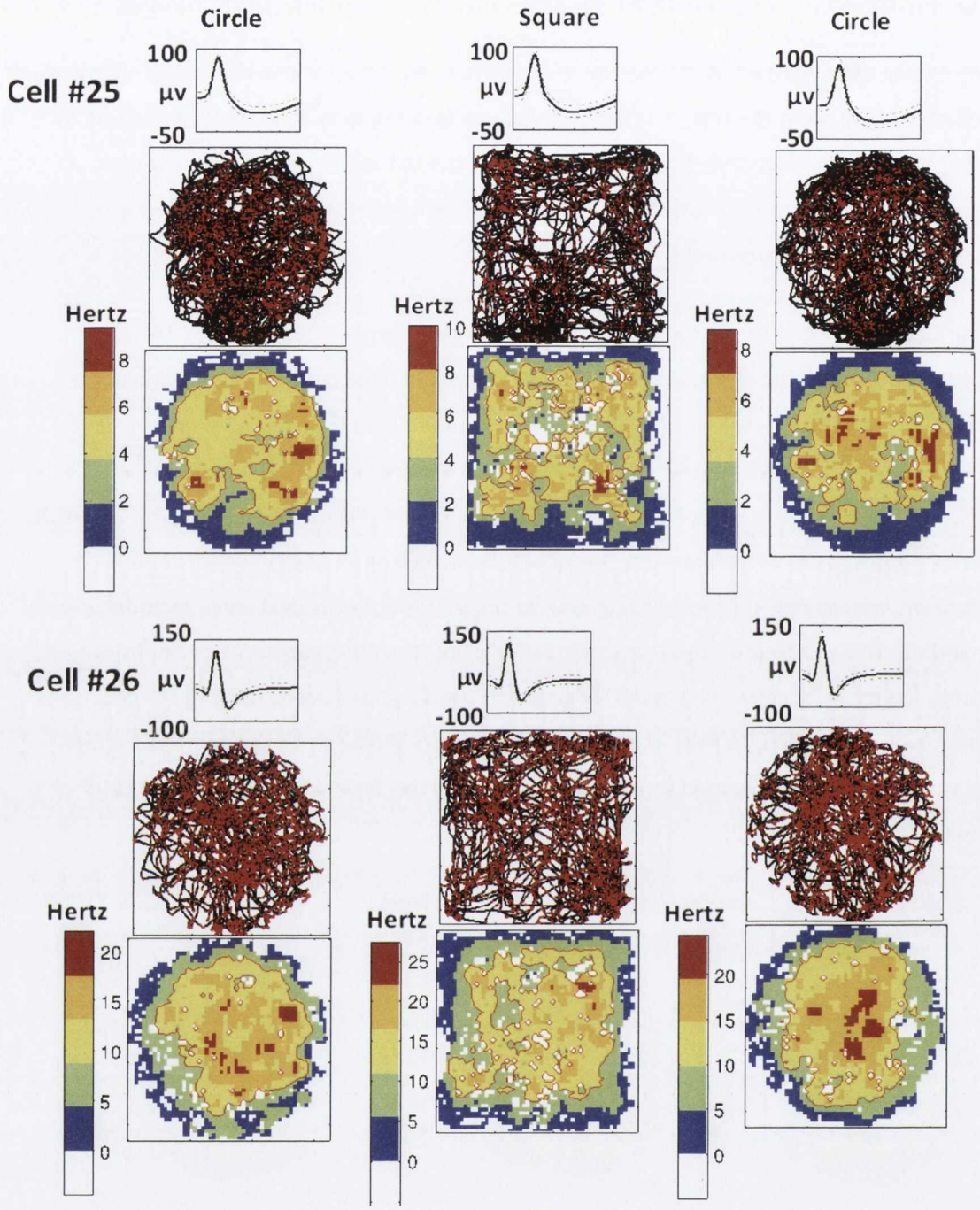


Figure 43. Waveform of and firing properties of centre units (cell #25 and #26) during circle, square then circle session. Firing rate map: peak firing rate is red, blue is 20% of peak firing rate. The firing properties for both cells were maintained in the square arena.

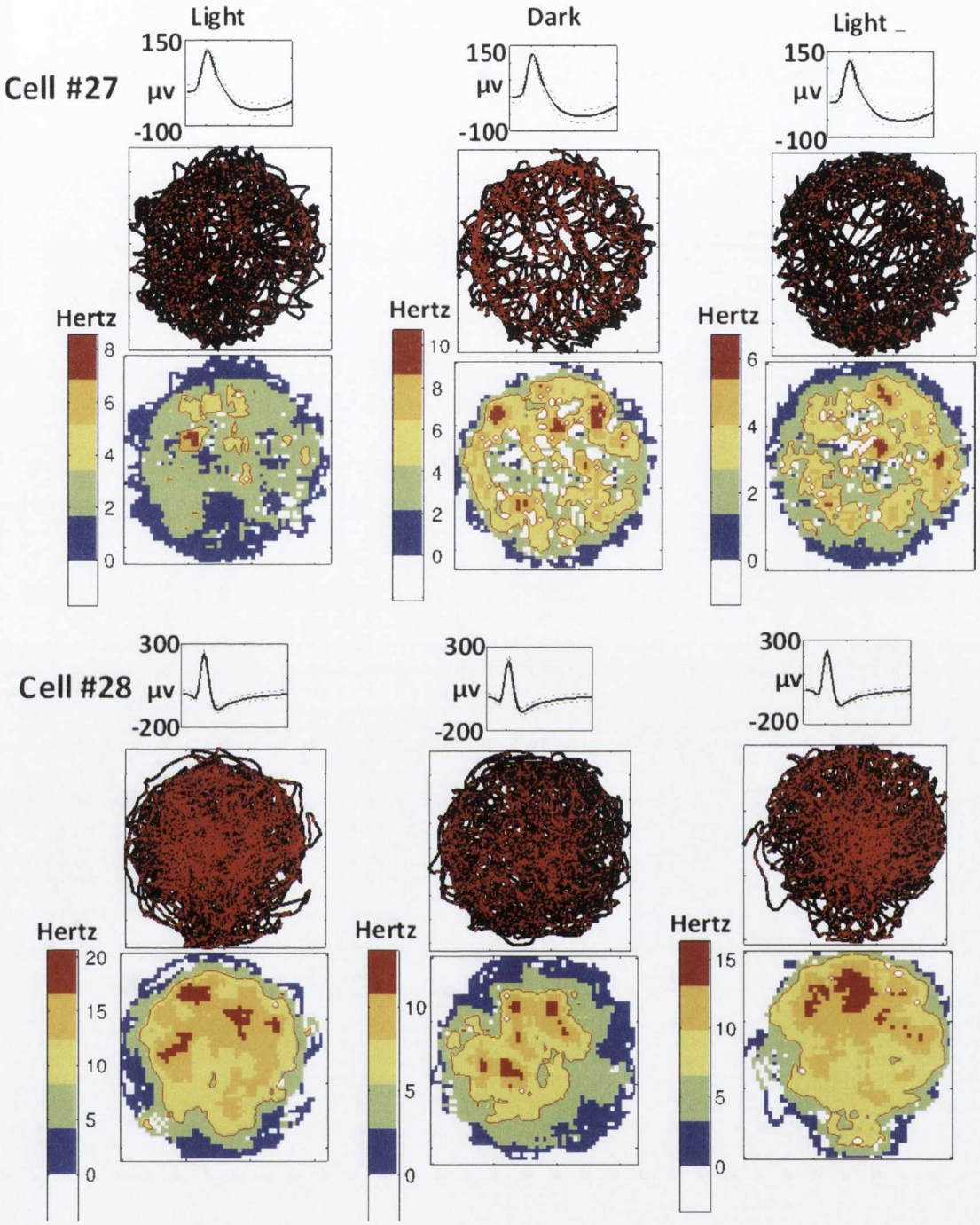


Figure 44. Waveform of and firing properties of centre units (cell #27 and #28) during light, dark then light session. Firing rate map: peak firing rate is red, blue is 20% of peak firing rate. The Firing properties for both cells were maintained in dark conditions.

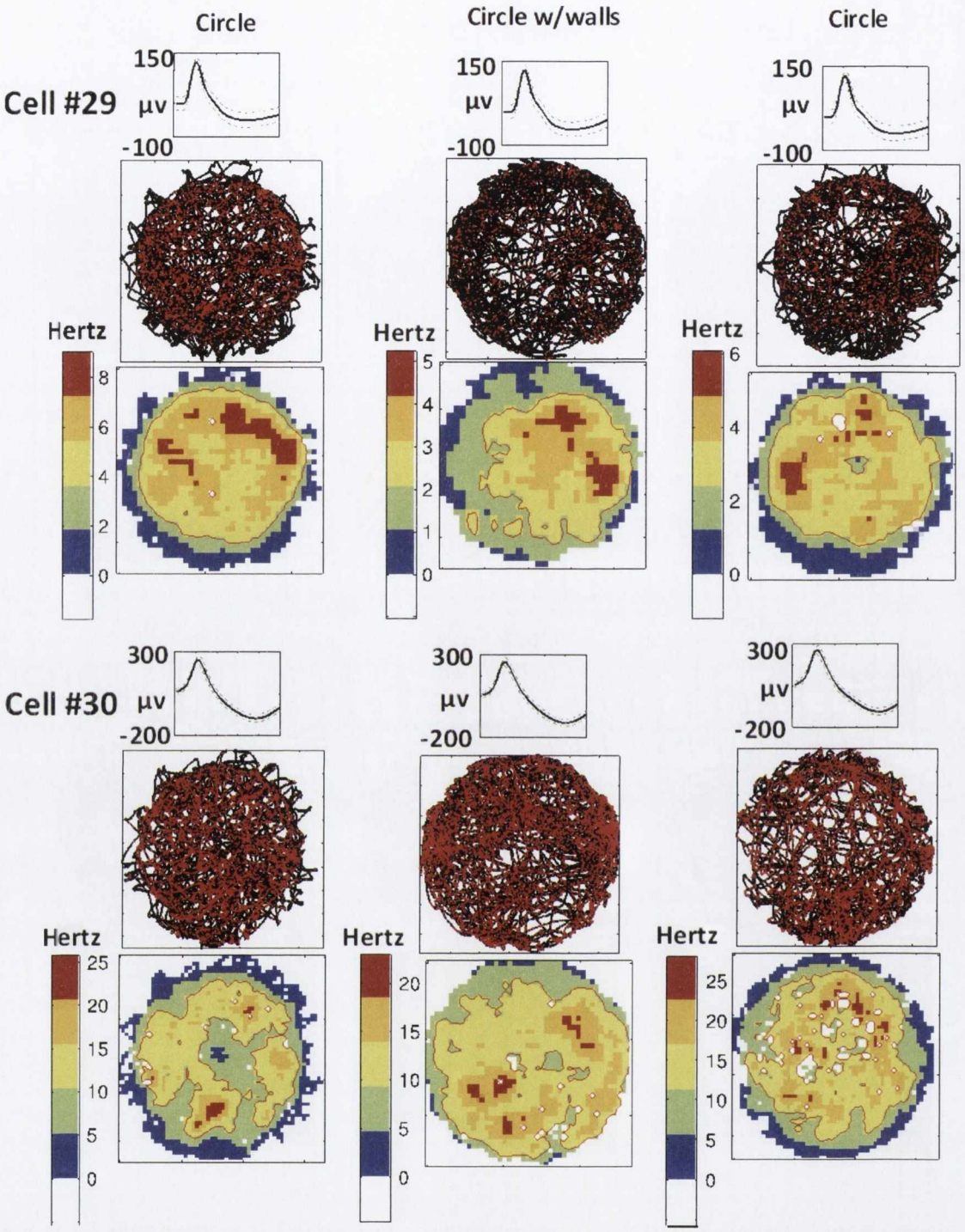


Figure 45. Waveform of and firing properties of centre units (cell #29 and #30) during circle, circle with walls then circle session. Firing rate map: peak firing rate is red, blue is 20% of peak firing rate.

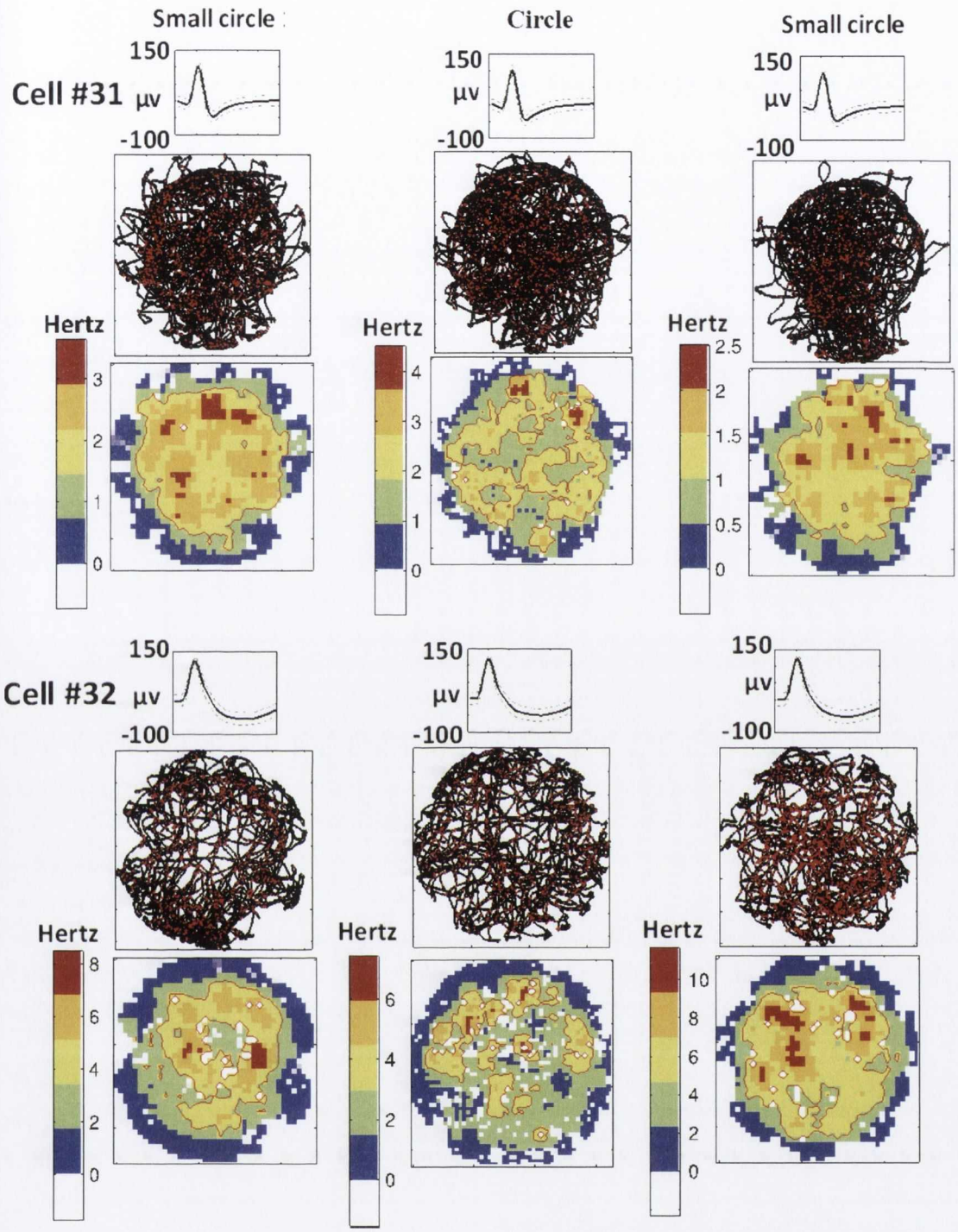


Figure 46. Waveform of and firing properties of centre units (cell #31 and #32) during small, large then small arena session. Firing rate map: peak firing rate is red, blue is 20% of peak firing rate. The lowest rate of firing activity, regardless of arena size, occurred when the rate moved its head over the arena perimeter.

4.5 Discussion

The anterior RSC of the rat contains a diverse group of cells whose firing properties appear to depend on the location of the rodent in the arena, or more specifically, its location to the environmental boundary. The activity of these cells were also found to correlate with self-generated movement information (e.g. running speed and angular head velocity). Theoretical models have predicted the existence of cells conveying environmental boundary information to place cells in the hippocampus, thus helping to create and maintain their place fields (Barry *et al.*, 2006; Bush *et al.*, 2014; Lever *et al.* 2009). Recent opinion suggests that during light conditions, information from visual cues (e.g. landmarks and boundaries) primarily drives place cell firing field formation (Bush *et al.*, 2014). During dark conditions, place field formation and maintenance is driven from idiothetic information, projected via grid cells in the mEC (Koenig *et al.*, 2011; McNaughton *et al.*, 2006; Poucet *et al.*, 2014).

During navigation in light conditions visual information about environmental boundaries and landmarks arrive at RSC via projections from visual areas 17 and 18b (Van Groen & Wyss, 1990; Van Groen & Wyss, 1992; Van Groen & Wyss, 2003; Wyass & Van Groen, 1992). Visual information of landmarks and boundaries are likely to be the primary input for units in anterior RSC whose firing activity are dependent on the rodent's proximity to the environmental boundaries. The RSC projects directly and indirectly to brain regions of the hippocampal formation which contain boundary cells thought to be important for determining place cells firing location (Van Groen & Wyss, 1990; Van Groen & Wyss, 1992; Van Groen & Wyss, 2003; Wyass & Van Groen, 1992). During light conditions the anterior RSC could support spatial navigation by conveying environmental boundary information to boundary cells in these brain areas.

During dark conditions rodents can navigate accurately in an environment using only self-motion cues (Etienne, 1992; Etienne & Jeffery, 2004; Mittelstaed M. & Mittelstaed H., 1980; Whishaw & Brooks, 1999; Whishaw *et al.*, 2001) and possibly memory of the environment (Cooper *et al.*, 2001). The anterior RSC is likely to contribute to the navigational process in the dark as the firing fields of all boundary sensitive units were present during dark recording conditions. Given the theoretical importance attributed to cells which encode boundary for place field activity this may explain why lesions of the RSC disrupt place cell activity, impair navigation in light and dark conditions (Cooper & Mizumori 1999; Cooper *et al.*, 2001; Cooper & Mizumori, 2001).

No previous single-unit study in the rodent RSC reported the presence of units active at the perimeter of the arena (Chen *et al.*, 1994a; Chen *et al.*, 1994b; Cho & Sharp 2001). Chen et al. (1994a) recorded RSC single-units as the rat navigated the radial-arm maze. The narrow arms of

the eight radial-arm maze restrict the movement of the rodent as well as imposing head directionality to one of eight possible directions. The firing activity of no unit in this chapter was found to be dependent on head direction. The imposed head directionality on the rodent as it traverses the arms of the radial-arm maze perhaps inhibited the formation of these units and that is why they were not reported. However, it is more likely that units reported in this chapter would be easier to visually identify in the open-field arena. Despite recording RSC single-units in the open-field arena Cho and Sharp (2001) did not report the presence of units with firing properties like those of perimeter units, corona units or gradient units. Cho and Sharp (2001) implanted their electrodes posterior to electrodes in this study, perhaps the anterior RSC conveys boundary information and the mid-caudal portion does not. The firing rates of some units in this chapter were disrupted by the presence of arena walls. It would be interesting to repeat Cho and Sharp's (2001) study and record in an arena with no walls to see if similar units recorded in this study are present in mid-caudal RSC.

The firing rate maps for centre firing units recorded in this study look similar to the firing rate maps of direction-dependent place cells which Cho and Sharp (2001). It would be interesting to perform direction-dependent place cell analysis on centre firing units, to see if they are direction-dependent place cells which were observed in mid-caudal RSC. Centre firing units, were the only class of unit whose firing activity was not positively or negatively correlated with angular head velocity but was strongly correlated with running speed. Visual inspection of firing rate maps, for these units, reveals that these units were almost silent as the rat leaned out over the arena perimeter when no arena walls were present. The rat cannot run or move forward when its head is out over the perimeter of the arena but only move its head, this could explain why these units were silent when the rodent's head moved over the arena perimeter.

The anterior RSC contains units which were active at discrete portions of the arena perimeter and, units which are active around the entire arena perimeter. The firing location of units which were active around the whole perimeter of the arena were maintained during all changes to the environment. The findings of this study suggest these units behave more like boundary cells described in the subiculum, which do not remap as frequently as boundary cells in mEC during changes to the environment (Lever *et* al., 2009; Solstad *et al.*, 2008). However, no report of boundary, which were active around the complete arena perimeter, were described in the subiculum (Lever *et* al., 2009). Units which were active around the complete arena perimeter have been described in the rodent claustrum (Jankowski & O'Mara, 2015), nucleus reuniens (Jankowski *et* al., 2015), rostral thalamus (Jankowski *et* al., 2015), post and para subiculum

(Boccara *et al.*, 2010). The rodent RSC is reciprocally connected to these structures which in-turn project or are reciprocally connected to brain regions in the hippocampal formation where boundary units are present (Van Groen & Wyss, 1990; Van Groen & Wyss, 1992; Van Groen & Wyss, 2003; Wyass & Van Groen, 1992). It is possible that the boundary signal observed in these structures could originate in the anterior RSC. Visual information conveying arena boundaries and somatosensory information (e.g. vibrissae) converge at the RSC. This information could be projected directly to the claustrum, nucleus reuniens or rostral thalamus to establish boundary units there. These structures could then relay environmental boundary information to boundary cells in mEC or subiculum or directly to the hippocampus. Therefore, it would be of interest to assess the effect of lesion of anterior RSC on the firing properties of boundary units in claustrum, nucleus reunions or rostral thalamus. Another experiment of interest would be to record boundary cells in the subiculum or border cells in the mEC with lesion of the anterior RSC. The results of both these experiments would provide more information on the role of the RSC for boundary cell formation.

The firing activity of perimeter units, which were active only at discrete portions of the arena perimeter, were not disrupted during dark conditions, change to arena shape or size. The firing properties of these cells were similar to boundary cells in subiculum, rather than boundary units in the mEC, which re-mapped frequently after changes to the environment (Lever *et* al., 2009; Solstad *et al.*, 2008). However, during recording trials with arena walls present, anterior RSC units which were active at a discrete portion of the arena became active around the entire arena perimeter. This type of re-mapping is unlike boundary cells in either the subiculum or the mEC. Further experiments are required to understand the functional significance of this type of re-mapping and what it signals to the spatial navigation network.

Another explanation for the change of firing characteristics of perimeter units active at discrete perimeter locations, could be due to the summation of information received locally in the anterior RSC. Visual as well as a sensory information, likely to be projected from partietal cortex, converge onto the anterior RSC. Alteration to the weight of one input, here it could be visual or tactile, as the rat could not see through the opaque arena wall but could feel it (e.g. vibrissae or nose poke), could change the units firing properties. It would be interesting to shave the rodent's whiskers and repeat the recording session with walls present to see if the partial perimeter unit re-maps. It would also be of interest to repeat this experiment with clear, Perspex arena walls. The rodent could see visual cues through the Perspex walls and if the partial perimeter cell does not remap then perhaps its firing activity visually driven.

Corona units were active throughout the arena but had an area of higher firing frequency around the perimeter of the arena or just before the arena perimeter. Interestingly, boundary cells which were recorded in subiculum on a raised arena with no walls were either active around the perimeter of the arena or were most active when the rodent leaned out over the arena perimeter (Lever *et* al., 2009). Firing rate maps for corona cells, in this study, do not appear have a maximal firing activity when the rat leans out over the perimeter of the arena. This is a visual observation, so further analysis is needed to establish if the higher firing frequency occurred at the perimeter of the arena perimeter, or when the rat leaned out over the arena. The area of higher firing activity either before, or around, the perimeter of the arena persists regardless of arena size and in dark conditions. The shape of the area of higher firing frequency also remaps to the shape of the environment as observed in square trials. The presence of perimeter walls extinguished the area of higher firing frequency around the perimeter of the arena for all, but one corona cell. The type of environmental boundary, be it a wall or sheer drop, modulates the firing properties of these cells. The purpose of corona units could be to convey the type of environmental boundary to other brain areas within the spatial navigation network.

A new type of unit, described here for the first time in the anterior RSC is the gradient unit. Gradient units have an area of peak firing frequency at the centre of the arena, which decreases in gradients to the outer most perimeter of the arena, in all directions, where the lowest firing frequency is observed. This distinctive firing pattern was maintained during dark recording trials, indicating the firing activity of these cells is not solely dependent on visual information. The firing pattern also re-scaled to cover the full area of both a small and large arena. This indicates that these units respond dynamically to the size of the environment to map it in its entirety. Firing rate patterns of gradient cells were present when the shape of the arena altered. The firing rate pattern covers the entire square arena and interestingly the gradients of firing rate appear to reflect the square shape of the arena. The shape of firing rate gradients, when the rat is reintroduced to the circular arena, reverts to being circular in shape.

Gradient unit firing pattern was maintained for 8 out of 11 units when arena walls were present. This indicates that within this group of units there is diversity, in terms, of their activity to boundary type. One "anti-border cell" was described in the mEC and it was recorded in the same location as boundary cells (Solstad *et al.*, 2008). This cell fired in the centre of the arena and had low activity around the boundary, similar to a gradient unit. However, the "anti-border cell" firing rate does not display the graded firing pattern of gradient units in anterior RSC (Solstad *et al.*, 2008). Gradient units also appear to be distinct from boundary cells in subiculum, which fired in

the centre of the arena, when arena walls were removed (Lever *et* al., 2009). Firstly, subiculuar boundary cells which were active at the centre of the arena, when walls were removed, did not display a clear gradient of highest firing activity at the centre of the arena to lowest firing activity at arena perimeter. Secondly, during walled trials these units displayed a peak rate of activity at one arena wall. No gradient unit in the anterior RSC ever remapped during any trial with walls to be preferentially active at one boundary of the arena. The functional role of gradient units was not determined in this study. However, one role for these units could be to provide a metric to measure distance from the centre of the arena to the perimeter. This information could be used locally by other units in the anterior RSC (e.g. corona, perimeter) or other spatial cells in other brain areas connected RSC to maintain their locational specificity.

The rodent anterior RSC contains a diverse group of units whose firing activity appear to be dependent on the type of arena boundary and distance from the arena boundary. Visual, vibrissae, somatosensory as well as self-generated motion information converge at the RSC. The units observed in this study, whose firing depends on the rat's location to the boundary, could be as a result of convergence and integration of sensory information converging at anterior RSC. The anterior RSC could be the primary input for boundary cell firing in postsubiculum, neucleus reuniens and claustrum. These structures project to mEC and subiculum, who in-turn, project boundary information directly to the CA1. In support of this theory, the anterior RSC receives a projection from CA1 of the hippocampus (Van Groen & Wyss, 1990; Van Groen & Wyss, 1992; Van Groen & Wyss, 2003; Wyass & Van Groen, 1992). This projection could provide the anterior RSC with ongoing feedback to regulate its activity. In order to test the importance of anterior RSC for boundary cell activity in other structures several lesion and recording studies would have to be undertaken. Lesion of the anterior portion of the RSC should disrupt boundary cell activity in postsubiculum, projections from postsubiculum to mEC are likely to be of importance for boundary cell activity in mEC. Lesion of anterior RSC should also disrupt boundary cells in nucleus reuniens and claustrum, these structures project directly to the CA fields of the hippocampus. Nucleus ruiniens and claustrum also project to subliculumm and mEC which convey boundary information directly to CA1 place cells (Vertes *et al.*, 2006; Wilhite *et al.*, 1986; Zingg *et al.*, 2014). The firing rate maps for all units in this study were unaltered during dark recording conditions. The firing rates of the majority of units in this chapter were correlated with running speed and/or angular head velocity. These correlates probably contribute to the persistence of these cells in dark conditions, providing further evidence that the anterior RSC contributes to navigation not only in light conditions but also dark conditions.

5. General discussion

The purpose of this study was to describe the spatial and non-spatial properties of single-units in the rodent anterior RSC. The anterior RSC contains HD units which constitute 15% of the overall unit population. The anterior RSC also contains a diverse group of units whose firing activity appeared to be dependent on the type of environmental boundary and distance from it. These units could be further differentiated based on their firing rate map properties, combined these units comprised 11% of all units recorded in the anterior RSC. Approximately 40% of units whose firing rates demonstrated no obvious spatial properties (e.g. head direction or place) were found to correlate with angular head velocity and/or running speed. There was a population (4% of all units recorded) of theta-modulated units and theta-skipping units (1% of all units recorded) recorded in the anterior RSC. The presence of spatially correlated units and theta-modulated units in anterior RSC, reported in this study for the first time, provide direct evidence that the anterior portion of the RSC is an important part of the spatial navigation network.

The majority of anterior RSC HD units were recorded from the Rgb region in this study, due to the starting depth of electrodes. The HD cells recorded had the same firing properties of HD units described elsewhere as the preferred firing direction and half peak-width was maintained during dark conditions (Goodridge *et al.*, 1998; Jankowski *et al.*, 2014; Taube *et al.*, 1990b). To provide further evidence that these units were HD units similar to those originally described by Taube *et al.* (1990a, b) then the preferred firing direction would have to be demonstrated to be dependent on external cues. To demonstrate this, rotation of the large extra-maze cue card should elicit the same rotation in preferred firing direction of the HD unit in anterior RSC. The firing activity of anterior RSC HD units were correlated with angular head velocity and running speed. These are self-generated motion cues which probably contributed to maintenance of the preferred firing direction during dark conditions. The HD signal observed in the RSC is thought to be projected from the ADN, ADN is also thought to project vestibular information to the RSC (Dillingham et al., 2014; Taube, 2007). A role of the RSC could be to integrate the vestibular signal from the ADN with the head direction signal from the ADN and then project this to the postsubiculum or EC. The anterior RSC could perform the same function but with projections from other brain areas which project the HD signal to anterior RSC, for example, the nucleus reuniens. Anterior RSC also receives projections from the primary and M1, M2 motor cortices (Vogt *et al.*, 1983). Another role of the anterior RSC could be to integrate efference copy from the motor cortex (e.g. running speed) with the HD signal projected to it, this would account for the HD units whose firing rate were correlated with running speed. The presence of HD units and

other units whose firing activity is correlated with angular head velocity and running speed are of theoretical importance for navigation, particularly path integration.

HD cells in the anterior RSC were found to anticipate future head direction by approximately 41ms. HD units in mid-caudal RSC were found to anticipate future heading direction by approximately 25ms, similar to the ADN which was approximately 23 ms (Cho and Sharp, 2001). The anticipatory time interval most similar to the anterior RSC was from HD cells in the mammillary bodies which was approximately 39 ms (Blair *et al.*, 1998). The head direction signal is thought to originate in the DTN and mammillary bodies then project to ADN which has reciprocal projections with the RSC (Taube, 2007). The reason anterior and mid-caudal RSC anticipatory time interval differ is not immediately clear. Perhaps, the projection from the mammillary bodies to ADN is topographical, so HD units which have larger anticipatory time intervals project to a discrete location within the ADN and HD units with smaller anticipatory time intervals project to other parts of the ADN. The ADN projection to RSC is topographical (Van Groen & Wyss, 1990; Van Groen & Wyss, 1992; Van Groen & Wyss, 2003; Wyass & Van Groen, 1992), so HD units with larger anticipatory time intervals could project to anterior RSC and HD units with smaller anticipatory time intervals project to the middle and posterior parts of RSC. Further studies are required to describe the projections from mammillary bodies to ADN to provide more information to support this hypothesis.

Approximately 11% of all units recorded in this study were sensitive to boundary type (presence of arena wall or sheer drop from platform) and/or the distance to the arena boundary. The area of high firing rate for some corona units appeared to mark approach to the arena boundary, while others appeared to fire at a higher frequency at the edge of the arena. Some other corona unit's highest rate of firing could have occurred at the extreme edge of the arena boundary (i.e. when rat leaned out over of the arena). Regardless of which aspect of arena boundary represented by these units, 11 of 12 corona units firing activity was disrupted when arena walls were present. It is not clear what the functional implications for these type of units are for spatial navigation. However, it is important for one to know the boundary of one's environment and type of boundary in order to accurately navigate, estimate distance or plan movements. The RSC is connected to the EC, postsubiculum and subiculum (Czajkowski *et al.*, 2012; Van Groen & Wyss, 1990; Van Groen & Wyss, 1992; Van Groen & Wyss, 2003; Wyass & Van Groen, 1992) which contain grid cells and other spatially correlated cells. One possible function of corona units could be to provide grid cells with a boundary reference in order to calibrate their spatial metrics when no walls are present. It is also possible, that disruption of corona units firing when walls

were present, was due to somatosensory information e.g. whiskers or nose touching the arena wall. This information is likely to be projected to the RSC via the parietal cortex (Burcham *et al.*, 1997; Reep *et al.*, 1994). Therefore, it would be interesting to record corona units with the arena walls present with the rat's whiskers shaved off to observe the effects on unit activity. It is possible nose touch to the arena wall is responsible for corona units lack of boundary firing specificity. To test this hypothesis it would be necessary to lesion the projection from parietal cortex to RSC then observe firing activity of corona unit when arena walls were present. The arena walls which were placed on the platform were opaque, therefore, the disruption to corona unit's boundary firing specificity could be due to lack of visual cues. To test this hypothesis the arena walls should be clear, Perspex so the rodent can see through the arena wall.

Gradient units recorded in the anterior RSC could work in conjunction with corona units in order to provide other spatial cells, like grid cells or place cells, in different parts of the brain with information about arena size or distance from the arena centre to boundary. Gradient units were present during dark trials and were present during trails with arena walls and without arena walls. The firing stability of these units across recording sessions may provide a stable reference for other spatially correlated units in other brain areas. It would be interesting to observe the firing pattern of gradient units with the arena divided into smaller sections e.g. compartments. If the graded firing pattern is present in each compartment, or if it is still maintained throughout the entire arena. Perimeter units were present during all recording sessions and may work in conjunction with gradient units and corona units to provide a metric of arena size and boundary type. During conditions when no walls are present gradient units could function with corona units to provide arena size and boundary information for other spatial cells (e.g. grid or place cells). If arena walls are present then gradient units could work in conjunction with perimeter units to provide environment size information for other spatial cells (e.g. grid or place cells). In order to test this hypothesis, it would be necessary to lesion anterior RSC and record grid cells in mEC, postsubiculum or place cells in either hippocampus, postsubiculum or mEC and observe any changes to their spatial firing metrics.

There were theta-modulated units recorded in the anterior RSC, which accounted for approximately 4% of the overall population of units recorded in this study. Cho and Sharp (2001) reported that approximately 45% of all units in mid-caudal RSC were theta-modulated. The presence of theta-modulated units strongly implicates the RSC is involved spatial navigation and spatial memory (Buzaki & Moser, 2013; Hasselmo, 2005; O'Keefe and Nadel, 1978). In previous studies, RSC theta was reported to be unlike hippocampal theta as it was described as only being

partially dependent on medial septal inputs (Borst *et al.*, 1987; Talk *et al.*, 2004). The CA1 of the hippocampus, which can locally generate a theta signal, projects only to the anterior RSC (Goutagny *et al.*, 2009) perhaps influencing theta activity there. This could explain why there are fewer theta modulated units in the anterior RSC than mid-caudal RSC which CA1 does not project to. It would therefore be of interest to examine the effect of temporal lesioning of the CA1 projection to the anterior RSC while recording theta-modulated units in the anterior RSC. The mammillary bodies along with the hippocampus are also involved in theta generation and propagation of the signal to the anterormedial (AM) and anteroventral (AV) thalamus (Dillingham *et al.*, 2014). The projections from AM and AV to the RSC could be topographical, with fewer projections to the anterior RSC than to posterior RSC, which could explain why fewer theta modulated units were observed in anterior RSC. Detailed histological analysis of the projection from AM and AV to RSC would have to be undertaken to examine this hypothesis.

Theta-skipping units were also observed in the anterior RSC in this study, but not described in previous studies where electrodes were implanted in mid-caudal RSC (Alexander & Nitz, 2015; Cho and Sharp, 2001). Theta-skipping units accounted for approximately 1% of all units recorded in this study. Theta-skipping units have also been described in the mEC and the nucleus reuniens of the thalamus (Brandon *et al.*, 2011; Brandon *et al.*, 2013; Jankowski *et al.*, 2014). Researchers have postulated that theta-skipping units may provide a pace-maker like function for synchronising some early components of the HD system (Jankowski *et al.*, 2014).The nucleus reuniens, which is reciprocally connected to the RSC, is a major source of direct thalamic projections to the CA fields of the rat hippocampus (McKenna & Vertes, 2004; Prasad and Chudasama, 2013; Vertes *et al.*, 2006). Perhaps the theta-skipping signal observed in the anterior RSC is projected from the nucleus reuniens. The firing activity of theta-skipping units in the mEC were also correlated to head direction (Brandon *et al.*, 2011). The theta-skipping signal in mEC was abolished when the medial septum was lesioned but head directionality was maintained (Brandon *et al.*, 2011). It would be interesting to record theta-skipping units in anterior RSC while the medial septum or nucleus reuniens was inactivated to observe the effect. If theta-skipping unit activity is abolished then it would provide more information on the possible source of the theta-skipping signal in anterior RSC.

In this study, it appears from inspection of the firing rate maps of theta-skipping units that there is place preference for firing. To test this hypothesis, the spatial information content (Skaggs) of theta-skipping units should demonstrate a positive correlation with theta-skipping index. It is also interesting that firing activity of theta-skipping units in nucleus reuniens demonstrated no place

preference for firing activity or preference for head direction (Jankowski *et al.*, 2014). It is possible that the in the anterior RSC the theta-skipping signal is projected there from the nucleus reuniens, the place preference could be a result of integration of this signal from CA1, subiculum or postsubiculum which all contain place cells. The RSC has been suggested to be important for integrating different spatial signals from different brain areas (Alexander & Nitz, 2015; Chen *et al.*, 1994a; Chen *et al.*, 1994b; Cho & Sharp, 2001; Mizumori *et al.*, 2001). To test this theory lesion of the CA1, subiculum or postubiculum projection to anterior RSC should decrease the spatial information content observed from theta-skipping units in anterior RSC.

Alexander and Nitz (2015) found several classes of unit associated with spatial navigation in mid-caudal RSC of the rodent. In their study the rodent had to navigate a "W" shaped maze from start to end. Alexander and Nitz (2015) demonstrated that RSC units had a higher activity when the rodent had to make a right or, left turn. These units are likely the angular head velocity units recorded in this study. For example, angular head velocity units, which were correlated for clockwise head turns only, were analogous to the units which were sensitive to right turns demonstrated by Alexander and Nitz (2015). Interestingly, Alexander and Nitz (2015) demonstrated units in the RSC mapped position in route centred space during light and dark conditions. Similar units were previous described in the rodent posterior parietal cortex (Nitz, 2006) which is connected to the RSC (Burcham *et al.*, 1997; Reep *et al.*, 1994). The "route cells" were defined based on Nitz (2006) previous work where they can either exhibit complex, but reliable, changes in activity across the route and some "route units" can demonstrate significant differences in firing intensity at different action sites (e.g. two right turns) (Alexander & Nitz). "Route units" were not described in this study as recordings were undertaken in an open-field arena. It would be interesting to record single-units in the anterior RSC while the rodent navigated a route maze to observe if these units are also present here.

In unfamiliar environments and in dark conditions rats have demonstrated the ability to leave home and find a goal location then return home in direct route, despite a complex outward path with many turns (Mittelstaedt & Mittelstaedt, 1980). This type of navigation is called path integration, and has been hypothesised to be a summation of outgoing journey vectors (McNaughton *et al.*, 2006; Mittelstaedt & Mittelstaedt, 1980). The vector is probably created from units whose firing activity correlate with angular head velocity and running speed or, HD units whose firing rates demonstrate these correlates. Rodents with lesioned RSC, demonstrate severe impairment in this task, as they cannot return to the starting position but non RSC lesion rodents can (Elduayen and Save, 2014). The anterior RSC contains HD units whose firing rates

were also correlated with angular head velocity and running speed. The RSC is connected to the EC, where grid cells are located. Grid cells are thought to provide a metric for measuring distance. It is therefore likely that the HD units in RSC work in conjunction with grid cells to provide an ongoing vector representation of the outgoing route, resulting in the rodent being able to calculate a direct route back home.

During navigation in dark conditions but in a familiar environment rodents use self-motion cues and memory of the environment (e.g. visual landmarks) to navigate accurately (Cooper *et al.*, 1999; Cooper *et al.*, 2001; Mizumori *et al.*, 2001). Cooper *et al.* (2001) placed rodents into a circular arena during, light conditions, from the same starting point and the rodent had to retrieve a food reward then return home, this task was repeated for many days. Rats without RSC lesion when placed into the arena from a novel location in the dark were found to return to the location where they were trained to return home and not the novel location which they entered the arena. If the rodent was simply using a path integration strategy, the rodent would return to the novel starting position, not the familiar location. RSC lesioned rats located the food reward but did not return to the site where they were trained to return, nor did they return to the novel site of entry. This demonstrates that RSC is important for path integration as the rodent did not return to the novel starting location during dark retrieval of food reward. Secondly, non-lesioned RSC rats during the dark returned home to the location which they were trained to return home to and not the novel starting position. This suggests that a function of the RSC, during dark conditions is to integrate memories of the environmental cues with self-motion cues. The anterior RSC, rather than middle or posterior portions of RSC, is most likely to facilitate this process. Anterior RSC is the only portion of the RSC which receives projections from CA1, where place cells are located, which are thought to be the neural substrates of the cognitive map. It would be interesting to repeat this experiment with only the anterior RSC is lesioned to see if the same deficits are observed.

Anatomical, behavioural and single-unit studies all indicate that that the RSC is important for spatial navigation. However, its exact role within the head direction pathway, thus far, is not known. It is, however, possible to hypothetically suggest roles or functions for the RSC based on current knowledge. The head direction signal is thought to project to the RSC from the ADN then back to ADN to the postsubiculum, or ADN to RSC then directly to postsubiculum where the signal enters the hippocampus via the EC (Taube, 2007). External visual cues are important for HD unit directional activity as they provide an anchor for preferred firing direction (Taube *et al.*, 1990b; Taube, 1995; Taube 2007). If visual cue is rotated 90 degrees in a familiar environment,

when the rat is not present, then upon entry to the familiar environment the HD unit will also rotate 90 degrees. The RSC could function to integrate current visual information about the external environment with the body's self-generated directional information. Interestingly, if the cue rotation is performed when the rat is present the effect on preferred firing direction is minimal (Taube *et al.*, 1990b). The RSC as well as receiving visual information also receives somatosensory, odour and tactile information via projections from the parietal cortex (Burcham *et al.*, 1997; Reep *et al.*, 1994). The RSC could function in this scenario to integrate all sensory information to assess if the environment has changed, this could function to prevent incorrect adjustments to the directional component of navigation.

The RSC as well as integrating sensory information into the head direction pathway, could also have a role of integrating this information for goal directed navigation. To navigate from a start point to a location where food is located, i.e. a goal location, is a complicated procedure which is known to involve the medial prefrontal cortex and hippocampus (Hok *et al.*, 2005; Hok *et al.*, 2007). However, based upon anatomical and electrophysiological data it is possible to hypothesis a model of goal navigation which involves the RSC. Upon entry to any novel environment, sensory information about the environment (visual, tactile and olfactory) is conveyed to the RSC, this information is likely integrated here and, projected to the hippocampus via intermediary structures (e.g. postsubiculum or mEC). The integrated sensory information would be important for creating and establishing a cognitive map of the environment (i.e. place cells in hippocampus). When the cognitive map is established, for that environment and the rat would like to navigate to another location within this environment for a food reward, this map or aspects of this map are likely to be projected to anterior RSC, possibly via the CA1. Integration of the heading direction in relation to external visual cues is likely to also occur in the RSC. Therefore, it is likely that current location and current heading direction are also integrated at the RSC. The medial prefrontal cortex is known to be involved in goal planning and signalling goal location (Hok *et al.*, 2005; Kesner & Churchwell, 2011). The RSC is directly connected to the medial prefrontal cortex as well as other frontal areas. The role of the RSC could be to relay information of current location and orientation to frontal areas, for goal-oriented navigation. The CA1 of the hippocampus also projects to frontal areas (Hoover & Vertes, 2007). The CA1 could project more information about the cognitive map e.g. where the goal is located to frontal areas. The frontal areas, could integrate information from the RSC and CA1 to form a route. The result of this integration, could be then sent back to the anterior RSC, where the route is then projected to the primary motor cortices for enactment. This is a hypothetical model of how the RSC could be involved in the creation of the hippocampal cognitive map and goal navigation.

Another potential role of the RSC is to provide sensory information to the hippocampus to update the cognitive map, on a regular basis. This would ensure that the internal representation of the environment is matched to the actual external representation. The RSC receives projections from visual areas 17 and 18b as well as somatosensory information from the parietal cortex (Burcham *et al.*, 1997; Reep *et al.*, 1994; Van Groen & Wyss, 1990; Van Groen & Wyss, 1992; Van Groen & Wyss, 2003; Wyass & Van Groen, 1992). The anterior RSC receives projections from the CA1 of the hippocampus which is likely to contain information from place cells. The RSC could function to integrate the external sensory information with the information received directly from CA1, or other intermediary structures (e.g. post subiculum, mEC), the integrated information could then projected back to the hippocampus, most likely via the RSC direct projection to the mEC or indirectly via postsubiculum or subiculum. This process, although hypothetical, is an efficient method for the brain to make sure the cognitive map, i.e. the internal representation of the environment, matches the actual external representation.

6. Conclusion

Anatomical connectivity studies suggested that the RSC could be important for spatial navigation due to its connections with the hippocampus, ATN and frontal areas. Behaviour studies provided the first empirical evidence that the RSC, when lesioned, impaired the rodent's ability to navigate correctly. Electrophysiological studies of single-units in the RSC demonstrated that their firing activity was correlated with location, head direction, running speed and angular head velocity. The presence theta-modulated units also strongly implicated the RSC had a role in spatial navigation. However, the RSC is one of the largest structures of the rodent brain and the weight of synaptic connections to and from important brain areas vary along its anterior-posterior axis. The anterior RSC also receives a projection from the dorsal CA1, which contains place cells, thought to the neural basis of the cognitive map.

Despite being implicated in spatial navigation, the spatial properties of single-units in anterior RSC were unknown. The aim of this study was to provide an accurate description of the spatial and non-spatial properties of single-units in the rodent anterior RSC. The presence of HD units and theta-modulated units confirm that the anterior RSC is involved in the spatial navigation network. Theta-skipping units in anterior RSC suggest this structure could be part of a network which involves the nucleus reuniens and EC, both of these structures project directly to the hippocampus. Boundary sensitive units (e.g. corona units) and gradient units present in the anterior RSC have never been described before in the RSC. Corona, perimeter and gradient units in anterior RSC could function together to establish and support boundary cell firing in other parts of the brain. Another function of corona, perimeter and gradient units could be to provide

other spatial cells (e.g. grid cells) in other brain areas with a stable, representative framework of the environment. The findings of this study suggest the rodent anterior RSC contains units with similar spatial properties to those of mid-caudal RSC. The presence of boundary sensitive and theta-skipping units unique to the anterior RSC suggest it may make an additional contribution to the spatial navigation network.

7. References

Aggleton, J. P., & Vann, S. D. (2004). Testing the importance of the retrosplenial navigation system: lesion size but not strain matters: a reply to Harker and Whishaw. Neuroscience Biobehavioral Reviews, 28(5), 525-531.

Albasser, M. M., Poirier, G. L., Warburton, E., & Aggleton, J. P. (2007). Hippocampal lesions halve immediate–early gene protein counts in retrosplenial cortex: distal dysfunctions in a spatial memory system. European Journal of Neuroscience, 26(5), 1254-1266.

Alexander, A.S., Nitz, D.A. (2015). Retrosplenial cortex maps the conjunction of internal and external spaces. Nature Neuroscience, 18(8), 1143-1151.

Andersen, P., Morris, R., Amaral, D., Bliss, T., & O'Keefe, J. (2006). The hippocampus book: Oxford University Press, USA.

Anderson, M. I., & O'Mara, S. M. (2003). Analysis of recordings of single-unit firing and population activity in the dorsal subiculum of unrestrained, freely moving rats. Journal of Neurophysiology, 90(2), 655-665.

Atlan, G., Terem, A., Peretz-Rivlin, N., Groysman, M., & Citri, A. (2016). Mapping synaptic cortico-claustral connectivity in the mouse. *Journal of Comparative Neurology*.

Auger, S. D., Mullally, S. L., & Maguire, E. A. (2012). Retrosplenial cortex codes for permanent landmarks. Public Library of Science One, 7(8), e43620.

Auger, S. D., Mullally, S. L., & Maguire, E. A. (2012). Retrosplenial cortex codes for permanent landmarks. *PLoS One*, *7*(8), e43620.

Auger, S. D., & Maguire, E. A. (2013). Assessing the mechanism of response in the retrosplenial cortex of good and poor navigators. *Cortex,49*(10), 2904-2913.

Awad, M., Warren, J. E., Scott, S. K., Turkheimer, F. E., & Wise, R. J. S. (2007). A common system for the comprehension and production of narrative speech. Journal of Neuroscience, 27(43), 11455-11464.

Baeg, E. H., Kim, Y. B., Jang, J., Kim, H. T., Mook-Jung, I., & Jung, M. W. (2001). Fast spiking and regular spiking neural correlates of fear conditioning in the medial prefrontal cortex of the rat. Cerebral Cortex, 11(5), 441-451.

Barnes, C. A., Mcnaughton, B. L., Mizumori, S. J. Y., Leonard, B. W., & Lin, L. H. (1990). Comparison of Spatial and Temporal Characteristics of Neuronal-Activity in Sequential Stages of Hippocampal Processing. Progress in Brain Research, 83, 287-300.

Barry, C., Ginzberg, L. L., O'Keefe, J., & Burgess, N. (2012). Grid cell firing patterns signal environmental novelty by expansion. Proceedings of the National Academy of Sciences of the United States of America, 109(43), 17687-17692

Barry, C., Hayman, R., Burgess, N., & Jeffery, K. J. (2007). Experience-dependent rescaling of entorhinal grids. Nature Neuroscience, 10(6), 682-684.

Barry, C., Lever, C., Hayman, R., Hartley, T., Burton, S., O'Keefe, J. Jeffery, K., Burgess, N. (2006). The boundary vector cell model of place cell firing and spatial memory. Reviews in the Neurosciences, 17(1-2), 71-97.

Bassett, J. P., & Taube, J. S. (2001). Neural correlates for angular head velocity in the rat dorsal tegmental nucleus. The Journal of Neuroscience, 21(15), 5740-5751.

Bassett, J. P., Tullman, M. L., & Taube, J. S. (2007). Lesions of the tegmentomammillary circuit in the head direction system disrupt the head direction signal in the anterior thalamus. The Journal of Neuroscience, 27(28), 7564-7577.

Bird, C. M., & Burgess, N. (2008). The hippocampus and memory: insights from spatial processing. Nature Reviews Neuroscience, 9(3), 182-194.

Blair, H. T., Cho, J., & Sharp, P. E. (1998). Role of the lateral mammillary nucleus in the rat head direction circuit: a combined single unit recording and lesion study. Neuron, 21(6), 1387-1397.

Blair, H. T., Lipscomb, B. W., & Sharp, P. E. (1997). Anticipatory time intervals of head-direction cells in the anterior thalamus of the rat: implications for path integration in the head-direction circuit. Journal of Neurophysiology, 78(1), 145-159.

Blair, H. T., & Sharp, P. E. (1995). Anticipatory head direction signals in anterior thalamus: evidence for a thalamocortical circuit that integrates angular head motion to compute head direction. The Journal of Neuroscience, 15(9), 6260-6270.

Blair, H. T., & Sharp, P. E. (1996). Visual and vestibular influences on head-direction cells in the anterior thalamus of the rat. Behavioral Neuroscience, 110(4), 643-660.

Boccara, C. N., Sargolini, F., Thoresen, V. H., Solstad, T., Witter, M. P., Moser, E. I., & Moser, M. B. (2010). Grid cells in pre-and parasubiculum. Nature Neuroscience, 13(8), 987-994.

Borst, J.G., Leung, L.W., MacFabe, D.F. (1987). Electrical activity of the cingulate cortex. II. Cholinergic modulation. Brain Research, 407, 81-93.

Bottini, G., Cappa, S., Geminiani, G., & Sterzi, R. (1990). Topographic disorientation—a case report. Neuropsychologia, 28(3), 309-312.

Bouton, M. E. (2002). Context, ambiguity, and unlearning: sources of relapse after behavioral extinction. *Biological psychiatry*, *52*(10), 976-986.

Bouton, M. E. (2004). Context and behavioral processes in extinction.*Learning & memory*, *11*(5), 485-494.

Brandon, M. P., Bogaard, A. R., Libby, C. P., Connerney, M. A., Gupta, K., & Hasselmo, M. E. (2011). Reduction of theta rhythm dissociates grid cell spatial periodicity from directional tuning. Science, 332(6029), 595-599.

Brandon, M. P., Bogaard, A. R., Schultheiss, N. W., & Hasselmo, M. E. (2013). Segregation of cortical head direction cell assemblies on alternating theta cycles. Nature Neuroscience, 16(6), 739-748.

Brun, V. H., Otnaess, M. K., Molden, S., Steffenach, H. A., Witter, M. P., Moser, M. B., & Moser, E. I. (2002). Place cells and place recognition maintained by direct entorhinal-hippocampal circuitry. Science, 296(5576), 2243-2246.

Bullock, T. H., Buzsaki, G., & McClune, M. C. (1990). Coherence of compound field potentials reveals discontinuities in the CA1-subiculum of the hippocampus in freely-moving rats. *Neuroscience*, *38*(3), 609-619.

Burcham, K. J., Corwin, J. V., Stoll, M. L., & Reep, R. L. (1997). Disconnection of medial agranular and posterior parietal cortex produces multimodal neglect in rats. Behavioural brain research, 86(1), 41-47.

Burgess, N., Maguire, E. A., & O'Keefe, J. (2002). The human hippocampus and spatial and episodic memory. Neuron, 35(4), 625-641.

Burgess, N., Spiers, H. J., & Paleologou, E. (2004). Orientational manoeuvres in the dark: dissociating allocentric and egocentric influences on spatial memory. Cognition, 94(2), 149-166.

Bush, D., Barry, C., & Burgess, N. (2014). What do grid cells contribute to place cell firing? Trends in Neurosciences, 37(3), 136-145.

Buzsaki, G., & Moser, E. I. (2013). Memory, navigation and theta rhythm in the hippocampal-entorhinal system. Nature Neuroscience, 16(2), 130-138.

Cacucci, F., Lever, C., Wills, T. J., Burgess, N., & O'Keefe, J. (2004). Theta-modulated place-by-direction cells in the hippocampal formation in the rat. The Journal of Neuroscience, 24(38), 8265-8277.

Chen, G., King, J. A., Burgess, N., & O'Keefe, J. (2013). How vision and movement combine in the hippocampal place code. Proceedings of the National Academy of Sciences, 110(1), 378-383.

Chen, L. L., Lin, L. H., Green, E. J., Barnes, C. A., & McNaughton, B. L. (1994). Head-direction cells in the rat posterior cortex. a. Anatomical distribution and behavioural modulation. Experimental Brain Research, 101(1), 8-23.

Chen, L. L., Lin, L.H., Barnes, C. A., & McNaughton, B. L. (1994). Head-direction cells in the rat posterior cortex. b. Contributions of visual and ideothetic information to the directional firing. Experimental brain research. 101(1), 24-34.

Cho, J., & Sharp, P. E. (2001). Head direction, place, and movement correlates for cells in the rat retrosplenial cortex. Behavioral Neuroscience, 115(1), 3-25.

Clark, B. J., Bassett, J. P., Wang, S. S., & Taube, J. S. (2010). Impaired head direction cell representation in the anterodorsal thalamus after lesions of the retrosplenial cortex. The Journal of Neuroscience, 30(15), 5289-5302.

Colom, L. V., & Bland, B. H. (1987). State-dependent spike train dynamics of hippocampal formation neurons: evidence for theta-on and theta-off cells. Brain Research, 422(2), 277-286.

Cooper, B. G., Manka, T. F., & Mizumori, S. J. (2001). Finding your way in the dark: the retrosplenial cortex contributes to spatial memory and navigation without visual cues. Behavioral Neuroscience, 115(5), 1012-1028.

Cooper, B. G., & Mizumori, S. J. (1999). Retrosplenial cortex inactivation selectively impairs navigation in darkness. Neuroreport, 10(3), 625-630.

Cooper, B. G., & Mizumori, S. J. (2001). Temporary inactivation of the retrosplenial cortex causes a transient reorganization of spatial coding in the hippocampus. The Journal of Neuroscience, 21(11), 3986-4001.

Cressant, A., Muller, R. U., & Poucet, B. (1997). Failure of centrally placed objects to control the firing fields of hippocampal place cells. Journal of Neuroscience, 17(7), 2531-2542.

Czajkowski, R., Sugar, J., Zhang, S. J., Couey, J. J., Ye, J., & Witter, M. P. (2013). Superficially projecting principal neurons in layer V of medial entorhinal cortex in the rat receive excitatory retrosplenial input. The Journal of Neuroscience, 33(40), 15779-15792.

de Almeida, L., Idiart, M., & Lisman, J. E. (2009). The Input-Output Transformation of the Hippocampal Granule Cells: From Grid Cells to Place Fields. Journal of Neuroscience, 29(23), 7504-7512.

Dilks, D. D., Julian, J. B., Kubilius, J., Spelke, E. S., & Kanwisher, N. (2011). Mirror-image sensitivity and invariance in object and scene processing pathways. *The Journal of Neuroscience*, *31*(31), 11305-11312

Dillingham, C. M., Frizzati, A., Nelson, A. J., & Vann, S. D. (2015). How do mammillary body inputs contribute to anterior thalamic function? Neuroscience & Biobehavioral Reviews, 54, 108-119.

Ekstrom, A. D., Kahana, M. J., Caplan, J. B., Fields, T. A., Isham, E. A., Newman, E. L., & Fried, I. (2003). Cellular networks underlying human spatial navigation. Nature, 425(6954), 184-188.

Elduayen, C., & Save, E. (2014). The retrosplenial cortex is necessary for path integration in the dark. Behavioural Brain Research, 272, 303-307.

Eleore, L., López-Ramos, J. C., Guerra-Narbona, R., & Delgado-García, J. M. (2011). Role of reuniens nucleus projections to the medial prefrontal cortex and to the hippocampal pyramidal CA1 area in associative learning. *PloS one*, *6*(8).

Epstein, R. A. (2008). Parahippocampal and retrosplenial contributions to human spatial navigation. Trends in Cognitive Sciences, 12(10), 388-396.

Etienne, A. S. (1992). Navigation of a small mammal by dead reckoning and local cues. Current Directions in Psychological Science, 1 (2) 48-52.

Etienne, A. S., & Jeffery, K. J. (2004). Path integration in mammals. Hippocampus, 14(2), 180-192.

Etienne, A. S., Maurer, R., Berlie, J., Reverdin, B., Rowe, T., Georgakopoulos, J., & Séguinot, V. (1998). Navigation through vector addition. Nature, 396(6707), 161-164.

Fenton, A. A., Kao, H. Y., Neymotin, S. A., Olypher, A., Vayntrub, Y., Lytton, W. W., & Ludvig, N. (2008). Unmasking the CA1 Ensemble Place Code by Exposures to Small and Large Environments: More Place Cells and Multiple, Irregularly Arranged, and Expanded Place Fields in the Larger Space. The Journal of Neuroscience, 28(44), 11250-11262.

Frank, L. M., Stanley, G. B., & Brown, E. N. (2004). Hippocampal plasticity across multiple days of exposure to novel environments. The Journal of Neuroscience, 24(35), 7681-7689.

Fuchs, A. F., & Kimm, J. (1975). Unit activity in vestibular nucleus of the alert monkey during horizontal angular acceleration and eye movement. Journal of Neurophysiology, 38(5), 1140-1161.

Fuhs, M. C., & Touretzky, D. S. (2006). A spin glass model of path integration in rat medial entorhinal cortex. The Journal of Neuroscience, 26(16), 4266-4276.

Fujisawa, S., & Buzsáki, G. (2011). A 4 Hz oscillation adaptively synchronizes prefrontal, VTA, and hippocampal activities. Neuron, 72(1), 153-165.

Garden, D. L., Massey, P. V., Caruana, D. A., Johnson, B., Warburton, E. C., Aggleton, J. P., & Bashir, Z. I. (2009). Anterior thalamic lesions stop synaptic plasticity in retrosplenial cortex slices: expanding the pathology of diencephalic amnesia. Brain, 132, 1847-1857.

Gevins, A., Smith, M.E., McEvoy, L., Yu,D. (1997). High-resolution EEG mapping of cortical activation related to working memory: Effects of task difficulty, type of processing, and practice. Cerebral Cortex, 374-385.

Giocomo, L. M., Zilli, E. A., Fransén, E., & Hasselmo, M. E. (2007). Temporal frequency of subthreshold oscillations scales with entorhinal grid cell field spacing. Science, 315(5819), 1719-1722.

Gonzalo-Ruiz, A., & Bayona, I. (2001). Localization of excitatory amino acid and neuropeptide markers in neurons of the subicular complex projecting to the retrosplenial granular cortex of the rat. European Journal of Anatomy, 5(3), 119-132.

Goodridge, J. P., Dudchenko, P. A., Worboys, K. A., Golob, E. J., & Taube, J. S. (1998). Cue control and head direction cells. Behavioral Neuroscience, 112(4), 749-761.

Goodridge, J. P., & Taube, J. S. (1997). Interaction between the postsubiculum and anterior thalamus in the generation of head direction cell activity. The Journal of Neuroscience, 17(23), 9315-9330.

Gothard, K. M., Skaggs, W. E., & McNaughton, B. L. (1996). Dynamics of mismatch correction in the hippocampal ensemble code for space: Interaction between path integration and environmental cues. The Journal of Neuroscience, 16(24), 8027-8040.

Goutagny, R., Jackson, J., & Williams, S. (2009). Self-generated theta oscillations in the hippocampus. Nature Neuroscience, 12(12), 1491-1493.

Gray, C. M., Maldonado, P. E., Wilson, M., & McNaughton, B. (1995). Tetrodes markedly improve the reliability and yield of multiple single-unit isolation from multi-unit recordings in cat striate cortex. Journal of neuroscience methods, 63(1), 43-54.

Guzowski, J. F., McNaughton, B. L., Barnes, C. A., & Worley, P. F. (1999). Environment-specific expression of the immediate-early gene Arc in hippocampal neuronal ensembles. Nature Neuroscience, 2(12), 1120-1124.

Hafting, T., Fyhn, M., Bonnevie, T., Moser, M. B., & Moser, E. I. (2008). Hippocampus-independent phase precession in entorhinal grid cells. Nature, 453(7199), 1248-1252.

Hafting, T., Fyhn, M., Molden, S., Moser, M. B., & Moser, E. I. (2005). Microstructure of a spatial map in the entorhinal cortex. Nature, 436(7052), 801-806.

Hales, J. B., Schlesiger, M. I., Leutgeb, J. K., Squire, L. R., Leutgeb, S., & Clark, R. E. (2014). Medial Entorhinal Cortex Lesions Only Partially Disrupt Hippocampal Place Cells and Hippocampus-Dependent Place Memory. Cell Reports, 9(3), 893-901.

Harker, K. T., & Whishaw, I. Q. (2004). Impaired place navigation in place and matching-to-place swimming pool tasks follows both retrosplenial cortex lesions and cingulum bundle lesions in rats. Hippocampus, 14(2), 224-231.

Harker, K. T., & Whishaw, I. Q. (2004). A reaffirmation of the retrosplenial contribution to rodent navigation: reviewing the influences of lesion, strain, and task. Neuroscience Biobehavioural Reviews, 28(5), 485-496.

Hartley, T., Burgess, N., Lever, C., Cacucci, F., & O'Keefe, J. (2000). Modeling place fields in terms of the cortical inputs to the hippocampus. Hippocampus, 10(4), 369-379.

Hasselmo, M. E. (2005). What is the function of hippocampal theta Rhythm? Linking behavioral data to phasic properties of field potential and unit recording data. Hippocampus, 15(7), 936-949.

Hasselmo, M. E. (2009). A model of episodic memory: Mental time travel along encoded trajectories using grid cells. Neurobiology of Learning and Memory, 92(4), 559-573.

Hayman, R. M., & Jeffery, K. J. (2008). How Heterogeneous Place Cell Responding Arises From Homogeneous Grids-A Contextual Gating Hypothesis. Hippocampus, 18(12), 1301-1313.

Henriksen, E. J., Colgin, L. L., Barnes, C. A., Witter, M. P., Moser, M. B., & Moser, E. I. (2010). Spatial Representation along the proximodistal axis of CA1. Neuron, 68(1), 127-137.

Hill, A. (1978). First occurrence of hippocampal spatial firing in a new environment. Experimental Neurology, 62(2), 282-297.

Hok, V., Lenck-Santini, P. P., Roux, S., Save, E., Muller, R. U., & Poucet, B. (2007). Goal-related activity in hippocampal place cells. The Journal of Neuroscience, 27(3), 472-482.

Hok, V., Save, E., Lenck-Santini, P. P., & Poucet, B. (2005). Coding for spatial goals in the prelimbic/infralimbic area of the rat frontal cortex. Proceedings of the National Academy of Sciences of the United States of America, 102(12), 4602-4607.

Hoover, W. B., & Vertes, R. P. (2007). Anatomical analysis of afferent projections to the medial prefrontal cortex in the rat. Brain Structure and Function, 212(2), 149-179.

Huxter, J., Burgess, N., & O'Keefe, J. (2003). Independent rate and temporal coding in hippocampal pyramidal cells. Nature, 425(6960), 828-832.

Ino, T., Doi, T., Hirose, S., Kimura, T., Ito, J., & Fukuyama, H. (2007). Directional disorientation following left retrosplenial hemorrhage: a case report with fMRI studies. Cortex, 43(2), 248-254.

Jankowski, M.M., Passecker, J., Nural, I.M., Vann, S.D, Erichsen, J. T., Aggleton, J.P., & O'Mara, S. M. (2015). Evidence for Spatially-Responsive Neurons in the Rostral Thalamus. Frontiers in Behavioral Neuroscience, 9 (256), 1-18.

Jankowski, M. M., Islam, M. N., Wright, N. F., Vann, S. D., Erichsen, J. T., Aggleton, J. P., & O'Mara, S. M. (2014). Nucleus reuniens of the thalamus contains head direction cells. Elife, 3, e03075. 1-10.

Jankowski, M. M., & O'Mara, S. M. (2015). Dynamics of Place, Boundary and Object Encoding In Rat Anterior Claustrum. Frontiers in Behavioral Neuroscience, 9, 250, 1-19.

Jeffery, K. J. (2007). Self-localization and the entorhinal-hippocampal system. Current Opinion in Neurobiology, 17(6), 684-691.

Jeffery, K. J., & Burgess, N. (2006). A metric for the cognitive map: found at last? Trends in Cognitive Sciences, 10(1), 1-3.

Jenkins, T. A., Vann, S. D., Amin, E., & Aggleton, J. P. (2004). Anterior thalamic lesions stop immediate early gene activation in selective laminae of the retrosplenial cortex: evidence of covert pathology in rats? European Journal of Neuroscience, 19(12), 3291-3304.

Jones, B. F., & Witter, M. P. (2007). Cingulate cortex projections to the parahippocampal region and hippocampal formation in the rat. Hippocampus, 17(10), 957-976.

Jones, M. W., & Wilson, M. A. (2005). Theta rhythms coordinate hippocampal–prefrontal interactions in a spatial memory task. *PLoS Biol*,*3*(12), e402.

Jung, M. W., Qin, Y., McNaughton, B. L., & Barnes, C. A. (1998). Firing characteristics of deep layer neurons in prefrontal cortex in rats performing spatial working memory tasks. Cerebral Cortex, 8(5), 437-450.

Jung, M. W., Wiener, S. I., & Mcnaughton, B. L. (1994). Comparison of Spatial Firing Characteristics of Units in Dorsal and Ventral Hippocampus of the Rat. The Journal of Neuroscience, 14(12), 7347-7356.

Katayama, K., Takahashi, N., Ogawara, K., & Hattori, T. (1999). Pure topographical disorientation due to right posterior cingulate lesion. *Cortex*,*35*(2), 279-282.

Keene, C. S., & Bucci, D. J. (2008). Contributions of the retrosplenial and posterior parietal cortices to cue-specific and contextual fear conditioning. *Behavioral neuroscience*, *122*(1), 89.

Keller, E. L., & Kamath, B. Y. (1975). Characteristics of head rotation and eye movement-related neurons in alert monkey vestibular nucleus. Brain Research, 100(1), 182-187.

Kesner, R. P., & Churchwell, J. C. (2011). An analysis of rat prefrontal cortex in mediating executive function. Neurobiology of Learning and Memory, 96(3), 417-431.

Kjelstrup, K. B., Solstad, T., Brun, V. H., Hafting, T., Leutgeb, S., Witter, M. P., Moser, E. I., Moser, M. B. (2008). Finite scale of spatial representation in the hippocampus. Science, 321(5885), 140-143.

Kobayashi, Y., & Amaral, D. G. (2000). Macaque monkey retrosplenial cortex: I. Three-dimensional and cytoarchitectonic organization. Journal of Comparative Neurology, 426(3), 339-365.

Kobayashi, Y., & Amaral, D. G. (2003). Macaque monkey retrosplenial cortex: II. Cortical afferents. Journal of Comparative Neurology, 466(1), 48-79.

Koenig, J., Linder, A. N., Leutgeb, J. K., & Leutgeb, S. (2011). The Spatial Periodicity of Grid Cells Is Not Sustained During Reduced Theta Oscillations. Science, 332(6029), 592-595.

Kramis, R., Vanderwolf, C. H., & Bland, B. H. (1975). Two types of hippocampal rhythmical slow activity in both the rabbit and the rat: relations to behavior and effects of atropine, diethyl ether, urethane, and pentobarbital. *Experimental neurology*, *49*(1), 58-85.

Kropff, E., Carmichael, J. E., Moser, M.B., & Moser, E. I. (2015). Speed cells in the medial entorhinal cortex. Nature. 523, 419-424

Kurotani, T., Miyashita, T., Wintzer, M., Konishi, T., Sakai, K., Ichinohe, N., & Rockland, K. S. (2013). Pyramidal neurons in the superficial layers of rat retrosplenial cortex exhibit a late-spiking firing property. Brain Structure Function, 218(1), 239-254.

Langston, R. F., Ainge, J. A., Couey, J. J., Canto, C. B., Bjerknes, T. L., Witter, M. P., Moser, E.I., Moser, M. B. (2010). Development of the Spatial Representation System in the Rat. Science, 328(5985), 1576-1580.

Leung, L. W., & Borst, J. G. G. (1987). Electrical activity of the cingulate cortex. I. Generating mechanisms and relations to behavior. *Brain research*,*407*(1), 68-80.

Leutgeb, S., Ragozzino, K., & Mizumori, S. (2000). Convergence of head direction and place information in the CA1 region of hippocampus. Neuroscience, 100(1), 11-19.

Lever, C., Burgess, N., Cacucci, F., Hartley, T., & O'Keefe, J. (2002). What can the hippocampal representation of environmental geometry tell us about Hebbian learning? Biological Cybernetics, 87(5-6), 356-372.

Lever, C., Burton, S., Jeewajee, A., O'Keefe, J., & Burgess, N. (2009). Boundary vector cells in the subiculum of the hippocampal formation. The Journal of Neuroscience, 29(31), 9771-9777.

Logothetis, N. K. (2008). What we can do and what we cannot do with fMRI.*Nature*, *453*(7197), 869-878.

Lyttle, D., Gereke, B., Lin, K. K., & Fellous, J. M. (2013). Spatial scale and place field stability in a grid-to-place cell model of the dorsoventral axis of the hippocampus. Hippocampus, 23(8), 729-744.

Maguire, E. (2001). The retrosplenial contribution to human navigation: a review of lesion and neuroimaging findings. Scandinavian Journal of Psychology, 42(3), 225-238.

McDonald, C. R., Crosson, B., Valenstein, E., & Bowers, D. (2001). Verbal encoding deficits in a patient with a left retrosplenial lesion. Neurocase, 7(5), 407-417.

McKenna, J. T., & Vertes, R. P. (2004). Afferent projections to nucleus reuniens of the thalamus. Journal of Comparative Neurology, 480(2), 115-142.

McNaughton, B. L., Battaglia, F. P., Jensen, O., Moser, E. I., & Moser, M. B. (2006). Path integration and the neural basis of the 'cognitive map'. Nature Reviews Neuroscience, 7(8), 663-678.

Meibach, R. C., & Siegel, A. (1977). Subicular projections to the posterior cingulate cortex in rats. Experimental Neurology, 57(1), 264-274.

Meunier, M., Jaffard, R., & Destrade, C. (1991). Differential involvement of anterior and posterior cingulate cortices in spatial discriminative learning in a T-maze in mice. Behavioural Brain Research, 44(2), 133-143.

Miller, A. M., Vedder, L. C., Law, L. M., & Smith, D. M. (2014). Cues, context, and long-term memory: the role of the retrosplenial cortex in spatial cognition. *Frontiers in human neuroscience*, *8*, 586.

Minoshima, S., Giordani, B., Berent, S., Frey, K. A., Foster, N. L., & Kuhl, D. E. (1997). Metabolic reduction in the posterior cingulate cortex in very early Alzheimer's disease. Annals of Neurology, 42(1), 85-94.

Mitchell, S. J., & Ranck, J. B. (1980). Generation of theta rhythm in medial entorhinal cortex of freely moving rats. *Brain research*, *189*(1), 49-66.

Mittelstaedt, M.-L., & Mittelstaedt, H. (1980). Homing by path integration in a mammal. Naturwissenschaften, 67(11), 566-567.

Miyashita, T., & Rockland, K. S. (2007). GABAergic projections from the hippocampus to the retrosplenial cortex in the rat. European Journal of Neuroscience, 26(5), 1193-1204.

Mizumori, S.J., & Williams, J. D. (1993). Directionally selective mnemonic properties of neurons in the lateral dorsal nucleus of the thalamus of rats. The Journal of neuroscience, 13(9), 4015-4028.

Mizumori, S. J., Cooper, B. G., Leutgeb, S., & Pratt, W. E. (2000). A neural systems analysis of adaptive navigation. Molecular Neurobiology, 21(1-2), 57-82.

Mizumori, S. J., Ragozzino, K. E., & Cooper, B. G. (2000). Location and head direction representation in the dorsal striatum of rats. Psychobiology, 28(4), 441-462.

Moghaddam, M., & Bures, J. (1996). Contribution of egocentric spatial memory to place navigation of rats in the Morris water maze. Behavioural Brain Research, 78(2), 121-129.

Monaco, J. D., & Abbott, L. F. (2011). Modular Realignment of Entorhinal Grid Cell Activity as a Basis for Hippocampal Remapping. The Journal of Neuroscience, 31(30), 9414-9425

Morgan, L. K., MacEvoy, S. P., Aguirre, G. K., & Epstein, R. A. (2011). Distances between real-world locations are represented in the human hippocampus. *The Journal of Neuroscience*, *31*(4), 1238-1245.

Morris, R., Pandya, D. N., & Petrides, M. (1999). Fiber system linking the mid-dorsolateral frontal cortex with the retrosplenial/presubicular region in the rhesus monkey. Journal of Comparative Neurology, 407(2), 183-192.

Morris, R. G. M. (1981). Spatial localization does not require the presence of local cues. Learning and Motivation, 12(2), 239-260.

Morris, R. G. M., Garrud, P., Rawlins, J. N. P., & Okeefe, J. (1982). Place Navigation Impaired in Rats with Hippocampal-Lesions. Nature, 297(5868), 681-683.

Moser, E. I., Kropff, E., & Moser, M.B. (2008). Place cells, grid cells, and the brain's spatial representation system. Annual Review of Neuroscience, 31, 69-89.

Muller, R.U. (1996). A quarter of a century of place cells. Neuron, 17(5), 813-822.

Muller, R. U., Bostock, E., Taube, J. S., & Kubie, J. L. (1994). On the directional firing properties of hippocampal place cells. The Journal of Neuroscience, 14(12), 7235-7251.

Muller, R. U., & Kubie, J. L. (1987). The effects of changes in the environment on the spatial firing of hippocampal complex-spike cells. The Journal of Neuroscience, 7(7), 1951-1968.

Muller, R. U., Kubie, J. L., Bostock, E.M, Taube, J.S., & Quirk, G. J. (1991). Spatial firing correlates of neurons in the hippocampal formation of freely moving rats. (pp.296-333). New York: Oxford University Press.

Muller, R. U., Kubie, J. L., & Ranck Jr, J. B. (1987). Spatial Firing Patterns of Hippocampal Complex-Spike Cells in a Fixed Environment. The Journal of Neuroscience, 7(7), 1935-1950.

Nakashiba, T., Young, J. Z., McHugh, T. J., Buhl, D. L., & Tonegawa, S. (2008). Transgenic inhibition of synaptic transmission reveals role of CA3 output in hippocampal learning. Science, 319(5867), 1260-1264.

Nelson, A. J. D., Hindley, E. L., Pearce, J. M., Vann, S. D., & Aggleton, J. P. (2015). The effect of retrosplenial cortex lesions in rats on incidental and active spatial learning. Frontiers in behavioral neuroscience, 9 (11), 1-16.

Nelson, A. J., Powell, A. L., Holmes, J. D., Vann, S. D., & Aggleton, J. P. (2015). What does spatial alternation tell us about retrosplenial cortex function? *Frontiers in behavioral neuroscience, 9.*

Neunuebel, J.P., Knierim, J.J. (2012). Spatial firing correlates of physiological distinct cell types of the rat dentate gyrus. The Journal of Neuroscience. 32, 3848-3858.

Nitz. D.A. (2006). Tracking route progression in the posterior parietal cortex. Neuron, 2(49), 747-756.

O'Keefe, J. (1976). Place units in the hippocampus of the freely moving rat. Experimental Neurology, 51(1), 78-109.

O'Keefe, J. (1979). A review of the hippocampal place cells. Progress in Neurobiology, 13(4), 419-439.

O'Keefe, J., & Burgess, N. (1996). Geometric determinants of the place fields of hippocampal neurons. Nature, 381(6581), 425-428.

O'Keefe, J., & Burgess, N. (2005). Dual phase and rate coding in hippocampal place cells: Theoretical significance and relationship to entorhinal grid cells. Hippocampus, 15(7), 853-866.

O'Keefe, J., & Dostrovsky, J. (1971). The hippocampus as a spatial map. Preliminary evidence from unit activity in the freely-moving rat. Brain Research, 34(1), 171-175.

O'Keefe, J., & Nadel, L. (1978). The hippocampus as a cognitive map.Oxford: Clarendon Press.

O'Keefe, J., & Recce, M. L. (1993). Phase relationship between hippocampal place units and the EEG theta-rhythm. Hippocampus, 3(3), 317-330.

O'Keefe, J., & Speakman, A. (1987). Single unit activity in the rat hippocampus during a spatial memory task. Experimental Brain Research, 68(1), 1-27.

O'Mara, S. M. (1995). Spatially selective firing properties of hippocampal formation neurons in rodents and primates. Progress in Neurobiology, 45(3), 253-274.

Paxinos, G., & Watson, C. (2005) The rat brain in stereotaxic coordinates. Burlington MA: Elsevier academic press.

Pothuizen, H. H., Aggleton, J. P., & Vann, S. D. (2008). Do rats with retrosplenial cortex lesions lack direction? European Journal of Neuroscience, 28(12), 2486-2498.

Poucet, B., Sargolini, F., Song, E. Y., Hangya, B., Fox, S., & Muller, R. U. (2014). Independence of landmark and self-motion-guided navigation: a different role for grid cells. Philosophical Transactions of the Royal Society B-Biological Sciences, 369(1635), 1-9.

Poucet, B., Thinus-Blanc, C., & Muller, R. U. (1994). Place cells in the ventral hippocampus of rats. Neuroreport, 5(16), 2045-2048

Prasad, J. A., & Chudasama, Y. (2013). Viral tracing identifies parallel disynaptic pathways to the hippocampus. The Journal of Neuroscience, 33(19), 8494-8503.

Quirk, G. J., Muller, R. U., Kubie, J. L., & Ranck Jr, J. B. (1992). The positional firing properties of medial entorhinal neurons: description and comparison with hippocampal place cells. The Journal of Neuroscience, 12(5), 1945-1963.

Ranck Jr, J. B. (1973). Studies on single neurons in dorsal hippocampal formation and septum in unrestrained rats: Part I. Behavioral correlates and firing repertoires. Experimental neurology, 41(2), 462-531.

Ranck Jr, J.B. (1984). Head direction cells in the deep cell layer of dorsal presubiculum in freely moving rats. Society for Neuroscience. Abstract 10:599

Rancz, E. A., Moya, J., Drawitsch, F., Brichta, A. M., Canals, S., & Margrie, T. W. (2015). Widespread Vestibular Activation of the Rodent Cortex. The Journal of Neuroscience, 35(15), 5926-5934.

Redish, A. D., Battaglia, F. P., Chawla, M. K., Ekstrom, A. D., Gerrard, J. L., Lipa, P., Rosenzweig, E.S., Worley, P.F., Guzowski, J.F., McNaughton, B.L., Barnes, C. A. (2001). Independence of firing correlates of anatomically proximate hippocampal pyramidal cells. The Journal of Neuroscience, 21(5), 1-6.

Reep, R.L., Chandler, H.C., King, V., & Corwin, J.V. (1994). Rat posterior parietal cortex: topography of corticocortical and thalamic connections. Experimental Brain Research, 100(1), 67-84.

Rolls, E. T., Stringer, S. M., & Elliot, T. (2006). Entorhinal cortex grid cells can map to hippocampal place cells by competitive learning. Network: Computation in Neural Systems, 17(4), 447-465.

Rotenberg, A., & Muller, R. U. (1997). Variable place-cell coupling to a continuously viewed stimulus: evidence that the hippocampus acts as a perceptual system. Philosophical Transactions of the Royal Society of London Series B: Biological Sciences, 352(1360), 1505-1513.

Royer, S., Sirota, A., Patel, J., & Buzsáki, G. (2010). Distinct representations and theta dynamics in dorsal and ventral hippocampus. The Journal of Neuroscience, 30(5), 1777-1787.

Sainsbury, R. S., Harris, J. L., & Rowland, G. L. (1987). Sensitization and hippocampal type 2 theta in the rat. *Physiology & Behavior*, *41*(5), 489-493.

Sargolini, F., Fyhn, M., Hafting, T., McNaughton, B. L., Witter, M. P., Moser, M.B., & Moser, E. I. (2006). Conjunctive representation of position, direction, and velocity in entorhinal cortex. Science, 312(5774), 758-762.

Save, E., Cressant, A., Thinus-Blanc, C., & Poucet, B. (1998). Spatial firing of hippocampal place cells in blind rats. the Journal of Neuroscience, 18(5), 1818-1826.

Save, E., Nerad, L., & Poucet, B. (2000). Contribution of multiple sensory information to place field stability in hippocampal place cells. Hippocampus, 10(1), 64-76.

Savelli, F., & Knierim, J. J. (2010). Hebbian analysis of the transformation of medial entorhinal grid-cell inputs to hippocampal place fields. The Journal of Neurophysiology, 103(6), 3167-3183.

Sharp, P. E., & Koester, K. (2008). Lesions of the mammillary body region severely disrupt the cortical head direction, but not place cell signal. Hippocampus, 18(8), 766-784.

Sharp, P. E., Tinkelman, A., & Cho, J. (2001). Angular velocity and head direction signals recorded from the dorsal tegmental nucleus of gudden in the rat: implications for path integration in the head direction cell circuit. Behavioral Neuroscience, 115(3), 571-588.

Shettleworth, S. J. (2009). *Cognition, evolution, and behavior*. Oxford University Press.

Shibata, H. (1994). Terminal Distribution of Projections from the Retrosplenial Area to the Retrohippocampal Region in the Rat, as Studied by Anterograde Transport of Biotinylated Dextran-Amine. Neuroscience Research, 20(4), 331-336.

Shinder, M. E., & Taube, J. S. (2010). Differentiating ascending vestibular pathways to the cortex involved in spatial cognition. Journal of Vestibular Research, 20(1), 3.

Sirota, A., Montgomery, S., Fujisawa, S., Isomura, Y., Zugaro, M., & Buzsáki, G. (2008). Entrainment of neocortical neurons and gamma oscillations by the hippocampal theta rhythm. *Neuron, 60*(4), 683-697.

Skaggs, W. E., Knierim, J. J., Kudrimoti, H. S., & McNaughton, B. L. (1995). A model of the neural basis of the rat's sense of direction. Advances in neural information processing systems, 7, 173-180.

Skaggs, W. E., & McNaughton, B. L. (1996). Theta Phase Precession in Hippocampal. Hippocampus, 6, 149-172.

Small, D. M., Zatorre, R. J., Dagher, A., Evans, A. C., & Jones-Gotman, M. (2001). Changes in brain activity related to eating chocolate: From pleasure to aversion. Brain, 124, 1720-1733.

Solstad, T., Boccara, C. N., Kropff, E., Moser, M.B., & Moser, E. I. (2008). Representation of geometric borders in the entorhinal cortex. Science, 322(5909), 1865-1868.

Solstad, T., Moser, E. I., & Einevoll, G. T. (2006). From grid cells to place cells: A mathematical model. Hippocampus, 16(12), 1026-1031.

Speakman, A., O'Keefe, J. (1990) Hippocampal complex spike cells do not change their place fields if the goal is moved within a cue controlled environment. The European Journal of Neuroscience. 2(6), 544-555.

Spiers, H. J., & Maguire, E. A. (2006). Thoughts, behaviour, and brain dynamics during navigation in the real world. Neuroimage, 31(4), 1826-1840.

Spiers, H. J., & Maguire, E. A. (2007). The neuroscience of remote spatial memory: A tale of two cities. Neuroscience, 149(1), 7-27.

St-Laurent, M., Petrides, M., & Sziklas, V. (2009). Does the cingulate cortex contribute to spatial conditional associative learning in the rat? Hippocampus, 19(7), 612-622.

Stackman, R. W., & Taube, J. S. (1997). Firing properties of head direction cells in the rat anterior thalamic nucleus: dependence on vestibular input. The Journal of Neuroscience, 17(11), 4349-4358.

Stackman, R. W., & Taube, J. S. (1998). Firing properties of rat lateral mammillary single units: head direction, head pitch, and angular head velocity. The Journal of Neuroscience, 18(21), 9020-9037.

Stensola, H., Stensola, T., Solstad, T., Froland, K., Moser, M. B., & Moser, E. I. (2012). The entorhinal grid map is discretized. Nature, 492(7427), 72-78.

Sugar, J., Witter, M. P., van Strien, N. M., & Cappaert, N. L. (2011). The retrosplenial cortex: intrinsic connectivity and connections with the (para) hippocampal region in the rat. An interactive connectome. Frontiers in Neuroinformatics, 5. 1-13.

Sutherland, R.J., Whishaw, I.Q., & Kolb, B. (1988). Contributions of cingulate cortex to two forms of spatial learning and memory. The Journal of Neuroscience, 8(6), 1863-1872.

Svoboda, E., McKinnon, M. C., & Levine, B. (2006). The functional neuroanatomy of autobiographical memory: A meta-analysis. Neuropsychologia, 44(12), 2189-2208.

Takahashi, N., Kawamura, M., Shiota, J., Kasahata, N., & Hirayama, K. (1997). Pure topographic disorientation due to right retrosplenial lesion.*Neurology*, *49*(2), 464-469.

Talk, A., Kang, E., Gabriel, M. (2004). Independent generation of the theta rhythm in the hippocampus and the posterior cingulate cortex. Brain Research, 1015, 15-24.

Taube, J.S. (1995). Head direction cells recorded in the anterior thalamic nuclei of freely moving rats. The Journal of Neuroscience. 15, 70-86.

Taube, J. S. (1995). Place cells recorded in the parasubiculum of freely moving rats. Hippocampus, 5(6), 569-583.

Taube, J. S. (2007). The head direction signal: origins and sensory-motor integration. Annual Review of Neuroscience. 30, 181-207.

Taube, J. S., & Bassett, J. P. (2003). Persistent neural activity in head direction cells. Cerebral Cortex, 13(11), 1162-1172.

Taube, J. S., Muller, R. U., & Ranck Jr, J. B. (1990). Head-direction cells recorded from the postsubiculum in freely moving rats. a. Description and quantitative analysis. The Journal of Neuroscience, 10(2), 420-435.

Taube, J. S., Muller, R. U., & Ranck Jr, J. B. (1990). Head-direction cells recorded from the postsubiculum in freely moving rats. b. Effects of environmental manipulations. The Journal of Neuroscience, 10(2), 436-447.

Thompson, L. T., & Best, P. J. (1989). Place cells and silent cells in the hippocampus of freely-behaving rats. The Journal of Neuroscience, 9(7), 2382-2390.

Thompson, L. T., & Best, P. J. (1990). Long-term stability of the place-field activity of single units recorded from the dorsal hippocampus of freely behaving rats. Brain Research, 509(2), 299-308.

Todd, T. P., & Bucci, D. J. (2015). Retrosplenial cortex and long-term memory: Molecules to behavior. *Neural plasticity, 2015.*

Tolman, E. C. (1948). Cognitive Maps in Rats and Men. The Psychological Review, 55(4), 189-208.

Tsanov, M., Chah, E., Noor, M. S., Egan, C., Reilly, R. B., Aggleton, J. P., Erichsen, J.T., Vann, S.D., O'Mara, S. M. (2014). The irregular firing properties of thalamic head direction cells mediate turn-specific modulation of the directional tuning curve. The Journal of Neurophysiology, 112(9), 2316-2331.

Tsanov, M., Chah, E., Vann, S. D., Reilly, R. B., Erichsen, J. T., Aggleton, J. P., & O'Mara, S. M. (2011). Theta-modulated head direction cells in the rat anterior thalamus. The Journal of Neuroscience, 31(26), 9489-9502.

Yartsev, M. & Ulanovsky, N. (2013). Representation of three-dimensional space in the hippocampus of freely flying bats. Science, 340 (6310), 367-372.

Vago, D. R., & Kesner, R. P. (2008). Disruption of the direct perforant path input to the CA1 subregion of the dorsal hippocampus interferes with spatial working memory and novelty detection. Behavioural Brain Research, 189(2), 273-283.

Van Cauter, T., Camon, J., Alvernhe, A., Elduayen, C., Sargolini, F., Save, E. (2013). Distinct roles of medial and lateral entorhinal cortex in spatial cognition. Cerebral Cortex. 23(2), 451-459.

Van Groen, T., & Michael Wyss, J. (1990). Connections of the retrosplenial granular a cortex in the rat. The Journal of Comparative Neurology, 300(4), 593-606.

Van Groen, T., & Wyss, J. M. (1992). Connections of the retrosplenial dysgranular cortex in the rat. The Journal of Comparative Neurology, 315(2), 200-216.

Van Groen, T., & Wyss, J. M. (2003). Connections of the retrosplenial granular b cortex in the rat. The Journal of Comparative Neurology, 463(3), 249-263.

Van Strien, N. M., Cappaert, N. L. M., & Witter, M. P. (2009). The anatomy of memory: an interactive overview of the parahippocampal-hippocampal network. Nature Reviews Neuroscience, 10(4), 272-282.

Vanderwolf, C. H. (1969). Hippocampal electrical activity and voluntary movement in the rat. Electroencephalography and clinical neurophysiology, 26(4), 407-418.

Vann, S.D, Brown, M.W., & Aggleton, J.P. (2000). Fos expression in the rostral thalamic nuclei and associated cortical regions in response to different spatial memory tests. Neuroscience, 101(4), 983-991.

Vann, S. D., & Aggleton, J. P. (2002). Extensive cytotoxic lesions of the rat retrosplenial cortex reveal consistent deficits on tasks that tax allocentric spatial memory. Behavioral Neuroscience, 116(1), 85.

Vann, S. D., & Aggleton, J. P. (2004). Testing the importance of the retrosplenial guidance system: effects of different sized retrosplenial cortex lesions on heading direction and spatial working memory. *Behavioural brain research*, *155*(1), 97-108.

Vann, S. D., & Aggleton, J. P. (2005). Selective dysgranular retrosplenial cortex lesions in rats disrupt allocentric performance of the radial-arm maze task. Behavioral Neuroscience, 119(6), 1682-1686.

Vann, S. D., Aggleton, J. P., & Maguire, E. A. (2009). What does the retrosplenial cortex do? Nature Reviews Neuroscience, 10(11), 792-802.

Vann, S.D., Wilton, L.K., Muir, J.L. Aggleton, J.P. (2003). Testing the importance of the caudal retrosplenial cortex for spatial memory in rats. Behavioural Brain Research, 140(1-2), 107-118.

Vertes, R. P., Hoover, W. B., Do Valle, A. C., Sherman, A., & Rodriguez, J. J. (2006). Efferent projections of reuniens and rhomboid nuclei of the thalamus in the rat. The Journal of Comparative Neurology, 499(5), 768-796.

Vogt, B. A., & Miller, M. W. (1983). Cortical connections between rat cingulate cortex and visual, motor, and postsubicular cortices. The Journal of Comparative Neurology, 216(2), 192-210.

Vogt, B. A., & Peters, A. (1981). Form and distribution of neurons in rat cingulate cortex: areas 32, 24, and 29. The Journal of Comparative Neurology, 195(4), 603-625.

Whishaw, I. Q., & Brooks, B. L. (1999). Calibrating space: exploration is important for allothetic and idiothetic navigation. Hippocampus, 9(6), 659-667.

Whishaw, I. Q., Maaswinkel, H., Gonzalez, C. L., & Kolb, B. (2001). Deficits in allothetic and idiothetic spatial behavior in rats with posterior cingulate cortex lesions. Behavioural Brain Research, 118(1), 67-76.

Whishaw, I. Q., & Vanderwolf, C. H. (1973). Hippocampal EEG and behavior: change in amplitude and frequency of RSA (theta rhythm) associated with spontaneous and learned movement patterns in rats and cats. *Behavioral biology*, *8*(4), 461-484.

Wiener, S. I. (1993). Spatial and behavioral correlates of striatal neurons in rats performing a self-initiated navigation task. The Journal of Neuroscience, 13(9), 3802-3817.

Wik, G., Fischer, H., Finer, B., Bragee, B., Kristianson, M., & Fredrikson, M. (2006). Retrospenial cortical deactivation during painful stimulation of fibromyalgic patients. International Journal of Neuroscience, 116(1), 1-8.

Wilhite, B. L., Teyler, T. J., & Hendricks, C. (1986). Functional relations of the rodent claustral-entorhinal-hippocampal system. Brain research, 365(1), 54-60.

Wills, T. J., Cacucci, F., Burgess, N., & O'Keefe, J. (2010). Development of the hippocampal cognitive map in preweanling rats. Science, 328(5985), 1573-1576.

Wilson, M. A., & Mcnaughton, B. L. (1993). Dynamics of the Hippocampal Ensemble Code for Space. Science, 261(5124), 1055-1058.

Winocur, G. (1982). Radial-arm maze behavior by rats with dorsal hippocampal lesions: Effects of cuing. *Journal of comparative and physiological psychology*, *96*(2), 155.

Witter, M. P., Groenewegen, H. J., Da Silva, F. L., & Lohman, A. H. M. (1989). Functional organization of the extrinsic and intrinsic circuitry of the parahippocampal region. *Progress in neurobiology*, *33*(3), 161-253.

Wyass, J. M., & Van Groen, T. (1992). Connections between the retrosplenial cortex and the hippocampal formation in the rat: a review. Hippocampus, 2(1), 1-11.

Yoon, T., Okada, J., Jung, M. W., & Kim, J. J. (2008). Prefrontal cortex and hippocampus subserve different components of working memory in rats .*Learning & memory*, *15*(3), 97-105.

Young, C. K., & McNaughton, N. (2009). Coupling of theta oscillations between anterior and posterior midline cortex and with the hippocampus in freely behaving rats. *Cerebral Cortex*, *19*(1), 24-40.

Zingg, B., Hintiryan, H., Gou, L., Song, M. Y., Bay, M., Bienkowski, M. S. Foster, N.N., Yamashita, S., Bowman, I., Toga, A.W., Dong, H. W. (2014). Neural Networks of the Mouse Neocortex. Cell, 156(5), 1096-1111.

Zugaro, M. B., Arleo, A., Berthoz, A., & Wiener, S. I. (2003). Rapid spatial reorientation and head direction cells. The Journal of Neuroscience, 23(8), 3478-3482.

Zugaro, M. B., Monconduit, L., & Buzsaki, G. (2005). Spike phase precession persists after transient intrahippocampal perturbation. Nature Neuroscience, 8(1), 67-71.

Zugaro, M. B., Tabuchi, E., & Wiener, S. I. (2000). Influence of conflicting visual, inertial and substratal cues on head direction cell activity. Experimental Brain Research, 133(2), 198-208.

8. Appendix – Conformation of ethical approval for experimentation.

Ethical Review of Licence for the attention of the Ethics Committee, Trinity College Dublin
Ref: 281109

This form which will be submitted for ethical review to a panel including both scientists and non-scientists. Please complete it in accordance with the procedure appended at the end of this document. Please fill in all sections, using as much space as you feel fit. The sections will expand to fit the input. Please ensure that all sections are as comprehensible to a non-scientist as possible, and that they are written either in layman's terms or fully explain all specialist terms.

Project title: *The effects of cognitive ageing on hippocampal function and the role of β–amyloid in Alzheimer's disease and theirs appropriate drug treatment.*

1. Name of licence holder: *Shane O'Mara*

2. Name(s) of person(s) carrying out the procedure: *Shane O'Mara*

3. Department of licence holder: Department of Psychology

4. Email address: smomara@tcd.ie Phone number: *01-896 8447*

5. Premises of work: *Trinity College Dublin, Dublin2*

6. Describe the area of study in layman's terms (e.g. trying to cure which disease, understand which general principle etc):

   This project is part of a research collaboration between GlaxoSmithKline (GSK), Trinity College Institute of Neuroscience (TCIN) in Dublin and National University of Ireland (NUI) in Galway. The overall objective of this project is to expedite the discovery and development of new medicines for the treatment of Alzheimer's disease (AD).

   We will investigate how cognitive ageing affect the brain's activity while the animals solve behavioural tasks (see section 7 below for a detailed explanation) and test different drug candidates to reverse this effect. Mechanisms of action of the loss of cognition and its reversal by these drugs will also be investigated.

7. What will this particular study accomplish (if all goes according to plan)?

   Experiments will be performed in a Plexiglas behavioural testing chamber with two retractable levers mounted on one wall; a photoelectric nose-poke port on the opposite wall, a 24V, 10W cue light above the nose-poke port, and a hopper mounted between the levers on the original wall where sucrose pellets are delivered. The Delayed non Match to Sample task (DNMS) requires the animal to press the retractable lever presented on a random basis in the left or right position (sample response) to initiate

the trial. This initiates the delay phase signalled by the cue light in which a nose-poke in a port located on the opposite wall must occur during a randomly timed 1–30 s interval. Animals typically nose-poke until the delay is over, then return to where both the left and right levers are extended (match/non-match phase). The correct response requires a press on the opposite lever pressed in the sample phase, constituting the non-match response, which is followed by delivery of a sucrose pellet into the hopper. An incorrect response (pressing the same lever pressed as in the sample phase) produces a 5 s time-out in which the overhead lights are turned off. Trials are separated by 10 s. Overall performance of the task declines in a linear manner as the duration of the delay interval is increased from 1 to 30 s. Middle-Aged (15 month) and aged (24month) rats are significantly impaired compared to young adult rats (6 month) when tested in this task for the longer delays (between 15 and 30 s), besides, this task is known to be dependent on structural parts of the hippocampal formation, the striatum and prefrontal cortex.

The second behavioural test used will be the water plus maze. This consists of a plus shaped maze containing water. The animal will be introduced to one arm of the maze and given 1 minute to find a submerged platform in another arm before being removed. The time taken to find the platform and the animals use of external cues to locate the platform are used as a measure of performance in this task. As before, studies have revealed that aged animals have a deficit in this task compared to young animals. This task is known to be dependent upon the hippocampus for spatial memory.

The third behavioural task to be used will be the novel object recognition task. In this task animals are habituated to a black circular arena with diameter of 1 metres. Following habituation animals will be exposed to two novel objects in the arena for 5 minutes. A delay of 10 minutes will pass and the animals will be put back in the arena with a previously seen object A, and a novel object C. Time spent exploring the novel object should exceed time with the previously encountered object, this is to test acquisition of the original 2 objects. The animal will be tested again at 24hr, where it is exposed to object A (familiar) and another novel object D. This is to test if the memory has been fully consolidated and the animal can identify the novel object D. This task is known to be dependent upon the dentate gyrus, a sub-region of the hippocampus and the perirhinal cortex.

Surgical Implantation of cannulae: Rats will be anaesthetised and maintained during the surgery with isofluorane, Ketamine and Xylazine will be used as analgesic agents to alleviate pain during the procedure. The bilateral cannulae implant will involve drilling 2 holes in the skull over the left and right ventricle and cannulae lowered slowly into each ventricle at a depth of 3.6mm below the surface of the brain. A guide cannula will be held in place and fixed to the skull with dental cement. The incision will be closed with surgical staples. Animlas will be decapitated within one month of the procedure. The Cannulae will be used to administer β-amyloid before testing in the delayed non match to sample task. Infusions will be at a rate of 1µl/min with a maximum volume of 10µl.

Long-term potentiation (LTP) in the hippocampus describes a long-lasting change in electrophysiological parameters at the synapse after titanic stimulation of an efferent input. It is considered to be a biological substrate for learning and memory. In this project, the proposal will be examined by comparing changes at the synapse in the hippocampal tissue prepared from animals in which LTP has been induced. LTP will be

induced in urethane-anaesthesised animals. Previous studies have reported an age related deficit maintaining LTP. Animals will be pre-treated with drug candidates to potentially reverse the age related deficit.

The aim of the present project is to firstly support previous data in findings of an age related deficit in these tasks and secondly, we will investigate the role of β-amyloid in the loss of cognition associated with Alzheimer's disease and thirdly we will explore the way we can reverse this behavioural impairment with potential drug candidates. Another important side of this research is the understanding of the mechanisms of action of the drug candidates in order to improve performance in the behavioural tasks. To fully unravel the mechanisms underlying the loss of cognition with age and its reversal with therapeutic drugs we will carry out biochemical analysis on brain regions associated with different behavioural tasks.

8. What species of animal will be used?

Hanvor Wistar or Long Evans Rats.

9. How many animals of each species and strain will be used? Justify this number with a description of the experimental design. Indicate any other supporting information you used to choose your sample size.

Our laboratory boasts a well-established system of advanced training in statistical analyses, with particular expertise in behavioural data handling. Previous work in our laboratory indicates that the minimum number of animals per plasticity group necessary to obtain statistically reliable results in similar experiments is approximately 8 rats. Working with this sample size, analyses of previous data have yielded a power of approximately 80%, when the alpha level is set at 0.05. With the aid of previously published data, we will perform power calculations to obtain the specific numbers of rats per group that we predict will be required for experiments that have not previously been undertaken in our laboratory. Taking into account the ethical priority to minimise the number of animals needed for any experiment, we will perform our calculations to achieve 80% power, when the alpha level is set at 0.05.

For each of all four experiments (assuming four different drug candidates) at least 32 animals (8 young rats without drug treatment, 8 young rats with, 8 middle-aged rats without and 8 middle-aged rats with) have to be used for each of the 3 behavioural experiments, resulting in a minimal number of 96 animals to complete each drug study and a total of 384. Additional studies will include cannulation study of 32 animals, involving β-amyloid infusion and the DNMS task (young rats without infusion, 8 young rats with β-amyloid infusion, 8 middle-aged rats without and 8 middle-aged rats with β-amyloid infusion). Finally LTP studies will include 16 animals (8 middle-age control and 8 middle-aged treated) per study with four potential drug candidates, given a total of 64. Together this results in a minimal number of 480 over 4 years to complete all studies. Note that the drug candidates will be selected on the basis of previous behavioural results obtained during the course of a separate study. Therefore, some of these compounds may or may not be included in the present project, resulting in an adjustable size of the groups.

10. Describe the procedure in terms comprehensible to the layman. Please emphasise the likely costs of the process in terms of animal welfare, i.e. which parts of the procedure may cause suffering, what type, to what degree and for how long?

Long-term potentiation (LTP) in the hippocampus describes a long-lasting change in electrophysiological parameters at the synapse after titanic stimulation of an efferent input. It is considered to be a biological substrate for learning and memory. In this project, the proposal will be examined by comparing changes at the synapse in the hippocampal tissue prepared from animals in which LTP has been induced. LTP will be induced in urethane-anaesthesised animals. Briefly, urethane will be administered intraperitoneally and the deeply anaesthetised animal will be placed in a head holder in a stereotaxic frame. The small cannula will be inserted into the brain ventricle to allow administration of 10µl volumes. Stimulating and recording electrodes will be stereotaxically placed in the perforant path and granule cells of the hippocampus respectively. Test shocks and 30 sec intervals will be delivered throughout the experiment but at a specific point, titanic stimulation (three trains of 50 shocks in 250msec) will be applied to the perforant path to induce LTP. 45 minutes after the tetenic stimulation the animal will be decapitated and the brain dissected for neurochemical analysis.

A second aspect of the surgery concerns the bilateral implantation of cannulas. Those cannulas will allow us to deliver a pharmacological substance that will block temporarily (ca. 90 minutes) *the neurons activity prior to the behavioural testing. The bilateral injections will be performed with stainless-steel injector needles inserted inside the implanted cannulas and fitted so that they protruded into the target area. The injectors are connected via a polyethylene catheter to microsyringes fitted to a micropump. The injection in itselfis given at a rate of 1µl/min. At the end of injection, injector needles will be left in place for 1 more minute to allow the diffusion of the solution. Immediately afterward, inlet cannulas will be replaced and the performance in the behavioural task will be recorded. During the injection, there is no need to restrain the rat; a well handled animal will typically rest on his homecage during the procedure.*

The duration of the DNMS experiment is approximately four months length. The acquisition of the delay non-match to sample task takes from three weeks to one month, after reaching the performance criterion the animals are recorded at base line for 3 weeks before drug dosing begins. The animals receive chronic drug administration according to the procedure described above for a period of up to 2 months. Drugs administration is stopped and recording is continued for a period of up to 1 month as a measure of longevity of drug effects.

All along the course of the DNMS study, the animals will be slightly food deprived allowing them a weight intake equal to 90% of their normal body weight. This procedure is necessary to encourage the animals to solve the behavioural task in maximised conditions. This implies that the animal's weight is monitored daily through the whole time study. There is no need to go under this percentage of body mass (e.g. up to 80%) as the sucrose pellets used to reinforce the behaviour are particularly appetitive for the rats.

The water plus maze experiments will involve animals being introduced to the arena for 5 consecutive days with a maximum of 1 minute per trial where the animal must try locate the hidden platform before being removed, dried with a towel and put back in its home cage. In the novel object recognition experiments animals will introduce to the arena for 5min exposure to 2 novel objects following habituation to the empty arena. For each test session the animal is exposed to the novel objet and the familiar object for a further 5 minutes to test acquisition and consolidation. Animals are then returned to their home cage

Chronic drug administration is carried out either by mixing the drug in the animal's food or water, or by subcutaneous injection when oral administration is not possible. Subcutaneous injection is relatively painless since injection is into the scruff of the neck, where rats experience relatively little pain; they are carried by their mother by the scruff as pups. Note however that the oral administration will be always *privileged as this procedure does not yield any supplementary stress and is similar to the normal intake in human subjects. In general terms, animals are always allowed to settle for a period of a few days upon arrival at the lab, and are well-handled by the experimenter so they are at ease with human contact and comfortable in their new surroundings.*

11. Severity banding:

Mild

12. How will pain be alleviated during and after the procedure?

Ketamine and Xylazine will be used as analgesic agents to alleviate pain during the cannulation procedure. Anaesthesia will be maintained during the surgery with isofluorane and post operative analgesia is provided by NSAID. Animals will receive the non-recoverable anestetic Urethane for LTP experiment.
Analgesic treatment is not anticipated as necessary for behavioural procedures.

13. What happens to the animals at the end of the experiment?

Animals are deeply anaesthetised and euthanised by a lethal overdose of anaesthetic, or by decapitation (for histology purposes).

14. Who is funding this work?

GlaxoSmithKline in collaboration with TCD.

15. Why is it necessary to use live animals for this study?

The experiments proposed can only be undertaken in animals because direct measurement of physiological brain function and tissue analyses are required in order to perform thorough investigations under controlled laboratory conditions.

16. If this is an application for licence renewal, what publications and noteworthy findings have come from the previously licensed period of work?

It is primary application for licence.

a. Publications:

Hennigan, A., Callaghan, C.K., Kealy, J., Rouine, J, Kelly A.M., Deficits in LTP and recognition memory in the genetically hypertensive rat are associated with decreased expression of neurotrophic factors and their receptors in the dentate gyrus, *Behavioural Brain Research*, 197, (2), 2009, p371 - 377

Callaghan, C., Loscher, C. and Kelly, Á. , Recognition memory in the rat is associated with increased BDNF release and ERK activation in the dentate gyrus , European Neuropsychopharmacology , 16, (1), 2006, ppS58

Callaghan, C and Kelly, Á. , Recognition memory in the rat is associated with increased BDNF release and ERK and PI3K activation in the dentate gyrus and perirhinal cortex, Irish Journal of Medical Science, 175, (3), 2006, pp45-

b. Noteworthy findings:

Neurotrophins play an important role mediating the acquisition and consolidation of recognition memory, acting mainly in the dentate gyrus and perirhinal cortex of the medial temporal lobe. BDNF appears to mediate its role through activation of the ERK/MAPK pathway and the Pi3K/Akt pathway it's the named brain regions. The main data produced as a result of the previous licence will be published early 2010.